UNIVERSIDAD AUTÓNOMA DE SAN LUIS POTOSÍ

FACULTADES DE INGENIERÍA, CIENCIAS QUÍMICAS y MEDICINA

UNIVERSIDAD DE GRANADA

FACULTAD DE CIENCIAS

Departamento de Química Inorgánica

PROGRAMA DE DOCTORADO EN QUÍMICA

VALORIZACIÓN SOSTENIBLE DE LA BIOMASA DE SARGAZO PARA LA REMOCIÓN DE CONTAMINANTES DEL AGUA MEDIANTE TECNOLOGÍAS DE ADSORCIÓN

SUSTAINABLE VALORIZATION OF SARGASSUM BIOMASS FOR THE REMOVAL OF POLLUTANTS FROM WATER BY ADSORPTION TECHNOLOGIES

Tesis que para obtener el grado de:

Doctorado en Ciencias Ambientales
Doctorado en Química

Presenta:

Lázaro Adrián González Fernández

Codirector: **Dr. Nahum Andrés Medellín Castillo**
Codirector: **Dr. Amado Enrique Navarro Frómeta**

SAN LUIS POTOSÍ, S. L. P. FECHA: Octubre de 2025

Esta Tesis está enmarcada en el Convenio de Cotutela de Tesis Doctoral suscrito entre la Universidad de Granada, España (UGR) y la Universidad Autónoma de San Luis Potosí, México (UASLP), de fecha 19 de noviembre de 2021.

VALORIZACIÓN SOSTENIBLE DE LA BIOMASA DE SARGAZO PARA LA REMOCIÓN DE CONTAMINANTES DEL AGUA MEDIANTE TECNOLOGÍAS DE ADSORCIÓN / SUSTAINABLE VALORIZATION OF SARGASSUM BIOMASS FOR THE REMOVAL OF POLLUTANTS FROM WATER BY ADSORPTION TECHNOLOGIES

This project was carried out at the Wastewater Treatment Research Laboratory affiliated with the Faculty of Engineering of the Universidad Autónoma de San Luis Potosí between August 2021 and June 2024 under the co-supervision of Dr. Nahum Andrés Medellín Castillo and Dr. Amado Enrique Navarro Frómeta.

Research stays were also conducted at the Department of Inorganic Chemistry affiliated with the Faculty of Sciences of the University of Granada, between September and November 2022 and between June and November 2024, under the supervision of Dr. Manuel Sánchez Polo, supported by the Mobility Scholarship among all institutions associated with the Ibero-American Postgraduate Association (AUIP) and the Heinrich Böll Foundation (Mexico and the Caribbean office). Similarly, a research stay was carried out at the Institute of Analytical and Bioanalytical Chemistry affiliated with Ulm University, Germany, between December 2024 and June 2025, under the supervision of Dr. Boris Mizaikoff, supported by the Research-Grants-One-Year-Grants for Doctoral Candidates from the Deutscher Akademischer Austauschdienst (DAAD).

The Doctoral Program in Environmental Sciences at the Universidad Autónoma de San Luis Potosí is part of the National System of Quality Postgraduate Studies (SNP) of the Secretariat of Sciences, Humanities, Technologies, and Innovation (SECIHITI). Scholarship number granted by SECIHITI: 800642. CVU number: 1014829.

The data from the work titled **VALORIZACIÓN SOSTENIBLE DE LA BIOMASA DE SARGAZO PARA LA REMOCIÓN DE CONTAMINANTES DEL AGUA MEDIANTE TECNOLOGÍAS DE ADSORCIÓN / SUSTAINABLE VALORIZATION OF SARGASSUM BIOMASS FOR THE REMOVAL OF POLLUTANTS FROM WATER BY ADSORPTION TECHNOLOGIES** are safeguarded by the Faculties of Engineering, Chemical Sciences, and Medicine and belong to the Universidad Autónoma de San Luis Potosí.

UNIVERSIDAD AUTÓNOMA DE SAN LUIS POTOSÍ

FACULTADES DE INGENIERÍA, CIENCIAS QUÍMICAS y MEDICINA

Programa Multidisciplinario de Posgrado en Ciencias Ambientales

UNIVERSIDAD DE GRANADA

FACULTAD DE CIENCIAS

Departamento de Química Inorgánica

VALORIZACIÓN SOSTENIBLE DE LA BIOMASA DE SARGAZO PARA LA REMOCIÓN DE CONTAMINANTES DEL AGUA MEDIANTE TECNOLOGÍAS DE ADSORCIÓN

SUSTAINABLE VALORIZATION OF SARGASSUM BIOMASS FOR THE REMOVAL OF POLLUTANTS FROM WATER BY ADSORPTION TECHNOLOGIES

Tesis que para obtener el grado de:

Doctorado en Ciencias Ambientales
Doctorado en Química

Presenta:

Lázaro Adrián González Fernández

SINODALES:

Presidente:	**Dr. Francisco Javier Pérez Vázquez**
Secretario:	**Dr. Nahum Andrés Medellín Castillo**
Vocal:	**Dra. Luisa María Pastrana Martínez**
Vocal:	**Dra. Lorena Díaz de León Martínez**
Vocal:	**Dra. Ana Conejo García**

SAN LUIS POTOSÍ, S. L. P. FECHA: Octubre de 2025

ACKNOWLEDGMENTS

To God above all, for giving me the opportunity, the strength, and the faith to get this far—for everything He does in our lives every day, even when we don't always notice it.

To my mom, who couldn’t physically make it with me to this point, but whom I know is still with me. Thank you for the light, the guidance, the love. To my dad, for helping me with everything, for his support and dedication. To my siblings and the rest of my family for their companionship and affection.

To my director, Dr. Nahum Andrés Medellín Castillo, who has gone above and beyond to bring me this far. I am deeply grateful for all the support provided throughout this project—for being my advisor and like a second father along the way.

To my co-director, Dr. Amado Enrique Navarro Frómeta, for all his guidance and help, for the knowledge he has shared with me, and for his support throughout these years.

To my second co-director in Spain, Dr. Manuel Sánchez Polo for his continuous support and guidance, the patience and all the shared knowledge.

To the members of my tutorial committee for their valuable guidance, suggestions, and critical insights throughout the development of this research. Their support and expertise were fundamental in shaping the course and quality of this work.

To my friends Yasmani, Susett, Juan Jesús, and Javier Ernesto for sharing with me some of the most meaningful moments of my academic and personal journey—for their friendship, laughter, and unwavering support along the way.

To my lab mates and colleagues, for all the moments we shared during the development of this thesis.

TECHNICAL ACKNOWLEDGMENTS

To Dr. Gladis Judith Labrada Delgado for her cooperation in obtaining the scanning electron micrographs and the EDS spectra of the samples.

To BSc. Laura Guadalupe Hernández de la Rosa, BSc. Gloria Korina Loredo Martínez and BSc. Miguel Angel Cortina Rangel for their support in training on various analytical techniques, the Flame Atomic Absorption Spectroscopy and ICP analyses.

To Dr. Roberto Leyva Ramos and Dr. Francisco Carrasco Marín for their support with the physisorption and XPS analysis and the guidance with the hydrothermal carbonization protocol.

To Dr. Raul Ocampo Pérez for his support with the kinetic experiments and analysis and access to his laboratory.

To MSc. Samuel Aguirre Contreras for his continuous support with the kinetic modelling using the COMOSOL Multiphysics software.

To Dr. Ventura Castillo Ramos for his support during the research stay in Granada, Spain and all the guidance in the analysis of the results obtained.

DEDICATIONS

To my mom, who is in heaven—this thesis is for you.

To my family, for all the support, understanding, and dedication throughout so many years.

To who I was and what remains of me in who I am today—and to all that I will become.

INDEX

RESUMEN

La contaminación de cuerpos de agua por metales pesados como el cadmio (Cd^{2+}) y el plomo (Pb^{2+}), así como por contaminantes emergentes como el ibuprofeno (IBU), constituye una amenaza ambiental y sanitaria de gran relevancia a nivel global. Estos compuestos son tóxicos, persistentes, no biodegradables y tienden a bioacumularse en organismos acuáticos, afectando cadenas tróficas y la salud humana. En este contexto, la presente tesis propone la valorización sostenible del alga marina Sargassum spp., frecuentemente considerada un residuo nocivo en las costas del Caribe mexicano, como materia prima para el desarrollo de biosorbentes eficientes en la remoción de dichos contaminantes. Se estudió la biomasa natural y sus derivados obtenidos por pirólisis (biochar) y carbonización hidrotermal (hidrochar), con rendimientos de conversión superiores al 30 %. Las muestras fueron caracterizadas mediante técnicas como FTIR, SEM/EDS, TGA, BET y análisis elemental (CHONS), revelando una alta densidad de grupos funcionales y superficies específicas de hasta 240 m^2/g en algunos biochars.

Los estudios de adsorción se realizaron en sistemas monocomponente y multicomponente, tanto en condiciones estáticas como dinámicas. Los materiales demostraron capacidades de adsorción máximas de hasta 478 mg/g para Pb(II) y 157 mg/g para Cd(II), y 103 mg/g para IBU bajo condiciones optimizadas. Se aplicaron modelos cinéticos de pseudo-primer y pseudo-segundo orden, así como modelos de isoterma de Langmuir, Freundlich y Radke-Prausnitz, con coeficientes de correlación mayores a 0.98. Además, se propuso y validó un modelo de difusión-permeación acoplado con dinámica de adsorción en lecho empacado, con buen ajuste predictivo para curvas de ruptura (%Desv < 5%).

Este trabajo representa una contribución novedosa al demostrar la aplicabilidad real del Sargazo no solo como biosorbente en fase líquida, sino como precursor de materiales carbonosos con alta eficiencia para la remoción simultánea de contaminantes metálicos y orgánicos. La integración de estudios termodinámicos, modelado matemático avanzado y evaluación en sistemas dinámicos refuerza la viabilidad de escalar esta tecnología como alternativa sustentable para el tratamiento de aguas contaminadas.

Palabras clave: Sargassum; Biochar; Hidrochar; Metales pesados; Contaminantes emergentes.

ABSTRACT

The contamination of water bodies by heavy metals such as cadmium (Cd^{2+}) and lead (Pb^{2+}), as well as by emerging pollutants like ibuprofen (IBU), represents a major environmental and public health concern at the global level. These compounds are toxic, persistent, non-biodegradable, and tend to bioaccumulate in aquatic organisms, affecting trophic chains and human health. In this context, the present thesis proposes the sustainable valorisation of the marine alga *Sargassum spp.*—often regarded as a harmful residue along the Mexican Caribbean coast—as a raw material for the development of efficient biosorbents for the removal of these pollutants. Natural biomass and its derivatives obtained through pyrolysis (biochar) and hydrothermal carbonization (hydrochar) were studied, achieving conversion yields above 30 %. The materials were characterized using techniques such as FTIR, SEM/EDS, TGA, BET, and CHONS elemental analysis, revealing a high density of functional groups and specific surface areas of up to 240 m^2/g in some biochars.

Adsorption studies were conducted in mono- and multi-component systems under both static and dynamic conditions. The materials exhibited maximum adsorption capacities of up to 478 mg/g for Pb(II), 157 mg/g for Cd(II), and 103 mg/g for IBU under optimized conditions. Pseudo-first and pseudo-second order kinetic models were applied, along with Langmuir, Freundlich, and Radke–Prausnitz isotherm models, all achieving correlation coefficients above 0.98. Additionally, a Diffusion–Permeation Model (DPM) coupled with packed-bed adsorption dynamics was proposed and validated, yielding a strong predictive fit for breakthrough curves (percentage deviation < 5%).

This work represents a novel contribution by demonstrating the real-world applicability of Sargassum not only as a biosorbent in aqueous media but also as a precursor for carbon-based materials with high efficiency for the simultaneous removal of metallic and organic pollutants. The integration of thermodynamic studies, advanced mathematical modeling, and evaluation under dynamic conditions strengthens the feasibility of scaling up this technology as a sustainable alternative for contaminated water treatment.

Keywords: Sargassum; Biochar; Hydrochar; Heavy metals; Emerging contaminants

INTRODUCTION

The contamination of water resources is a widespread phenomenon nowadays. In particular, potable and drinkable water has been significantly affected, often losing its intended purpose (Vasilachi et al., 2021). Water pollution originates from numerous sources, which can generally be classified into two main categories: direct and indirect sources. Direct sources include effluent discharges from industries and refineries, as well as pollutants entering water supplies from soil/groundwater systems and the atmosphere through rainwater deposition. Indirect sources pertain to contaminants infiltrating water supplies via soil/groundwater systems and atmospheric deposition, such as acid rain (González-Fernández et al., 2023).

A significant group of contaminants of concern is heavy metals, which are widely used across multiple industries, including mining, metallurgy, electronics, electroplating, and metal finishing. These industries generate large volumes of wastewater containing dissolved metal ions, which, if improperly treated, infiltrate water bodies and accumulate in aquatic ecosystems (Singh et al., 2022). Unlike organic pollutants, heavy metals are non-biodegradable, meaning they persist in the environment and can bioaccumulate in living organisms over time. The presence of these metals in industrial effluents is highly undesirable due to their toxicity to both lower and higher organisms within the trophic chain, ultimately impacting biodiversity and human health (Zaynab et al., 2022).

Heavy metal pollution is particularly problematic because many of these elements are essential in trace amounts for biological functions but become toxic at elevated concentrations. Metals such as cadmium (Cd) and lead (Pb) are especially hazardous due to their high mobility, persistence, and strong affinity for biological tissues. They enter aquatic ecosystems through various pathways, including direct industrial discharge, atmospheric deposition, leaching from landfills, and agricultural runoff containing metal-based pesticides and fertilizers. Once introduced into the water, heavy metals interact with dissolved organic matter, sediments, and biota, often undergoing complex chemical transformations that influence their bioavailability and toxicity (Mitra et al., 2022).

The toxicity of heavy metals primarily arises from their ability to bind to proteins, enzymes, and DNA, disrupting essential biological functions. Heavy metals can mimic essential metal ions (such as calcium, zinc, and magnesium) and displace them in biochemical processes, leading to oxidative

stress, enzyme inhibition, and cellular damage. In aquatic environments, heavy metals have been shown to reduce reproductive success, impair growth, and cause developmental abnormalities in fish, amphibians, and invertebrates. In humans, chronic exposure to heavy metals through contaminated drinking water, seafood, or crops irrigated with polluted water has been linked to neurological disorders, kidney damage, cancer, and other severe health conditions (Abd Elnabi et al., 2023).

Cadmium (Cd) is a highly toxic, non-essential heavy metal widely used in industrial applications such as battery manufacturing, electroplating, pigment production, and plastic stabilization. It is a byproduct of zinc, lead, and copper mining and refining, which releases large amounts of cadmium into the environment. Agricultural practices also contribute significantly to cadmium contamination, as phosphate fertilizers often contain cadmium impurities that leach into the soil and water (Zhang et al., 2023). One of the primary concerns with cadmium contamination is its high solubility in water and strong bioaccumulation potential. Once introduced into aquatic systems, cadmium readily binds to organic matter, sediments, and biological tissues, making it difficult to remove. Long-term exposure to cadmium is associated with severe health effects, including kidney dysfunction, bone demineralization (osteomalacia and osteoporosis), respiratory damage, and cancer. Cadmium also has a long biological half-life, meaning it remains in human tissues for decades, further exacerbating its toxic effects (NULI et al., 2024).

In aquatic organisms, cadmium interferes with calcium metabolism, leading to skeletal deformities, reduced growth rates, and reproductive impairment. Many studies have reported high cadmium concentrations in fish, molluscs, and crustaceans, making seafood a primary source of human exposure. Due to its severe toxicity, the World Health Organization (WHO) and the U.S. Environmental Protection Agency (EPA) have set stringent limits on cadmium concentrations in drinking water, typically below 0.005 mg/L. However, in many industrialized and mining regions, cadmium levels often exceed these safety thresholds, necessitating urgent remediation strategies (Lee et al., 2023).

Lead (Pb) is another highly toxic heavy metal with widespread industrial applications, including battery production, ammunition manufacturing, plumbing materials, and pigments. Historically, lead was also used in gasoline (tetraethyl lead) and paints, leading to extensive environmental

contamination. Although the use of lead in these applications has been restricted in many countries, legacy pollution from industrial emissions, mining waste, and lead-based paint continues to pose a significant threat (Collin et al., 2022).

Lead contamination in water primarily originates from corroded lead pipes, industrial effluents, and mining runoff. Unlike cadmium, which remains in water primarily in dissolved form, lead is more likely to bind to sediments and suspended particles, making it persistent in aquatic ecosystems. However, changes in pH, salinity, and the presence of organic ligands can remobilize lead from sediments, making it bioavailable to aquatic organisms (Garai et al., 2021).

The toxic effects of lead are well-documented, with neurological damage being one of the most severe consequences of exposure. Lead is a potent neurotoxin that disrupts synaptic transmission, leading to cognitive impairment, behavioural disorders, and developmental delays, particularly in children. Even at low concentrations, lead exposure has been linked to decreased IQ, learning disabilities, and attention deficits. In adults, chronic lead exposure increases the risk of hypertension, cardiovascular diseases, kidney damage, and anaemia (Collin et al., 2022).

In aquatic life, lead affects enzymatic activity, osmoregulation, and reproductive success. Fish exposed to lead-contaminated water exhibit gill damage, reduced swimming performance, and metabolic disturbances, leading to population declines. Regulatory agencies, including the WHO and EPA, have established strict lead concentration limits in drinking water, typically below 0.01 mg/L. However, incidents of lead-contaminated water supplies, such as the Flint water crisis in the United States, highlight the ongoing challenges of lead pollution and the need for effective remediation technologies (Kolarova & Napiórkowski, 2021).

Given the severe environmental and health risks posed by cadmium and lead contamination, there is a growing interest in developing sustainable and cost-effective remediation technologies. Conventional heavy metal removal methods, such as chemical precipitation, ion exchange, and membrane filtration, are often expensive and generate secondary waste that requires further disposal. In contrast, biosorption, which utilizes biological materials like algae, bacteria, fungi, and agricultural waste to capture heavy metal ions from aqueous solutions, has emerged as a promising alternative (Shankar et al., 2023).

Alongside heavy metals, contaminants of emerging concern (CECs) have garnered increasing attention. These include pharmaceuticals, personal care products, endocrine-disrupting chemicals, and microplastics. Unlike traditional pollutants, CECs are often introduced into water bodies through domestic wastewater, agricultural runoff, and improper disposal of consumer products. Ibuprofen, a widely used non-steroidal anti-inflammatory drug (NSAID), exemplifies the issue of pharmaceutical contamination. It enters aquatic systems primarily through domestic wastewater, as conventional wastewater treatment plants are ineffective at removing pharmaceuticals. Studies have detected ibuprofen residues in rivers, lakes, and even drinking water sources, raising concerns over its ecological and health impacts (Blasco & Trombini, 2023).

Although ibuprofen is less acutely toxic than heavy metals, its chronic exposure poses risks to aquatic organisms. Research indicates that ibuprofen can disrupt endocrine systems, alter reproductive functions, and impair growth in fish and amphibians. Moreover, the synergistic effects of ibuprofen combined with other pharmaceuticals or pollutants, such as heavy metals, can exacerbate toxicological outcomes. The presence of ibuprofen and other pharmaceuticals in water also threatens microbial communities essential for nutrient cycling and ecosystem stability. Continuous exposure to sub-lethal concentrations of pharmaceuticals can lead to the development of antibiotic-resistant bacteria, posing a significant public health threat (Jan-Roblero & Cruz-Maya, 2023).

Recently, another water quality issue has emerged: Sargassum, a type of marine macroalga that periodically reaches Caribbean beaches. Reports indicate that Sargassum currently represents one of the most pressing environmental issues in Mexico, resembling an uncontrolled algal epidemic. The Mexican Caribbean is experiencing severe environmental degradation due to this brown macroalga, which has disrupted coastal ecosystems and caused the death of marine species, including turtles and fish (Devault et al., 2021).

Beyond its ecological impact, Sargassum has also had significant economic consequences by affecting tourism-dependent activities. Additionally, it poses a potential health hazard due to its decomposition on beaches and its high content of arsenic and heavy metals. However, Sargassum itself is not inherently problematic; if governments implemented protection and management

strategies, its potential benefits could be better understood and even leveraged for environmental applications, such as in constructed wetlands (Saetan et al., 2021).

Among biological materials, marine algae, particularly *Sargassum spp.*, have demonstrated exceptional biosorption capabilities for heavy metals and CEC removal. *Sargassum* is a fast-growing, naturally abundant macroalga that contains functional groups such as carboxyl, hydroxyl, sulfonate, and amino groups, which actively bind to metal ions through complexation, ion exchange, and electrostatic interactions (Davis et al., 2003). The high surface area, porous structure, and chemical composition of *Sargassum spp.* make it an ideal biosorbent for cadmium and lead removal from industrial effluents and contaminated water bodies (González Fernández et al., 2024).

Studies have shown that untreated, chemically modified, and carbonized forms of *Sargassum spp.* exhibit high adsorption capacities for Cd^{2+} and Pb^{2+} ions, with removal efficiencies often exceeding 80–90 % under optimal conditions (Jayakumar et al., 2021). The efficiency of metal adsorption depends on factors such as pH, contact time, initial metal concentration, and biosorbent dosage (Rekha et al., 2025). Research has also demonstrated that pyrolyzed *Sargassum spp.* (biochar and hydrochar) exhibits enhanced metal removal efficiency, offering a highly stable and reusable material for wastewater treatment applications (Arora et al., 2024; Chambers et al., 2023).

Heavy metal and CEC pollution, particularly from cadmium, lead and ibuprofen represents a serious environmental and public health challenge. These toxic pollutants persist in ecosystems, bioaccumulate in organisms, and pose severe health risks through direct and indirect exposure. The development of sustainable, cost-effective remediation strategies is crucial for mitigating their impact. Biosorption, particularly using marine macroalgae like *Sargassum spp.*, has emerged as a viable, eco-friendly solution for cadmium, lead and CEC removal from contaminated water. Future research should focus on optimizing biosorption conditions, scaling up the process for industrial applications, and integrating biosorbent-based technologies with existing water treatment systems to enhance heavy metal remediation efforts.

JUSTIFICATION

The contamination of water bodies by heavy metals and CEC represents one of the most pressing environmental challenges. Industries such as mining, metal smelting, fuel and energy production from petroleum, fertilizer and pesticide manufacturing, and pharmaceuticals generate waste containing both heavy metals and organic micropollutants. These pollutants often enter aquatic environments due to improper treatment or disposal, posing serious risks to ecosystems and human health.

When heavy metals accumulate in ecosystems at concentrations exceeding permissible levels, they exert significant toxic effects on cells, primarily by disrupting protein function or causing protein denaturation. Moreover, these metals can undergo bioaccumulation and biomagnification within the trophic chain, leading to severe environmental consequences for marine ecosystems and human health (Zaynab et al., 2022). Similarly, CECs, such as pharmaceuticals (e.g., ibuprofen), personal care products, and endocrine-disrupting chemicals, persist in the environment due to their low degradability and continuous introduction through domestic and industrial wastewater (Yadav et al., 2021).

Pharmaceuticals like ibuprofen are of particular concern due to their widespread use and incomplete removal in conventional wastewater treatment plants. These compounds can interfere with hormonal regulation, reproduction, and metabolic processes in aquatic organisms. Additionally, the combined presence of heavy metals and CECs may lead to synergistic toxic effects, intensifying their impact on aquatic life. Addressing this dual pollution challenge requires sustainable and efficient remediation strategies, such as biosorption, which has demonstrated potential in removing both metallic and organic contaminants from water.

The biosorption of heavy metals by marine algae and seagrasses is primarily attributed to the properties of their cell walls, where electrostatic attraction and complexation play crucial roles. These cell walls typically consist of a fibrillar skeleton and an amorphous matrix. The fibrillar skeleton is primarily composed of cellulose, while the amorphous matrix consists mainly of alginic acid (alginate) and a smaller proportion of sulfate polysaccharides (fucoidans). Among the functional groups involved, carboxyl groups are the most abundant in the cell walls of these biosorbents. The second most prevalent acidic functional group is sulfonic acid, found in

fucoidans, which plays a secondary role unless metal binding occurs under low pH conditions. Hydroxyl groups within polysaccharides are also present, but they are less abundant and only exhibit negative charges at pH levels above 10, limiting their role in metal adsorption (Davis et al., 2003).

The search for novel materials and techniques to treat wastewater from industrial and mining activities has become a significant challenge in recent years. Conventional methods for heavy metal removal often prove ineffective at low metal concentrations, are costly, and have low efficiency under real-world conditions. Recent studies have explored alternative methodologies for contaminant adsorption, particularly for heavy metals, using biologically derived materials such as bacteria, algae, fungi, and industrial, agricultural, and urban waste. These alternatives have demonstrated high feasibility, low cost, and remarkable removal efficiency. Among these techniques, biosorption has emerged as a promising approach, involving the selective transfer of solutes from a liquid phase onto solid biological material, driven by various physical and chemical mechanisms (González et al., 2011).

Due to their natural origin and the elimination of residual sludge during the removal process, biosorption-based treatments not only reduce the environmental impact of contaminated water discharge but also allow for metal recovery and potential reintegration into productive cycles. From an economic perspective, marine algae and seagrasses have attracted significant attention in biotechnology due to their natural abundance. They frequently accumulate on beaches, where they are considered waste material. Utilizing them as biosorbents for heavy metals and radionuclide removal aligns with the principle of "waste for waste removal." Fishing vessels inadvertently collect large quantities of algae and seagrasses along with fish schools, which could be commercially repurposed instead of being discarded as "trash" (Devault et al., 2021).

Marine algae grow naturally on continental shelves in seas and oceans. Pacific coastlines, in particular, are frequently covered with marine algae that accumulate along shores without any beneficial use, often generating unpleasant odours as they degrade. However, the high diversity of marine algae enhances their selectivity and efficiency in heavy metal adsorption. Studies have demonstrated varying adsorption capacities among red, green, and brown algae, depending on their

chemical composition and specific adsorption sites (e.g., fucanoids, alginates, and phosphorylated proteins) (Davis et al., 2003).

Despite their promising potential, biosorption remains largely confined to laboratory-scale batch processes. While the underlying mechanisms of biosorption are being elucidated, the precise nature of metal-ion interactions and influencing factors remain incompletely understood. Furthermore, the optimized conditions identified in laboratory studies often fail to align with real wastewater conditions, which involve variables such as ionic strength, interfering ions, detergents, acidity, and organic content.

OBJECTIVES

General objective

Characterize the biomass and biochar/hydrochar derivatives of *Sargassum spp.* for their potential use as materials for removing contaminants from aqueous matrices through adsorption processes under both static and dynamic conditions, within single- and multi-component systems.

Specific objectives

1. Perform a physicochemical characterization of *Sargassum spp.* biomass using various analytical (acid-base titrations, nitrogen physisorption, scanning electron microscopy, etc.), spectrophotometric, and instrumental techniques.
2. Evaluate the influence of physical treatments (pyrolysis and hydrocarbonization) on *Sargassum spp.* biomass by analysing its physicochemical properties.
3. Characterize the biochars and hydrochars derived from *Sargassum spp.* biomass using multiple analytical, spectrophotometric, and instrumental techniques.
4. Determine the optimal experimental conditions for pollutants adsorption using natural and carbonized materials for batch and continuous methods.
5. Analyse the kinetics, thermodynamics, and equilibrium of the adsorption of the contaminants on natural and carbonized materials applying theoretical models.

PUBLISHED LITERATURE

Paper 1: Fundamentals in applications of algae biomass: A review

Journal: Journal of Environmental Management

Impact Factor (JCR): 8.7

Quartile: Q1

Volume: 338, 2023

ISSN: 0301-4797

https://doi.org/10.1016/j.jenvman.2023.117830

https://www.sciencedirect.com/science/article/pii/S0301479723006187

Fundamentals in applications of algae biomass: A review

Lázaro Adrián González Fernández[1], Ventura Castillo Ramos[2], Manuel Sánchez Polo[2] and Nahum Andrés Medellín Castillo[1,3]*

[1]*Multidisciplinary Postgraduate Program in Environmental Sciences. Av. Manuel Nava 201, 2nd. floor, University Zone, 78000, San Luis Potosí, S.L.P., Mexico.*

[2]*Department of Inorganic Chemistry, Faculty of Science, University of Granada, 18071, Granada, Spain.*

[3]*Center for Research and Postgraduate Studies of the Faculty of Engineering. Dr. Manuel Nava No. 8, West University Zone, 78290, San Luis Potosí, S.L.P., Mexico.*

*Corresponding author: nahum.medellin@uaslp.mx

Abstract

Algae play an extremely important ecological role. They form the basis of trophic webs, produce oxygen that allows the respiration of many of the organisms in aquatic environments, absorb CO_2, and serve as refuge areas and habitats for thousands of species. Many species can also absorb organic pollutants from seawater. Algae have been used for many centuries by humans as a source of food, fertilizer, fodder, and for the extraction of compounds with antifungal, antiviral, anticancer, and antibacterial properties. More recently, some species have been used for the production of biofuels. It has been shown that mixing small proportions of algae with the feed of cattle can reduce methane emissions from their digestive activity by more than 95 %.

One of the most widespread but least known applications of algae is the extraction of their phycocolloids for utilization in food, pharmaceutical, wine, and textile industries, among others. These compounds have gelling, stabilizing, and thickening properties and are therefore frequently included in creams, ice creams, cheeses, jellies, flavored milks, sauces, shampoos, medications, toothpaste, and many other products. The phycocolloids agar and carrageenan are extracted from red algae, whereas alginate is extracted from brown algae, being used in dental impressions, emulsifying lotions, and paints, among others, and in the preparation of wine and beer.

Algae are of particular interest in the research and development of new biosorbent materials, not only because of their high adsorption capacity, but also because they are present in the seas and oceans in abundant and easily accessible quantities. Marine algae are a promising biosorbent for the removal of heavy metals and various pollutants and, due to their intrinsic

characteristics, have received increasing attention in recent decades. Their application as biosorbents for the sorption of heavy metals and radionuclides could be interpreted as the use of waste to remove waste.

Algae have attracted particular interest in the field of biotechnology for economic reasons, given that large amounts are naturally produced and left lying on beaches as waste material. The composition of algae biomass makes it a promising candidate for an extensive list of applications that continues to lengthen. The development of appropriate technologies and policies can transform the presence of algae in coastal ecosystems from an unpleasant and potentially harmful phenomenon into a source of major benefits.

This review discusses the capacity of algae biomass to remove pollutants and also delves into its applicability in the production of dyes, oils, and biofuels and for animal feed and fertilizer industries, among others. Further research is warranted on strategies to convert a biomass that is currently considered waste into a means of addressing environmental problems.

1. Introduction

The search for new materials and techniques for the treatment of wastewater from industrial and mining processes has intensified in recent times and poses a major challenge. Growing manufacturing and metalworking sectors require the extraction of increasing amounts of heavy metals, and this activity can be responsible for aquatic environments with higher concentrations of metals than permitted by water quality criteria. Heavy metals in ionic form are discharged into rivers and seas from tanning, photography, pigmentation, plastics, battery and metallurgical industries, among others, without due environmental control (Gin et al., 2002) .

The effects of heavy metals on plants include necrosis at the tips of leaves, the inhibition of root growth, or the death of the plant. In humans, ingestion of heavy metals can cause skin rashes, ulcers, respiratory and immune system disorders, kidney and liver damage, genetic alterations, hypertension, and even death. According to the World Health Organization (WHO), the maximum concentration of heavy metal ions in water should range from 0.01 to 1.00 ppm, but concentrations up to 450 ppm have been reported in effluents (Guibal et al., 2001). Satisfactory results have been obtained in the elimination of toxic metals from wastewater using various techniques, including microprecipitation, electrodeposition, osmosis, adsorption, filtration,

ultracentrifugation, and ion exchange resins. However, these methods are not effective for low heavy metal concentrations in solution, being costly in relation to the low yield obtained under real-life conditions (Guibal et al., 2001).

Alternative methodologies have recently been developed for heavy metal adsorption using biological materials such as bacteria, algae, fungi, and industrial, agricultural, and urban waste, achieving high removal efficiency at a low cost. These techniques include biosorption, i.e., the selective transfer of solute(s) from a liquid phase to a batch of solid particles of biological material, which involves various physical and chemical mechanisms depending on certain factors. In the case of algae, their natural origin and the elimination of residual sludge during the removal process mean that this system not only removes the contaminating metal, reducing the environmental impact at the discharge site, but also allows its recovery for use in a new production cycle. The utilization of algae for the biosorption of heavy metals can be interpreted as using waste to dispose of waste.

For instance, fishing boats drag a large amount of algae along with fish in their nets, typically considered worthless and needing removal, but potentially of value as bioadsorber (Volesky, 1990). Algae offer a powerful biotechnological tool for the elimination of heavy metals. Moreover, besides the capacity of algae biomass to remove pollutants, it has recently proven useful in the production of dyes, oils, and biofuels and for animal feed and fertilizer industries, among many others.

Marine algae are relatively low in nitrogen and phosphorous but contain over 60 trace elements as well as fungal and disease prevention agents. The use of algae for composting was found to improve soil consistency and increase water retention in sandy or gritty soils and to serve as a top or side additive.

2. Bibliometric Analysis

Bibliometric analysis facilitates the review of large amounts of scientific literature. It functions in the same way as a systematic review and can be combined with rigorous techniques to guarantee the quality of the information processed and the results obtained (Nobanee et al., 2021). In the present study, the Web of Science (WoS) was searched for publications identifying Sargassum as a problem, using the search string "sargassum" and "invasion"; 68 studies were retrieved, with the

earliest being only 25 years ago. Figure 1 shows a significant increase over time in scientific papers on the environmental problems posed by Sargassum from 1997 onwards. More than 40% of retrieved studies were published in the past five years.

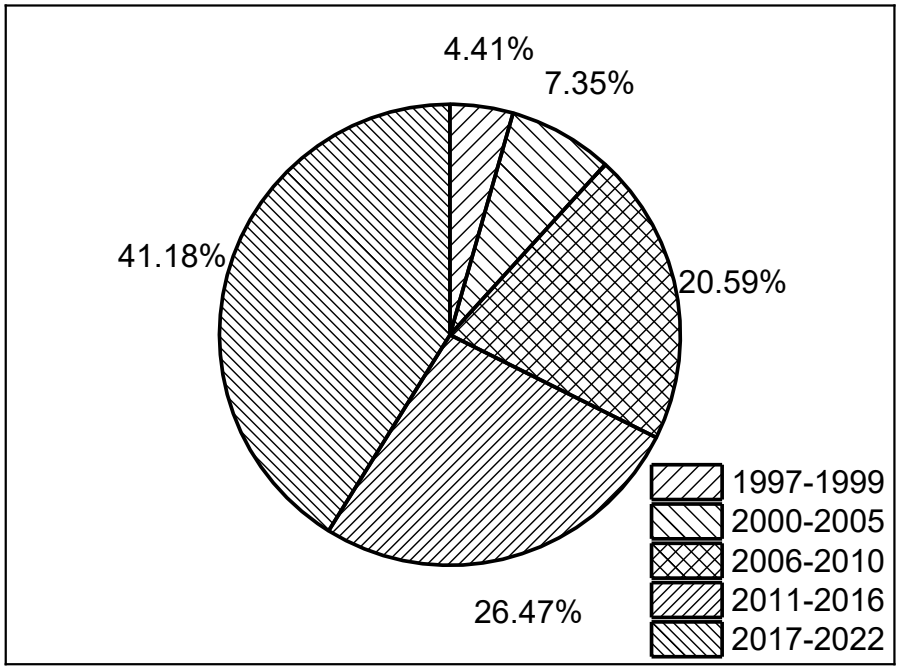

Figure 1. Distribution of publications on Sargassum as a problem from 1997 to 2022.

As shown in Table 1, most of the studies were conducted in Spain (n=19), followed by the USA (n=15), Portugal (n=10), Germany (n= 7), and Australia and England (n= 6 in each).

Table 1: Countries with the highest number of publications related to Sargassum as an environmental problem.

Order	Countries	Number of publications
1	Spain	19
2	USA	15
3	Portugal	10
4	Germany	7
5	Australia	6
5	England	6

The Web of Science (WoS) database was also used to select studies by using the search string "sargassum" and "applications" or "sargassum" and "uses" or "sargassum" and "valorization". The aim was to evaluate the interest of the scientific community in solving the problem of Sargassum and generating a use for or adding value to its biomass. Over the past five years, 161 publications have addressed this issue, with the largest number appearing in 2021, as depicted in Figure 2. The results were also grouped according to the country of the study, journal, and research area, among other parameters. Analyses were also conducted of the most frequently cited authors during this five-year period and of the studies with the largest number of citations.

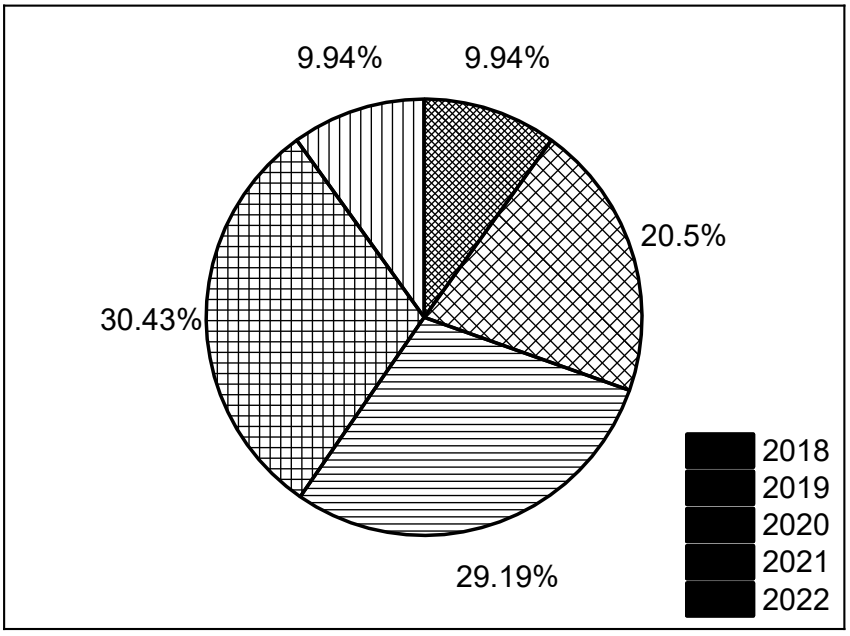

Figure 2. Distribution of publications by year of publication.

The People's Republic of China heads the list of countries with the largest number of studies (Figure 3) with 21 publications, followed by India (n=18), South Korea (n=18), Portugal (n=14, Egypt, (n=12), Spain (n=12) and Brazil, France, Iran, and Mexico (n= 11 each).

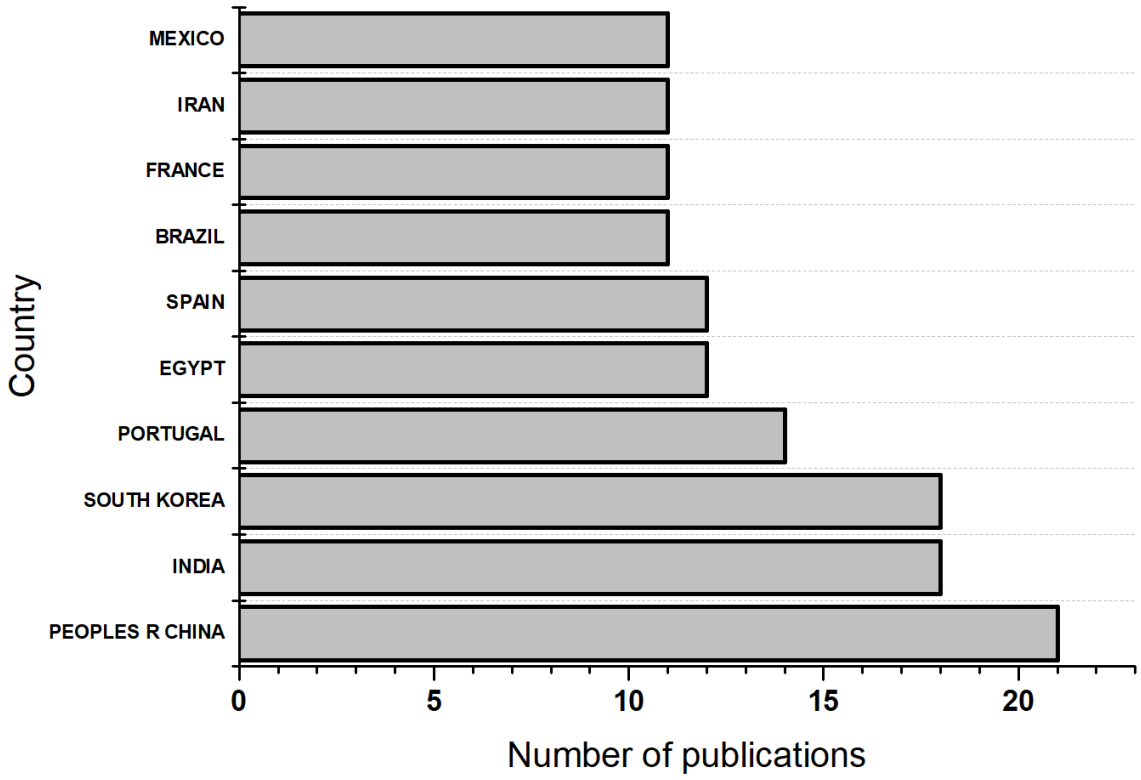

Figure 3. Top ten countries by number of publications.

The journal with the largest number of publications on this issue (Figure 4) is the Journal of Applied Phycology (n=15 articles), followed by Marine Drugs (n=12), Algal Research Biomass Biofuels and Bioproducts, Botanica Marina, International Journal of Biological Macromolecules and RSC Advances (n=4 each), and Antioxidants, Bionanoscience, Journal of Food Processing and Preservation, and PEERJ (n=3 each). By scientific field (Figure 5), the largest number of items were in Biotechnology Applied Microbiology (n=37), followed by Marine Freshwater Biology (n=30), Environmental Sciences Ecology (n=26), Pharmacology Pharmacy (n=24), and Chemistry (n=20). By WoS category (Figure 6), studies were most frequently grouped in Biotechnology Applied Microbiology (n=37), followed by Marine Freshwater Biology (n=30), Environmental Sciences (n=21), Medicinal Chemistry (n=19), and Pharmacology Pharmacy (n=18). Other

categories included Biochemistry Molecular Biology, Food Science Technology, and Plant Sciences.

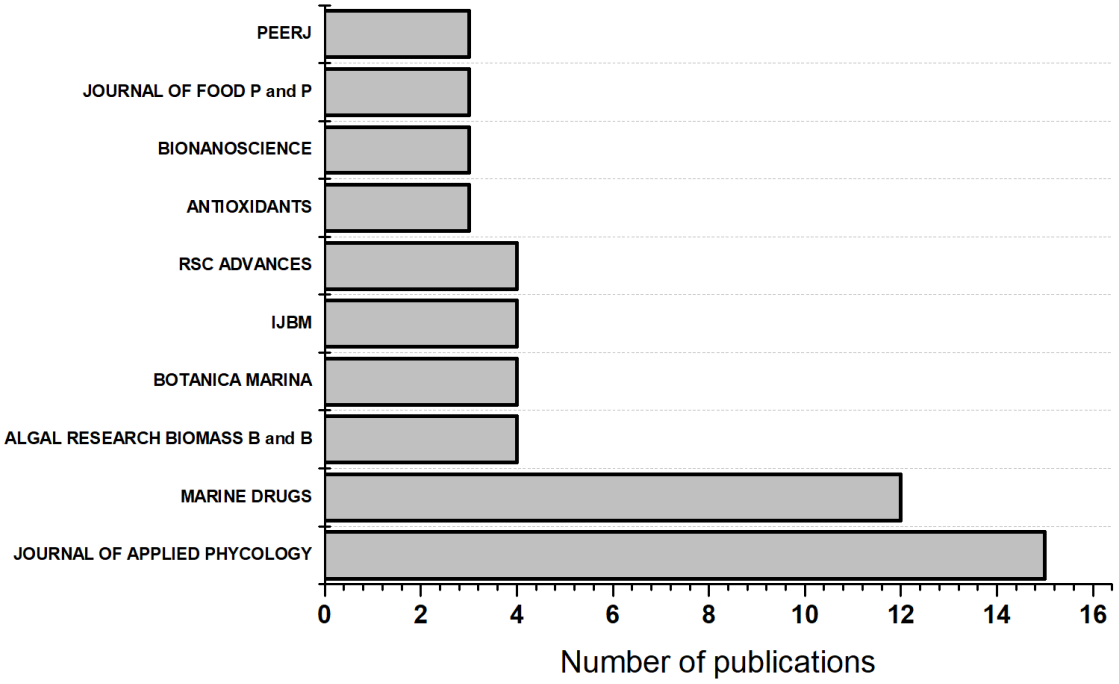

Figure 4. Top ten journals by number of publications.

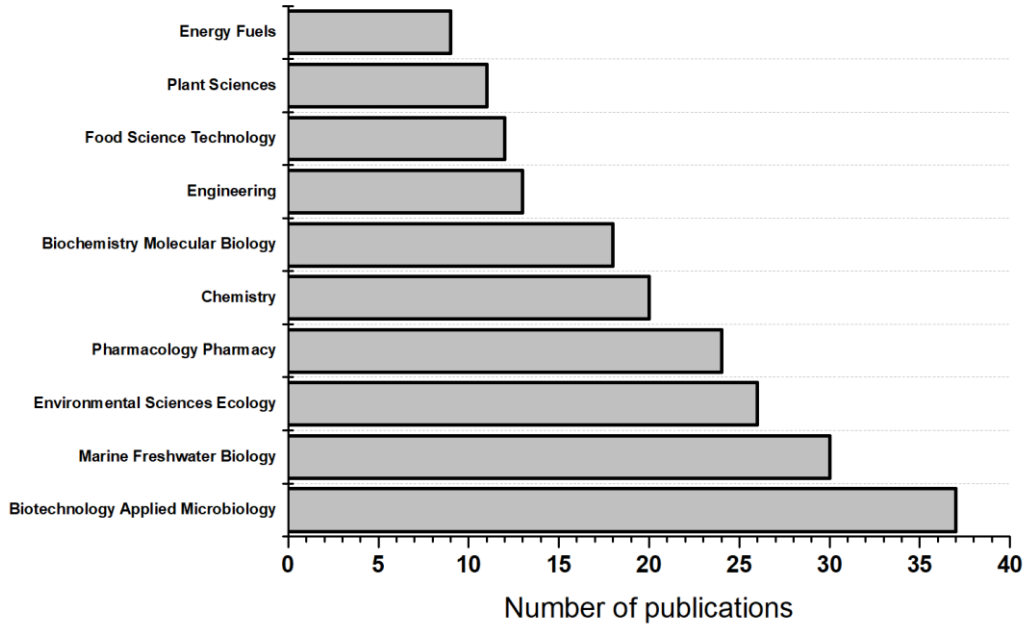

Figure 5. Top ten research areas by number of publications.

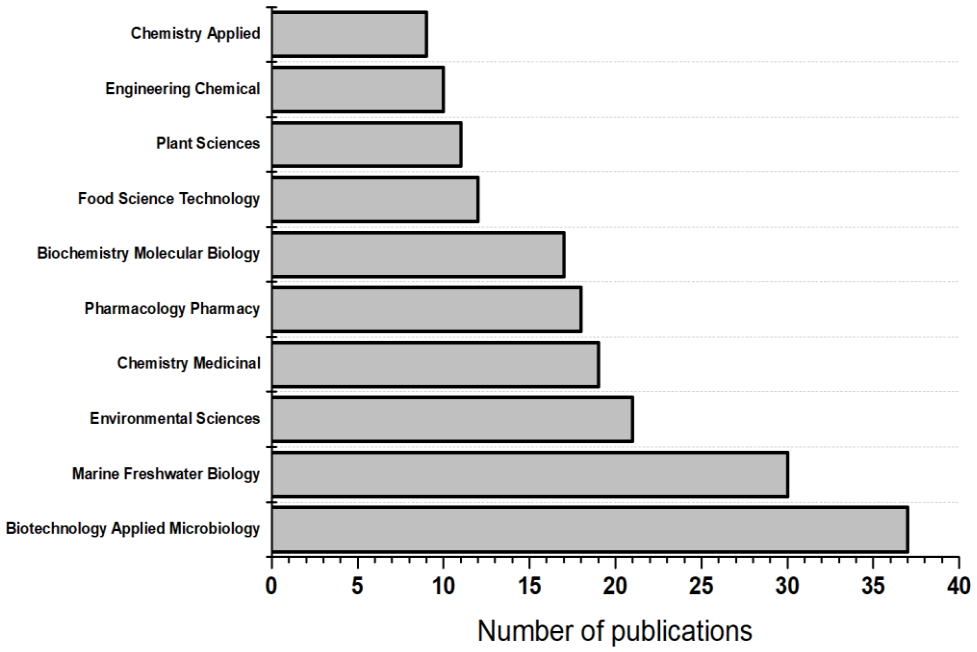

Figure 6. Number of publications by WoS Category.

Table 2 shows the top 15 main authors, ranked according to the number of their publications on this topic, and Figure 7 displays the number of citations they received. The most cited author is Yeon YJ (n=33 citations), followed by Kim HS (n=22) and Ahn G (n=21).

Table 2. Top 15 Authors according to the number of publications.

Order	Author	Number of publications
1	Ahn G	5
1	Fernando IPS	5
1	Jeon YJ	5
4	Dominguez H	4
4	Sanjeewa KKA	4
4	Torres MD	4
7	Florez-Fernandez N	3
7	Je JG	3
7	Mohapatra BR	3
7	Ramavandi B	3
7	Stiger-pouvreau V	3
7	Van Tussenbroek BI	3
7	Wu MJ	3
7	Yousefzadi M	3
7	Zubia M	3

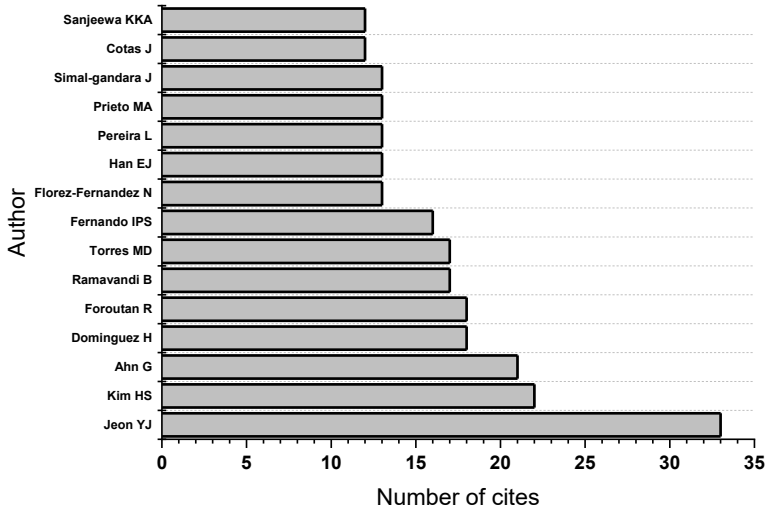

Figure 7. Top 15 most cited authors.

3. Brown Algae

The typical wall of brown algae consists of a fibrillar skeleton fixed in an unstructured viscous matrix (Figure 8).

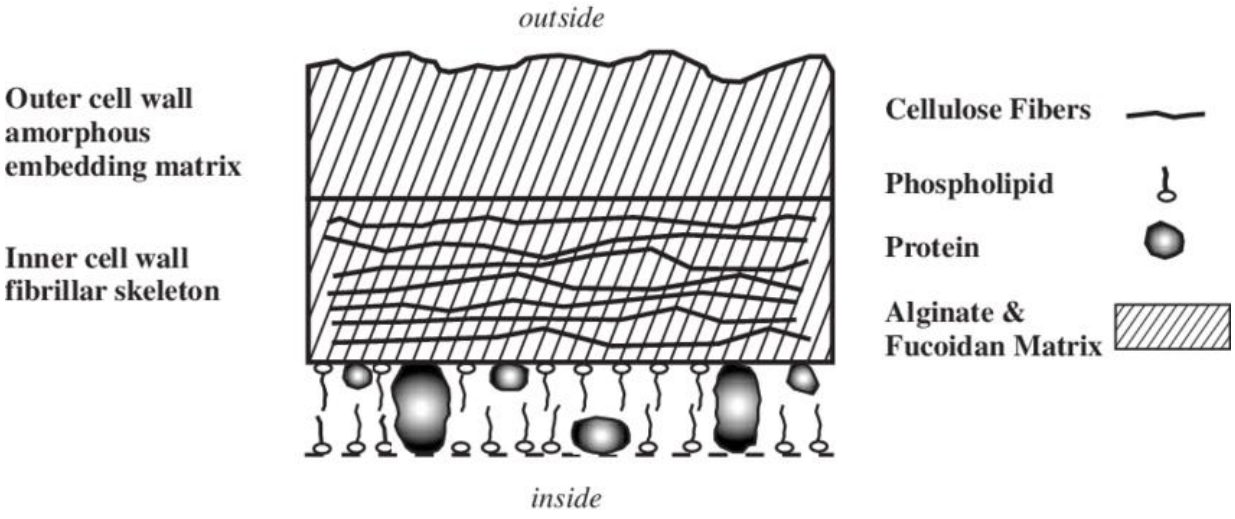

Figure 8. Brown algae cell wall structure (After Davis et al., 2003).

The most common fibrillar component is cellulose. Alginic acid is the primary constituent of the amorphous matrix of this type of algae and is responsible for binding heavy metals through

their carboxyl groups. The alginate content (from alginic acid) represents 10–40 % of the dry weight of the algae according to their environmental conditions, life cycle, and health status.

Alginic acid (Figure 9) is a polysaccharide composed of α-1,4-guluronic $(–G–)_n$ and β-1,4-D-mannuronic $(–M–)_n$ acids arranged in a non-regular manner (amorphous matrix) in discrete blocks of $(–G–)_n$, $(–M–)_n$, which present structural differences and different proportions in the alginate, thereby determining differences in the physical properties and reactivity of the polysaccharides.

The M:G ratio varies among different species. The affinity for pollutants increases with a higher proportion of G blocks (Davis et al., 2003). Dissociation constants of the different functional groups in the algal cell wall are displayed in Table 3. Mannuronic and guluronic acid constants are pKa=3.38 and 3.65, respectively. The polymer has a similar pKa value.

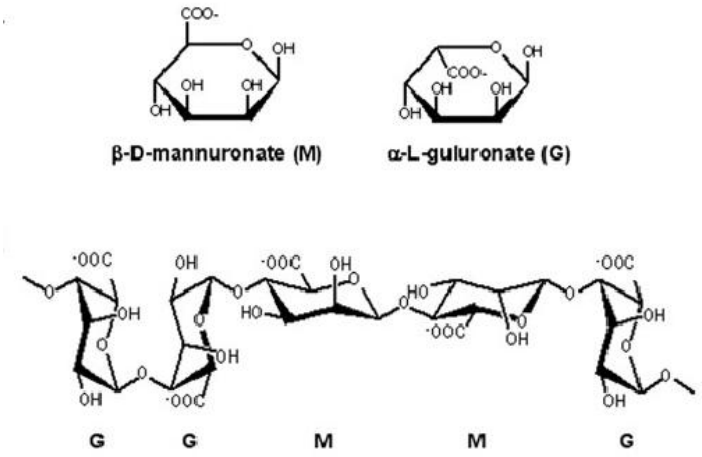

Figure 9. Monomeric and polymeric structure of alginate (After Davis et al., 2003).

Table 3. Functional groups in the algal cell wall involved in the adsorption of pollutants**.**

Functional group	Site	pKa
Carboxylic	Uronic acid	3.0-4.4
Sulphate	Cysteic acid	1.3
Phosphate	Polysaccharides	0.94-2.1
Imidazole	Histidine	6.0-7.0
Hydroxyl	Phenol-Tyrosine	9.5-10.5
Ammine	Cytidine	4.1

There is a wide diversity of marine algae, and the adsorption capacity and selectivity for heavy metals are known to vary among red, green and brown algae (Murphy et al., 2007). The chemical

composition and presence of different adsorption centers (fucanoids, alginates, phosphated proteins, etc.) can increase the adsorption of certain metals according to their size, degree of solvation, the presence of chelating ions and molecular sieves, and the ion exchange with species present in the algae (de la Rocha et al., 2009; Rojas et al., 2005). Marine algae are innocuous and have an inorganic content rich in calcium, magnesium, sodium, and potassium, meaning that algae-based biosorbents are acceptable for water cleaning or wastewater treatments.

4. Marine algae as option for bioremediation

Marine algae grow naturally on the continental shelves of seas and oceans. Shores on the Pacific coast are generally covered with marine algae that can become unsightly and foul-smelling over time and are considered waste materials, with no beneficial use (Cuizano & Navarro, 2008).

Crist et al. (1992) and Ragan (1986) studied the mechanisms by which heavy metals are fixed in brown algae, which incorporate the metals in high concentrations through polyanionic polysaccharides present in the cell wall and the affinity between metals and polyphenols. Finally, the high alginate content makes brown algae an ideal model for investigating metal-algae interactions at molecular level. The fact that a single functional group is responsible for the adsorption of heavy metals allows the application of various techniques to elucidate the mechanism. These include determination of the ionization constant (Navarro, 2006) of the algae, the ionic strength, the desorption of adsorbed metals by chelating species and acids, and the ion exchange, and analysis of images captured by infrared spectroscopy and scanning electron microscopy, among others. Marine algae appear to be the only adsorbents whose adsorption capacity is almost exclusively (> 90%) attributable to alginates (N. A. Cuizano et al., 2007; Davis et al., 2003; González et al., 2011; Lodeiro et al., 2004; Tapia et al., 2011).

It is important to determine the modifications that can strengthen the adsorption capacity, thermal-mechanical properties and selectivity of algae. Chemical modifications of algae are largely performed to facilitate contact between heavy metal ions and the functional groups that participate in the adsorption equilibrium and to cross-link or create new chains of biopolymers (Volesky, 1990). The main substances used include: $CaCl_2$, for the crosslinking of polyalginic chains; *formaldehyde and glutaraldehyde*, for the crosslinking of polyalginate chains between adjacent functional groups, mainly hydroxyl groups; *NaOH*, for reducing the protonation of

adsorbent functional groups, exchanging sodium ions in functional groups and facilitating ion exchange by increasing electrostatic attraction towards heavy metal cations; and *HCl,* for acid washing to produce competition between light metals and protons on the adsorbent surface, with the latter displacing the former; acid treatment can also lead to the dissolution of damaged outer polysaccharides from the algal cell wall, creating new adsorption sites. However, this type of biomass modification does not always improve the adsorption effectiveness, and the capacity for heavy metal removal can be reduced by the solubilization of different forms of alginate in the presence of NaOH (Volesky, 1990) .

Chemical modifications have not been found to increase the adsorption capacity of algae and do not appear to be a cost-effective approach, although they may be useful to improve biomass stability in continuous processes (columns) (Leyte-Vidal et al., 2019) . There has been much less published research on biosorption with algae than with other biomaterials, and there has been little investigation on multimetallic or dynamic systems. One study (Brinza et al., 2007) reported a higher metal adsorption capacity for brown algae than for green and red algae and some other adsorbents (Table 4). Bakkaloglu et al., 1998 investigated the metal biosorption capacity of various types of biomasses, including bacteria (*S. rimosus*), yeasts (*S. cerevisiae*), fungi (*P. chrysogenum*), activated sludge, and marine algae (*A. nodosum* and *F. vesiculosus*), finding that copper, zinc, and nickel were removed more effectively by *A. nodosum* than by the other adsorbents. In another investigation, the capacity to adsorb calcium ions was found to be greatest for the algae *L. trabeculata* than for chitosan, cross-linked chitosan, or rice hulls, observing a higher affinity for the algae in comparison to the other adsorbents (A. E. Navarro, 2006).

Despite increasing evidence that marine algae are a promising biosorbent of heavy metals and other pollutants, their application in biosorption is currently limited to discontinuous processes, largely in the laboratory setting. Although the mechanisms of biosorption are under investigation, the type of metal ion-adsorbent interaction and influential factors have not been fully elucidated. In addition, the real-life conditions of wastewater have not been completely matched in studies, including ionic strength, interfering ions, detergents, acidity, and organic content, among other factors.

In regard to the adsorption mechanism, further research is required on the factors that influence the equilibrium state (e.g., pH, temperature) and on the role that the co-ion (anion) plays in the biosorption process. In addition, there is a need to develop mathematical models of equilibrium and kinetics that are related to real wastewater conditions (e.g., pH, ionic content). It is also important to explore the possibility of recovering heavy metals removed from the water and adsorbed on the biosorbent. The biosorption of heavy metals by marine algae has been widely studied over recent decades, but many questions remain about the optimization of this process. Nevertheless, it is possible that the utilization of marine algae is one of the best ecological weapons available for the decontamination of our planet.

5. Using marine algae to produce biochar

Biochar is a carbon-rich material obtained from the thermochemical decomposition of organic waste in the absence of oxygen at temperatures that generally range between 300 and 700 ˚C and (pyrolysis). Pyrolysis stabilizes the carbon present in organic matter in a form that is more resistant to chemical and biological decomposition and does not degrade in soil, avoiding the emission of carbon into the atmosphere observed when non-pyrolyzed organic matter decomposes. Biochar has properties that can improve the soil, increase the productivity of crops, and contribute to carbon sequestration, relevant to the fight against climate change.

Interest in the application of biochar, a relatively recent idea, mainly resulted from the discovery of substances similar in nature to biochar in dark soils of the Amazon, known as *Terra preta do indio*. Generally, land in the Amazon forest is very poor in nutrients, but these dark soils are rich in organic carbon and highly fertile (Lehmann, 2007) .

Biochar can be used to improve the soil and the efficiency of resource utilization, to remediate and/or protect against environmental contamination, and to mitigate greenhouse gases (Chan & Xu, 2012). Biochar can also retain metallic elements or contaminants (J. Wang et al., 2021). In this way, a manure biochar was found to retain cadmium (Břendová et al., 2017), and good results were obtained using biochar as adsorbent for a rice crop in cadmium-contaminated soil. Verheijen et al., 2012 reported that biochar can also favor the sorption from soils and sediments of organic compounds such as herbicides, pesticides, enzymes, and polycyclic aromatic hydrocarbons, helping to avoid harmful short- and long-term effects.

Table 4. Removal percentages and adsorption capacities of some adsorbents for different pollutants.

Adsorbent	Adsorbate	pH	% Rem, q	Reference
Pretreated *Laminaria japónica*	Cu(II)	4.8	95.0 %	(Liu et al., 2009)
	Cd(II)	4.8	66.0 %	
	Zn(II)	4.8	60.0 %	
Lessonia nigrescens	Cd(II)	3.7	37.0 mg g^{-1}	(Gutiérrez et al., 2015)
Durvillaea antarctica	Cd(II)	3.7	45.0 mg g^{-1}	
Sargassum muticum treated with Ca	Cd(II)	No control	50.6 mg g^{-1}	(Carro et al., 2015)
	Hg(II)	No control	60.2 mg g^{-1}	
Ascophyllum nodosum	Cd(II)	4.9	215 mg g^{-1}	(Holan et al., 1993)
	Ni(II)	6.0	136 mg g^{-1}	(Holan & Volesky, 1994)
	Pb(II)	6.0	478 mg g^{-1}	
Fucus vesiculosus	Cd(II)	3.5	73.0 mg g^{-1}	(Holan et al., 1993)
	Ni(II)	3.5	23.0 mg g^{-1}	(Holan & Volesky, 1994)
	Pb(II)	6.0	600 mg g^{-1}	
Padina gymnospora	Ni(II)	3.5	10.0 mg g^{-1}	(Holan & Volesky, 1994)
	Pb(II)	3.5	65.0 mg g^{-1}	
Padina tetrastomatica	Pb(II)	4.5	217.4 mg g^{-1}	(Jalali et al., 2002)
	Cd(II)	5.0	59.6 mg g^{-1}	(Hashim & Chu, 2004)
Sargassum spp.	Cd(II)	6.0	157.4 mg g^{-1}	(Tobin et al., 1984)
	Cr(VI)	4	69.0 mg g^{-1}	(Sala Cossich et al., 2002)
	Cr(VI)	3.5	67.6 mg g^{-1}	(Silva et al., 2003)
	Cu(II)	3.5	68.6 mg g^{-1}	
Sargassum baccularia	Cd(II)	5.0	83.2 mg g^{-1}	(Hashim & Chu, 2004)
Sargassum fluitans	Ni(II)	3.5	24.0 mg g^{-1}	(Holan & Volesky, 1994)
Sargassum fluitans	Pb(II)	3.5	330 mg g^{-1}	
Sargassum hystrix	Pb(II)	4.5	285 mg g^{-1}	(Jalali et al., 2002)
Sargassum natans	Cd(II)	3.5	132 mg g^{-1}	(Holan et al., 1993)
	Ni(II)	3.5	24.0 mg g^{-1}	(Holan & Volesky, 1994)
	Pb(II)	3.5	253 mg g^{-1}	
	Pb(II)	4.5	238 mg g^{-1}	(Jalali et al., 2002)
Undaria pinnatifida	Pb(II)	4.0	403 mg g^{-1}	(Kim et al., 1999)
Activated Carbon from *Sargassum spp.*	Cr(VI)	2.0	91.98 %	(Akbar Esmaeili & Ghasemi, 2012)
	Cu(II)	4.0	~ 97 %	(A Esmaeili et al., 2010)
Activated Carbon from *Sargassum fusiforme*	Congo Red	7.0	234 mg g^{-1}	(Ma et al., 2020)
Pretreated Ulva lactuca	Pb(II)	5.0	19.7 mg g^{-1}	(Bulgariu & Bulgariu, 2014)
	Zn(II)	5.0	3.9 mg g^{-1}	
	Co(II)	5.0	5.9 mg g^{-1}	
Caulerpa fastigiata	Cd(II)	5.5	2.8 mg g^{-1}	(Sarada et al., 2014)

%Rem: Percentage of remotion; q: adsorption capacity.

Seaweeds have attracted interest as an energy source because they have a rapid growth rate (from 10 to 340 times that of oil crops) and require a smaller area for cultivation. They can be grown under unfavourable conditions, as in the case of wastewater, meaning that bioenergy can be generated without taking land suitable for food production (Chisti, 2007) .

Algae can be converted into energy by biochemical or thermochemical conversion (Amin, 2009). In relation to the former, the production of biodiesel requires a specific type of algae that can generate an oil content representing between 30 and 75% of its dry weight. In this way, biodiesel or ethanol can be produced from the fermentation of green algae such as *Chlorococcus littoral* (Ueno et al., 1998). In thermochemical conversion, all types of algae can be converted into energy products through heat-assisted reactions, and biochar is generated as a by-product of this process (Metzger et al., 1991).

Biochar from algae biomass has a lower carbon content, surface area, and CEC in comparison to lignocellulose-containing material but has a higher pH and a higher–content of nitrogen, ashes, and inorganic elements (P, K, Ca, and Mg). Hence, algae biochar can be useful to reduce the acidity of soil and increase its content of inorganic nutrients (Bird et al., 2011). However, despite these advantages, there have been only a few studies on biochar production from algae. Notably, Bird et al., 2011 used macroalgae and seagrasses from fresh water and marine ecosystems and obtained biochar that was more than 30% of the dry weight of the raw material. Likewise, Chaiwong et al., 2012 used slow pyrolysis and produced biochar that was 28-31% of the weight of various species of algae obtained from fresh water. Acceptable biochar yields were also reported by Yuan & Macquarrie, 2015 from the biorefining of *Ascophylum nosodum*. Choi et al., 2016 and Chiodo et al., 2016 also described the satisfactory performance and properties of biochar obtained from the brown algae *Saccharina japonica* and the *Posidonea* species *Oceanica* (seagrass) and from *Lacustrine Alga* (algae), respectively.

6. Natural brown dye extracted from marine algae

Brown algae are used as a high-intensity colorant for fabrics, and alginate extracted from sargassum is employed as a fabric thickener to prevent colour fading (Abbott, 1996). The striking brown colour extracted from brown algae such as sargassum contains fucoxanthin, a yellowish-brown pigment belonging to the xanthophyll family of carotenoid pigments (Hii et al., 2010) . Natural brown-hued colorants are difficult to find and isolate and brown algae could yield natural

dyes that could replace artificial colorants in food, pharmaceuticals, and cosmetics among others. Fucoxanthin has also been found to have antioxidant properties and to exert beneficial health effects, promoting weight loss and acting as an anticancer and anti-inflammatory agent (Maeda et al., 2008; Miyashita & Hosokawa, 2007), supporting the potential value of seaweed algae as a functional food ingredient. Brown algae possess greater antioxidant properties in comparison to red or green algae, offering compounds not found on land. Crude extracts, fractions, and pure components of brown algae are similar and often superior to antioxidants of synthetic origin (Balboa et al., 2013) .

Natural pigments are generally unstable, being involved in chemical reactions that affect the color of the final product. They are very easily affected by such environmental factors as light, temperature, oxygen, and water pH (Timberlake & Henry, 1986). Spray drying has proven highly useful in these cases to coat the pigment with an encapsulating agent and thereby reduce negative effects of these factors (Saénz et al., 2009) . It has been widely used for drying foods and in the production of drugs and other thermosensitive substances in which the solvent can rapidly evaporate. Spray drying can also be used to encapsulate a biologically active compound within a protective matrix that is inert to the compound (Saénz et al., 2009). This procedure improves the efficacy and range of application of food additives, increases the shelf life of the product, and reduces its costs. (Ray et al., 2016) . In addition, good quality powders can be produced with high stability, facilitating storage, handling, transportation, and application in comparison to liquid concentrates (Tonon et al., 2008).

Tun Norbrillinda et al., 2016 extracted a natural brown dye from brown algae by soaking the algae biomass in a water bath filled with distilled water at 95-98 °C for about 3.5 hours. The extract was then spray dried using maltodextrin DE 10 as an encapsulation agent producing a microbiologically stable powder with a brownish yellow shade. The colorant was also found to have antioxidant activity, favoring its use as a natural brown dye in multiple products and foods, including beverages and desserts.

Yip et al., 2014 extracted pigments from *Sargassum binderi* using methanol:chloroform:water, as part of the fucoidan extraction process in which pigments are waste. Fucoxanthin and chlorophyll were identified in the extract, which therefore has potential as a bioingredient and functional food. It was found to remain stable under normal storage conditions.

7. Fabrication of cellulose nanofibers from waste brown algae

Cellulose nanofibers, a nanocomposite developed from cellulose, the main component of plants, are attracting attention for their lightness, resistance, and environmental qualities. They are already used in a wide variety of articles, such as adult diapers, screens, automobiles, or airplanes (Rezaei et al., 2015). Interest centres on their physical properties, being five-fold lighter and five-fold stronger than steel. As nanometre-scale fibres, they allow visible light to pass through and can be made transparent. The large specific surface area of this material means that it is also suitable for the manufacture of filters that collect dust and other small particles or of deodorizing substances that absorb microscopic odour-carrying particles (Huang et al., 2016).

Food wrappers using cellulose nanofiber film, which have a strong barrier effect against the penetration of oxygen and other gases, are effective to keep food fresh. These nanofibers also have high viscosity, even when immersed in water, opening up their possible usefulness as a food additive to reinforce the sensation of body or chewiness of food (Ghaderi et al., 2014).

Cellulose can be obtained from practically any plant: from timber, wheat or rice straw, or the stems of corn, cotton, or marine algae, among numerous others, minimizing the environmental impact of its extraction. Brown algae are considered a more accessible and better-quality source in comparison to terrestrial plants, whose cellulose contains lignin, affecting the processing cost. Most species of brown algae do not contain this compound, allowing the extraction of quality cellulose without additional purification steps (Trivedi et al., 2013). In addition, cellulose extracted from brown algae contains a network that resembles a sponge, very different from the structure observed in cellulose of plant origin (Strømme et al., 2002). Furthermore, as already noted, seaweeds are a low-cost source of biomass that grow rapidly without the need for arable land, drinking water, fertilizers, or pesticides (Trivedi et al., 2013). Finally, milder conditions are required for the extraction and isolation of cellulose from seaweeds in comparison to lignin-containing plant cellulose (John et al., 2011).

Gao et al., 2018 found that cellulose isolated from brown algae after alginate extraction was cellulose I, present in the rigid chain 416 conformation in dilute solution. Addition of these nanofibers to milk produced an appreciable thickening effect due to absorption of the cellulose by casein micelles *via* hydrogen bonds, resulting in a weak gel-like structure. Paniz et al., 2020

combined alkaline treatment, bleaching, and freeze-drying of the Antarctic algae *Cystosphaera jacquinottii* to produce cellulose, obtaining a porous sponge-like cellulosic material.

8. Production of algal oil and bio-oil

Algal fuel, algal biofuel, and algal oil offer alternatives to liquid fossil fuels and common biofuels (e.g., from corn and sugarcane) as a source of energy-rich oil. Various companies and government agencies are funding efforts to reduce capital and operating costs and achieve commercially viable algal fuel production (Adeniyi et al., 2018).

Algal fuel releases CO_2 when burned; however, unlike fossil fuel, biofuels only release CO_2 recently removed from the atmosphere *via* photosynthesis with growth of the algae or plants. The energy crisis and the global food crisis have sparked interest in algae farming to produce biodiesel and other biofuels. One of the attractive features of algal fuels is that algae do not need land suitable for agriculture and can grow in saline and wastewaters, with minimal impact on freshwater resources. In addition, they have a high flash point, and are biodegradable and relatively harmless to the environment if spilled (Saad et al., 2019). It has been estimated that the cost per unit mass is higher for algae than other second-generation biofuel crops due to the high capital and operating costs involved but that algae 10- to 100-fold more fuel per unit area (Mu et al., 2020).

Brown algae can be converted into various types of fuels according to the technique and the part of cells used. The lipid or oily portion of the algal biomass can be extracted and converted into biodiesel using a similar process to that applied for any other vegetable oil or can be converted into a petroleum replacement for petroleum-based fuels. Alternatively, or after lipid extraction, the carbohydrate content of the algae can be fermented to produce bioethanol or butanol fuel (Kumar et al., 2015). Some species of algae, notably sargassum, can produce 60 % or more of their dry weight as oil (Mu et al., 2020). Because the cells grow in aqueous suspension, with more efficient access to water, CO_2, and dissolved nutrients, microalgae can produce large amounts of biomass and usable oil in high-rate algal ponds or photobioreactors. This oil can be converted into biodiesel for utilization in motor vehicles. Rural communities could reap economic benefits from the regional production of microalgae and their transformation into biofuels (Konur, 2021).

Growth rates can be faster for microalgae than for terrestrial crops because they do not produce structural compounds (e.g., cellulose) for leaves, stems, or roots and can grow floating in a rich nutrient medium. Microalgae can convert a much higher fraction of their biomass to oil

(60%) in comparison to conventional crops (e.g., 2-3 % for soybeans). The yield per unit area of Sargassum oil is estimated to be 58700 and 136900 L ha^{-1} $year^{-1}$ depending on the lipid content, which is 10- to 23-fold higher than palm oil, the next highest yielding crop (5 950 L ha^{-1} $year^{-1}$) (Mu et al., 2020).

Sargassum can be used to produce green diesel (also known as renewable diesel, hydrotreated vegetable oil, or hydrogen-derived renewable diesel) through a hydrotreating process that breaks the molecules down into the shorter hydrocarbon chains used in diesel engines. Given that it has the same chemical properties as petroleum-based diesel, it does not require new engines, pipelines, or infrastructure for its utilization and distribution (Douvartzides et al., 2019). However, it has not yet been produced at a cost that is competitive with oil. Although hydrotreating is currently the most common method to produce fuel-like hydrocarbons, catalytic decarboxylation and decarbonylation are alternative processes that offer some advantages over hydrotreating, as highlighted in studies by Santillan-Jimenez & Crocker, 2012 and Peng et al., 2012.

Research is ongoing into the catalytic conversion of renewable fuels by decarboxylation. Deoxygenation is not a major concern in oil refining because the concentration of oxygen in crude oil is only around 0.5 %, and catalysts are not specifically formulated for hydrogenating oxygenates. Hence, one of the critical technical challenges in achieving economically viable hydrodeoxygenation of algae oil is related to the development of effective catalysts (Galadima et al., 2022).

Kumar et al., 2015 used biomass from *Sargassum wightii* algae to produce algal oil and bio-oil, examining the optimal pre-treatment methods, solvent systems, exposure times and temperatures. The best oil yield (2.1 %) was obtained when ultrasonication was combined with the extraction of chloroform: methanol in a 2:1 ratio. The highest bio-oil yield was 25 % of the dry weight of the biomass, and the bio-oil produced in this way was a complex mixture of alcohols, ketones, aldehydes, fatty acids, esters, and nitrogen-containing heterocyclic compounds.

Farobie et al., 2022 conducted a comprehensive investigation into bio-oil production from *Sargassum* spp. *via* slow pyrolysis. The resulting bio-oil mainly contained carboxylic acids, furan derivatives, aliphatic hydrocarbons, and *N*-aromatic compounds. Bio-oil yields were around 30 % when the temperature was set at 400 ºC and the retention time at 50 min. The authors affirmed

that the effective valorisation of *Sargassum* sp. would be beneficial not only for environmental mitigation but also for producing high-value chemicals.

9. Other options

9.1 Constructed wetlands

Constructed wetlands are a type of Natural Treatment System (NTS) that mimics the conditions of natural wetlands. They consist of shallow lagoons or channels usually planted with typical wetlands species, with a substrate that provides a surface on which bacteria can settle and also acts to eliminate suspended solids produced in the filtration process (H. Wang et al., 2021).

Wetlands can be characterized by free flow or subsurface flow. Free-flowing wetlands are ponds or channels in which the water is exposed to the atmosphere and emerging plants are rooted in an impermeable layer. The input of water is usually continuous, and wastewaters normally undergo a previous treatment.

The advantages of NTSs over conventional treatments include their robustness against variations in flow and load, the simplicity of their operation, the almost zero energy consumption (zero if the wastewater is transferred by gravity), integration of the landscape in the rural environment and, when the flow is subsurface, the absence of bad odors and the non-proliferation of mosquitoes.

However, a larger surface area is needed for the implementation of NTSs in comparison to conventional approaches. In addition, one of the main problems of wetlands with subsurface flow is clogging of the bed (Knowles et al., 2011); therefore, previous treatment of the influent is necessary to minimize the presence of fats, oils, sand, and suspended solids and thereby prolong the wetland's useful life.

The substrate, sediments, and vegetation debris in constructed wetlands are important for several reasons:

- They support many of the living organisms in the wetland.

- The permeability of the substrate promotes the movement of water through the wetland.

- Many chemical and biological (especially microbial) transformations take place within the substrate.

- They provide storage for many contaminants.

- The accumulation of vegetation debris increases the amount of organic matter in the wetland, giving rise to the exchange of matter and fixation of microorganisms and providing a source of carbon that is at the same time a source of energy for key biological reactions in the wetland (Lara, 1999).

The environment is directly responsible for the extraction of some contaminating substances through physical and chemical interactions. The granular size of the medium directly affects the hydraulic flow of the wetland and, therefore, the flow of water to be treated. In this way, the absorption capacity and filtration are greater if the granular bed is made up of large amounts of clay and silt, when the adsorption is large and the hole diameter is small. However, this medium also has a high hydraulic resistance and produces very low flow rates, limiting the flow that can be treated (Arias Triguero, 2004). In contrast, the adsorption capacity and filtering power of the medium are lower if the granular bed comprises gravel and sand, but the hydraulic conductivity is higher. The granular medium indirectly contributes to the elimination of pollutants by supporting the growth of plants and colonies of microorganisms responsible for biodegrading activity (biofilms).

Besides gravel and sand, organic substrates can be used in constructed wetlands. This has been little studied, although experiments have been performed with compost (Aslam et al., 2007), rice husks (Tee et al., 2009), and wood mulch (Saeed & Sun, 2011), among others. The addition of organic substrates offers various environmental benefits, using waste that is highly abundant and can often pose a risk of forest fires. They can also adsorb organic compounds, creating a larger surface area for the growth of microorganism colonies, and their greater porosity reduces the likelihood of clogging.

Solid organic materials are cheap and readily available in areas of mining or other activities. They are a promising option for utilization in constructed wetlands because they can provide a carbon source to fuel bacterial sulfate reduction, among numerous post-decomposition biological and biochemical processes, and they can also serve as microbial carriers and adsorbents for metals and organic compounds (Gibert et al., 2005). Many researchers have highlighted the effectiveness for environmental pollution remediation of packed batch or column bioreactors with substrate mixtures combining organic solids (e.g., cattle manure, crop straw, sludge, compost, wood chips,

chitin, etc.) with inorganic supports (Genty et al., 2018; Neculita et al., 2007; Singh & Chakraborty, 2020).

However, the decomposition rate of complex organic substances is often unstable and uncertain and is accompanied by a gradual decrease in carbon supply, requiring the continual replacement of depleted media to maintain microbial activity and the performance of the system, especially at high system power loads (Neculita et al., 2007; X. Wang et al., 2018). Furthermore, there is a tendency to hydraulic clogging in some labile organic media due to their low permeability (Sheoran et al., 2010).

9.2 Use as compost and soil quality improver

Seaweeds are relatively low in nitrogen and phosphorous but contain over 60 trace elements as well as fungal and disease prevention agents. The use of algae for composting was found to improve soil consistency and increase water retention in sandy or gritty soils and to serve as a top or side additive (Michalak & Chojnacka, 2013).

The entire composting process lasts approximately five months. After the completion of active composting, irrigation and regular turning are halted, and the piles are then allowed to cure for 4 to 8 weeks (Dougherty, 1999; Misra et al., 2003). Compost requires adequate proportions of nitrogen and carbon (Misra et al., 2003). Food waste (including vegetables, meat, dairy, and bread) can be used as the main source of nitrogen, while wood chips and litter have been used as primary carbon inputs and as loading agents to promote airflow through compost piles.

Seaweed is best used to amend soil for young plants as a dilution of compost tea, which drains out of the composting bins or is simply the by-product of soaking the seaweed for a few days (Abou-El-Hassan & El-Batran, 2020). Algae can be used to produce compost tea with an aerator or with the addition of microbial inoculants to stimulate microbial activity and create a less odoriferous brew. These items can be found at garden centers, online, or at pet stores that sell aquarium equipment. The resulting liquid seaweed fertilizer can be diluted with water and then foliar fed to the plants or added around the plant roots. It not only feeds the plants but neutralizes pests, viruses, and fungi (St. Martin, 2015). Further advantages of using seaweed as compost are that it can applied dry or wet and it does not clump or overflow. Moreover, dogs, cats, and birds do not appear to like the rough texture or smell of composted dried seaweed (Michalak et al., 2017).

9.3 Animal nutrition

The composition of algae varies between species and within the same species, depending on the phase of their biological cycle at harvesting and on the growth conditions. There are very few published studies on the nutritional value of seaweed as livestock feed, mostly when used as an additive to supply bioactive compounds or micronutrients rather than as a substantive source of macronutrients (Becker, 2007). However, Bikker et al., 2020, recently explored the usefulness of intact seaweeds as a source of macronutrients. They harvested algae from the coastal waters of Ireland, Scotland, and France (n=13 samples), including six different species of brown (*Laminaria digitata*, *Saccharina latissimi* and *Ascophyllum nodosum*), red (*Palmaria palmata* and *Chondrus crispus*), and green (*Ulva lactuca*) algae. After drying on the same shoreline, exposed to the elements, they were processed to reduce their particle size. Nutrient content widely varied within and between species, ranging from 4.5 to 24.8 % for proteins, from 35.1 to 69.1 % for non-starch polysaccharides, and from 17.3 to 44.5 % for ashes. Brown algae species had the highest concentration of non-starch polysaccharides, and red and green species the highest concentrations of amino acids (up to 26.5 %).

Intestinal organic matter and nitrogen digestibility and total tract organic matter digestibility (digestibility coefficients: 0.81, 0.89, and 0.88, respectively) were lower for the seaweeds than for soybean meal (digestibility coefficients: 0.84, 0.98 and 0.97, respectively). Maximum gas production was higher for *S. latissima*, *L digitata*, *P. palmata,* and *U. lactuca* than for alfalfa. The protein content and amino acid profile of *P. palmata* and *U. lactuca* indicate that they may be a valuable protein source for cattle, although their high content of non-starch polysaccharides and low in vitro digestibility may contraindicate their inclusion in diets for monogastrics. Results of the fermentation of *L. digitata*, *S. latissima* and *P. palmata* suggest that they may have higher nutritional value for ruminants. However, their high ash content is a drawback for any livestock species, although this likely results from contamination with sand while drying on the beach and could be addressed by washing the seaweed before processing.

The above findings on the variability between and within species underscore the need for a nutrient analysis before the incorporation of algae in a balanced diet. However, their protein content and amino acid profile, especially in red and green algae (e.g., *P. palmata* and *U. lactuca*), indicate their potential value as a source of supplemental protein for livestock, particularly

ruminants. Extraction of the protein and reduction in the ash content would favor the inclusion of these algae in animal diets.

10. Conclusions

Algae are widely used in food industry, agriculture, cosmetics, and medicine. They are seen as offensive waste on the beach at one extreme and as a highly nutritious superfood at the other. As a source of hydrocolloids, algae are used as thickeners for numerous products, including ice cream, toothpaste, cosmetics, shampoo, pet food, baby food, dairy products, creams, instant soups, and many other articles.

They are also considered as biological activators and organic biostimulants that increase the nutrient content and its availability for rapid assimilation during plant development. In addition, the application of seaweed extracts and the enzymes they contain to the foliage of plants strengthens their defences and improves their nutrition and physiology, increasing their resistance to stress.

The incorporation of seaweed extracts in soil and foliage fixes nitrogen from the air, increasing the nutrition of crops and their vigour. Brown algae and red algae are the most widely used types, and brown algae are a particularly important source of nitrogen due to their high protein content. They also contain organic nitrogen, which is readily assimilated and provides important elements such as calcium, phosphorus, potassium, and magnesium. Brown algae have been reported to contain a high percentage of organic matter, minerals, vitamins, carbohydrates, lipids, and natural phytohormones.

Red algae have a high protein content, increasing the concentration of assimilable nitrogen. They also provide assimilable phosphorus and potassium to plants. It has been reported that the natural gums and carbohydrates they contain help to retain soil moisture and increase the absorption of minerals from the soil.

Algae can be used in constructed wetlands, in the production of biochar and dyes, and as a soil additive or improver, among many other applications. Further research is warranted on strategies to convert a biomass that is currently considered waste into a means of addressing environmental problems.

References

Abbott, I. A. (1996). Ethnobotany of seaweeds: clues to uses of seaweeds. *Fifteenth International Seaweed Symposium*, 15–20.

Abou-El-Hassan, S., & El-Batran, H. S. (2020). Integration of some bio compounds with compost tea to produce sweet corn without mineral fertilizers. *Middle East J. of Agric. Res*, *9*(3), 645–652.

Adeniyi, O. M., Azimov, U., & Burluka, A. (2018). Algae biofuel: current status and future applications. *Renewable and Sustainable Energy Reviews*, *90*, 316–335.

Amin, S. (2009). Review on biofuel oil and gas production processes from microalgae. *Energy Conversion and Management*, *50*(7), 1834–1840.

Aslam, M. M., Malik, M., Baig, M. A., Qazi, I. A., & Iqbal, J. (2007). Treatment performances of compost-based and gravel-based vertical flow wetlands operated identically for refinery wastewater treatment in Pakistan. *Ecological Engineering*, *30*(1), 34–42.

Bakkaloglu, I., Butter, T. J., Evison, L. M., Holland, F. S., & Hancockt, I. C. (1998). Screening of various types biomass for removal and recovery of heavy metals (Zn, Cu, Ni) by biosorption, sedimentation and desorption. *Water Science and Technology*, *38*(6), 269–277.

Balboa, E. M., Conde, E., Moure, A., Falqué, E., & Domínguez, H. (2013). In vitro antioxidant properties of crude extracts and compounds from brown algae. *Food Chemistry*, *138*(2–3), 1764–1785.

Becker, E. W. (2007). Micro-algae as a source of protein. *Biotechnology Advances*, *25*(2), 207–210.

Bikker, P., Stokvis, L., Van Krimpen, M. M., Van Wikselaar, P. G., & Cone, J. W. (2020). Evaluation of seaweeds from marine waters in Northwestern Europe for application in animal nutrition. *Animal Feed Science and Technology*, *263*, 114460.

Bird, M. I., Wurster, C. M., de Paula Silva, P. H., Bass, A. M., & De Nys, R. (2011). Algal biochar–production and properties. *Bioresource Technology*, *102*(2), 1886–1891.

Břendová, K., Száková, J., Lhotka, M., Krulikovská, T., Punčochář, M., & Tlustoš, P. (2017). Biochar physicochemical parameters as a result of feedstock material and pyrolysis

temperature: predictable for the fate of biochar in soil? *Environmental Geochemistry and Health*, *39*(6), 1381–1395.

Brinza, L., Dring, M. J., & Gavrilescu, M. (2007). MARINE MICRO AND MACRO ALGAL SPECIES AS BIOSORBENTS FOR HEAVY METALS. *Environmental Engineering & Management Journal (EEMJ)*, *6*(3).

Bulgariu, L., & Bulgariu, D. (2014). Enhancing biosorption characteristics of marine green algae (Ulva lactuca) for heavy metals removal by alkaline treatment. *Journal of Bioprocessing & Biotechniques*, *4*(1), 1.

Carro, L., Barriada, J. L., Herrero, R., & de Vicente, M. E. S. (2015). Interaction of heavy metals with Ca-pretreated Sargassum muticum algal biomass: Characterization as a cation exchange process. *Chemical Engineering Journal*, *264*, 181–187.

Chaiwong, K., Kiatsiriroat, T., Vorayos, N., & Thararax, C. (2012). Biochar production from freshwater algae by slow pyrolysis. *Maejo International Journal of Science and Technology*, *6*(2), 186.

Chan, K. Y., & Xu, Z. (2012). Biochar: nutrient properties and their enhancement. In *Biochar for environmental management* (pp. 99–116). Routledge.

Chiodo, V., Zafarana, G., Maisano, S., Freni, S., & Urbani, F. (2016). Pyrolysis of different biomass: direct comparison among Posidonia Oceanica, Lacustrine Alga and White-Pine. *Fuel*, *164*, 220–227.

Chisti, Y. (2007). Biodiesel from microalgae. *Biotechnology Advances*, *25*(3), 294–306.

Choi, J. H., Kim, S.-S., Suh, D. J., Jang, E.-J., Min, K.-I., & Woo, H. C. (2016). Characterization of the bio-oil and bio-char produced by fixed bed pyrolysis of the brown alga Saccharina japonica. *Korean Journal of Chemical Engineering*, *33*(9), 2691–2698.

Crist, R. H., Oberholser, K., McGarrity, J., Crist, D. R., Johnson, J. K., & Brittsan, J. M. (1992). Interaction of metals and protons with algae. 3. Marine algae, with emphasis on lead and aluminum. *Environmental Science & Technology*, *26*(3), 496–502.

Cuizano, N. A., Llanos, B. P., Chang, L., & Navarro, A. E. (2007). Equilibrio ácido-base de algas marinas del litoral peruano elucida su alta afinidad por contaminantes ambientales. *Revista*

de La Sociedad Química Del Perú, *73*(2), 85–93.

Cuizano, N., & Navarro, A. (2008). Biosorción de metales pesados por algas marinas: Posible solución a la contaminación a bajas concentraciones. In *Anales de la Real Sociedad Española de Química, ISSN 1575-3417, Nº. 2, 2008, pags. 120-125* (Vol. 104).

Davis, T. A., Volesky, B., & Mucci, A. (2003). A review of the biochemistry of heavy metal biosorption by brown algae. *Water Research*, *37*(18), 4311–4330.

de la Rocha, S. R., Sánchez-Muniz, F. J., Gómez-Juaristi, M., & Marín, M. T. L. (2009). Trace elements determination in edible seaweeds by an optimized and validated ICP-MS method. *Journal of Food Composition and Analysis*, *22*(4), 330–336.

Dougherty, M. (1999). *Field Guide to On-Farm Composting (NRAES 114)*. Natural Resource, Agriculture, and Engineering Service (NRAES).

Douvartzides, S. L., Charisiou, N. D., Papageridis, K. N., & Goula, M. A. (2019). Green diesel: Biomass feedstocks, production technologies, catalytic research, fuel properties and performance in compression ignition internal combustion engines. *Energies*, *12*(5), 809.

Esmaeili, A, Ghasemi, S., & Sohrabipour, J. (2010). Biosorption of copper from wastewater by activated carbon preparation from alga Sargassum sp. *Natural Product Research*, *24*(4), 341–348.

Esmaeili, Akbar, & Ghasemi, S. (2012). *Investigation of Cr (VI) adsorption by dried brown algae Sargassum sp. and its activated carbon*.

Farobie, O., Amrullah, A., Bayu, A., Syaftika, N., Anis, L. A., & Hartulistiyoso, E. (2022). In-depth study of bio-oil and biochar production from macroalgae Sargassum sp. via slow pyrolysis. *RSC Advances*, *12*(16), 9567–9578.

Galadima, A., Masudi, A., & Muraza, O. (2022). Towards sustainable catalysts in hydrodeoxygenation of algae-derived oils: A critical review. *Molecular Catalysis*, 112131.

Gao, H., Duan, B., Lu, A., Deng, H., Du, Y., Shi, X., & Zhang, L. (2018). Fabrication of cellulose nanofibers from waste brown algae and their potential application as milk thickeners. *Food Hydrocolloids*, *79*, 473–481.

Genty, T., Bussière, B., Benzaazoua, M., Neculita, C. M., & Zagury, G. J. (2018). Changes in

efficiency and hydraulic parameters during the passive treatment of ferriferous acid mine drainage in biochemical reactors. *Mine Water and the Environment*, *37*(4), 686–695.

Ghaderi, M., Mousavi, M., Yousefi, H., & Labbafi, M. (2014). All-cellulose nanocomposite film made from bagasse cellulose nanofibers for food packaging application. *Carbohydrate Polymers*, *104*, 59–65.

Gibert, O., de Pablo, J., Cortina, J. L., & Ayora, C. (2005). Municipal compost-based mixture for acid mine drainage bioremediation: Metal retention mechanisms. *Applied Geochemistry*, *20*(9), 1648–1657.

Gin, K. Y.-H., Tang, Y.-Z., & Aziz, M. A. (2002). Derivation and application of a new model for heavy metal biosorption by algae. *Water Research*, *36*(5), 1313–1323.

González, F., Romera, E., Ballester, A., Blázquez, M. L., Muñoz, J. Á., & García-Balboa, C. (2011). Algal biosorption and biosorbents. In *Microbial biosorption of metals* (pp. 159–178). Springer.

Guibal, E., Sweeney, N. V. O., Zikan, M. C., Vincent, T., & Tobin, J. M. (2001). Competitive sorption of platinum and palladium on chitosan derivatives. *International Journal of Biological Macromolecules*, *28*(5), 401–408.

Gutiérrez, C., Hansen, H. K., Hernández, P., & Pinilla, C. (2015). Biosorption of cadmium with brown macroalgae. *Chemosphere*, *138*, 164–169.

Hashim, M. A., & Chu, K. H. (2004). Biosorption of cadmium by brown, green, and red seaweeds. *Chemical Engineering Journal*, *97*(2–3), 249–255.

Hii, S., Choong, P., Woo, K., & Wong, C. (2010). Stability studies of fucoxanthin from Sargassum binderi. *Australian Journal of Basic and Applied Sciences*, *4*(10), 4580–4584.

Holan, Z. R., & Volesky, B. (1994). Biosorption of lead and nickel by biomass of marine algae. *Biotechnology and Bioengineering*, *43*(11), 1001–1009.

Holan, Z. R., Volesky, B., & Prasetyo, I. (1993). Biosorption of cadmium by biomass of marine algae. *Biotechnology and Bioengineering*, *41*(8), 819–825.

Huang, P., Zhao, Y., Kuga, S., Wu, M., & Huang, Y. (2016). A versatile method for producing functionalized cellulose nanofibers and their application. *Nanoscale*, *8*(6), 3753–3759.

Jalali, R., Ghafourian, H., Asef, Y., Davarpanah, S. J., & Sepehr, S. (2002). Removal and recovery of lead using nonliving biomass of marine algae. *Journal of Hazardous Materials*, *92*(3), 253–262.

John, R. P., Anisha, G. S., Nampoothiri, K. M., & Pandey, A. (2011). Micro and macroalgal biomass: a renewable source for bioethanol. *Bioresource Technology*, *102*(1), 186–193.

Kim, Y. H., Park, J. Y., Yoo, Y. J., & Kwak, J. W. (1999). Removal of lead using xanthated marine brown alga, Undaria pinnatifida. *Process Biochemistry*, *34*(6–7), 647–652.

Knowles, P., Dotro, G., Nivala, J., & García, J. (2011). Clogging in subsurface-flow treatment wetlands: occurrence and contributing factors. *Ecological Engineering*, *37*(2), 99–112.

Konur, O. (2021). Algal biodiesel fuels: A scientometric review of the research. *Biodiesel Fuels Based on Edible and Nonedible Feedstocks, Wastes, and Algae*, 669–694.

Kumar, P. S., Pavithra, J., Suriya, S., Ramesh, M., & Kumar, K. A. (2015). Sargassum wightii, a marine alga is the source for the production of algal oil, bio-oil, and application in the dye wastewater treatment. *Desalination and Water Treatment*, *55*(5), 1342–1358.

Lehmann, J. (2007). Bio-energy in the black. *Frontiers in Ecology and the Environment*, *5*(7), 381–387.

Liu, Y., Cao, Q., Luo, F., & Chen, J. (2009). Biosorption of Cd2+, Cu2+, Ni2+ and Zn2+ ions from aqueous solutions by pretreated biomass of brown algae. *Journal of Hazardous Materials*, *163*(2–3), 931–938.

Lodeiro, P., Cordero, B., Grille, Z., Herrero, R., & Sastre de Vicente, M. E. (2004). Physicochemical studies of cadmium (II) biosorption by the invasive alga in Europe, Sargassum muticum. *Biotechnology and Bioengineering*, *88*(2), 237–247.

Ma, M., Ying, H., Cao, F., Wang, Q., & Ai, N. (2020). Adsorption of congo red on mesoporous activated carbon prepared by CO2 physical activation. *Chinese Journal of Chemical Engineering*, *28*(4), 1069–1076.

Maeda, H., Tsukui, T., Sashima, T., Hosokawa, M., & Miyashita, K. (2008). Seaweed carotenoid, fucoxanthin, as a multi-functional nutrient. *Asia Pacific Journal of Clinical Nutrition*, *17*.

Metzger, P., Largeau, C., & Casadevall, E. (1991). Lipids and macromolecular lipids of the

hydrocarbon-rich microalga Botryococcus braunii. Chemical structure and biosynthesis. Geochemical and biotechnological importance. In *Fortschritte der Chemie organischer Naturstoffe/Progress in the Chemistry of Organic Natural Products* (pp. 1–70). Springer.

Michalak, I., & Chojnacka, K. (2013). Algal compost–toward sustainable fertilization. *Reviews in Inorganic Chemistry*, *33*(4), 161–172.

Michalak, I., Wilk, R., & Chojnacka, K. (2017). Bioconversion of Baltic seaweeds into organic compost. *Waste and Biomass Valorization*, *8*(6), 1885–1895.

Misra, R. V, Roy, R. N., & Hiraoka, H. (2003). *On-farm composting methods*. Rome, Italy: UN-FAO.

Miyashita, K., & Hosokawa, M. (2007). 12 Beneficial Health Effects of Seaweed Carotenoid, Fucoxanthin. *Marine Nutraceuticals and Functional Foods*, 297.

Mu, D., Xin, C., & Zhou, W. (2020). Life cycle assessment and techno-economic analysis of algal biofuel production. *Microalgae Cultivation for Biofuels Production*, 281–292.

Murphy, V., Hughes, H., & McLoughlin, P. (2007). Cu (II) binding by dried biomass of red, green and brown macroalgae. *Water Research*, *41*(4), 731–740.

Navarro, A. E. (2006). Propiedades ácido-básicas de Lentinus edodes y cinética de biosorción de Cadmio (II). *Revista Latinoamericana de Recursos Naturales*, *2*(2), 47–54.

Neculita, C., Zagury, G. J., & Bussière, B. (2007). Passive treatment of acid mine drainage in bioreactors using sulfate-reducing bacteria: Critical review and research needs. *Journal of Environmental Quality*, *36*(1), 1–16.

Nobanee, H., Al Hamadi, F. Y., Abdulaziz, F. A., Abukarsh, L. S., Alqahtani, A. F., AlSubaey, S. K., Alqahtani, S. M., & Almansoori, H. A. (2021). A bibliometric analysis of sustainability and risk management. *Sustainability*, *13*(6), 3277.

Paniz, O. G., Pereira, C. M. P., Pacheco, B. S., Wolke, S. I., Maron, G. K., Mansilla, A., Colepicolo, P., Orlandi, M. O., Osorio, A. G., & Carreño, N. L. V. (2020). Cellulosic material obtained from Antarctic algae biomass. *Cellulose*, *27*(1), 113–126.

Peng, B., Yuan, X., Zhao, C., & Lercher, J. A. (2012). Stabilizing catalytic pathways via redundancy: selective reduction of microalgae oil to alkanes. *Journal of the American*

Chemical Society, *134*(22), 9400–9405.

Piña Leyte-Vidal, J. J., González-Fernández, L. A., Gutiérrez-Artiles, O., Márquez-Llauger, L., & Del Cristo, T. A. (2019). Caracterización de tres bioindicadores de contaminación por metales pesados. *Revista Cubana de Química*, *31*(2), 293–308.

Ragan, M. A. (1986). Phlorotannins, brown algal polyphenols. *Progress in Phycological Research*, *4*, 177–241.

Ray, S., Raychaudhuri, U., & Chakraborty, R. (2016). An overview of encapsulation of active compounds used in food products by drying technology. *Food Bioscience*, *13*, 76–83.

Rezaei, A., Nasirpour, A., & Fathi, M. (2015). Application of cellulosic nanofibers in food science using electrospinning and its potential risk. *Comprehensive Reviews in Food Science and Food Safety*, *14*(3), 269–284.

Rojas, G., Silva, J., Flores, J. A., Rodriguez, A., Ly, M., & Maldonado, H. (2005). Adsorption of chromium onto cross-linked chitosan. *Separation and Purification Technology*, *44*(1), 31–36.

Saad, M. G., Dosoky, N. S., Zoromba, M. S., & Shafik, H. M. (2019). Algal biofuels: current status and key challenges. *Energies*, *12*(10), 1920.

Saeed, T., & Sun, G. (2011). A comparative study on the removal of nutrients and organic matter in wetland reactors employing organic media. *Chemical Engineering Journal*, *171*(2), 439–447.

Saénz, C., Tapia, S., Chávez, J., & Robert, P. (2009). Microencapsulation by spray drying of bioactive compounds from cactus pear (Opuntia ficus-indica). *Food Chemistry*, *114*(2), 616–622.

Sala Cossich, E., Granhen Tavares, C. R., & Kakuta Ravagnani, T. M. (2002). Biosorption of chromium (III) by Sargassum sp. biomass. *Electronic Journal of Biotechnology*, *5*(2), 6–7.

Santillan-Jimenez, E., & Crocker, M. (2012). Catalytic deoxygenation of fatty acids and their derivatives to hydrocarbon fuels via decarboxylation/decarbonylation. *Journal of Chemical Technology & Biotechnology*, *87*(8), 1041–1050.

Sarada, B., Prasad, M. K., Kumar, K. K., & Murthy, C. V. R. (2014). Cadmium removal by macro algae Caulerpa fastigiata: Characterization, kinetic, isotherm and thermodynamic studies.

Journal of Environmental Chemical Engineering, *2*(3), 1533–1542.

Sheoran, A. S., Sheoran, V., & Choudhary, R. P. (2010). Bioremediation of acid-rock drainage by sulphate-reducing prokaryotes: a review. *Minerals Engineering*, *23*(14), 1073–1100.

Silva, E. A., Cossich, E. S., Tavares, C. G., Cardozo Filho, L., & Guirardello, R. (2003). Biosorption of binary mixtures of Cr (III) and Cu (II) ions by Sargassum sp. *Brazilian Journal of Chemical Engineering*, *20*, 213–227.

Singh, S., & Chakraborty, S. (2020). Performance of organic substrate amended constructed wetland treating acid mine drainage (AMD) of North-Eastern India. *Journal of Hazardous Materials*, *397*, 122719.

St. Martin, C. C. G. (2015). Potential of compost tea for suppressing plant diseases. *CABI Reviews*, *2014*, 1–38.

Strømme, M., Mihranyan, A., & Ek, R. (2002). What to do with all these algae? *Materials Letters*, *57*(3), 569–572.

Tapia, P., Santander, M., Pavez, O., Valderrama, L., Guzman, D., & Romero, L. (2011). Bio sorption of copper ions with biomass of algae and dehydrated waste of olives. *Revista de Metalurgia*, *47*(1), 15–28.

Tee, H. C., Seng, C. E., Noor, A. M., & Lim, P. E. (2009). Performance comparison of constructed wetlands with gravel-and rice husk-based media for phenol and nitrogen removal. *Science of the Total Environment*, *407*(11), 3563–3571.

Timberlake, C. F., & Henry, B. S. (1986). Plant pigments as natural food colours. *Endeavour*, *10*(1), 31–36.

Tobin, J. M., Cooper, D. G., & Neufeld, R. (1984). Uptake of metal ions by Rhizopus arrhizus biomass. *Applied and Environmental Microbiology*, *47*(4), 821–824.

Tonon, R. V, Brabet, C., & Hubinger, M. D. (2008). Influence of process conditions on the physicochemical properties of açai (Euterpe oleraceae Mart.) powder produced by spray drying. *Journal of Food Engineering*, *88*(3), 411–418.

Trivedi, N., Gupta, V., Reddy, C. R. K., & Jha, B. (2013). Enzymatic hydrolysis and production of bioethanol from common macrophytic green alga Ulva fasciata Delile. *Bioresource*

Technology, *150*, 106–112.

Tun Norbrillinda, M., Mahanom, H., Nur Elyana, N., & Nur Intan Farina, S. (2016). Optimization of spray drying process of Sargassum muticum color extract. *Drying Technology*, *34*(14), 1735–1744.

Ueno, Y., Kurano, N., & Miyachi, S. (1998). Ethanol production by dark fermentation in the marine green alga, Chlorococcum littorale. *Journal of Fermentation and Bioengineering*, *86*(1), 38–43.

Verheijen, F. G. A., Montanarella, L., & Bastos, A. C. (2012). Sustainability, certification, and regulation of biochar. *Pesquisa Agropecuária Brasileira*, *47*(5), 649–653.

Volesky, B. (1990). Biosorption and biosorbents. *Biosorption of Heavy Metals*.

Wang, H., Sheng, L., & Xu, J. (2021). Clogging mechanisms of constructed wetlands: A critical review. *Journal of Cleaner Production*, 126455.

Wang, J., Shi, L., Zhai, L., Zhang, H., Wang, S., Zou, J., Shen, Z., Lian, C., & Chen, Y. (2021). Analysis of the long-term effectiveness of biochar immobilization remediation on heavy metal contaminated soil and the potential environmental factors weakening the remediation effect: A review. *Ecotoxicology and Environmental Safety*, *207*, 111261.

Wang, X., Zhang, J., Chang, V. W. C., She, Q., & Tang, C. Y. (2018). Removal of cytostatic drugs from wastewater by an anaerobic osmotic membrane bioreactor. *Chemical Engineering Journal*, *339*, 153–161.

Yip, W. H., Joe, L. S., Mustapha, W. A. W., Maskat, M. Y., & Said, M. (2014). Characterisation and stability of pigments extracted from Sargassum binderi obtained from Semporna, Sabah. *Sains Malaysiana*, *43*(9), 1345–1354.

Yuan, Y., & Macquarrie, D. J. (2015). Microwave assisted step-by-step process for the production of fucoidan, alginate sodium, sugars and biochar from Ascophyllum nodosum through a biorefinery concept. *Bioresource Technology*, *198*, 819–827.

Book Chapter 1: Valorization of brown algae biomass and by-products

Book: Bioresources and bioprocess in biotechnology for a sustainable future

Editorial: Taylor and Francis Group (CRC Press)

ISBN (online): 9781003410041

https://doi.org/10.1201/9781003410041

https://www.taylorfrancis.com/chapters/edit/10.1201/9781003410041-3/valorization-brown-algae-biomass-products-l%C3%A1zaro-gonz%C3%A1lez-fern%C3%A1ndez-nahum-andr%C3%A9s-medell%C3%ADn-castillo-amado-enrique-navarro-fr%C3%B3meta-candy-carranza-%C3%A1lvarez-rogelio-flores-ram%C3%ADrez-paola-elizabeth-d%C3%ADaz-flores-leonardo-sep%C3%BAlveda-torre-nancy-ver%C3%B3nica-p%C3%A9rez-aguilar

Valorization of brown algae biomass and by-products

Lázaro A. González Fernández[1], Nahum Andrés Medellín Castillo[2], Amado Enrique Navarro Frómeta[3], Candy Carranza Álvarez[4], Rogelio Flores Ramírez[5], Paola Elizabeth Díaz Flores[6] and Leonardo Sepúlveda Torres[7]

[1]*Multidisciplinary Postgraduate Program in Environmental Sciences, Autonomous University of San Luis Potosí, Av. Manuel Nava 201, 2o. piso, Zona Universitaria, 78000, San Luis Potosí, S.L.P., México.*

[2]*Postgraduate studies and research center, School of Engineering, Autonomous University of San Luis Potosí, Av. Dr. Manuel Nava #8, Edificio P, Zona Universitaria, 78290, San Luis Potosí, S.L.P., México.*

[3]*Technological University of Izúcar of Matamoros, Prolongación Reforma 168, Santiago Mihuacán, 74420 Izúcar de Matamoros, Pue., México.*

[4]*School of Professional Studies Huasteca Zone ,Romualdo del Campo 501 Fracc. Rafael Curiel, 79060, Cd Valles, S.L.P., México.*

[5]*Coordination for the Innovation and Application of Science and Technology, Av. Sierra Leona #550, Col. Lomas 2a. Sección, 78210, San Luis Potosí, S.L.P., México.*

[6]*School of Agronomy and Veterinary Medicine, Carretera San Luis Potosí - Matehuala Km. 14.5, Ejido Palma de la Cruz, 78321, Soledad de Graciano Sánchez, S.L.P., México.*

[7]*School of Chemical Sciences, Blvd. V. Carranza s/n. Col. República Oriente C.P.25280 Saltillo, Coah. México.*

**Corresponding author:* nahum.medellin@uaslp.mx

1. Introduction

Although the term algae is used generically to refer to aquatic plants and gives the impression of defining a homogeneous group of plants, the truth is that it comprises the most varied, complex, and plastic group (morphologically, biochemically, and physiologically) of the Vegetal kingdom. The macroalgae and seagrass beds have been used for centuries as green manure (or semi-composted) in almost all coastal agricultural areas and, above all, island areas, where they assure that their use exempts them from practicing crop rotation. In some North Sea islands, they have even formed the basis of the existence of agriculture since the agricultural land has been (and continues) manufacturing man mixing sand and silt with the arriving macroalgae (Zuli & Shouyu, 2019).

Despite being a relatively unknown group, algae offer many possibilities in terms of their use. Perhaps the best known is the one they have as food, and although this culture is not extended, in some countries, especially on the Asian coast, they are a daily ingredient in their dishes. They

have also been used as fertilizers, and in many coastal towns, it is possible to see people collecting algae to give them this use. With the arrival of new technologies, they have become used industrially as a source of chemical products, or in the production of shampoos or creams, while the food industry has incorporated them into everyday foods such as custards and ice cream or jams. Its use also covers the field of medicine, in which, since ancient times, they have been used to combat diseases and all kinds of illnesses (Baghel et al., 2020).

Marine algae are innocuous species with an inorganic content rich in calcium, magnesium, sodium, and potassium, which are identified in cellular processes. Consequently, algae-based biosorbents can be accepted when applied to water cleaning or wastewater treatment.

In coastal regions, seaweeds are fundamental primary producers, and several species are being considered as raw material for their diversity of products of economic importance, which has resulted in an increase in their demand. Therefore, it is necessary to monitor the bioaccumulation of certain xenobiotics in them because, for example, there are some that are used for direct or indirect human consumption or for livestock consumption (Hashemian et al., 2019).

2. Brown algae and food products

There is scientific evidence showing that incorporating seaweed and/or seaweed isolates in food matrices can positively affect the nutritional, organoleptic, textural, healthy, and even improved preservation characteristics of foods and beverages. Seaweeds that are consumed directly can belong to several groups of algae. Among them, the most important are red algae (*Rhodophyta*, Fig. 1a), brown algae (*Phaeophyta*), and green algae (*Chlorophyta*). All of them live in very diverse environments with extreme changes in salinity, temperature, lighting, and nutrients, with an extraordinary ability to adapt (Stevenson, 2014).

a) b) c)

Figure 1. The most important algae groups: a) red algae, b) brown algae, and c) green algae.

Specifically, brown algae are a rich source of iodine. This is an aspect of great interest due to the recent importance of iodine deficiency in European population groups. In addition, they have interesting antioxidant, antimicrobial and anti-inflammatory properties that can affect lowering cholesterol and blood pressure or help with digestion and weight control. Despite its multiple advantages, seaweed also poses some limitations at a nutritional level, so food technologists must work on advances that allow overcoming the current obstacles for its incorporation as a valuable ingredient in more fortified foods and healthy (Küpper & Carrano, 2019).

For example, the iodine content of raw brown seaweed may be too high for daily intake. In addition, they have a high salt content, which limits the amounts that can be incorporated into food products and dishes. It should also be noted that depending on the location of the algae culture, they can also accumulate certain heavy metals. Another important aspect to consider in the application of algae as an ingredient in food is the bioavailability of its proteins or other nutrients present in its composition. This bioavailability is closely related to its structural properties and the possible presence of antinutrient compounds, thus limiting its absorption after ingestion (Blikra et al., 2022).

All these elements show the need for technological innovations in cultivation, processing, and subsequent technological adaptations to optimize this raw material as a feed ingredient. These innovations seek to improve the food safety, digestibility, nutritional value, and flavor of brown algae.

The incorporation of algae as an ingredient in foods favors their texture and palatability; improves its physical properties, performance in certain products, and enables the substitution of certain additives. Thus, proteins and fibers favor solubility, water retention capacity, emulsifying activity, foam stability, viscosity, and gelation (Palasí Mascarós, 2015).

For example, the functionality of algae in processed meat products, such as hamburgers, sausages, and meat emulsions, has multiple benefits from a technological point of view. Algae can influence pH due to acidic components such as fucoidans and alginic acid; in stability thanks to the antioxidants that retard the rancidity of these products; its high content of mineral salts allows to reduce the addition of salt and improve the properties of water retention in the food, in addition to reducing the percentage of saturated fats (Quitral et al., 2019). Its application in cereal-based products, such as bread, flour or pasta, is also notable, where it improves the interaction between starch granules and protein matrix (Ścieszka & Klewicka, 2019).

On the other hand, the use of algae in food has been more focused on incorporating its extracts, rich in certain components, into food for human consumption. The most obvious example is the *phycocolloids*, which are the structural component of the cell walls of algae. It is a set of polysaccharides that contribute to stabilizing emulsions, suspensions, and foams, in addition to controlling the growth of crystals (Jensen, 1993).

3. Brown algae as bioindicators

In aquatic ecosystems, pollution by organic or inorganic sources causes a series of physicochemical changes in the water, which affect the composition and distribution of communities (Ospina Alvarez & Peña, 2004). In aquatic organisms, the effects of being subjected to a toxic discharge occur over time from individual responses (biochemical and physiological) to population, community, and ecosystem responses; and the magnitude of the changes registered in the organisms depends on the duration of the disturbance of the initial conditions of the aquatic system, its intensity and nature (Pinilla, 2000).

In recent years, a large number of environmental agencies around the world use methods for evaluating water quality based on the use of biological communities (Barbour, 2001). The reasons for the use of living organisms to monitor water quality are mainly the low cost and ease of implementing this type of study, compared to expensive chemical or toxicity analyses.

Bioindicators constitute a large group of plant, fungal or animal species whose presence or status in a given ecosystem provides information on certain ecological characteristics of the ecosystem, or the possible environmental impact of some practices on it. These are mainly used for the evaluation of the environmental quality of ecosystems. All bioindicators must meet a series of requirements for their use, such as: dispersion and abundance in the territory, sedentary lifestyle and tolerating pollutants in concentrations similar to those of the contaminated ecosystem without lethal effects (Markert et al., 2003; Phillips, 1977; St-Cyr & Campbell, 1994, 2000).

Algae are frequently used as bioindicators of water quality, since they are easily sampled and indicate the presence of contaminants quite clearly, due to their sensitivity to changes in the characteristics of the environment they inhabit (Markert et al., 2003).

The most used are diatoms, which are part of the phytoplankton of both marine and freshwater environments. They show the trophic state of the environment according to its abundance (from ultraoligotrophic to hypereutrophic), as well as the mineralization of the water or its salinity. They are also very sensitive to water acidification and bioaccumulate a wide variety of contaminants. Being microorganisms, they detect short-term changes and present a rapid response to those changes (Piña Leyte-Vidal et al., 2019).

Macroalgae are also used as bioindicators, generally in the marine environment. Like diatoms, they bioaccumulate various pollutants, such as heavy metals or PAHs. This property means that species of the *Fucus*, *Ulva*, *Ascophyllum* or *Enteromorpha* genera are used as sentinel organisms against certain pollutants. Being phototrophic organisms, their greater or lesser abundance can also indicate the transparency of the water in the environment (Russo et al., 2021).

In a work carried out by Méndez-Rodríguez et al., 2022 on the accumulation of metals in macroalgae, reported that Fe, Mn, and Zn were the most abundant elements in all species analyzed. Next came Cu, Ni, Co and Cd. However, the levels of most of the metals analyzed varied widely, depending on the collection sites and the particular species. Also, Haritonidis & Malea, 1999 carried out a study on the bioaccumulation of metals in the macroalgae Ulva rigida in the Thermaikos Gulf (Greece). The temporal and spatial trend of contamination provided by the results on the detected concentrations of metals in macroalgae may not correspond to that evaluated in other bioindicator species such as molluscs and barnacles.

4. Heavy metals biosorption with brown algae biomass

The great diversity of marine algae allows it to increase its selectivity and efficiency. Different adsorption capacities and selectivity have been discovered by red, green, and brown algae against various heavy metals (Murphy et al., 2007). The chemical composition and presence of different adsorption centres (fucanoids, alginates, phosphated proteins, etc.) (Rojas et al., 2005) allow greater adsorption of certain metals due to their size, degree of solvation, presence of chelating ions, molecular sieves, ion exchange with species present in the algae, etc. (de la Rocha et al., 2009; Rojas et al., 2005).

The mechanisms by which heavy metals are fixed in brown algae have been studied by Crist et al., 1992 and Ragan, 1986. These state that they incorporate these metals in high concentrations through polyanionic polysaccharides present in the cell wall and by the affinity between metals and polyphenols. Finally, the high content of alginates (Fig. 2) in seaweeds (compared to the other functional groups identified as adsorption centres) makes them ideal models to identify the biosorption mechanism, specially to investigate metal-algae interactions at the molecular level.

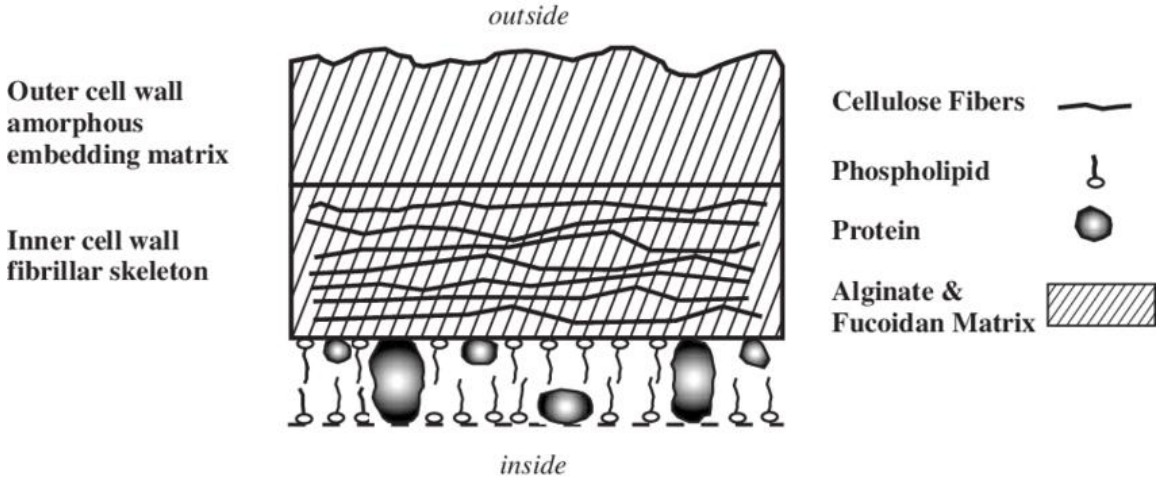

Figure 2. Cell wall structure in brown algae. After Schiewer & Volesky, 2000.

The existence of a single functional group responsible for the adsorption of heavy metals allows its mechanism to be clearly elucidated by means of different techniques, such as the determination of the ionization constant (Navarro, 2006) of algae, ionic strength effect, desorption of adsorbed metals by chelating species and acids, ion exchange, infrared spectroscopy, scanning electron microscopy, etc. Marine algae are perhaps the only adsorbents whose adsorption capacity

is due exclusively to alginates in more than 90 % (Cuizano et al., 2007; Davis et al., 2003; González et al., 2011; Lodeiro et al., 2004; Tapia et al., 2011).

Marine algae are innocuous species with an inorganic content rich in calcium, magnesium, sodium, and potassium, which are identified in cellular processes. Consequently, algae-based biosorbents can be accepted when applied to water cleaning or wastewater treatment.

Marine algae are a promising biosorbent of heavy metals and various pollutants and, due to their intrinsic characteristics, have received increasing attention in recent decades. Unfortunately, despite its recent development, biosorption is reduced to discontinuous processes at the laboratory level. The biosorption mechanism is being elucidated, but the type of metal ion-adsorbent interaction and its factors are unknown. Likewise, the optimal conditions reached are not completely adjusted to the conditions of conventional wastewater (ionic strength, interfering ions, detergents, acidity, organic content, etc.).

Algae arouse superior interest in developing new biosorbent materials, not only because of their adsorption capacity, but also because they are present in abundant quantities and are easily accessible in seas and oceans. Still, there are only a few publications on biosorption using algae in relation to the investigations using other biomaterials; moreover, there are a few regarding multimetallic systems and dynamical systems. According to the literature, brown algae have a higher metal adsorption capacity than red and green algae (Brinza et al., 2007)**.**

In the near future, many aspects should be considered regarding the adsorption mechanism, such as studying it more intensively using various techniques and combinations of them, as well as the factors that influence the equilibrium state such as pH, temperature, and the role that the co-ion (anion) plays in the biosorption process.

Better mathematical models of equilibrium and kinetics are also required that are adapted to real conditions, including parameters that conventional models neglect. This could be strengthened by a better application of biosorption technology, such as improving the physical-chemical conditions with pH and ionic content similar to those of real wastewater, and finally analyzing the possibility of recovering the heavy metal after being removed from the wastewater. solution and adsorbed on the biosorbent.

Even though the biosorption of heavy metals by marine algae has been extensively studied during the last decades, there are still many unanswered questions and aspects to be determined for its complete optimization, but what can be sure is that the use of marine algae is one of the best ecological weapons we have for the decontamination of our planet.

Algae bind only the free metal ions, through two physical-chemical processes. The first process is rapid and reversible and involves adsorption of the metal ion on the outer surface of the cell wall. This process can be ionic or by complex formation with cell wall ligands. The polymers that make up the cell wall are rich in carboxylic, phosphoryl, hydroxyl, and aromatic groups that can bind cations or produce organic complexes that can influence metal absorption. The second mechanism of metal incorporation is slower, it is regulated by cellular metabolism and metals are stored in the cytoplasm in vacuoles rich in polyphenols (Garnham et al., 1992).

As a product of this accumulation, the algae can reach trace element contents several orders of magnitude higher than in the water. Another version of how heavy metals are bound to algae was studied by Crist et al., 1988 and Ragan, 1986, who state that these metals are incorporated in large concentrations through polyanionic polysaccharides present in the cell wall, and by affinity between metals and polyphenols (Fig.3).

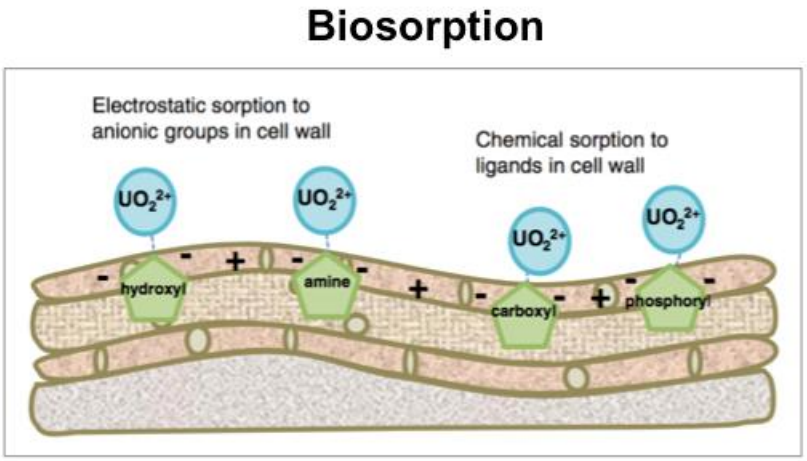

Figure 3. Mechanisms by which contaminants bind to adsorbents during the biosorption process.

5. Algal bio-oil

The great dependence on energy and the high pollution generated by fossil fuels has led us to promote the development of renewable energy sources with a low environmental impact. This is

how biofuels are presented as a great alternative to fossil fuels, since fuels such as biodiesel, biogas, and bioethanol can be produced from biomass (Singh et al., 2022).

One of the alternatives that have attracted much interest in recent decades is the use of algae biomass to produce bioethanol. Algae have high concentrations of carbohydrates in the form of polysaccharides (sugar polymers), which are released after fragmentation using enzymes and can be fermented to bioethanol (Maity & Mallick, 2022).

Algae can be processed differently to obtain a broad spectrum of products. For some time now, its use as an alternative to current biomass raw materials for the generation of biofuels has been gaining increasing interest among the scientific community, business people, and the general public. In fact, algae are recognized as a potential source for biodiesel production due to their high oil content and rapid growth. However, this is not the only application (Yaashikaa et al., 2022).

Biofuel extraction technology is relatively simple. It includes a first pressing stage with which approximately 70 % of the oil is extracted and a second stage with an organic solvent reaches up to 99 %, although the latter makes the process more expensive (Brar et al., 2022). Given the high viscosity that the original virgin oil reaches, it can be used directly in diesel engines once they have been adapted to operate with this highly viscous fuel. The triglycerides that make up vegetable oils can also be transformed into monoesters and glycerine by means of the trans-esterification reaction with methanol. The molecules that make up the biodiesel resulting from this last process have a lower molecular weight, and its viscosity is substantially lower, so it can be used as fuel in compression engines. Obviously, the biodiesel obtained by either of the two routes does not contain sulphur, is not toxic, and is easily biodegradable (Deshpande et al., 2022).

6. Brown algae as fertilizers

The use of algae as a fertilizer dates back to the 19th century, when the inhabitants of the coasts collected the large brown algae dragged by the tide and contributed them to their land. At the beginning of the 20th century, a small industry based on the drying and grinding of algae developed but was weakened by the arrival of synthetic chemical fertilizers (Farnham et al., 2019).

Brown algae and its derivatives improve the soil and invigorate the plants, increasing the yields and quality of the crops, so as this practice spreads, it will replace the use of synthetic chemical products with organic ones, thus favouring a sustainable agriculture. Algae have better

properties than fertilizers because they release nitrogen more slowly, and they are also rich in microelements and do not generate adventitious seeds (Islek, 2022).

Thanks to its high fibre content, macro and micronutrients, amino acids, vitamins, and plant phytohormones, algae act as a soil conditioner and contribute to moisture retention. In addition, due to their mineral content, they are a useful fertilizer and a source of trace elements (Davis et al., 2003).

Algae such as *Ascophyllum nodosum* (Fig. 4a.), *Fucus serratus* (Fig. 4b.), *Sargassum spp.* (Fig. 4c. and 4d.), and *Laminaria* (Fig. 4e.) are used to cultivate potatoes, artichokes, citrus, orchids, and grasses. *Corallines* (Fig. 2f.), a calcified red algae has a high carbonate content, and are used as well as soil conditioners, to correct the pH in acid soils. Brown algae are also capable of activating the immune system of the crops, generating higher production of higher quality and more resistant to diseases and environmental stress (Baroud et al., 2021).

a)

b)

c)

d)

e)

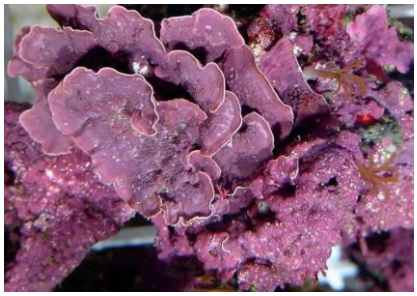

f)

7. Bibliography

Baghel, R. S., Suthar, P., Gajaria, T. K., Bhattacharya, S., Anil, A., & Reddy, C. R. K. (2020). Seaweed biorefinery: A sustainable process for valorising the biomass of brown seaweed. *Journal of Cleaner Production*, *263*, 121359.

Barbour, M. T. (2001). Rapid Bioassessment Protocols for Use in Steams and Wadeable Rivers: Periphyton. *Benthic Macroinvertebrates and Fish*.

Baroud, S., Tahrouch, S., El Mehrach, K., Sadki, I., Fahmi, F., & Hatimi, A. (2021). Effect of brown algae on germination, growth and biochemical composition of tomato leaves (Solanum lycopersicum). *Journal of the Saudi Society of Agricultural Sciences*, *20*(5), 337–343.

Blikra, M. J., Henjum, S., & Aakre, I. (2022). Iodine from brown algae in human nutrition, with an emphasis on bioaccessibility, bioavailability, chemistry, and effects of processing: A systematic review. *Comprehensive Reviews in Food Science and Food Safety*, *21*(2), 1517–1536.

Brar, P. K., Örmeci, B., & Dhir, A. (2022). Algae: A cohesive tool for biodiesel production alongwith wastewater treatment. *Sustainable Chemistry and Pharmacy*, *28*, 100730.

Brinza, L., Dring, M. J., & Gavrilescu, M. (2007). MARINE MICRO AND MACRO ALGAL SPECIES AS BIOSORBENTS FOR HEAVY METALS. *Environmental Engineering & Management Journal (EEMJ)*, *6*(3).

Crist, R. H., Oberholser, K., McGarrity, J., Crist, D. R., Johnson, J. K., & Brittsan, J. M. (1992). Interaction of metals and protons with algae. 3. Marine algae, with emphasis on lead and aluminum. *Environmental Science & Technology*, *26*(3), 496–502.

Crist, R. H., Oberholser, K., Schwartz, D., Marzoff, J., Ryder, D., & Crist, D. R. (1988). Interactions of metals and protons with algae. *Environmental Science & Technology*, *22*(7), 755–760.

Cuizano, N. A., Llanos, B. P., Chang, L., & Navarro, A. E. (2007). Equilibrio ácido-base de algas marinas del litoral peruano elucida su alta afinidad por contaminantes ambientales. *Revista de La Sociedad Química Del Perú*, *73*(2), 85–93.

Davis, T. A., Volesky, B., & Mucci, A. (2003). A review of the biochemistry of heavy metal

biosorption by brown algae. *Water Research*, *37*(18), 4311–4330.

de la Rocha, S. R., Sánchez-Muniz, F. J., Gómez-Juaristi, M., & Marín, M. T. L. (2009). Trace elements determination in edible seaweeds by an optimized and validated ICP-MS method. *Journal of Food Composition and Analysis*, *22*(4), 330–336.

Deshpande, G., Shrikhande, S., Patle, D. S., & Sawarkar, A. N. (2022). Simultaneous optimization of economic, environmental, and safety criteria for algal biodiesel process retrofitted using dividing wall column and multistage vapor recompression. *Process Safety and Environmental Protection*.

Farnham, W., Murfin, C., Critchley, A., & Morrell, S. (2019). Distribution and control of the brown alga Sargassum muticum. *International Seaweed Symposium (Xth)*, 277–282.

Garnham, G. W., Codd, G. A., & Gadd, G. M. (1992). Kinetics of uptake and intracellular location of cobalt, manganese and zinc in the estuarine green alga Chlorella salina. *Applied Microbiology and Biotechnology*, *37*(2), 270–276.

González, F., Romera, E., Ballester, A., Blázquez, M. L., Muñoz, J. Á., & García-Balboa, C. (2011). Algal biosorption and biosorbents. In *Microbial biosorption of metals* (pp. 159–178). Springer.

Haritonidis, S., & Malea, P. (1999). Bioaccumulation of metals by the green alga Ulva rigida from Thermaikos Gulf, Greece. *Environmental Pollution*, *104*(3), 365–372.

Hashemian, M., Ahmadzadeh, H., Hosseini, M., Lyon, S., & Pourianfar, H. R. (2019). Production of microalgae-derived high-protein biomass to enhance food for animal feedstock and human consumption. In *Advanced bioprocessing for alternative fuels, biobased chemicals, and bioproducts* (pp. 393–405). Elsevier.

ISLEK, C. (2022). GREEN FERTILIZER AND ALGAL BIOFERTILIZER. *Introduction and Application of Organic Fertilizers as Protectors of Our Environment*, 182.

Jensen, A. (1993). Present and future needs for algae and algal products. *Fourteenth International Seaweed Symposium*, 15–23.

Küpper, F. C., & Carrano, C. J. (2019). Key aspects of the iodine metabolism in brown algae: a brief critical review. *Metallomics*, *11*(4), 756–764.

Lodeiro, P., Cordero, B., Grille, Z., Herrero, R., & Sastre de Vicente, M. E. (2004). Physicochemical studies of cadmium (II) biosorption by the invasive alga in Europe, Sargassum muticum. *Biotechnology and Bioengineering*, *88*(2), 237–247.

Maity, S., & Mallick, N. (2022). Trends and advances in sustainable bioethanol production by marine microalgae: A critical review. *Journal of Cleaner Production*, 131153.

Markert, B. A., Breure, A. M., & Zechmeister, H. G. (2003). Definitions, strategies and principles for bioindication/biomonitoring of the environment. In *Trace Metals and other Contaminants in the Environment* (Vol. 6, pp. 3–39). Elsevier.

Méndez-Rodríguez, L., Piñón-Gimate, A., Casas-Valdez, M., Cervantes-Duarte, R., & Arreola-Lizárraga, J. A. (2022). Macroalgae from two coastal lagoons of the Gulf of California as indicators of heavy metal contamination by anthropogenic activities. *Journal of the Marine Biological Association of the United Kingdom*, 1–13.

Murphy, V., Hughes, H., & McLoughlin, P. (2007). Cu (II) binding by dried biomass of red, green and brown macroalgae. *Water Research*, *41*(4), 731–740.

Navarro, A. E. (2006). Propiedades ácido-básicas de Lentinus edodes y cinética de biosorción de Cadmio (II). *Revista Latinoamericana de Recursos Naturales*, *2*(2), 47–54.

Ospina Alvarez, N., & Peña, E. J. (2004). Alternativas de monitoreo de calidad de aguas: algas como bioindicadores. *Acta Nova*, *2*(4), 513–517.

Palasí Mascarós, J. T. (2015). *Caracterización físico-química y nutricional de algas en polvo empleadas como ingrediente alimentario*. Universitat Politècnica de València.

Phillips, D. J. H. (1977). The use of biological indicator organisms to monitor trace metal pollution in marine and estuarine environments—a review. *Environmental Pollution (1970)*, *13*(4), 281–317.

Piña Leyte-Vidal, J. J., González-Fernández, L. A., Gutiérrez-Artiles, O., Márquez-Llauger, L., & Del Cristo, T. A. (2019). Caracterización de tres bioindicadores de contaminación por metales pesados. *Revista Cubana de Química*, *31*(2), 293–308.

Pinilla, G. (2000). Indicadores biológicos en ecosistemas acuáticos continentales de Colombia. *Bogotá: Universidad Jorge Tadeo Lozano*.

Quitral, V., Jofré, M. J., Rojas, N., Romero, N., & Valdés, I. (2019). Algas marinas como ingrediente funcional en productos cárnicos. *Revista Chilena de Nutrición*, *46*(2), 181–189.

Ragan, M. A. (1986). Phlorotannins, brown algal polyphenols. *Progress in Phycological Research*, *4*, 177–241.

Rojas, G., Silva, J., Flores, J. A., Rodriguez, A., Ly, M., & Maldonado, H. (2005). Adsorption of chromium onto cross-linked chitosan. *Separation and Purification Technology*, *44*(1), 31–36.

Russo, D., Salinas-Ramos, V. B., Cistrone, L., Smeraldo, S., Bosso, L., & Ancillotto, L. (2021). Do We Need to Use Bats as Bioindicators? *Biology*, *10*(8), 693.

Schiewer, S., & Volesky, B. (2000). Biosorption by marine algae. In *Bioremediation* (pp. 139–169). Springer.

Ścieszka, S., & Klewicka, E. (2019). Algae in food: A general review. *Critical Reviews in Food Science and Nutrition*, *59*(21), 3538–3547.

Singh, A., Prajapati, P., Vyas, S., Gaur, V. K., Sindhu, R., Binod, P., Kumar, V., Singhania, R. R., Awasthi, M. K., & Zhang, Z. (2022). A comprehensive review of feedstocks as sustainable substrates for next-generation biofuels. *BioEnergy Research*, 1–18.

St-Cyr, L., & Campbell, P. G. C. (1994). Trace metals in submerged plants of the St. Lawrence River. *Canadian Journal of Botany*, *72*(4), 429–439.

St-Cyr, L., & Campbell, P. G. C. (2000). Bioavailability of sediment-bound metals for Vallisneria americana Michx, a submerged aquatic plant, in the St. Lawrence River. *Canadian Journal of Fisheries and Aquatic Sciences*, *57*(7), 1330–1341.

Stevenson, J. (2014). Ecological assessments with algae: a review and synthesis. *Journal of Phycology*, *50*(3), 437–461.

Tapia, P., Santander, M., Pavez, O., Valderrama, L., Guzman, D., & Romero, L. (2011). Bio sorption of copper ions with biomass of algae and dehydrated waste of olives. *Revista de Metalurgia*, *47*(1), 15–28.

Yaashikaa, P. R., Devi, M. K., Kumar, P. S., & Pandian, E. (2022). A review on biodiesel paroduction by algal biomass: Outlook on lifecycle assessment and techno-economic analysis. *Fuel*, *324*, 124774.

Zuli, W. U., & Shouyu, Z. (2019). Effect of Typhoon on the Distribution of Macroalgae in the Seaweed Beds of Gouqi Island, Zhejiang Province. *Journal of Agricultural Science and Technology*, *21*(9), 159.

Book Chapter 2: Heavy metal pollution in water: Cause and remediation strategies

Book: Current Status of Marine Water Microbiology

Editorial: Springer Nature Singapore

ISBN (online): 978-981-99-5022-5

ISBN (print): 978-981-99-5021-8

https://doi.org/10.1007/978-981-99-5022-5_10

https://link.springer.com/chapter/10.1007/978-981-99-5022-5_10

Heavy metal pollution in water: Cause and remediation strategies

Lázaro Adrián González-Fernández[1], Nahum Andrés Medellín-Castillo[1,2], Amado Enrique Navarro Frómeta[3], Candy Carranza-Álvarez[4], Ventura Castillo-Ramos[5], Manuel Sánchez-Polo[5], Javier E. Vilasó-Cadre[6], Paola Elizabeth Díaz-Flores[2,7], Lourdes Morales-Oyervides[8], Nancy Verónica Pérez-Aguilar[8], René Loredo-Portales[9]*

[1]*Multidisciplinary Postgraduate Program in Environmental Sciences. Av. Manuel Nava 201, 2nd. floor, University Zone, 78000, San Luis Potosí, S.L.P., Mexico.*

[2]*Center for Research and Postgraduate Studies of the School of Engineering. Dr. Manuel Nava No. 8, West University Zone, 78290, San Luis Potosí, S.L.P., Mexico.*

[3]*Technological University of Izúcar de Matamoros. De Reforma 168, Campestre la Paz, 74420, Izúcar de Matamoros, Pue., Mexico.*

[4]*School of Professional Studies Huasteca Zone. Romualdo del Campo 501, Rafael Curiel, 79060, Ciudad Valles, S.L.P, Mexico.*

[5]*Department of Inorganic Chemistry, School of Science, University of Granada, 18071, Granada, Spain.*

[6]*Institute of Metallurgy. Sierra Leona #550, Lomas 2a sección, 78350, San Luis Potosí, S. L. P., Mexico.*

[7]*School of Agronomy and Veterinary Medicine. Carretera San Luis Potosí - Matehuala Km. 14.5 Ejido Palma de la Cruz, 78321, Soledad de Graciano Sánchez, S.L.P., Mexico.*

[8]*School of Chemical Sciences, Autonomous University of Cohauila, Blvd. V. Carranza s/n, República Oriente, 25280, Saltillo, Coah., Mexico.*

[9]*Department of Environmental Sciences, Division of Life Sciences, Ex Hacienda El Copal km 9, Carretera Irapuato-Silao, 36500, Irapuato, Gto., Mexico.*

**Corresponding author:* nahum.medellin@uaslp.mx

Abstract

Contamination by heavy metals and metalloids in water resources, soil, and air is one of the most severe problems that compromise food and water safety and public health globally and locally. Water naturally contains heavy metals; however, its increase, although sometimes also determined by natural enrichment when passing through aquifers containing rocks with a high concentration of this material, is mostly linked to human activity, such as mining and industry, which generates waste such as lead, mercury, cadmium, arsenic, and chromium, which reach rivers and contaminate groundwater. The danger of heavy metals is greater since they are not chemically or biologically degradable. Once emitted, they can remain in the environment for hundreds of years. In addition, its concentration in living beings increases as they are ingested by others, so the ingestion of

contaminated plants or animals can cause symptoms of poisoning. Today we know a great variety of methods and techniques that can be used for the removal of heavy metals from water, each of which shows advantages and disadvantages that must be analyzed. The search for new materials and alternatives for the disinfection of water contaminated with heavy metals, as well as the optimization of those that we know today, is a permanent task for the scientific community.

Keywords: Heavy metals; water; contamination; remediation.

1. Water pollution

Water is essential in supporting human life and preserving biological diversity on earth. Water quality is vital as water sources are used for various purposes: domestic use, industrial activities, agricultural irrigation, and other economic activities. However, the problem of water contamination by heavy metals has greatly affected water quality due to rapid urbanization, population increase, and deficient water treatment systems.

Water pollution and its increasing scarcity mean that more and more people in different parts of the world have poor access to water, directly affecting their health and way of life. Therefore, it is essential to understand the causes and consequences of water pollution (Van der Perk, 2014).

Humans and their intervention in nature are the main ones responsible for water pollution. Only 3 % of the planet's water is freshwater (water that can be drunk) and, although there are drinking water purification mechanisms, such as desalination, which help water consumption, the first and most urgent thing to do is to avoid its contamination (Chaudhry & Malik, 2017).

The World Health Organization (WHO) defines contaminated water as "water whose composition has been modified so that it does not meet the conditions for the use that will allow it to reach its natural state". Oceans, rivers, canals, lakes, and reservoirs are all at the mercy of pollution (Moss, 2008).

No form of life can survive without clean water, from humans to animals, plants, and organisms. In short, without clean water, there is no life. But how does water become polluted? The leading causes of water pollution are:

- The dumping of industrial waste and garbage in rivers, canals, and seas. Above all, from companies that dump large quantities of polluting products derived from their industrial

processes. Hydrocarbons, wastewater, detergents, plastics, and other solid waste end up in rivers and seas, where, in addition to their environmental impact, many of them end up being ingested by animals or small marine organisms (Dwivedi, 2017).

- Rising temperatures. Global warming also causes the alteration of water by reducing oxygen in its composition (Chaudhry & Malik, 2017).
- Agrochemicals. Fertilizers and pesticides, generally used by food companies, are absorbed by the soil, filtered by subway channels, and affect the water, and the surrounding plants and can also reach drinking water reservoirs (Khanna & Gupta, 2018).

Water pollution has devastating effects on protecting the environment and the planet's health. Some of the most important consequences of the different types of water pollution are the destruction of biodiversity, contamination of the food chain involving toxic transmission to food, and shortages of drinking water (Inyinbor Adejumoke et al., 2018).

According to UN data, 2 million tons of sewage flow daily into the world's waters. The most important source of pollution is the lack of adequate management and treatment of human, industrial and agricultural waste. Freshwater animals are becoming extinct five times faster than land animals (Azevedo-Santos et al., 2021; Schwarzenbach et al., 2010).

If the mechanism of constant pollution in which we live is not stopped or changed, by 2050, there could be more plastics in the ocean than fish. Recycling, minimizing waste generation, consuming less, and caring for and valuing water consumption seems to be the only possible solutions to a problem for which we are all responsible.

2. Heavy metals

Contamination by heavy metals and metalloids in water resources, soil, and the air is one of the most severe problems that compromise food and water safety and public health globally and locally. Heavy metal is usually defined as a chemical element with metallic properties and high density, although some consider that it is necessary to refer to the atomic number or weight or to some of its chemical or toxicity properties to differentiate it from other metals (Malik et al., 2019).

Some heavy materials such as iron, cobalt, copper, manganese, molybdenum, and zinc are beneficial and necessary for species such as humans in small quantities. Metals such as mercury, lead or chromium can become harmful in large concentrations or after transformations, as they

increase in toxicity and bioaccumulation potential since they accumulate in the body and are not eliminated either by feces, urine, or sweat. For example, mercury is more toxic in the form of methylmercury or dimethylmercury, and Cr(VI) is highly dangerous; instead Cr(III) is an essential nutrient for humans (L. Yang et al., 2020).

Water naturally contains heavy metals, its increase, may be due to natural enrichment when passing through aquifers containing rocks with a high concentration of this material or linked to human activity, such as mining and industry, which generates waste such as lead, mercury, cadmium, arsenic, and chromium, which reach rivers and contaminate groundwater (Bolisetty et al., 2019).

Industrial and mining activity releases toxic metals into the environment, which are very harmful to human health and almost all life forms. In addition, metals from anthropogenic emission sources, including the combustion of leaded gasoline, are found in the atmosphere as suspended material that we breathe (Rai et al., 2019).

For example, mercury, zinc, lead, copper, cadmium, chromium, and nickel are used in paint in the textile and printing industry and for electroplating metals, as well as for processing paper in the paper industry and as an additive in the fur industry, and arsenic is also used as an additive in the plastics industry (Briffa et al., 2020). Table 1 Describes the main sources of heavy metals and their effect on human health.

Heavy metals are more dangerous since they are not chemically or biologically degradable. Once emitted, they can remain in the environment for hundreds of years. In addition, its concentration in living beings increases as others ingest them, so ingesting contaminated plants or animals can cause poisoning symptoms.

Table 1. Origin of pollution and health effects of some heavy metals.

Heavy metal	Source of pollution	Health Effects	Maximum concentration level in the water (mg L^{-1})		
			WHO	FAO	USA
Arsenic (As)	Mining of ores, arsenical pesticides, fossil fuels burning	Hyperkeratosis, cancer, brain damage, dizziness, and fatigue	10	100	10
Cadmium (Cd)	Fertilizers, electroplating, battery manufacturing metal-plating, rayon industries, mining	Lung and kidney damage, cancer, cardiovascular diseases	3	10	5

Copper (Cu)	Metal-plating, rayon industries, mining	Normocytic anemia, bone frailness, gastrointestinal disturbances	2000	200	1300
Chromium (Cr)	Leather industries, dye production, electroplating	Skin irritation, dermatitis, kidney and liver damage, hair loss	50	100	100
Lead (Pb)	Textile industries, automotive sector, petroleum refining	Nervous system damage, brain damage, fatigue	10	5000	15
Mercury (Hg)	Pesticides, batteries, paper industry	Arthritis, circulatory and nervous system damage, kidney damage.	6	-	2
Nickell (Ni)	Alloy industries, pigment manufacturing sector, tannery industry wastewater	Asthma, dermatitis, cancer, and respiratory failure	70	200	-

3. Bibliometric analysis

Bibliometric indicators are instruments for measuring scientific productions and make it possible to analyse the impact caused by scientific work. They are statistical data deduced from scientific publications. Their use is based on the important role of publications in disseminating new knowledge, a role assumed at all levels of the scientific process. With these indicators, it is possible to determine the growth of any scientific area by considering the number of published works, the collaboration of authors, research centres, the impact of communications, countries, institutions, the production of scientists, considering the number of citations received, among others.

The topic of water pollution by heavy metals has been the subject of research for many decades. Over time, the knowledge generated on the theme has evolved. Only in the last decade, a large number of works have been generated that contribute to its development. To carry out an analysis of the subject in this decade, a search was done on the Web of Science following the criterion that the sequence of words "Heavy metal pollution in water" appeared in the title or the abstract of the scientific publications.

The first result obtained reveals that 5388 scientific research papers have been published in WoS meeting the search requirements, which are distributed by years, as seen in Fig. 1. Since 2014 and up to 2021, the number of publications has steadily increased, which indicates that the interest of the international scientific community in this topic. So far in 2022, the number of publications is also high, and this shows that it is still novel and that there are still niches of opportunity for the generation of new knowledge.

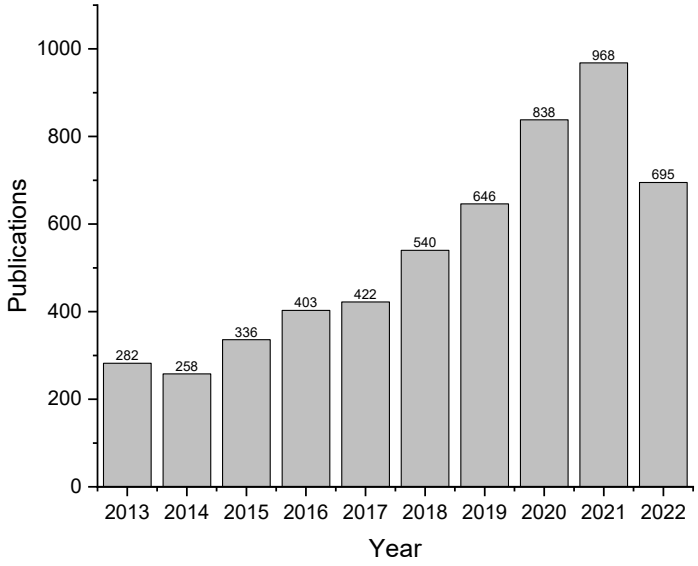

Figure 1. Distribution of publications by year (2013-2022).

The analysis of the documents requires a statistical analysis of their origin, i.e., the key journals in the field. These journals address the main trends in research on the subject under analysis. Table 2 shows the journals with the highest number of articles published in this field, representing 22.4 % of all the articles considered. The top three journals are Environmental Science and Pollution Research (285 articles, 5.3 %), Science of The Total Environment (166 articles, 3.1 %), and Environmental Monitoring and Assessment (138 articles, 2.6 %). In terms of impact factors, most of the selected journals have an impact factor above 3.0, indicating their dominant academic influence.

Table 2. Key journals for publications in the field of heavy metal water pollution.

Order	Journals	Articles	%
1	Environmental Science and Pollution Research	285	**5.3**
2	Science of the Total Environment	166	**3.1**
3	Environmental Monitoring and Assessment	138	**2.6**
4	Chemosphere	120	**2.2**
5	Water	92	**1.7**
6	Environmental Earth Sciences	85	**1.6**
7	Desalination and Water Treatment	84	**1.6**
8	International Journal of Environmental Research and Public Health	84	**1.6**
9	Environmental Pollution	81	**1.5**
10	Fresenius Environmental Bulletin	73	**1.3**

Among the compiled information, the authors with the most publications are ordered from highest to lowest in Table 3. It can be seen that the author who has published the most papers on

water pollution by heavy metals is Liu Y with 42, followed by Li Y and Zhang Y with 37 each, and Li J and Wang Y with 33 each.

Table 3. Order of authors with the highest number of publications.

Order	Author	Publications
1	Liu Y.	42
2	Li Y.	37
3	Zhang Y.	37
4	Li J.	33
5	Wang Y.	33
6	Kumar A.	30
7	Wang J.	29
8	Kumar V.	26
9	Li H.	25
10	Wang L.	25

The 5388 research papers developed in this decade are distributed according to the different research areas as shown in Fig. 2. Approximately 50% of the publications have been developed in the area of Environmental Sciences and Ecology (ESE), followed in order by Engineering, Water Resources (WR) and Chemistry.

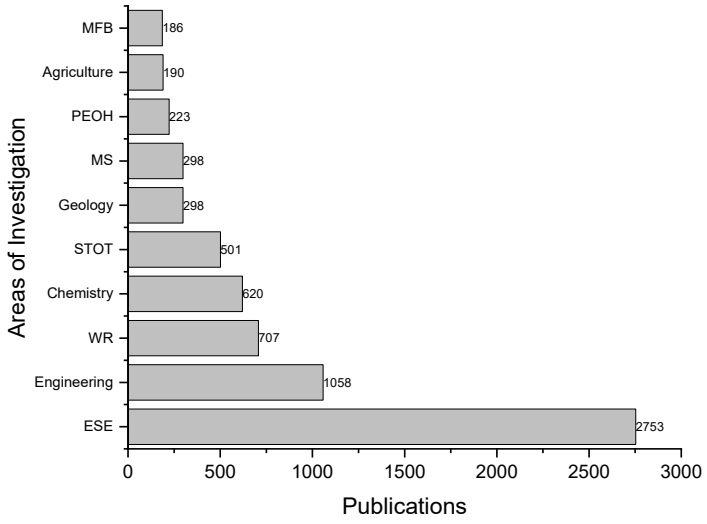

Figure 2. Number of publications by area of knowledge.

According to the WoS categories, publications are mainly grouped around Environmental Sciences, as shown in Fig. 3. This category accounts for about 50% of the works that have been developed. It is followed by Water Resources (WR), Environmental Engineering (EE), and Chemical Engineering (CE).

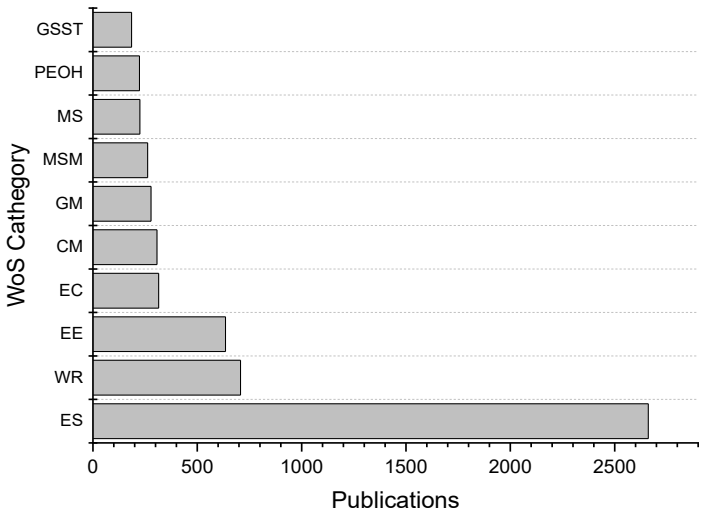

Figure 3. Publications according to Web of Science categories.

The Asia-Pacific and Middle East region dominates the list of the ten countries that have published the most on this topic, as shown in Fig. 4a. The list (Fig. 4b) is headed by the People's Republic of China, which accounts for about 44% of all publications in the last decade, followed by India with 17% and the United States of America with 7%.

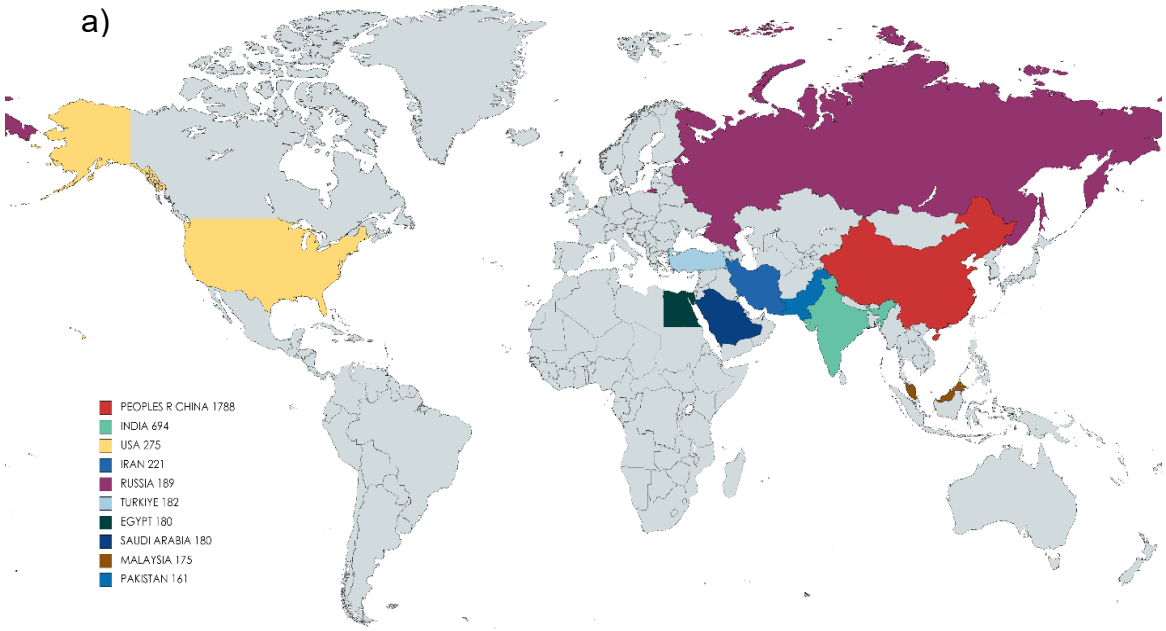

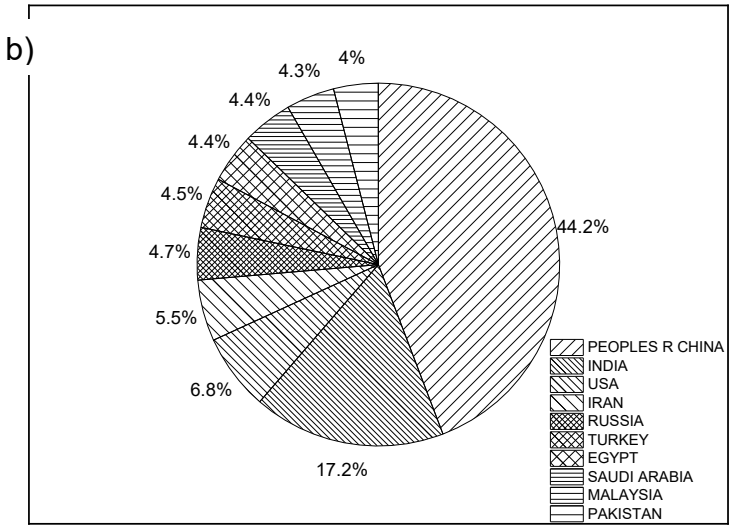

Figure 4. Distribution by country of publications on water pollution by heavy metals.

Table 4 shows the 10 articles with the highest citations in the last decade. "A review on the adsorption of heavy metals by clay minerals, with special focus on the past decade" by author Mohammad Kashif Uddin published in Chemical Engineering Journal in 2017, tops the list with 990 citations.

Table 4. Research papers with the highest number of citations.

Title	Source Title	Publication Year	Total Citations
A review on the adsorption of heavy metals by clay minerals, with special focus on the past decade	Chemical Engineering Journal	2017	990
Adsorption of heavy metals on conventional and nanostructured materials for wastewater treatment purposes: A review	Ecotoxicology And Environmental Safety	2018	764
A comparative review of biochar and hydrochar in terms of production, physico-chemical properties and applications	Renewable & Sustainable Energy Reviews	2015	739
Heavy metal pollution in surface water and sediment: A preliminary assessment of an urban river in a developing country	Ecological Indicators	2015	727
Efficient techniques for the removal of toxic heavy metals from aquatic environment: A review	Journal Of Environmental Chemical Engineering	2017	691
Adsorption of divalent metal ions from aqueous solutions using graphene oxide	Dalton Transactions	2013	592
Impacts of soil and water pollution on food safety and health risks in China	Environment International	2015	575
A review on modification methods to cellulose-based adsorbents to improve adsorption capacity	Water Research	2016	565
Sustainable technologies for water purification from heavy metals: review and analysis	Chemical Society Reviews	2019	552
Metal-organic frameworks for heavy metal removal from water	Coordination Chemistry Reviews	2018	512

4. Remediation

4.1 Precipitation

Precipitation is the most common method for removing toxic heavy metals down to parts per million levels in water, because some metal salts are insoluble in water and precipitate when the appropriate anion is added (Charerntanyarak, 1999). Although the process is cost-effective, its efficiency is affected by low pH values and the presence of other salts (ions). The process requires the addition of other chemicals, which eventually leads to the generation of a high-water content sludge, which is costly to dispose of.

Before selecting a chemical precipitation system for metal separation, several factors should be considered, including the demonstrated ability of the system to meet discharge limits, the capital expenditure required, the cost of operation and maintenance, the amount of pollutant and hydraulic quantity presently permitted, and those proposed for the future, the frequency, volume and characteristics of discharges, and the water conservation and recovery potential (BrbootI et al., 2011).

Chemical precipitation is most often carried out using sodium hydroxide, sulfate compounds (alum or ferric sulfate), or sulfides (sodium sulfide or iron sulfide) (Bhattacharyya et al., 1979). The addition of these compounds to metal-bearing wastewater forms metal hydroxides or metal sulfides, respectively, and the water solubility is limited. Precipitation is ineffective when the metal is in deficient concentrations since an excess of a precipitating agent is needed to form a precipitate. In many cases, the solid formed is not stable enough to separate from the solution. To overcome these difficulties, a co-precipitation treatment is often used, which consists of adding iron hydroxide to the precipitating agent to form a precipitate. It consists of adding iron or aluminum hydroxide with the precipitating agent to act as a coagulant or to adsorb the metals that have not precipitated (L. K. Wang et al., 2005).

Hydroxide precipitation accompanied by coagulation-flocculation is widely used to reduce the concentration of metals such as lead, zinc, copper, and iron in wastewater. The precipitation process is highly dependent on the pH of the solution. When the pH ranges from 8.0 to 11.0, the removal can be greater than 99 % for most heavy metals (Pang et al., 2009). Although this value is high, it is only achieved when the starting concentrations of the metals are in the order of parts

per million and decreases drastically when working at lower concentration orders (Vardhan et al., 2019). Additionally, large amounts of solids are formed (Pohl, 2020).

The use of sulfide-containing or sulfide-derived compounds is characterized by lower solubility than when metal hydroxides are used, which allows higher percentages of metal ion removal to be achieved using shorter times. However, this process generates metal sulfides of very low solubility, is very sensitive to the added concentration of the precipitating agent, and can generate hydrogen sulfide as a by-product, which has toxic effects on animals, humans, and the environment (M. Kumar et al., 2021). All these limitations make it necessary to search for novel precipitating agents such as potassium/sodium thiocarbonate and 2,4,6-trimercaptothiazine (Pohl, 2020).

In addition, organic anions have been used to precipitate heavy metals in effluents from the mining and metallurgical industries. Such is the case of 1,3-benzenediamidoethanethiol dianion, which was developed to selectively and irreversibly bind soft heavy metals from an aqueous solution. The results for metals such as iron show that their concentration may be reduced from 194 ppm to 0.009 ppm with this dianion at pH 4.5 (Matlock et al., 2002).

4.2 Electrochemical methods

Electrochemical methods have been widely used for the removal of metals from pollutants in water. They present important advantages such as high separation efficiency; generally, no toxic substances are used, so they are safe and environmentally friendly. They are selective and controlled methods, and, under optimal electrochemical cell design, they are economical methods (Muddemann et al., 2019).

Fig. 5 shows the main electrochemical methods for treating metals in water and their electrochemical basis. Most of them involve the electrolysis process, either directly or indirectly.

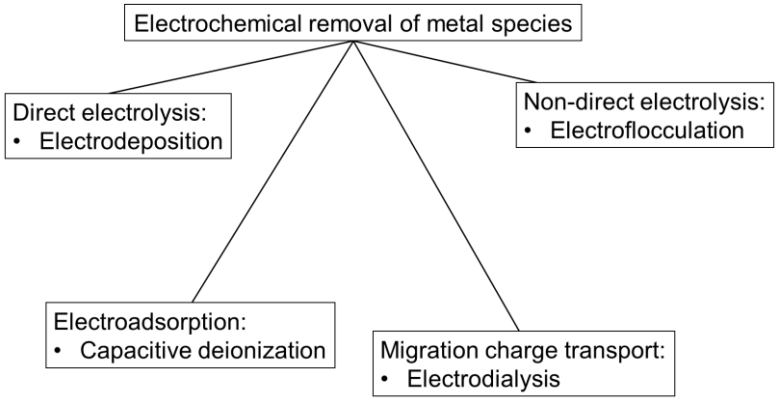

Figure 5. Electrochemical methods for the removal of metals from water.

Electrodeposition is a direct electrolysis that involves the reduction of ions to the metallic state or an insoluble compound so that a solid deposition on the cathode occurs (Paunovic & Schlesinger, 2006). In an electrodeposition process, many parameters must be controlled to achieve optimal results, for example, the material, shape, and position of the electrodes, voltage, current density, agitation, and the type of reactor (Carpanedo de Morais Nepel et al., 2020).

The electrodeposition process can be carried out at constant potential (potentiostatic) or constant current density (galvanostatic) (Tatiparti & Ebrahimi, 2012; Vincent et al., 2020). Cathodes of the same electrodeposited metal, as well as inert stainless-steel electrodes have been used (Kuleyin & Uysal, 2020). Advanced materials such as carbon nanotubes and graphene composites or graphene oxide electrodes have also been introduced (Stando et al., 2021). This method has been used for the removal of copper, cadmium, chromium, lead, uranium, zinc, antimony, nickel, and gold from wastewater (Carpanedo de Morais Nepel et al., 2020; Gu et al., 2020; Kuleyin & Uysal, 2020; T; Vincent et al., 2020; W. Wang et al., 2020; C. Wang et al., 2021; Wu et al., 2022).

Some treatment methods use electrolysis to separate the metal ions without their direct participation in the charge transfer reaction at the electrode. Electroflocculation is one of the most commonly used (Fig. 6). It consists of generating a metal hydroxide by taking advantage of the anodic oxidation of a sacrificial electrode, usually aluminum or iron, and the reduction reaction of water that generates OH- ions.

These hydroxides are colloidal, and in a first stage, destabilization and coagulation occurs, i.e., the aggregation of particles; these aggregates end up agglomerating and forming flocs, which

adsorb the contaminating metal ions on their surface. The flocs formed can be collected at the bottom of the tank when they sediment, or they can be floated on gas bubbles generated by the electrolysis of water or an auxiliary electrolyte. This separation of gas bubbles is known as electroflotation.

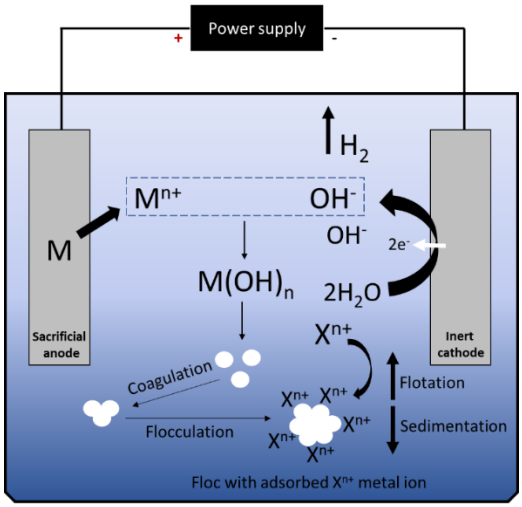

Figure 6. Schematic of an electrochemical cell for removing X^{n+} metal cations by electroflocculation.

Capacitive deionization consists of the electroadsorption of ions by passing through a cell containing two porous electrodes polarized by a potential difference (Fig. 7). This method has been widely used for water desalination and removal of pollutant ions. The electric field between the electrodes causes the migration of anions towards the positive electrode and cations towards the negative electrode, establishing an electrical double layer in the pores of the material that stores the ions. This double layer behaves as a capacitor, allowing energy storage and recovery when the electrodes are depolarized (Shocron et al., 2022).

The main advantages of this technology are its high efficiency, the regeneration of the electrodes, and the recovery of part of the energy supplied (I. Cohen et al., 2013). The electrode material is of special importance since there must be a high porosity with sufficient size to adsorb the ions. Charcoal has been widely used; however, the development of new advanced materials with better textural and electrical properties can be an important improvement to the efficiency of this method because, for example, the more charge an electrode can store, the more effective the deionization process is (Zhao et al., 2020). In some cells, ion exchange membranes are used to

increase the number of ions retained inside the electrodes, which significantly improves the deionization results (L. Wang & Lin, 2019).

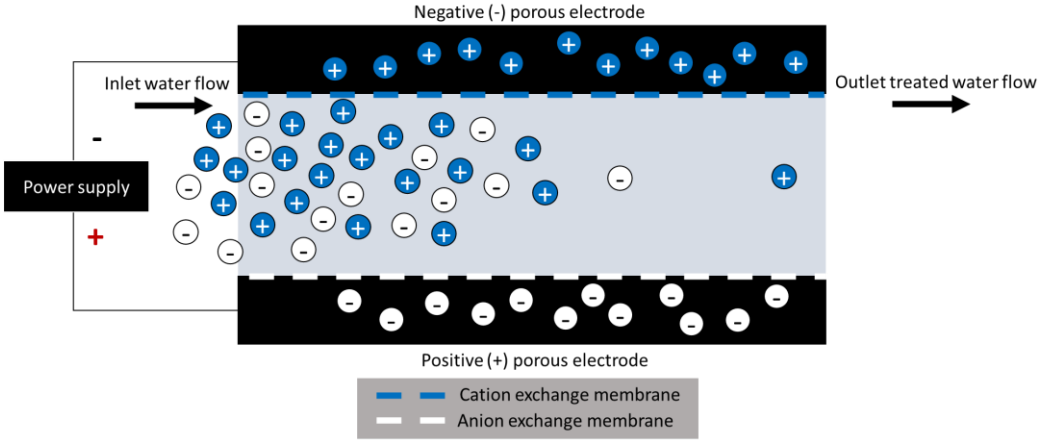

Figure 7. Schematic of a capacitive deionization cell to remove cations and anions in solution.

Different designs of capacitive deionization cells differ fundamentally in the use or not of ion exchange membranes, in the direction of the solution flow concerning the electric field between the electrodes, and in the type of electrodes. Some cells can combine capacitive and faradaic mechanisms (Tang et al., 2019). Flow electrode cells have recently appeared, where the anode and cathode are suspended particles (C. Zhang et al., 2021).

Capacitive deionization cells can operate at constant voltage and current (L. Wang & Lin, 2018). The regeneration of the active sites of the electrodes can be done at an open circuit or by reverse polarization of the electrodes. The latter regenerates more active sites, increasing the capacity for a new deionization cycle. In the treatment of metal contaminants, capacitive deionization has been used primarily for the removal of arsenic, cadmium, chromium, copper, iron, lead, uranium, vanadium, zinc, iron, calcium, magnesium, and sodium (Chen et al., 2020; Kalfa et al., 2020).

Finally, electrodialysis consists of establishing a potential difference between two electrodes between which there are anion and cation exchange membranes (Fig. 8). The electric field causes the migration of the charged species towards the oppositely charged electrode and the selective membranes prevent the diffusion of the counterions. Electrodialysis technologies use cells with several anion and cation exchange membranes placed alternately, significantly improving separation (Ladole et al., 2021).

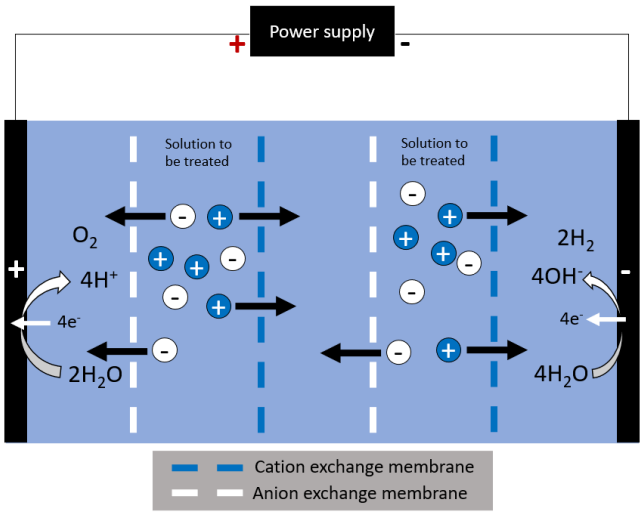

Figure 8. Schematic of the electrodialysis process for removing cations and anions in solution.

Water oxidation and reduction reactions usually occur at the cathode and anode, and when the concentration of chlorides is sufficient, their oxidation also occurs. These electrolysis reactions generate ions that maintain electrical neutrality. Electrolytes are commonly introduced into the anode and cathode half-cells (Hutten, 2016).

4.3 Membrane-based methods

Heavy metals removal from water by membrane technology has been widely employed in practical applications and research since ultrafiltration (Bhattacharyya et al., 1978) and reverse osmosis (Sato et al., 1977) membranes were first demonstrated in the 1970s for the removal of Cu(II), Ni(II) and Zn(II). The separation of metal ions by membrane technologies is primarily based on size exclusion, Donna mechanism (charge repulsion), and adsorption capabilities of the membranes themselves. A membrane acts as a barrier, preventing certain compounds from passing through (Abdullah et al., 2019).

Usually, membrane performance is measured in terms of selectivity and flux rate (flow per unit area per unit of time). Permeate is the purified stream and retentate is the rejected stream (Ruhal & Choudhury, 2012). Membranes can be classified according to their pore size, nature, and working principle. Several types of membranes are widely used in research, including microfiltration and ultrafiltration membranes (MF and UF), nanofiltration membranes (NF), reverse osmosis membranes (RO), liquid and supported liquid membranes (LM and SLM), as well as electrodialysis (ED).

4.4 Micro and ultra-filtration membranes

Due to their large pore sizes (0.1 – 10 um), microfiltration is non-viable for heavy metal ions removal in water. In the case of ultrafiltration (0.01 – 0.1 um), pores are still too large to be effective in rejecting metal ions. However, extensive work and research have been conducted on UF processes to make it a viable option in removing heavy metals.

There are two main ways to make UF processes workable: first, by manipulating the water matrix where the metal pollutants are present, increasing their size with complexation or micelle agents and thus being size excluded by the UF membrane (Huang & Feng, 2019; Tortora et al., 2016; Xiang et al., 2022). Second, by manipulating the UF membrane´s properties themselves, cladding functional groups or adsorbents to improve their rejection performances. This second option is derived from fabricating a subclass of UF membranes, called Mixed Matrix Membranes (Algieri et al., 2021; Mungray et al., 2012).

When talking about Mixed Matrix Membranes based on embedding adsorptive species in the membrane, their performance is only based on the nature of these species and the operational conditions (Abdullah et al., 2019). Wang et al. (R. Wang et al., 2013) prepared a membrane by electrospinning with a very high charge density and large surface area based on polyacrylonitrile (PAN)/polyethylene terephthalate functionalized with cellulose nanofibers capable of removing bacteria and viruses by size extrusion and simultaneously adsorbing up to 100 mg and 260 mg of Cr(VI) and Pb(II), respectively, with a permeation rate of 1300 L $m^{-2}h^{-1}psi^{-1}$. By the application of a two-nozzle approach, electrospun PVA/PAN nanofibers were applied by Liu et al. (Liu et al., 2020) for the removal of Cr(VI) and Cd(II) ions.

PAN fibers were modified by surface grafting and hydrolysis by crosslinking methods boosting their separation performances. Chelating action plus electrostatic interactions with metal ions were removal pathways achieved by a ring-opening reaction of the epoxy group with iminodiacetic acid, forming the functional PDF-g-PGMA/IDAA membrane. It can reach 100% rejection in heavy metal ions following Pb^{2+} > Cu^{2+}> Cd^{2+}. Ceramic microfilters were functionalized by Kim et al. (J.-H. Kim et al., 2021) with Mg being able to remove a wide range of heavy metals, including Fe, Cu, Ni, Zn, Cr, Pb, and As through precipitation, separation, and sorption. Life spam of the filter was considerably improved due to the fouling reduction after its functionalization with Mg.

4.5 Nanofiltration membranes

Nanofiltration membranes have a pore size of 1 – 10 nm (Gao et al., 2014). Their transmembrane pressure (4.0 – 10.0 bar) is, therefore, lower than reverse osmosis membranes but higher than ultrafiltration membranes. Nanofiltration has become a widely used commercial process due to its pore size and loose selective thin film structure, favorable for metal ions exclusion in water. Most commercial nanomembranes are fabricated of aliphatic amine monomers, such as piperazine, having a negatively charged surface because of carboxylic and sulfonic species on the polyamide surface (Abdullah et al., 2019).

By grafting 0.6 %wt. Ethylenediamine carbon nanotubes on a polyether sulfone, a composite nanomembrane positively charged, was fabricated by Peydayesh et al. (Peydayesh et al., 2020) with excellent heavy metals rejection following the order Zn (96.7 %) > Mg (95.01 %) > Cd (92.4 %) > Cu (91.9 %) > Ca (91.3 %) > Ni (90.7 %) > Pb (90.5 %), due to Donnan exclusion mechanism. Another positively charged aliphatic polyamide nanomembrane synthesized by direct polymerization of polyethyleneimine on a polyether sulfone support was developed by Li et al. (P. Li et al., 2022). It was able to effectively reject Mn (98.78 %) > Zn (98.32 %) > Ni (97.74 %) > Cu (95.67 %) > Cd (90.49 %) at concentrations of 1000 ppm.

Also, grafting polyethyleneimine to a nanomembrane using 2-chloro-1-methyl iodopyridine as an active agent derived in a film able to separate toxic heavy metals ($CuCl_2$ 96 %, $NiCl_2$ 95.8 %, $CrCl_3$ 98.0 %), as well as dyes and divalent/monovalent salts (Qi et al., 2019). By surface coating and crosslinking method with glutaraldehyde, Ye et al. (Ye et al., 2019) were able to cast polyelectrolyte complex nanoparticles with ammonium groups to develop novel complex nanomembranes effectively charged, providing a strong repulsion to metal cations, reaching up to 95% of Mg, Cu, and Zn rejection.

Al-Rashdi et al., 2013 studied the effect of pH on the retention performance of a commercial nanomembrane (NF270). They found that rejection improves when the pH is below the isoelectric point, indicating that the Donnan exclusion mechanism played a key role. At a concentration of 1000 ppm and pH = 1.5 and 4 bar, rejections of 99 %, 89 %, and 74 % for Cd, Mn, and Pb, respectively were found.

4.6 Reverse osmosis membranes

Compared to NF membranes, RO membranes are denser and have a pore size ranging from 0.1 to 1.0 nm. In terms of efficiency, it is one of the best alternatives for contaminants removal as it mostly allows water to pass through (Chon et al., 2014; Dialynas & Diamadopoulos, 2009; Harharah et al., 2022; B. Verma et al., 2021). Its working principle is based on osmosis but works in the direction of water moving from high concentrated phase to low concentrated by applying an external pressure (Abdullah et al., 2019) (Fig. 9). More than 98 % of Cu, Cr, and Ni removal was achieved by a commercial low-pressure RO membrane (ULPROM/ES 20) at metal concentrations of 10 mg L^{-1} (Ozaki et al., 2002).

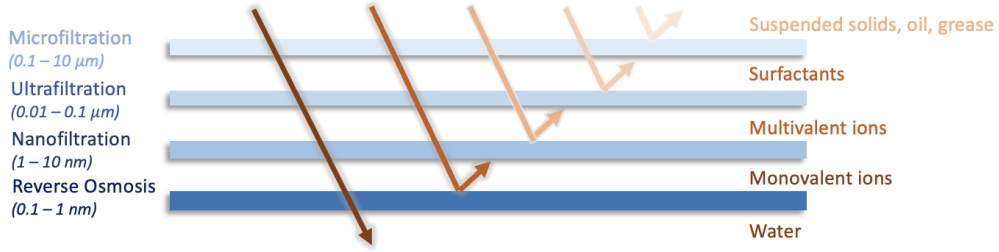

Figure 9. Schematic representation of several filtration processes and rejected contaminants.

A combination between UF and RO was applied by Petrinic et al., 2015a to remove suspended contaminants such as metal elements and organic/inorganic compounds, reaching 91.3 % – 99.8 % of removal efficiencies. Similar studies highlight the necessity of combining RO with other membrane filtration processes, as the study reported by Ricci et al., 2015, where a system comprised of sequential MF, UF, and RO units was implemented to recover noble metals above 95 %.

Ni(II) was completely removed by merging UF and RO units (Petrinic et al., 2015b), playing the pH a key role in the removal efficiency. Mnif et al., 2017 achieved a Cr(VI) rejection of 99.9 % at a pH = 8, whilst if the pH dropped to 3, the efficiencies decreased to 91 % (Çimen, 2015).

Considering the operating pressures (20-30 bar) and energy needed (≈ 2.5 kWh m^{-3}) for RO processes (Aumesquet-Carreto et al., 2022), a prevailing need to combine RO with other filtration units arises to increase its feasibility and applications in heavy metals removal from water (Chung et al., 2014).

4.7 Supported liquid membranes

Liquid membranes are formed by a layer of immiscible liquid being the barrier to the feed solution contaminated with heavy metals (Abdullah et al., 2019). There are several types of liquid membranes described in the literature. The most widely used in heavy metal removal are polymer inclusion membranes (Zulkefeli et al., 2018) and supported liquid membranes (Yesil & Tugtas, 2019). Emulsion liquid membranes (Ahmad et al., 2011) are found to be unstable for practical applications and bulk liquid membranes (S. H. Chang, 2016) do not have enough surface area for the current application.

An emerging class of supported liquid membranes is supported ionic liquid membranes (Abdullah et al., 2019). Ionic liquids offer the advantages of versatility and easy tunability of their physicochemical properties through a proper selection of the anion-cation pairs that conform to them (Ramos, Han, Zhang, et al., 2020). A plethora of different anion-cation combinations can be done (around 10^8) (Ramos, Han, & Yeung, 2020), offering a vast research area to be studied in removing heavy metals from water bodies.

Common supports for ionic liquids are polypropylene, polyvinyl chloride, polyethylene terephthalate, among other polymeric materials. In contrast, the most used ionic liquids are imidazolium and phosphonium based cations such as trihexyltetradecyl phosphonium chloride (Regel-Rosocka et al., 2015) and [OMIM][BF4] (Abebe et al., 2017) that work as supported liquid membranes for effective remediation (> 85 %) of heavy metals as Zn, Pb, Cd and As (Imdad & Dohare, 2022).

A recent work developed by Zheng et al. (Zheng et al., 2022) demonstrates the viability of supported liquid membranes for heavy metals removal. They grafted the ionic liquid 1-vinyl-3-butyl imidazolium tetrafluoroborate on polyether sulfone by radiation and electrospinning processes, obtaining nanofibrous membranes able to adsorb up to 187.3 mg g^{-1} of Cd(II) with good recyclability over cycles, and also removing dyes and possessing antimicrobial properties.

4.8 Electrodialysis

Electrodialysis consists of several ion exchange membranes (anionic and cationic) stacked together under the action of an electric field, concentrating the electrolytes in a concentrated stream (Min et al., 2019) (Fig. 10). Cations can pass through the anionic membranes but are retained in the

cationic layers, in a similar way as anions with the cationic membranes. This process can generate hydrogen gas and oxygen/chlorine in the anode (Abdullah et al., 2019).

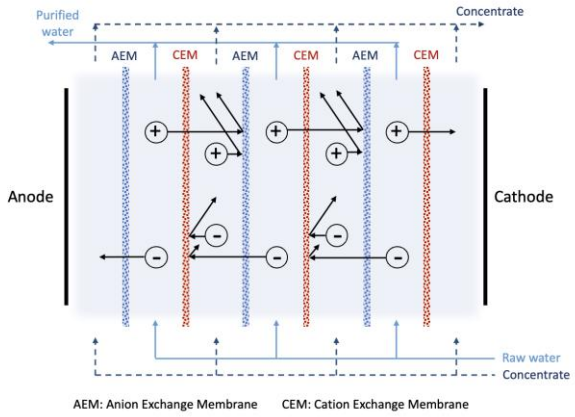

Figure 10. Scheme of electrodialysis working principle for heavy metals removal in water.

Compared to MF, UF, NF, and RO, electrodialysis reduces the use of chemicals and causes less secondary environmental pollution (Babilas & Dydo, 2018; Gurreri et al., 2020; Min et al., 2021a). In ED, operational parameters play an important role in heavy metal separation. The most determinant variables are the applied current and voltage, temperature, pH, and membrane properties (Juve et al., 2022). Increasing temperatures lead to higher removal efficiency of the ions, enhancing their mobility towards the concentrate (Benneker et al., 2018) but increasing energy costs and making the process less viable.

The surface charge of ED membranes and morphologies has an important impact on heavy metal separations. It can be enhanced by the presence of specific functional groups that alter the hydrophobic/hydrophilic properties of the membrane to increment selectivity (Irfan et al., 2019). Most ED membranes are based on a polymeric matrix with attached acid or quaternary ammonium groups (Juve et al., 2022; Ran et al., 2017).

The selection of appropriate membrane technology for removing heavy metals from water bodies requires consideration of several factors. Other pollutants present in water may affect the efficiency of the membrane. For instance, when adsorptive membranes reach their saturation point, they must be regenerated, a process that may not be feasible for practical use. For heavy metals removal to be viable, membrane technologies with energy implications, such as RO and ED, must be optimized. Additionally, it is important to carefully select the chemicals introduced into water

bodies (complexation/micelle agents) and consider their impact on the environment. It is also necessary to consider the generation of byproducts of remediation as a determinant parameter in selecting a membrane technology.

Table 5 summarizes the advantages and disadvantages of each membrane technology covered in this section.

Table 5. Summary of membrane processes for heavy metals removal

Membrane process	Advantages	Disadvantages	Refs.
Ultrafiltration	Cost-effective and low transmembrane pressures. Effective for macro- metal ions.	Generation of byproducts. High maintenance costs and fouling risks.	(Xiang et al., 2022)
Nanofiltration	Better metal ions rejection compared to UF and lower operational costs.	Lower water permeation and high energy consumption compared to UF. Fouling control.	(Xiang et al., 2022)
Reverse Osmosis	Performance in heavy metal rejection. Easy operation and no added chemicals needed.	Energy requirements and water permeability. Membrane fouling and durability.	(Imdad & Dohare, 2022)
Supported Liquid Membranes	Low cost and high efficiency. Good stability and selectivity. High water permeability.	Risk of leakage. Need of regeneration after saturation point. High material costs.	(Imdad & Dohare, 2022)
Electrodialysis	Excellent metal separation and reusability.	High energy and operational costs. Membrane clogging due to macromolecules. Fouling.	(Imdad & Dohare, 2022)

4.9 Phytoremediation and microbiological interactions

Phytoremediation is a green technology also called agroremediation, botanoremediation, or green remediation; it is a sustainable and green approach to remediate soil (Alonso-Bravo et al., 2018), water (Viramontes-Acosta et al., 2020) and even air (Ortiz-Cáceres, 2020). This technique successfully uses cosmopolitan plant species that can remove and store organic and inorganic contaminants in high concentrations in their roots and plant tissues (Ashraf et al., 2019).

Several technologies are available to remediate soils contaminated by heavy metals. However, physicochemicals are more expensive (e.g., excavation of contaminants, material, and chemical/physical treatment) or fail to achieve a long-term solution or aesthetics. For this reason, phytoremediation can provide a cost-effective, simple, feasible, durable, aesthetically pleasing, and publicly accepted solution for the remediation of contaminated sites.

Implementing phytoremediation is straightforward because it does not require expert personnel or expensive high-quality equipment. Phytoremediation is a decontamination process that is mediated by plants, and their biomass. It includes a wide variety of plants such as grasses,

shrubs, and trees that, in symbiosis with microorganisms, favor the restoration of the environment (soil, water, and air), through the degradation, accumulation, and stabilization of pollutants. Phytoremediation is considered a green technology with the potential to reduce the generation of secondary waste and remove contaminants (organic pollutants, heavy metals, etc.) from the soil (Shah & Daverey, 2020).

Phytoremediation plants must comply with the following characteristics (González-Gómez, 2010; González-Chávez, 2017; López et al., 2004):

- The plant must be tolerant to high concentrations of heavy metals and carry out its development in the presence of this.
- Being an accumulator of heavy metals, remediation must be carried out since this is the important purpose of phytoremediation.
- It must have an immediate increase and high productivity rate since this enables good pollutant removal rates and optimizes phytoremediation processes. The plant must maintain its reproductive capacity in the presence of disturbances through succession.
- Plants must be easy to harvest.
- They must have stress resistance since it is fundamental that the plant can resist stress situations generated by chemical, physical, biological, or climatic conditions.
- Being local species, representative of the natural society, it is advisable to use native plants to alter the local ecosystem as little as possible.
- Among the main factors affecting phytoremediation are biomass, pH, microorganism, speciation, and chelators in the soil (Marrero-Coto et al., 2012).

4.9.1 Phytoremediation mechanisms

Plants can develop several mechanisms to remove contaminants (Fig. 11) from the rhizosphere to the aerial tissues, among which phytostabilization, which consists of stabilizing them in the rhizosphere, phytodegradation, which consists of changing the oxidation state of the elements to eliminate them at the root level, phytostimulation, which is assisted by microorganisms, phytodegradation, and phytovolatilization, which consist of removing the contaminants at the leaf level once the plants have transformed them, are the most important mechanisms to be able to apply phytoremediation as a decontamination technology.

However, the most important mechanism to apply phytoremediation as a decontamination technology is phytoextraction, which consists of extracting contaminants from the rhizosphere and transporting them to aerial tissues. Among the factors that affect this mechanism are biomass, temperature, pH, light, ion exchange capacity, cation exchange capacity, salinity, the type of element if it is organic or inorganic, as well as microorganisms since these can change the pH due to the substances they secrete, provide nutrients and phytohormones (X. Zhang et al., 2018).

The mechanisms of soil and water phytoremediation can be divided into four subsets, as described in Fig. 11. These soil and water toxic metal remediation technology are: 1) phytoextraction, also called phytoaccumulation, is the process that takes place in plants found in soil contaminated by heavy metals; 2) phytovolatilization, which is the evaporation of certain metals from the aerial tissues of plants; 3) phytostabilization, which is the use of plants to be able to remove the bioavailability of toxic metals in contaminated soils; and 5) phytostimulation, the use of plant roots to remove toxic metals (Kushwaha et al., 2015).

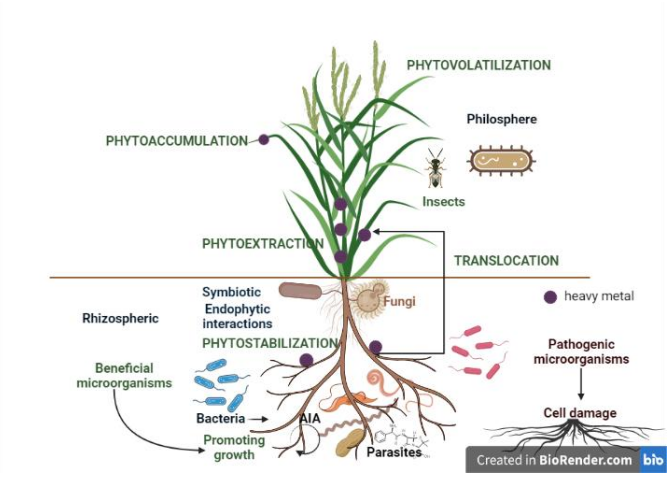

Figure 11. Phytoremediation mechanisms and biological interactions.

The biological changes that occur mainly in nature are called natural depletion and are assisted by plant-microorganism interaction. A phytoremediation plant executes any of the above mechanisms in three stages: absorption or uptake, excretion, and detoxification of pollutants. The uptake of contaminants is done through root tissue and leaves through the stomata and cuticle of the epidermis. This uptake happens in the rhizome dermis of the adolescent roots, which can uptake compounds by osmosis defined by external factors such as temperature and soil pH.

Other relevant components that influence the uptake of contaminants are their molecular weight and hydrophobicity, which determine that these molecules cross plant cell membranes. After crossing the membrane, contaminants are distributed throughout the plant. Contaminants absorbed by plant roots will be excreted by the leaves (phytovolatilization). Once the concentration of contaminants is high, only small fractions (less than 5 %) are removed without changing their chemical composition.

4.9.2 Interactions of plants with microorganisms

Phytoremediation plants can grow naturally in contaminated sites and tolerate high concentrations of heavy metals because they have developed mechanisms to do so or have achieved symbiosis with the microbiota of the environment in which they develop. Roots are the main tissue involved in the absorption of metals through association and interaction with soil microorganisms.

Among these associations are those established with bacteria and endophytic and/or mycorrhizal fungi (EMF), a symbiotic interaction between soil microorganisms and roots. These associations give plants stress resistance, improve plant biomass, their antioxidant system, and their potential to accumulate metals.

Therefore, the success of phytoremediation also depends on beneficial associations between microorganisms and plants (Vigliotta et al., 2016), because beneficial microorganisms promote the growth of roots and air tissues, but pathogenic microorganisms damage plant tissue (Fig. 12). Rajkumar et al., 2009 reported that inoculation of soils with *Psudomona aureginosa* significantly increased the bioavailability of Cr and Pb compared to uninoculated controls. In addition, they also observed that *P. aureginosa* significantly enhanced Cr and Pb accumulation in maize tissues.

Rajkumar et al., 2009 mentioned that in this case, the enhancement of heavy metal uptake may be due to the production of siderophores, particularly pyoverdine (dihydroquinoline type chromophore, with a peptide chain of 6-12 amino acids) and phytochelatins (cysteine-rich protein); Siderophore Production by Bacteria (SPB) resistant to metals may increase the efficiency of phytoextraction directly, improving the accumulation of metals in plant tissues.

Siderophore production by rhizospheric bacteria solubilizes unavailable forms of heavy metal-containing minerals through complexation. Plants can take up metals from the siderophore-

metal complex, possibly mediated by root processes, such as chelate degradation and metal release, direct uptake of the siderophore-metal complex, or by a ligand exchange reaction.

Recent studies with hyperaccumulator plants have revealed that inoculation of soils/seeds with metal-resistant endophytic bacteria enhances plant growth and accelerates the phytoremediation process naturally or artificially in metal-contaminated soils, improving nutrient acquisition, cell elongation, metal accumulation or stabilization, and metal stress relief in plants. Likewise, these microorganisms can passively activate or promote plant growth through various mechanisms such as nitrogen fixation, phosphate solubilization, siderophore production, phytohormones, and ACC deaminase (Ma et al., 2011).

Rolón-Cárdenas et al., 2021 obtained four bacterial isolates from the rhizosphere of *T. latifolia,* showing that they have biochemical activity for the promotion of seedling growth exposed to various concentrations of cadmium. The bacterial isolates characterized in this study are of the genus *Pseudomona*. In addition to exhibiting high tolerance to Cd, these bacteria probably present high tolerance to other heavy metals because the gene that confers tolerance to Cd also confers tolerance to other heavy metals. On the other hand, Ma et al., 2016 found that *Pseudomonas libanensis* TR1 and *Pseudomonas reactans* Ph3R3 are resistant to multiple metals such as Cd, Cr, Cu, Ni, Pb, and Zn.

In recent studies, the effect of *Pseudomonas* sp. on the promotion of plant growth of roots of *T. latifolia* plants tolerant to high concentrations of Cd (500-750 ppm) and Pb (5-50 ppm) was evaluated (Fig. 2), demonstrating that bacterial isolates (*Pseudomonas rhodesiae*) can increase up to 50 % Cd removal compared to plants without bacterial inoculation (Moctezuma Granados, 2017), as well as that *P. rhodesiae* increases Cd translocation to shoots (Rolón-Cárdenas et al., 2021). Recently, the effect of endophytic and/or mycorrhizal fungi (EMF) associated with *T. latifolia*, the interactions of this plant species with EMF, and the mechanisms of EMF in the promotion of plant growth and phytoextraction of heavy metals are being evaluated.

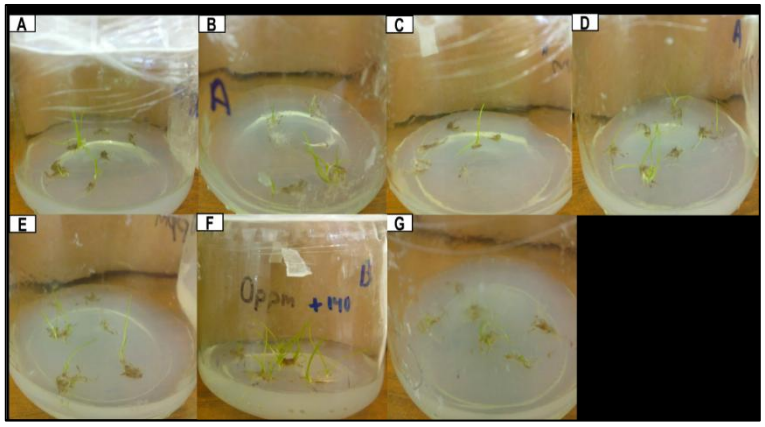

Figure 12. Growth stimulation assay of *T. latifolia in vitro* in the presence of lead. A) 0 ppm Pb; B) 5 ppm Pb; C) 10 ppm Pb; D) 25 ppm Pb; E) 50 ppm Pb; F) 25 ppm Pb plus GRC140; G) 50 ppm plus GRC140.

4.10 Treatment wetlands

Treatment wetlands (TW), also called artificial or constructed wetlands, are nature-based systems that can be used for the treatment of wastewater of very varied composition and are ideal for operation in small communities or socio-economic objectives and even for isolated users. Through physical, chemical, and biological processes, as well as their multiple combinations, they effectively remove many types of contaminants.

Microorganisms present in TW play an important role in the removal processes of different contaminants, including metals (J. Wang et al., 2022). Although domestic and municipal waters do not contain significant amounts of metals and metalloids such as boron, selenium, and arsenic (Březinová & Vymazal, 2015), industrial waters such as the metal-mechanical, mining, and textile industries, among others, have these pollutants in concentrations that represent a threat to human health and ecosystems, also considering that in many places these wastewaters are mixed in municipal drainage systems without any prior treatment.

Since conventional treatment systems and some advanced treatments generally imply higher costs in their installation, operation, and maintenance (Sylwan & Thorin, 2021), it is necessary, then, to evaluate the effectiveness of TW and the way to improve it since it is a green technology with collateral benefits for human communities and ecosystems, in the removal of toxic metals and metalloids, an aspect that has been recently reviewed (Nisa et al., 2022; S. Singh et al., 2022).

Toxic metals and metalloids are removed in TW through a combination of biotic and abiotic mechanisms, including filtration processes, sedimentation, precipitation and coprecipitation, sorption and ion exchange, biosorption, redox processes, including those mediated by microorganisms present in the system and phytoremediation processes carried out by the present macrophytes such as rhizofiltration, phytostabilization, phytoaccumulation and phytovolatilization (Yu et al., 2021).

Figure 13 schematically presents these processes. In general, the predominant role in the removal of metals is played by the processes that occur in the substrate and sediments, with the role of macrophytes being of less importance (Ventura et al., 2021). The greatest accumulation of metals is observed in sediments and by being confined in them, the possible toxic effect on aquatic biota is reduced, as has been demonstrated in the evaluation of the removal of Cu and other divalent metal ions in a wetland system for more than 20 years (Knox et al., 2021).

Although some of these elements are essential for the metabolic processes of macrophytes and microorganisms in treatment wetlands, their presence above certain levels can affect the biota of these systems and, consequently their removal. Likewise, the different species of macrophytes have different metal removal capacities, depending on the biomass ratio in their roots, stems, and leaves (Schück & Greger, 2020). This explains the different results reported in the literature when evaluating the removal percentages (Batool & Saleh, 2020).

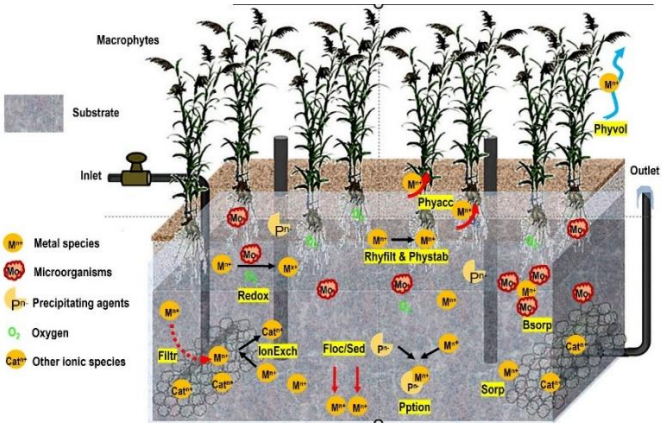

Figure 13. Abiotic and biotic removal processes in TW. Filtr – filtration; IonExch – ion exchange; Floc/Sed – flocculation/sedimentation; Pption – precipitation; Sorp – sorption; Bsorp – biosorption; Redox – oxidation/reduction processes; Rhyfilt & Phystab – rhyzofiltration and phytostabilization; Phyacc – phytoaccumulation; Phyvol – phytovolatilization.

Due to the above, more and more attention is currently paid to the processes of improved removal of metals and metalloids in treatment wetlands, which includes, among others, the use of substrates with properties that intensify physical processes such as ionic exchange or precipitation, a more careful selection of macrophytes, including polycultures, bioaugmentation with suitable microorganisms, the use of hybrid systems, the use of external additives and treatment intensification mechanisms such as artificial aeration and recirculation, among others (Yu et al., 2022).

Some examples of improved metal removal in treatment wetlands are illustrative of this. Regarding the selection of the substrate, the use of biochar and organic waste has shown to be effective, improving the removal of metals in mining waste, improving the binding capacity of the substrate, and intensifying the biotic removal mechanisms (G. Wang et al., 2023). In systems with intermittent aeration, filled with biochar, the volatilization and assimilation processes of Hg(II) by plants are increased, which contribute to better removal of this toxic metal (J. Chang et al., 2022).

Likewise, using zeolites combined with organic fillers is effective for removing Cu in the treatment of leachate from sanitary landfills (Wdowczyk et al., 2022). Inoculation with arbuscular mycorrhizal fungi and the use of aeration in vertical wetlands improve the removal of Pb, Zn, Cu, and Cd (Xu et al., 2022). The coupling of TW with microbial fuel cells, together with an adequate selection of the substrate and macrophyte has been shown to improve the removal of Zn and Ni in sludge (L. Wang et al., 2022).

4.11 Adsorption

For solutions with a high concentration of heavy metals, some of the technologies mentioned above can be used; however, when the concentrations are low (less than 100 mg L^{-1}), more economical and efficient methods (such as adsorption) are required (Volesky, 2003).

Adsorption is a separation process by which certain components of a fluid phase (liquid or gas) are transferred to a solid substrate, becoming physically or chemically bound on the surface of the adsorbent (Ruthven, 1984). Adsorption is an effective method of removal at low levels of metal ions. However, the economic viability of this process depends on an effective means of regenerating the solid once its adsorption capacity is exhausted (Suzuki & Suzuki, 1990).

The adsorbent is characterized by its high porosity, with extremely small pore sizes resulting in its internal surface area much larger than the external surface area. Differences in molecular weight or polarity cause some molecules to be retained more strongly than others, which makes the adsorption process selective (R. T. Yang, 2003).

Physical adsorption is caused mainly by Van der Waals and electrostatic forces, which occur between the molecules of the adsorbate and the atoms that make up the surface of the adsorbent. These adsorbents are mainly characterized by surface properties such as surface area and polarity. The ion is adsorbed by the solid depending on the relative charge between the two. This process can be slow or fast, depending on the composition of the adsorbent, the adsorbate, and the temperature (Bruch et al., 2007).

Chemical adsorption is due to forces of a chemical nature and is a process that depends on the temperature, the chemical nature of the solid, and the concentration of the species to be adsorbed (Webb, 2003). The two types of adsorption do not necessarily occur independently; thus, in natural systems, it is common for both to occur on the same solid surface (X. Wang et al., 2015).

Common materials that have been used for contaminant adsorption include activated carbon, silica gel, activated alumina, and graphene. These commercially available adsorbent materials are highly efficient for removing heavy metals thanks to their high specific area and abundant functional groups that are present on the surface and that allow the adsorption process to exist (Table 6).

Table 6. Most common adsorbents applied in adsorption remediation.

Adsorbent	Example/Raw materials	Advantages	Disadvantages
Activated Carbon	Wood, peat, coconut shells, coals	Pore size distribution, Surface chemistry, mineral matter content, chemical nature which can be easily modified, chemical treatment available, cost-effective technology	Commercial activated carbon is quite expensive Secondary pollution generated by spent activated carbons Rapid saturation High cost of reactivation
Polymeric materials	Alginate, silk, lignin, chitosan, cellulose, cyclodextrin	Suitable and cost effective, biodegradable, and biocompatible, chemical stability, tailorable structure, high adsorption, and rate capacity	Denaturation by extreme temperature, performance depends on pH, not suitable for column step

Agricultural residues	Fruit peels Bagasse, coir pith, maize cob, sawdust, bark	Large quantities available, low or no cost, strong affinity and high selectivity towards heavy metals due to the abundant availability of binding groups on the Surface area, easy acquiring	Effectiveness depends on pH and temperature, not suitable for industrial scale yet
Industrial wastes	Fly ash, red mud, sludge, metal hydroxide sludge	Higher area and porosity, low or no cost, large quantities available	Additional cost for processing, not suitable for industrial scale yet
Magnetic adsorbents	Hematite, magnetite, spinel ferrite, Ilmenite	Small size, large Surface area, large number of active sites, high operation efficiency, low cost	Additional cost for processing, not suitable for industrial scale yet

The most commonly used adsorbents with high adsorption capacity are chitosan, zeolite, lignin, and activated carbon (AC) (R. T. Yang, 2003); however, some of these adsorbents, such as activated carbon, have a high cost in the adsorption process, which limits their use in wastewater treatment. AC, because of its non-polar surface and low cost, is the adsorbent of choice for removing a wide range of pollutants; however, as it is not selective, it can also adsorb harmless components that are in higher proportions than the more dangerous pollutants such as heavy metals (Mariana et al., 2021), for this reason, various solid materials are recently being developed that improve, in certain applications, the properties of AC (Abdulrasheed et al., 2018).

The high adsorption capacity of AC is due to their high internal surface area, and porosity and pore size distribution plays an important role. In general, micropores (smaller than 2 nm) provide the increased area and retention capacity. In comparison, mesopores (between 2 and 50 nm) and macropores (larger than 50 nm) are necessary to retain large molecules, such as dyes or colloids, and favor access and rapid diffusion of the molecules to the internal surface of the solid (Rodriguez-Reinoso, 1997).

The structure of ACs is important because, on its surface, different functional groups from chemical activation make it chemically reactive (Bandosz et al., 1992). This is due to the interaction of the free radicals on the carbon surface with atoms such as oxygen and nitrogen from the activation method. Fig. 14 shows the main functional groups that can occur on the surface of an AC.

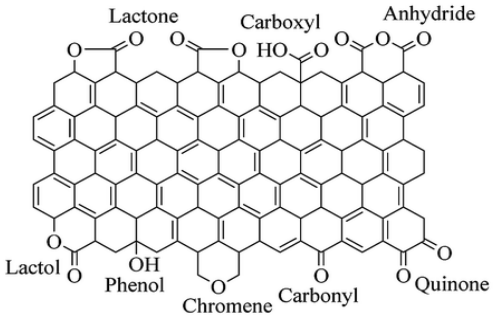

Figure 14. Main functional groups in activated carbons.

Rossner et al., 2009 used an AC, a carbonaceous resin, and two high silica zeolites to evaluate the removal of a mixture of contaminants from lake water. Adsorption isotherm experiments were conducted with a mixture of 28 emerging contaminants at environmentally relevant concentrations (approximately 200-900 ng L^{-1}). Among the adsorbents tested, AC was the most effective, and the doses of activated carbon typically used to control taste and odour in drinking water (<10 mg L^{-1}) were sufficient to achieve efficient removal for most of the emerging contaminants tested.

Table 7 shows the adsorption capacity of different AC for heavy metals and their dependence on the conditions under which adsorption occurs.

Table 7. Adsorption capacity of different AC for heavy metals.

AC	Metal	pH	q (mg g^{-1}) or R (%)	Ref.
AC from *Sargassum spp.*	Cr(VI)	2.0	91.92 %	(Esmaeili & Ghasemi, 2012)
	Cu(II)	4.0	97.0 %	(Esmaeili et al., 2010)
AC from apricot stone	Ni(II)	6.0	98.51 %	(Kobya et al., 2005)
	Co(II)	6.0	99.11 %	
	Cd(II)	6.0	99.68 %	
	Cu(II)	6.0	97.48 %	
	Pb(II)	6.0	99.93 %	
	Cr(III)	6.0	98.99 %	
	Cr(VI)	1.0	99.99 %	
AC from pulverized waste tires	Pb(II)	NC	322.5 mg g^{-1}	(Shahrokhi-Shahraki et al., 2021)
	Cu(II)		185.2 mg g^{-1}	
	Zn(II)		71.9 mg g^{-1}	
Commercial AC	Pb(II)		42.5 mg g^{-1}	
	Cu(II)		15.0 mg g^{-1}	
	Zn(II)		14.0 mg g^{-1}	
AC from coconut shell	Pb(II)	6.0	92.72 mg g^{-1}	(Anirudhan & Sreekumari, 2011)
	Cu(II)	6.0	73.60 mg g^{-1}	

NC: No control of pH.

Recent studies have established alternative methodologies for the adsorption of contaminants, such as heavy metals, using materials of biological origin, such as bacteria, algae and fungi, industrial, agricultural, and urban wastes, due to their high feasibility, low cost, and high removal efficiency. One of the techniques used for these processes is biosorption, which consists of the selective transfer of one or more solutes from a liquid phase to a batch of solid particles of biological material and involves the participation of various physical and chemical mechanisms depending on different factors such as pH or temperature (Abdi & Kazemi, 2015).

Due to the natural origin of the substrates and the elimination of residual sludge during the removal process, this alternative is a system that not only removes the polluting metal, reducing the environmental impact generated on the environment in which it is discharged but also allows it to be recovered and integrated into a new productive cycle (Volesky, 2003).

4.12 Bioremediation

Human beings, with our daily activities, generate enormous amounts of waste, which affect the environment (soil, water, and air, mainly). In short, environmental pollution threatens our well-being (Van der Perk, 2014). Fortunately, the scientific community has developed techniques to try to restore environments damaged by pollution. One of these techniques is bioremediation, which is defined as a biotechnological process that uses organisms to recover a polluted environment, whether it is a terrestrial or an aquatic environment (Vidali, 2001).

Ecosystems can naturally attenuate pollution, i.e., they purify and regenerate soil or water in the face of pollution of anthropogenic origin. Millions of microorganisms, including yeasts, non-pathogenic bacteria and fungi are capable of degrading toxic substances, especially heavy metals, reducing their toxic character or even rendering them harmless to the environment and human health. It is a process that happens every day in a prolonged way. Bioremediation replicates this capacity of nature but accelerates the process (Sales da Silva et al., 2020).

Bioremediation uses living organisms; however, not all organisms can be used in the bioremediation of environments. In fact, organisms are chosen according to their qualities to immobilize, mineralize or degrade pollutant compounds and special attention is paid to their enzymes. In general, the organisms most commonly used in bioremediation processes are bacteria, fungi, and plants (Fig. 15 a), b) and c), respectively). Sometimes, organisms are genetically

modified, so their qualities are closer to those required for bioremediation (Iwamoto & Nasu, 2001).

a) b) c)

Figure 15. The most common organisms used in bioremediation processes: a) bacteria, b) fungi, and c) plants.

Bioremediation processes commonly involve oxidation-reduction reactions where reduced contaminants are oxidized, and oxidized contaminants are reduced (Ihsanullah et al., 2020). Many different types of contaminants can be removed with this technique: polycyclic aromatic hydrocarbons, petroleum, pesticides, chlorophenols, heavy metals, dyes, sulfates, etc. (Kour et al., 2021; Lellis et al., 2019; S. Verma & Kuila, 2019). Bioremediation is so complex that it can be classified into multiple types depending on the criteria chosen. Here are two types of bioremediation classification.

According to the bioremediation strategy:

Biostimulation: This type of bioremediation strategy takes advantage of the particularities of the organisms already in the soil or water body to be treated and seeks to adapt the environmental conditions to enhance their development and the consequent degradation of pollutants. In short, biostimulation consists of incorporating nutrients or modifying environmental variables such as soil or water pH (Adams et al., 2015).

Bioaugmentation: This other bioremediation strategy involves the incorporation of organisms, which can degrade compounds, into a contaminated environment. In this way, the aim is to optimize the remediation process (Adams et al., 2015).

Depending on the organisms used for bioremediation:

Enzymatic degradation: This technique refers to the exclusive use of enzymes to remediate a contaminated environment.

Microbial bioremediation: In this case, it refers to using bacteria and fungi to remediate the contaminated site. Species that are capable of metabolizing contaminating compounds are sought.

Phytoremediation: Bioremediation is carried out exclusively by plants. There are several types of phytoremediation depending on the qualities of the plants: some are capable of degrading the compounds, others of immobilizing them in their leaves, etcetera.

Bioremediation is generally used to remediate environments that hydrocarbons, such as petroleum, pesticides, heavy metals, etc. have contaminated. Plants can extract heavy metals from substrates by adsorbing them (S. Verma & Kuila, 2019). Examples of plant species used for the remediation of environments contaminated with heavy metals include *Thlaspi caerulescens* (Fig. 16a), which adsorbs cadmium (Luo & Zhang, 2021), and *Chrysopogon zizanioides* (Fig. 16b), which adsorbs zinc and lead (Punamiya et al., 2010).

a)

b)

Figure 16. Plants used for heavy metals adsorption: a) *Thlaspi caerulescens* and b) *Chrysopogon zizanioides*.

The fungus *Pycnoporus sanguineus* also has high efficiency in adsorbing heavy metals in aqueous solution (Yahaya & Don, 2014), particularly lead, cadmium, and copper. In addition, this fungal species could be used for soil bioremediation, specifically for soils contaminated with oil spills, since it can grow on this compound and tolerate high temperatures (Sales da Silva et al., 2020).

4.13 Novel/recent methods

The study of mechanisms and methodologies for the removal of heavy metals in aqueous matrices has had a considerable boom in the last decade, so much so that numerous studies have been developed with novel and promising methods to reduce the concentration of heavy metals in water to levels that are safe for use in different daily activities.

4.13.1 Biofiltration

Biofiltration uses microorganisms attached to a porous medium to break down contaminants in wastewater streams. These microorganisms can grow in a biofilm on the surface of the medium or be suspended in the aqueous phase around the particles that make it up. Some parameters like O2 content, temperature, pH, initial concentration of the pollutant, etc. regulate the removal efficiency of biofilters. The removal efficiency can be improved by chemical or genetic modification of the filter media or microorganisms, respectively.

The possibility of an effective application of biofilters to remove toxic heavy metals from contaminated water is high, especially on a large scale. Microbial cloning can improve the efficiency of the elimination and, therefore, the reduction of the cost of the treatment as reported by (Srivastava & Majumder, 2008). This technique is capable of removing heavy metals up to levels of the order of ppb, which makes it a highly applicable technique, as well as being relatively cheap. Its scope of application extends to wastewater from industries such as fertilizers, chemicals, dyes, paper and pulp, textiles, pharmaceuticals, pigments, etc. In short, biofilters are a beneficial emerging technology for treating wastewater contaminated with heavy metals.

4.13.2 Forward Osmosis

Forward osmosis is a membrane separation technology that is considered an economical method for wastewater treatment due to its low pollution potential and energy-saving characteristics. Currently, osmosis is Thin Film Composite membranes manufactured by creating a dense layer of polyamide by interfacial polymerization on a support layer. However, the dense and hydrophobic polyamide layer leads to lower separation efficiency. Therefore, there is an urgent need to improve the separation performance of TFC membranes in wastewater treatment (He et al., 2022).

4.13.3 Novel Nanomaterials

In the last 5 to 10 years, developing new environmentally friendly nanomaterials with excellent sorption capabilities, performance, and stability has enabled massive advances in heavy metal ion capture.

Fang et al., 2018 synthesized a ZnS nanocrystal adsorbent to remove Hg^{2+}, Cu^{2+}, $Pb^{2+,}$ and Cd^{2+} from wastewater. This adsorbent showed a high adsorption capacity based on the ion exchange reaction. In addition, it was shown that the adsorption capacity towards metallic species increases when the K_{sp} of its sulfide has an increasingly low value. Additionally, it was shown that the adsorbed heavy metal could be replaced by another heavy metal when the sulfide of the latter is more stable than that of the former. This mutual substitution character of the metal sulfides was used to separate multiple heavy metals. According to the results, all other heavy metals could be adsorbed and separated from the wastewater one by one. The results showed that this cation exchange-based sequential adsorption and separation method is promising for removing and recovering multiple heavy metals from wastewater.

Metalorganic frameworks (MOFs) are formed by the coordination of a metal ion such as Zr(IV), Mg(II), Fe(III), Ca(II), Al(III), Zn(II), Cu(II), Cd(II), Co(II), Ln(III) or Ti(III) and an organic ligand such as amines, benzoic acid, sulfonates, phosphates, carboxylates, etc. (J. Li et al., 2018; Y. Wu et al., 2018). MOFs are attractive materials for adsorption and have gained popularity compared to other traditional materials such as activated carbons, silica gel, or activated alumina (Ricco et al., 2015; J.-C. Yang & Yin, 2017). Some MOFs have shown an excellent adsorption capacity for metals like As(V) (C. Wang et al., 2015), Cu(II) (Y. Zhang et al., 2015), Hg(II) (Liang et al., 2016) and Cr(VI) (Q. Yang et al., 2016).

Carbon materials are widely used in the removal of heavy metals. Recently, carbon nitride materials have attracted a revival activity. This material is synthesized as thin two-dimensional sheets, giving it a large surface area, large pore volumes, and large exposed sites on the surface, thus possessing excellent characteristics for photocatalysis and has gained significant attention for heterogeneous catalysis and adsorption applications (Lin et al., 2015).

Among all the graphitic carbon nitriles, g-C_3N_4 has been reported as the most stable allotrope, which exhibits a controllable structure, products that are not harmful to environmental health, high chemical stability, and resistance to temperature changes in addition to other physical

and chemical properties that have allowed their introduction in the field of adsorption (Shen et al., 2007; Y. Wang et al., 2010).

Metal oxides are promising adsorbent materials due to their high adsorption capacity, susceptibility to modification and easy synthesis, high economic value, and the fact that they can be widely produced. Nanometer metal oxides, in particular, show great potential to remove most trace metal contaminants, making them beneficial materials.

For example, it has been reported that they generally show adsorption capacities between 10 and 200 times greater than conventional adsorbents such as activated carbon. This is because it has a highly reactive surface, which benefits the adsorption of contaminants (L. Wang et al., 2020). Nanoparticles tend to aggregate easily, but the surface modification of nanometric metal oxides can improve the adsorption performance. Chai et al., 2021 reported that the introduction of amine groups in Fe_3O_4 increases the adsorption capacity of Cr(VI), for example.

Nanometric metal oxides have a large number of active sites on their surface that allow them to interact with various contaminants. Additionally, smaller particles exhibit faster adsorption kinetics as they have a lower resistance to diffusion. Reduction or oxidation has been suggested to occur between metal oxides and some specific multivalent heavy metal ions, for example, Cr(III), Cr(VI), As(III), As(V), Sb(III), Sb(V), etc. as they have a low affinity towards adsorption sites. Metal oxides involved in redox reactions include Fe_3O_4, MnO_2, TiO_2, and CeO_2 (Chai et al., 2021).

5. Challenges in heavy metal pollution in water

One of the biggest problems humanity will face in the coming decades will be the scarcity of drinking water due to climate change, which will increase periods of drought, as well as the high rate of pollution that many of the main drinking water sources have. From large pieces of trash to invisible chemicals, a wide range of pollutants end up in our planet's lakes, rivers, streams, groundwater, and eventually, our oceans.

Water pollution, along with drought, inefficiency, and population growth, has contributed to a freshwater crisis that threatens the sources we depend on for drinking water and other vital needs (Mekonnen & Hoekstra, 2016). Water pollution can cause human health problems, wildlife poisoning, and long-term damage to the ecosystem.

As is evident, the only way to solve the water contamination problem comes from two sides: not contaminate it and clean what is already contaminated. In this way, pollution that ends up destroying both aquifers and other types of water reserves can be avoided and minimized, so it is a battle that must be fought simultaneously on all fronts. As time goes by, new and diverse forms of treatment for contaminated water are emerging, which allows a greater range of possibilities in the field of water resources decontamination processes.

The main challenge is to change the remediation approach that we currently have and convert it into a systematic approach to prevention. Strategies must be directed towards preventing metallic contaminants from ending up in the water, especially the water used in the usual tasks of human beings.

While the reduction of the discharges of heavy metals in the water is achieved, the technologies used for their removal must be made more and more friendly to the environment, minimizing the use of new chemical species and the generation of residuals. All of the above must be achieved while maintaining high energy efficiency and economic profitability.

6. Conclusions

Environmental pollution is positioned as one of the most important problems affecting society in the XXI century. The loss of air quality, water resources, and soils available for agricultural activities has increased exponentially. A growing problem of contamination by heavy metals is identified at a global and local level, which severely compromises health, food safety, and the environment. Due to its high toxicity, the impact on health caused by prolonged exposure or bioaccumulation of heavy metals is alarming. Depending on the type of metal or metalloid, conditions ranging from damage to vital organs to carcinogenic developments occur (Rai et al., 2019).

It is currently widely accepted that the distribution, mobility, biological availability, and toxicity of chemical elements are not a function of their total concentration but rather depend on the chemical form in which they are found. It is necessary to know the chemical species of the elements to understand the chemical and biochemical reactions in which they intervene and therefore, obtain information regarding the essential and toxic nature of the chemical elements and the remediation strategies to apply in order to reduce or minimize the effects of the contaminant in human and environmental health. Speciation analyzes will become an essential tool for risk

assessment in the environment, allowing more effective trace element diagnoses and controls to be performed.

Today we know a great variety of methods and techniques that can be used to remove heavy metals from aqueous matrices, each of which shows advantages and disadvantages that must be analyzed. The search for new materials and alternatives for the disinfection of water contaminated with heavy metals, as well as the optimization of those that we know today, is a permanent task for the scientific community.

7. Bibliography

Abdi, O., & Kazemi, M. (2015). A review study of biosorption of heavy metals and comparison between different biosorbents. *J Mater Environ Sci*, *6*(5), 1386–1399.

Abdullah, N., Yusof, N., Lau, W. J., Jaafar, J., & Ismail, A. F. (2019). Recent trends of heavy metal removal from water/wastewater by membrane technologies. *Journal of Industrial and Engineering Chemistry*, *76*, 17–38.

Abdulrasheed, A. A., Jalil, A. A., Triwahyono, S., Zaini, M. A. A., Gambo, Y., & Ibrahim, M. (2018). Surface modification of activated carbon for adsorption of SO2 and NOX: A review of existing and emerging technologies. *Renewable and Sustainable Energy Reviews*, *94*, 1067–1085.

Abebe, A., Tilahun, S., Mesfine, M., & Atlabachew, M. (2017). Removal of cadmium ions from aqueous solution using very small ionic liquids to water ratio without metal chelator and pH modifications. *Ethiopian Journal of Science and Technology*, *10*(1), 51–64.

Adams, G. O., Fufeyin, P. T., Okoro, S. E., & Ehinomen, I. (2015). Bioremediation, biostimulation and bioaugmention: a review. *International Journal of Environmental Bioremediation & Biodegradation*, *3*(1), 28–39.

Agarwal, I. C., Rochon, A. M., Gesser, H. D., & Sparling, A. B. (1984). Electrodeposition of six heavy metals on reticulated vitreous carbon electrode. *Water Research*, *18*(2), 227–232. https://doi.org/10.1016/0043-1354(84)90073-3

Ahmad, A. L., Kusumastuti, A., Derek, C. J. C., & Ooi, B. S. (2011). Emulsion liquid membrane for heavy metal removal: An overview on emulsion stabilization and destabilization. *Chemical Engineering Journal*, *171*(3), 870–882.

Algieri, C., Chakraborty, S., & Candamano, S. (2021). A way to membrane-based environmental remediation for heavy metal removal. *Environments*, *8*(6), 52.

Alonso-Bravo, J. N., Montaño-Arias, N. M., Santoyo-Pizano, G., Márquez-Benavides, L., Saucedo-Martinez, B. C., & Sánchez-Yáñez, J. M. (2018). Biorecuperación y fitorremediación de suelo impactado por aceite residual automotriz. *Journal of the Selva Andina Research Society*, *9*(1), 45–51.

Al-Rashdi, B. A. M., Johnson, D. J., & Hilal, N. (2013). Removal of heavy metal ions by nanofiltration. *Desalination*, *315*, 2–17.

Anirudhan, T. S., & Sreekumari, S. S. (2011). Adsorptive removal of heavy metal ions from industrial effluents using activated carbon derived from waste coconut buttons. *Journal of Environmental Sciences*, *23*(12), 1989–1998.

Arana Juve, J. M., Christensen, F. M. S., Wang, Y., & Wei, Z. (2022). Electrodialysis for metal removal and recovery: A review. *Chemical Engineering Journal*, *435*, 134857. https://doi.org/10.1016/J.CEJ.2022.134857

Ashraf, S., Ali, Q., Zahir, Z. A., Ashraf, S., & Asghar, H. N. (2019). Phytoremediation: Environmentally sustainable way for reclamation of heavy metal polluted soils. In *Ecotoxicology and Environmental Safety* (Vol. 174, Issue November 2018, pp. 714–727). Elsevier Inc. https://doi.org/10.1016/j.ecoenv.2019.02.068

Aumesquet-Carreto, M.-Á., Ortega-Delgado, B., & García-Rodríguez, L. (2022). Opportunities of Reducing the Energy Consumption of Seawater Reverse Osmosis Desalination by Exploiting Salinity Gradients. *Membranes*, *12*(11), 1045.

Azevedo-Santos, V. M., Brito, M. F. G., Manoel, P. S., Perroca, J. F., Rodrigues-Filho, J. L., Paschoal, L. R. P., Goncalves, G. R. L., Wolf, M. R., Blettler, M., & Andrade, M. C. (2021). Plastic pollution: A focus on freshwater biodiversity. *Ambio*, *50*(7), 1313–1324.

Babilas, D., & Dydo, P. (2018). Selective zinc recovery from electroplating wastewaters by electrodialysis enhanced with complex formation. *Separation and Purification Technology*, *192*, 419–428.

Balali-Mood, M., Naseri, K., Tahergorabi, Z., Khazdair, M. R., Sadeghi, M., Kumar, R., & Chawla, J. (2021). Toxic mechanisms of five heavy metals: mercury, lead, chromium, cadmium, and arsenic. *Frontiers in Pharmacology*, *5*(4), 643972.

Bandosz, T. J., Jagiello, J., & Schwarz, J. A. (1992). Comparison of methods to assess surface acidic groups on activated carbons. *Analytical Chemistry*, *64*(8), 891–895.

Benneker, A. M., Klomp, J., Lammertink, R. G. H., & Wood, J. A. (2018). Influence of temperature gradients on mono- and divalent ion transport in electrodialysis at limiting currents. *Desalination*, *443*, 62–69. https://doi.org/10.1016/j.desal.2018.05.005

Bhattacharyya, D., Jumawan Jr, A. B., & Grieves, R. B. (1979). Separation of toxic heavy metals by sulfide precipitation. *Separation Science and Technology*, *14*(5), 441–452.

Bhattacharyya, D., Moffitt, M., & Grieves, R. B. (1978). Charged membrane ultrafiltration of toxic metal oxyanions and cations from single-and multisalt aqueous solutions. *Separation Science and Technology*, *13*(5), 449–463.

Bolisetty, S., Peydayesh, M., & Mezzenga, R. (2019). Sustainable technologies for water purification from heavy metals: review and analysis. *Chemical Society Reviews*, *48*(2), 463–487.

BrbootI, M. M., AbiD, B. A., & Al-ShuwaikI, N. M. (2011). Removal of heavy metals using chemicals precipitation. *Eng. Technol. J*, *29*(3), 595–612.

Březinová, T., & Vymazal, J. (2015). Evaluation of heavy metals seasonal accumulation in Phalaris arundinacea in a constructed treatment wetland. *Ecological Engineering*, *79*, 94–99.

Briffa, J., Sinagra, E., & Blundell, R. (2020). Heavy metal pollution in the environment and their toxicological effects on humans. *Heliyon*, *6*(9), e04691.

Bruch, L. W., Cole, M. W., & Zaremba, E. (2007). *Physical adsorption: forces and phenomena*. Courier Dover Publications.

Cardoso, L. G., Duarte, J. H., Costa, J. A. V., de Jesus Assis, D., Lemos, P. V. F., Druzian, J. I., de Souza, C. O., Nunes, I. L., & Chinalia, F. A. (2021). Spirulina sp. as a bioremediation agent for aquaculture wastewater: production of high added value compounds and estimation of theoretical biodiesel. *BioEnergy Research*, *14*(1), 254–264.

Carpanedo de Morais Nepel, T., Landers, R., Gurgel Adeodato Vieira, M., & Florêncio de Almeida Neto, A. (2020). Metallic copper removal optimization from real wastewater using pulsed electrodeposition. *Journal of Hazardous Materials*, *384*, 121416. https://doi.org/10.1016/J.JHAZMAT.2019.121416

Chai, W. S., Cheun, J. Y., Kumar, P. S., Mubashir, M., Majeed, Z., Banat, F., Ho, S.-H., & Show, P. L. (2021). A review on conventional and novel materials towards heavy metal adsorption in wastewater treatment application. *Journal of Cleaner Production*, *296*, 126589. https://doi.org/https://doi.org/10.1016/j.jclepro.2021.126589

Chang, J., Peng, D., Deng, S., Chen, J., & Duan, C. (2022). Efficient treatment of mercury (II)-containing wastewater in aerated constructed wetland microcosms packed with biochar. *Chemosphere*, *290*, 133302.

Chang, S. H. (2016). Types of bulk liquid membrane and its membrane resistance in heavy metal removal and recovery from wastewater. *Desalination and Water Treatment*, *57*(42), 19785–19793.

Charerntanyarak, L. (1999). Heavy metals removal by chemical coagulation and precipitation. *Water Science and Technology*, *39*(10–11), 135–138.

Chaudhry, F. N., & Malik, M. F. (2017). Factors affecting water pollution: a review. *J Ecosyst Ecography*, *7*(225), 1–3.

Chen, R., Sheehan, T., Ng, J. L., Brucks, M., & Su, X. (2020). Capacitive deionization and electrosorption for heavy metal removal. *Environmental Science: Water Research & Technology*, *6*(2), 258–282. https://doi.org/10.1039/C9EW00945K

Chin, J. F., Heng, Z. W., Teoh, H. C., Chong, W. C., & Pang, Y. L. (2021). Recent development of magnetic biochar crosslinked chitosan on heavy metal removal from wastewater–Modification, application and mechanism. *Chemosphere*, 133035.

Chon, K., Cho, J., Kim, S. J., & Jang, A. (2014). The role of a combined coagulation and disk filtration process as a pre-treatment to microfiltration and reverse osmosis membranes in a municipal wastewater pilot plant. *Chemosphere*, *117*, 20–26.

Chung, S., Kim, S., Kim, J.-O., & Chung, J. (2014). Feasibility of combining reverse osmosis–ferrite process for reclamation of metal plating wastewater and recovery of heavy metals. *Industrial & Engineering Chemistry Research*, *53*(39), 15192–15199.

Çimen, A. (2015). Removal of chromium from wastewater by reverse osmosis. *Russian Journal of Physical Chemistry A*, *89*(7), 1238–1243.

Cohen, I., Avraham, E., Soffer, A., & Aurbach, D. (2013). Water Desalination by Capacitive Deionization - Advantages Limitations and Modification. *ECS Transactions*, *45*(17), 43–59. https://doi.org/10.1149/04517.0043ECST/XML

Cohen, M. A. (2013). Water pollution from oil spills. *Encyclopedia of Energy, Natural Resource, and Environmental Economics*, *3*, 121–126.

Cui, J., Xie, Y., Sun, T., Chen, L., & Zhang, W. (2021). Deciphering and engineering photosynthetic cyanobacteria for heavy metal bioremediation. *Science of The Total Environment*, *761*, 144111.

Dialynas, E., & Diamadopoulos, E. (2009). Integration of a membrane bioreactor coupled with reverse osmosis for advanced treatment of municipal wastewater. *Desalination*, *238*(1–3), 302–311.

Durairaj, S., Sivakumar, D., Shankar, D., Gomathi, V., & Nandakumaar, A. (2014). Application of electro-dialysis on removal of heavy metals. *Poll Res*, *33*(3), 627–631. https://www.researchgate.net/publication/287762453

Dwivedi, A. K. (2017). Researches in water pollution: A review. *International Research Journal of Natural and Applied Sciences*, *4*(1), 118–142.

Esmaeili, A., & Ghasemi, S. (2012). *Investigation of Cr (VI) adsorption by dried brown algae Sargassum sp. and its activated carbon*.

Esmaeili, A., Ghasemi, S., & Sohrabipour, J. (2010). Biosorption of copper from wastewater by activated carbon preparation from alga Sargassum sp. *Natural Product Research*, *24*(4), 341–348.

Eunice, G., Niño, A., Carlos, •, Barrera, A. C., García, A. B., Elisabeth, •, & Lumbaque, C. (2013). La Electrocoagulación como un Tratamiento Eficiente para la Remoción de Metales Pesados Presentes en Aguas Residuales. *Revista Facultad de Ciencias Básicas*, *9*(2), 306–317. https://doi.org/10.18359/RFCB.389

Fan, L., Xu, X., Wang, G., Yang, J., & Han, T. L. Z. (2012). Experimental Research for Heavy Metal Lead and Zinc Smelting Wastewater by Electroflocculation. *Advanced Materials Research*, *534*, 217–220. https://doi.org/10.4028/WWW.SCIENTIFIC.NET/AMR.534.217

Fang, L., Li, L., Qu, Z., Xu, H., Xu, J., & Yan, N. (2018). A novel method for the sequential removal and separation of multiple heavy metals from wastewater. *Journal of Hazardous Materials*, *342*, 617–624.

Gao, J., Sun, S.-P., Zhu, W.-P., & Chung, T.-S. (2014). Chelating polymer modified P84 nanofiltration (NF) hollow fiber membranes for high efficient heavy metal removal. *Water Research*, *63*, 252–261.

Genchi, G., Sinicropi, M. S., Lauria, G., Carocci, A., & Catalano, A. (2020). The effects of cadmium toxicity. *International Journal of Environmental Research and Public Health*, *17*(11), 3782.

Gherasim, C. V., Křivčík, J., & Mikulášek, P. (2014). Investigation of batch electrodialysis process for removal of lead ions from aqueous solutions. *Chemical Engineering Journal*, *256*, 324–334. https://doi.org/10.1016/J.CEJ.2014.06.094

González Gómez, J. D. (2010). *Fitorremediación-una herramienta viable para la descontaminación de aguas y suelo*.

González-Chávez, M. C. A. (2017). Definiciones y problemática en la investigación científica en aspectos de fitoremediación de suelos. *Agro Productividad*, *10*(4).

Gu, J. nan, Liang, J., Chen, C., Li, K., Zhou, W., Jia, J., & Sun, T. (2020). Treatment of real deplating wastewater through an environmental friendly precipitation-electrodeposition-oxidation process: Recovery of silver and copper and reuse of wastewater. *Separation and Purification Technology*, *248*, 117082. https://doi.org/10.1016/J.SEPPUR.2020.117082

Gupta, V. K., Moradi, O., Tyagi, I., Agarwal, S., Sadegh, H., Shahryari-Ghoshekandi, R., Makhlouf, A. S. H., Goodarzi, M., & Garshasbi, A. (2016). Study on the removal of heavy metal ions from industry waste by carbon nanotubes: effect of the surface modification: a review. *Critical Reviews in Environmental Science and Technology*, *46*(2), 93–118.

Gurreri, L., Tamburini, A., Cipollina, A., & Micale, G. (2020). Electrodialysis applications in wastewater treatment for environmental protection and resources recovery: A systematic review on progress and perspectives. *Membranes*, *10*(7), 146.

Harharah, R. H., Abdalla, G. M. T., Elkhaleefa, A., Shigidi, I., & Harharah, H. N. (2022). A Study of Copper (II) Ions Removal by Reverse Osmosis under Various Operating Conditions. *Separations*, *9*(6), 155.

Huang, Y., & Feng, X. (2019). Polymer-enhanced ultrafiltration: Fundamentals, applications and recent developments. *Journal of Membrane Science*, *586*, 53–83.

Hughes, M. F. (2002). Arsenic toxicity and potential mechanisms of action. *Toxicology Letters*, *133*(1), 1–16.

Hutten, I. M. (2016). Filtration Mechanisms and Theory. *Handbook of Nonwoven Filter Media*, 53–107. https://doi.org/10.1016/B978-0-08-098301-1.00002-2

Ihsanullah, I., Jamal, A., Ilyas, M., Zubair, M., Khan, G., & Atieh, M. A. (2020). Bioremediation of dyes: Current status and prospects. *Journal of Water Process Engineering*, *38*, 101680.

Imdad, S., & Dohare, R. K. (2022). A critical review on heavy metals removal using ionic liquid membranes from the industrial wastewater. *Chemical Engineering and Processing-Process Intensification*, 108812.

Inyinbor Adejumoke, A., Adebesin Babatunde, O., Oluyori Abimbola, P., Adelani Akande Tabitha, A., Dada Adewumi, O., & Oreofe Toyin, A. (2018). Water pollution: effects, prevention, and climatic impact. *Water Challenges of an Urbanizing World*, *33*, 33–47.

Irfan, M., Xu, T., Ge, L., Wang, Y., & Xu, T. (2019). Zwitterion structure membrane provides high monovalent/divalent cation electrodialysis selectivity: Investigating the effect of functional groups and operating parameters. *Journal of Membrane Science*, *588*, 117211.

Iwamoto, T., & Nasu, M. (2001). Current bioremediation practice and perspective. *Journal of Bioscience and Bioengineering*, *92*(1), 1–8.

Jarvis, P., & Fawell, J. (2021). Lead in drinking water–an ongoing public health concern? *Current Opinion in Environmental Science & Health*, *20*, 100239.

Jing, G., Ren, S., Pooley, S., Sun, W., Kowalczuk, P. B., & Gao, Z. (2021). Electrocoagulation for industrial wastewater treatment: an updated review. *Environmental Science: Water Research & Technology*, *7*(7), 1177–1196. https://doi.org/10.1039/D1EW00158B

Juve, J.-M. A., Christensen, F. M., Wang, Y., & Wei, Z. (2022). Electrodialysis for metal removal and recovery: A review. *Chemical Engineering Journal*, 134857.

Kalfa, A., Shapira, B., Shopin, A., Cohen, I., Avraham, E., & Aurbach, D. (2020). Capacitive deionization for wastewater treatment: Opportunities and challenges. *Chemosphere*, *241*, 125003. https://doi.org/10.1016/J.CHEMOSPHERE.2019.125003

Khanna, R., & Gupta, S. (2018). Agrochemicals as a potential cause of ground water pollution: a review. *Int J Chem Stud*, *6*(3), 985–990.

Khelifa, A., Moulay, S., & Naceur, A. W. (2005). Treatment of metal finishing effluents by the electroflotation technique. *Desalination*, *181*(1–3), 27–33. https://doi.org/10.1016/J.DESAL.2005.01.011

Kim, J.-H., Lee, S. Y., Rha, S., Lee, Y. J., Jo, H. Y., & Lee, S. (2021). Treatment of Heavy Metal Wastewater by Ceramic Microfilter Functionalized with Magnesium Oxides. *Water, Air, & Soil Pollution*, *232*(12), 1–13.

Kim, N., Lee, J., Kim, S., Hong, S. P., Lee, C., Yoon, J., & Kim, C. (2020). Short Review of Multichannel Membrane Capacitive Deionization: Principle, Current Status, and Future Prospect. *Applied Sciences 2020, Vol. 10, Page 683*, *10*(2), 683. https://doi.org/10.3390/APP10020683

Knox, A. S., Paller, M. H., Seaman, J. C., Mayer, J., & Nicholson, C. (2021). Removal, distribution and retention of metals in a constructed wetland over 20 years. *Science of The Total Environment*, *796*, 149062.

Kobya, M., Demirbas, E., Senturk, E., & Ince, M. (2005). Adsorption of heavy metal ions from aqueous solutions by activated carbon prepared from apricot stone. *Bioresource Technology*, *96*(13), 1518–1521.

Koparal, S. S., Özgür, R., Öğütveren, Ü. B., & Bergmann, H. (2004). Antimony removal from model acid solutions by electrodeposition. *Separation and Purification Technology*, *37*(2), 107–116. https://doi.org/10.1016/J.SEPPUR.2003.09.001

Kour, D., Kaur, T., Devi, R., Yadav, A., Singh, M., Joshi, D., Singh, J., Suyal, D. C., Kumar, A., & Rajput, V. D. (2021). Beneficial microbiomes for bioremediation of diverse contaminated environments for environmental sustainability: present status and future challenges. *Environmental Science and Pollution Research*, *28*(20), 24917–24939.

Kuleyin, A., & Uysal, H. E. (2020). Recovery of Copper Ions from Industrial Wastewater by Electrodeposition. *Int. J. Electrochem. Sci*, *15*, 1474–1485. https://doi.org/10.20964/2020.02.39

Kumar, M., Nandi, M., & Pakshirajan, K. (2021). Recent advances in heavy metal recovery from wastewater by biogenic sulfide precipitation. *Journal of Environmental Management*, *278*, 111555.

Kumar, R., & Chawla, J. (2014). Removal of cadmium ion from water/wastewater by nano-metal oxides: a review. *Water Quality, Exposure and Health*, *5*(4), 215–226.

Kumar, S., & Sharma, A. (2019). Cadmium toxicity: effects on human reproduction and fertility. *Reviews on Environmental Health*, *34*(4), 327–338.

Kushwaha, A., Rani, R., Kumar, S., & Gautam, A. (2015). Heavy metal detoxification and tolerance mechanisms in plants: Implications for phytoremediation. *Environmental Reviews*, *24*(1), 39–51.

Kyzas, G. Z., & Matis, K. A. (2016). Electroflotation process: A review. *Journal of Molecular Liquids*, *220*, 657–664. https://doi.org/10.1016/J.MOLLIQ.2016.04.128

Ladole, M. R., Patil, S. S., Paraskar, P. M., Pokale, P. B., & Patil, P. D. (2021). Desalination Using Electrodialysis. *Advances in Science, Technology and Innovation*, 15–38. https://doi.org/10.1007/978-3-030-72873-1_2/COVER

Lellis, B., Fávaro-Polonio, C. Z., Pamphile, J. A., & Polonio, J. C. (2019). Effects of textile dyes on health and the environment and bioremediation potential of living organisms. *Biotechnology Research and Innovation*, *3*(2), 275–290.

Li, J., Wang, X., Zhao, G., Chen, C., Chai, Z., Alsaedi, A., Hayat, T., & Wang, X. (2018). Metal–organic framework-based materials: superior adsorbents for the capture of toxic and radioactive metal ions. *Chemical Society Reviews*, *47*(7), 2322–2356.

Li, P., Lan, H., Chen, K., Ma, X., Wei, B., Wang, M., Li, P., Hou, Y., & Niu, Q. J. (2022). Novel high-flux positively charged aliphatic polyamide nanofiltration membrane for selective removal of heavy metals. *Separation and Purification Technology*, *280*, 119949.

Li, T., Xiao, K., Yang, B., Peng, G., Liu, F., Tao, L., Chen, S., Wei, H., Yu, G., & Deng, S. (2019). Recovery of Ni(II) from real electroplating wastewater using fixed-bed resin adsorption and subsequent electrodeposition. *Frontiers of Environmental Science & Engineering 2019 13:6*, *13*(6), 1–12. https://doi.org/10.1007/S11783-019-1175-7

Liang, L., Chen, Q., Jiang, F., Yuan, D., Qian, J., Lv, G., Xue, H., Liu, L., Jiang, H.-L., & Hong, M. (2016). In situ large-scale construction of sulfur-functionalized metal–organic framework and its efficient removal of Hg (II) from water. *Journal of Materials Chemistry A*, *4*(40), 15370–15374.

Lin, Q., Li, L., Liang, S., Liu, M., Bi, J., & Wu, L. (2015). Efficient synthesis of monolayer carbon nitride 2D nanosheet with tunable concentration and enhanced visible-light photocatalytic activities. *Applied Catalysis B: Environmental*, *163*, 135–142. https://doi.org/https://doi.org/10.1016/j.apcatb.2014.07.053

Liu, X., Jiang, B., Yin, X., Ma, H., & Hsiao, B. S. (2020). Highly permeable nanofibrous composite microfiltration membranes for removal of nanoparticles and heavy metal ions. *Separation and Purification Technology*, *233*, 115976.

López, R. A. N., Vong, Y. M., Borges, R. O., & Olguín, E. J. (2004). Fitorremediación: fundamentos y aplicaciones. *Revista Ciencia*, 69–83.

Lopez-Ramon, M. V., Stoeckli, F., Moreno-Castilla, C., & Carrasco-Marin, F. (1999). On the characterization of acidic and basic surface sites on carbons by various techniques. *Carbon*, *37*(8), 1215–1221.

Luo, J.-S., & Zhang, Z. (2021). Mechanisms of cadmium phytoremediation and detoxification in plants. *The Crop Journal*, *9*(3), 521–529.

Ma, Y., Rajkumar, M., Luo, Y., & Freitas, H. (2011). Inoculation of endophytic bacteria on host and non-host plants—effects on plant growth and Ni uptake. *Journal of Hazardous Materials*, *195*, 230–237.

Ma, Y., Rajkumar, M., Zhang, C., & Freitas, H. (2016). Inoculation of Brassica oxyrrhina with plant growth promoting bacteria for the improvement of heavy metal phytoremediation under drought conditions. *Journal of Hazardous Materials*, *320*, 36–44.

Maarof, H. I., Daud, W. M. A. W., & Aroua, M. K. D. (2017). Recent trends in removal and recovery of heavy metals from wastewater by electrochemical technologies. *Reviews in Chemical Engineering*, *33*(4), 359–386. https://doi.org/10.1515/REVCE-2016-0021/ASSET/GRAPHIC/J_REVCE-2016-0021_CV_002.JPG

Malik, L. A., Bashir, A., Qureashi, A., & Pandith, A. H. (2019). Detection and removal of heavy metal ions: a review. *Environmental Chemistry Letters*, *17*(4), 1495–1521.

Mariana, M., HPS, A. K., Mistar, E. M., Yahya, E. B., Alfatah, T., Danish, M., & Amayreh, M. (2021). Recent advances in activated carbon modification techniques for enhanced heavy metal adsorption. *Journal of Water Process Engineering*, *43*, 102221.

Marrero-Coto, J., Amores-Sánchez, I., & Coto-Pérez, O. (2012). Phytoremediation, a technology that involves plants and microorganisms in environmental remediation. *ICIDCA Sobre Los Derivados de La Caña de Azúcar*, *46*(3), 52–61.

Masese, F. O., Raburu, P. O., Mwasi, B. N., & Etiégni, L. (2012). Effects of deforestation on water resources: integrating science and community perspectives in the Sondu-Miriu River Basin, Kenya. *New Advances and Contributions to Forestry Research*, *268*, 1–18.

Matlock, M. M., Howerton, B. S., & Atwood, D. A. (2002). Chemical precipitation of heavy metals from acid mine drainage. *Water Research*, *36*(19), 4757–4764.

Mekonnen, M. M., & Hoekstra, A. Y. (2016). Four billion people facing severe water scarcity. *Science Advances*, *2*(2), e1500323.

Merzouk, B., Gourich, B., Sekki, A., Madani, K., & Chibane, M. (2009). Removal turbidity and separation of heavy metals using electrocoagulation–electroflotation technique: A case study. *Journal of Hazardous Materials*, *164*(1), 215–222. https://doi.org/10.1016/J.JHAZMAT.2008.07.144

Mickova, I. (2015). Advanced Electrochemical Technologies in Wastewater Treatment. Part II: Electro-Flocculation and Electro-Flotation. *Undefined*.

Min, K. J., Choi, S. Y., Jang, D., Lee, J., & Park, K. Y. (2019). Separation of metals from electroplating wastewater using electrodialysis. *Energy Sources, Part A: Recovery, Utilization, and Environmental Effects*, *41*(20), 2471–2480.

Min, K. J., Kim, J. H., & Park, K. Y. (2021a). Characteristics of heavy metal separation and determination of limiting current density in a pilot-scale electrodialysis process for plating wastewater treatment. *Science of the Total Environment*, *757*, 143762.

Min, K. J., Kim, J. H., & Park, K. Y. (2021b). Characteristics of heavy metal separation and determination of limiting current density in a pilot-scale electrodialysis process for plating wastewater treatment. *Science of the Total Environment*, *757*. https://doi.org/10.1016/j.scitotenv.2020.143762

Mnif, A., Bejaoui, I., Mouelhi, M., & Hamrouni, B. (2017). Hexavalent chromium removal from model water and car shock absorber factory effluent by nanofiltration and reverse osmosis membrane. *International Journal of Analytical Chemistry*, *2017*.

Moctezuma Granados, C. E. (2017). Evaluación de Pseudomonas endófitas de la raíz de Typha latifolia en la fitoextracción de Cd (II). *REPOSITORIO NACIONAL CONACYT*.

Mohammadi, T., Razmi, A., & Sadrzadeh, M. (2004). Effect of operating parameters on Pb2+ separation from wastewater using electrodialysis. *Desalination*, *167*(1–3), 379–385. https://doi.org/10.1016/J.DESAL.2004.06.150

Moss, B. (2008). Water pollution by agriculture. *Philosophical Transactions of the Royal Society B: Biological Sciences*, *363*(1491), 659–666.

Moussa, D. T., El-Naas, M. H., Nasser, M., & Al-Marri, M. J. (2017). A comprehensive review of electrocoagulation for water treatment: Potentials and challenges. *Journal of Environmental Management*, *186*, 24–41. https://doi.org/10.1016/J.JENVMAN.2016.10.032

Muddemann, T., Haupt, D., Sievers, M., & Kunz, U. (2019). Electrochemical Reactors for Wastewater Treatment. *ChemBioEng Reviews*, *6*(5), 142–156. https://doi.org/10.1002/CBEN.201900021

Mungray, A. A., Kulkarni, S. v, & Mungray, A. K. (2012). Removal of heavy metals from wastewater using micellar enhanced ultrafiltration technique: a review. *Central European Journal of Chemistry*, *10*(1), 27–46.

Murcott, S. (2012). *Arsenic contamination in the world*. IWA publishing.

Nisa, K. U., Tarfeen, N., & Nisa, Q. (2022). Potential role of wetlands in remediation of metals and metalloids: a review. *Metals Metalloids Soil Plant Water Systems*, 427–444.

Ortiz Cáceres, E. A. (2020). *Análisis y propuesta de técnicas de fitorremediación para disminuir la presencia de compuestos orgánicos volátiles en el aire en la industria de pinturas de Lima Metropolitana, durante el período 2014 al 2019*.

Ozaki, H., Sharma, K., & Saktaywin, W. (2002). Performance of an ultra-low-pressure reverse osmosis membrane (ULPROM) for separating heavy metal: effects of interference parameters. *Desalination*, *144*(1–3), 287–294.

Pang, F. M., Teng, S. P., Teng, T. T., & Omar, A. K. M. (2009). Heavy metals removal by hydroxide precipitation and coagulation-flocculation methods from aqueous solutions. *Water Quality Research Journal*, *44*(2), 174–182.

Pavesi, T., & Moreira, J. C. (2020). Mechanisms and individuality in chromium toxicity in humans. *Journal of Applied Toxicology*, *40*(9), 1183–1197.

Perez-Cadenas, A. F., Maldonado-Hodar, F. J., & Moreno-Castilla, C. (2003). On the nature of surface acid sites of chlorinated activated carbons. *Carbon*, *41*(3), 473–478.

Petrinic, I., Korenak, J., Povodnik, D., & Hélix-Nielsen, C. (2015a). A feasibility study of ultrafiltration/reverse osmosis (UF/RO)-based wastewater treatment and reuse in the metal finishing industry. *Journal of Cleaner Production*, *101*, 292–300.

Petrinic, I., Korenak, J., Povodnik, D., & Hélix-Nielsen, C. (2015b). A feasibility study of ultrafiltration/reverse osmosis (UF/RO)-based wastewater treatment and reuse in the metal finishing industry. *Journal of Cleaner Production*, *101*, 292–300.

Peydayesh, M., Mohammadi, T., & Nikouzad, S. K. (2020). A positively charged composite loose nanofiltration membrane for water purification from heavy metals. *Journal of Membrane Science*, *611*, 118205.

Pohl, A. (2020). Removal of heavy metal ions from water and wastewaters by sulfur-containing precipitation agents. *Water, Air, & Soil Pollution*, *231*(10), 1–17.

Punamiya, P., Datta, R., Sarkar, D., Barber, S., Patel, M., & Das, P. (2010). Symbiotic role of Glomus mosseae in phytoextraction of lead in vetiver grass [Chrysopogon zizanioides (L.)]. *Journal of Hazardous Materials*, *177*(1–3), 465–474.

Qi, Y., Zhu, L., Shen, X., Sotto, A., Gao, C., & Shen, J. (2019). Polythyleneimine-modified original positive charged nanofiltration membrane: removal of heavy metal ions and dyes. *Separation and Purification Technology*, *222*, 117–124.

Rai, P. K., Lee, S. S., Zhang, M., Tsang, Y. F., & Kim, K.-H. (2019). Heavy metals in food crops: Health risks, fate, mechanisms, and management. *Environment International*, *125*, 365–385.

Rajkumar, M., Ae, N., & Freitas, H. (2009). Endophytic bacteria and their potential to enhance heavy metal phytoextraction. *Chemosphere*, *77*(2), 153–160.

Ramos, V. C., Han, W., & Yeung, K. L. (2020). A comparative study between ionic liquid coating and counterparts in bulk for toluene absorption. *Green Chemical Engineering*, *1*(2), 147–154. https://doi.org/10.1016/J.GCE.2020.10.008

Ramos, V. C., Han, W., Zhang, X., Zhang, S., & Yeung, K. L. (2020). Supported ionic liquids for air purification. *Current Opinion in Green and Sustainable Chemistry*, *25*, 100391. https://doi.org/10.1016/j.cogsc.2020.100391

Regel-Rosocka, M., Rzelewska, M., Baczynska, M., Janus, M., & Wisniewski, M. (2015). Removal of palladium (II) from aqueous chloride solutions with cyphos phosphonium ionic liquids as metal ion carriers for liquid-liquid extraction and transport across polymer inclusion membranes. *Physicochemical Problems of Mineral Processing*, *51*.

Ricci, B. C., Ferreira, C. D., Aguiar, A. O., & Amaral, M. C. S. (2015). Integration of nanofiltration and reverse osmosis for metal separation and sulfuric acid recovery from gold mining effluent. *Separation and Purification Technology*, *154*, 11–21.

Ricco, R., Konstas, K., Styles, M. J., Richardson, J. J., Babarao, R., Suzuki, K., Scopece, P., & Falcaro, P. (2015). Lead (II) uptake by aluminium based magnetic framework composites (MFCs) in water. *Journal of Materials Chemistry A*, *3*(39), 19822–19831.

Rodriguez-Reinoso, F. (1997). Activated carbon. *Introduction to Carbon Technologies*.

Rolón-Cárdenas, G. A., Arvizu-Gómez, J. L., Pacheco-Aguilar, J. R., Vázquez-Martínez, J., & Hernández-Morales, A. (2021). Cadmium-tolerant endophytic Pseudomonas rhodesiae strains isolated from Typha

latifolia modify the root architecture of Arabidopsis thaliana Col-0 in presence and absence of Cd. *Brazilian Journal of Microbiology*, *52*(1), 349–361.

Rossner, A., Snyder, S. A., & Knappe, D. R. U. (2009). Removal of emerging contaminants of concern by alternative adsorbents. *Water Research*, *43*(15), 3787–3796.

Ruhal, R., & Choudhury, B. (2012). Membrane Separation and Design. *Handbook of Food Process Design*, 769–788.

Ruthven, D. M. (1984). *Principles of adsorption and adsorption processes*. John Wiley & Sons.

Saha, R., Nandi, R., & Saha, B. (2011). Sources and toxicity of hexavalent chromium. *Journal of Coordination Chemistry*, *64*(10), 1782–1806.

Sales da Silva, I. G., Gomes de Almeida, F. C., Padilha da Rocha e Silva, N. M., Casazza, A. A., Converti, A., & Asfora Sarubbo, L. (2020). Soil bioremediation: Overview of technologies and trends. *Energies*, *13*(18), 4664.

Sato, T., Imaizumi, M., Kato, O., & Taniguchi, Y. (1977). RO applications in wastewater reclamation for re-use. *Desalination*, *23*(1–3), 65–76.

Schück, M., & Greger, M. (2020). Screening the capacity of 34 wetland plant species to remove heavy metals from water. *International Journal of Environmental Research and Public Health*, *17*(13), 4623.

Schwarzenbach, R. P., Egli, T., Hofstetter, T. B., Von Gunten, U., & Wehrli, B. (2010). Global water pollution and human health. *Annual Review of Environment and Resources*, *35*(1), 109–136.

Shah, V., & Daverey, A. (2020). Phytoremediation: A multidisciplinary approach to clean up heavy metal contaminated soil. *Environmental Technology & Innovation*, *18*, 100774.

Shahrokhi-Shahraki, R., Benally, C., El-Din, M. G., & Park, J. (2021). High efficiency removal of heavy metals using tire-derived activated carbon vs commercial activated carbon: Insights into the adsorption mechanisms. *Chemosphere*, *264*, 128455.

Shekhawat, K., Chatterjee, S., & Joshi, B. (2015). Chromium toxicity and its health hazards. *International Journal of Advanced Research*, *3*(7), 167–172.

Shen, H., Jiang, H., Mao, H., Pan, G., Zhou, L., & Cao, Y. (2007). Simultaneous determination of seven phthalates and four parabens in cosmetic products using HPLC-DAD and GC-MS methods. *Journal of Separation Science*, *30*(1), 48–54.

Shocron, A. N., Atlas, I., & Suss, M. E. (2022). Predicting ion selectivity in water purification by capacitive deionization: Electric double layer models. *Current Opinion in Colloid & Interface Science*, *60*, 101602. https://doi.org/10.1016/J.COCIS.2022.101602

Singh, R., Singh, S., Parihar, P., Singh, V. P., & Prasad, S. M. (2015). Arsenic contamination, consequences and remediation techniques: a review. *Ecotoxicology and Environmental Safety*, *112*, 247–270.

Singh, S., Benny, C. K., & Chakraborty, S. (2022). An overview on the application of constructed wetlands for the treatment of metallic wastewater. *Biodegradation and Detoxification of Micropollutants in Industrial Wastewater*, 103–130.

Smara, A., Delimi, R., Chainet, E., & Sandeaux, J. (2007). Removal of heavy metals from diluted mixtures by a hybrid ion-exchange/electrodialysis process. *Separation and Purification Technology*, *57*(1), 103–110. https://doi.org/10.1016/J.SEPPUR.2007.03.012

Srivastava, N. K., & Majumder, C. B. (2008). Novel biofiltration methods for the treatment of heavy metals from industrial wastewater. *Journal of Hazardous Materials*, *151*(1), 1–8.

Stando, G., Hannula, P. M., Kumanek, B., Lundström, M., & Janas, D. (2021). Copper recovery from industrial wastewater - Synergistic electrodeposition onto nanocarbon materials. *Water Resources and Industry*, *26*, 100156. https://doi.org/10.1016/J.WRI.2021.100156

Suzuki, M., & Suzuki, M. (1990). *Adsorption engineering* (Vol. 14). Kodansha Tokyo.

Sylwan, I., & Thorin, E. (2021). Removal of heavy metals during primary treatment of municipal wastewater and possibilities of enhanced removal: A review. *Water*, *13*(08), 1121.

Tang, W., Liang, J., He, D., Gong, J., Tang, L., Liu, Z., Wang, D., & Zeng, G. (2019). Various cell architectures of capacitive deionization: Recent advances and future trends. *Water Research*, *150*, 225–251. https://doi.org/10.1016/J.WATRES.2018.11.064

Tatiparti, S. S. v., & Ebrahimi, F. (2012). Potentiostatic versus galvanostatic electrodeposition of nanocrystalline Al-Mg alloy powders. *Journal of Solid State Electrochemistry*, *16*(3), 1255–1262. https://doi.org/10.1007/S10008-011-1522-5/FIGURES/6

Tonini, G. A., & Ruotolo, L. A. M. (2017). Heavy metal removal from simulated wastewater using electrochemical technology: optimization of copper electrodeposition in a membraneless fluidized bed electrode. *Clean Technologies and Environmental Policy*, *19*(2), 403–415. https://doi.org/10.1007/S10098-016-1226-8

Tortora, F., Innocenzi, V., Prisciandaro, M., Vegliò, F., & Mazziotti di Celso, G. (2016). Heavy metal removal from liquid wastes by using micellar-enhanced ultrafiltration. *Water, Air, & Soil Pollution*, *227*(7), 1–11.

Van der Perk, M. (2014). *Soil and water contamination*. CRC Press.

Vardhan, K. H., Kumar, P. S., & Panda, R. C. (2019). A review on heavy metal pollution, toxicity and remedial measures: Current trends and future perspectives. *Journal of Molecular Liquids*, *290*, 111197.

Ventura, D., Ferrante, M., Copat, C., Grasso, A., Milani, M., Sacco, A., Licciardello, F., & Cirelli, G. L. (2021). Metal removal processes in a pilot hybrid constructed wetland for the treatment of semi-synthetic stormwater. *Science of The Total Environment*, *754*, 142221.

Verduzco, L. E., Oliva, J., Oliva, A. I., Macias, E., Garcia, C. R., Herrera-Trejo, M., Pariona, N., & Mtz-Enriquez, A. I. (2019). Enhanced removal of arsenic and chromium contaminants from drinking water by electrodeposition technique using graphene composites. *Materials Chemistry and Physics*, *229*, 197–209. https://doi.org/10.1016/J.MATCHEMPHYS.2019.03.006

Verma, B., Balomajumder, C., Sabapathy, M., & Gumfekar, S. P. (2021). Pressure-driven membrane process: a review of advanced technique for heavy metals remediation. *Processes*, *9*(5), 752.

Verma, S., & Kuila, A. (2019). Bioremediation of heavy metals by microbial process. *Environmental Technology & Innovation*, *14*, 100369.

Vidali, M. (2001). Bioremediation. an overview. *Pure and Applied Chemistry*, *73*(7), 1163–1172.

Vigliotta, G., Matrella, S., Cicatelli, A., Guarino, F., & Castiglione, S. (2016). Effects of heavy metals and chelants on phytoremediation capacity and on rhizobacterial communities of maize. *Journal of Environmental Management*, *179*, 93–102.

Vincent, M., Laurio, O., Velandres, J. A., Alfafara, C. G., Migo, V. P., Concepcion, M., Detras, M., Sunga-Amparo, J. M., & Mendoza, M. (2020). Potentiostatic Electrodeposition as an Option to the Traditional Recovery of Silver in Artisanal Gold Smelting Wastewater in Bulacan, Philippines. *Philippine Engineering Journal*, *41*(1), 67–86. https://journals.upd.edu.ph/index.php/pej/article/view/7148

Viramontes-Acosta, A., Hernández-López, M., Velasquez-Chavez, T. E., & Mendez-Almaraz, R. (2020). Construcción de un Humedal para la fitorremediación de agua residual en el Instituto Tecnológico Superior de Lerdo. *Revista Ciencia*, *1*.

Volesky, B. (2003). Sorption and biosorption, BV Sorbex. *Inc., St. Lambert, Quebec*, *326*.

Voskoboinikov, G. M., Matishov, G. G., Metelkova, L. O., Zhakovskaya, Z. A., & Lopushanskaya, E. M. (2018). Participation of the green algae Ulvaria obscura in bioremediation of sea water from oil products. *Doklady Biological Sciences*, *481*(1), 139–141.

Wang, C., Li, T., Yu, G., & Deng, S. (2021). Removal of low concentrations of nickel ions in electroplating wastewater by combination of electrodialysis and electrodeposition. *Chemosphere*, *263*, 128208. https://doi.org/10.1016/J.CHEMOSPHERE.2020.128208

Wang, C., Liu, X., Chen, J. P., & Li, K. (2015). Superior removal of arsenic from water with zirconium metal-organic framework UiO-66. *Scientific Reports*, *5*(1), 1–10.

Wang, G., Yu, G., Chi, T., Li, Y., Zhang, Y., Wang, J., Li, P., Liu, J., Yu, Z., & Wang, Q. (2023). Insights into the enhanced effect of biochar on cadmium removal in vertical flow constructed wetlands. *Journal of Hazardous Materials*, *443*, 130148.

Wang, J., Long, Y., Yu, G., Wang, G., Zhou, Z., Li, P., Yang, Y. Z. K., & Wang, S. (2022). A Review on Microorganisms in Constructed Wetlands for Typical Pollutant Removal: Species, Function, and Diversity. *Environmental Monitoring and Remediation Using Microbiotechnology*, 845725176.

Wang, L. K., Vaccari, D. A., Li, Y., & Shammas, N. K. (2005). Chemical precipitation. In *Physicochemical treatment processes* (pp. 141–197). Springer.

Wang, L., & Lin, S. (2018). Membrane Capacitive Deionization with Constant Current vs Constant Voltage Charging: Which Is Better? *Environmental Science and Technology*, *52*(7), 4051–4060. https://doi.org/10.1021/ACS.EST.7B06064/SUPPL_FILE/ES7B06064_SI_001.PDF

Wang, L., & Lin, S. (2019). Mechanism of Selective Ion Removal in Membrane Capacitive Deionization for Water Softening. *Environmental Science and Technology*, *53*(10), 5797–5804. https://doi.org/10.1021/ACS.EST.9B00655/SUPPL_FILE/ES9B00655_SI_001.PDF

Wang, L., Shi, C., Pan, L., Zhang, X., & Zou, J.-J. (2020). Rational design, synthesis, adsorption principles and applications of metal oxide adsorbents: a review. *Nanoscale*, *12*(8), 4790–4815.

Wang, L., Xu, D., Zhang, Q., Liu, T., & Tao, Z. (2022). Simultaneous removal of heavy metals and bioelectricity generation in microbial fuel cell coupled with constructed wetland: an optimization study on substrate and plant types. *Environmental Science and Pollution Research*, *29*(1), 768–778.

Wang, R., Guan, S., Sato, A., Wang, X., Wang, Z., Yang, R., Hsiao, B. S., & Chu, B. (2013). Nanofibrous microfiltration membranes capable of removing bacteria, viruses and heavy metal ions. *Journal of Membrane Science*, *446*, 376–382.

Wang, W., Shu, G., Tian, H., & Zhu, X. (2020). Removals of Cu(II), Ni(II), Co(II) and Ag(I) from wastewater and electricity generation by bimetallic thermally regenerative electro-deposition batteries. *Separation and Purification Technology*, *235*, 116230. https://doi.org/10.1016/J.SEPPUR.2019.116230

Wang, X., Gao, Y., Wang, J., Wang, Z., & Chen, L. (2015). Chemical adsorption: another way to anchor polysulfides. *Nano Energy*, *12*, 810–815.

Wang, Y., Di, Y., Antonietti, M., Li, H., Chen, X., & Wang, X. (2010). Excellent visible-light photocatalysis of fluorinated polymeric carbon nitride solids. *Chemistry of Materials*, *22*(18), 5119–5121.

Wdowczyk, A., Szymańska-Pulikowska, A., & Gałka, B. (2022). Removal of selected pollutants from landfill leachate in constructed wetlands with different filling. *Bioresource Technology*, *353*, 127136.

Webb, P. A. (2003). Introduction to chemical adsorption analytical techniques and their applications to catalysis. *Micromeritics Instrument Corp. Technical Publications*, 1–12.

Wu, C., Gao, J., Liu, Y., Jiao, W., Su, G., Zheng, R., & Zhong, H. (2022). High-gravity intensified electrodeposition for efficient removal of Cd2+ from heavy metal wastewater. *Separation and Purification Technology*, *289*, 120809. https://doi.org/10.1016/J.SEPPUR.2022.120809

Wu, Y., Pang, H., Yao, W., Wang, X., Yu, S., Yu, Z., & Wang, X. (2018). Synthesis of rod-like metal-organic framework (MOF-5) nanomaterial for efficient removal of U (VI): batch experiments and spectroscopy study. *Science Bulletin*, *63*(13), 831–839.

Xiang, H., Min, X., Tang, C.-J., Sillanpää, M., & Zhao, F. (2022). Recent advances in membrane filtration for heavy metal removal from wastewater: A mini review. *Journal of Water Process Engineering*, *49*, 103023.

Xu, Z., Li, K., Li, W., Wu, C., Chen, X., Huang, J., Zhang, X., & Ban, Y. (2022). The positive effects of arbuscular mycorrhizal fungi inoculation and/or additional aeration on the purification efficiency of combined heavy metals in vertical flow constructed wetlands. *Environmental Science and Pollution Research*, 1–15.

Yahaya, Y. A., & Don, M. M. (2014). Pycnoporus sanguineus as potential biosorbent for heavy metal removal from aqueous solution: A review. *Journal of Physical Science*, *25*(1), 1.

Yang, J.-C., & Yin, X.-B. (2017). CoFe2O4@ MIL-100 (Fe) hybrid magnetic nanoparticles exhibit fast and selective adsorption of arsenic with high adsorption capacity. *Scientific Reports*, *7*(1), 1–15.

Yang, L., Zhang, Y., Wang, F., Luo, Z., Guo, S., & Strähle, U. (2020). Toxicity of mercury: Molecular evidence. *Chemosphere*, *245*, 125586.

Yang, Q., Zhao, Q., Ren, S., Lu, Q., Guo, X., & Chen, Z. (2016). Fabrication of core-shell Fe3O4@ MIL-100 (Fe) magnetic microspheres for the removal of Cr (VI) in aqueous solution. *Journal of Solid State Chemistry*, *244*, 25–30.

Yang, R. T. (2003). *Adsorbents: fundamentals and applications*. John Wiley & Sons.

Ye, C.-C., An, Q.-F., Wu, J.-K., Zhao, F.-Y., Zheng, P.-Y., & Wang, N.-X. (2019). Nanofiltration membranes consisting of quaternized polyelectrolyte complex nanoparticles for heavy metal removal. *Chemical Engineering Journal*, *359*, 994–1005.

Yesil, H., & Tugtas, A. E. (2019). Removal of heavy metals from leaching effluents of sewage sludge via supported liquid membranes. *Science of the Total Environment*, *693*, 133608.

Yu, G., Li, P., Wang, G., Wang, J., Zhang, Y., Wang, S., Yang, K., Du, C., & Chen, H. (2021). A review on the removal of heavy metals and metalloids by constructed wetlands: Bibliometric, removal pathways, and key factors. *World Journal of Microbiology and Biotechnology*, *37*(9), 1–12.

Yu, G., Wang, G., Chi, T., Du, C., Wang, J., Li, P., Zhang, Y., Wang, S., Yang, K., & Long, Y. (2022). Enhanced removal of heavy metals and metalloids by constructed wetlands: A review of approaches and mechanisms. *Science of The Total Environment*, 153516.

Zamora-Ledezma, C., Negrete-Bolagay, D., Figueroa, F., Zamora-Ledezma, E., Ni, M., Alexis, F., & Guerrero, V. H. (2021). Heavy metal water pollution: A fresh look about hazards, novel and conventional remediation methods. *Environmental Technology & Innovation*, *22*, 101504.

Zhang, C., Ma, J., Wu, L., Sun, J., Wang, L., Li, T., & Waite, T. D. (2021). Flow Electrode Capacitive Deionization (FCDI): Recent Developments, Environmental Applications, and Future Perspectives. *Environmental Science and Technology*, *55*(8), 4243–4267. https://doi.org/10.1021/ACS.EST.0C06552/ASSET/IMAGES/LARGE/ES0C06552_0008.JPEG

Zhang, X., Li, X., Yang, H., & Cui, Z. (2018). Biochemical mechanism of phytoremediation process of lead and cadmium pollution with Mucor circinelloides and Trichoderma asperellum. *Ecotoxicology and Environmental Safety*, *157*, 21–28.

Zhang, Y., Zhao, X., Huang, H., Li, Z., Liu, D., & Zhong, C. (2015). Selective removal of transition metal ions from aqueous solution by metal–organic frameworks. *RSC Advances*, *5*(88), 72107–72112.

Zhao, X., Wei, H., Zhao, H., Wang, Y., & Tang, N. (2020). Electrode materials for capacitive deionization: A review. *Journal of Electroanalytical Chemistry*, *873*, 114416. https://doi.org/10.1016/J.JELECHEM.2020.114416

Zheng, X., Ni, C., Xiao, W., Liang, Y., & Li, Y. (2022). Ionic liquid grafted polyethersulfone nanofibrous membrane as recyclable adsorbent with simultaneous dye, heavy metal removal and antibacterial property. *Chemical Engineering Journal*, *428*, 132111.

Zulkefeli, N. S. W., Weng, S. K., & Abdul Halim, N. S. (2018). Removal of heavy metals by polymer inclusion membranes. *Current Pollution Reports*, *4*(2), 84–92.

Paper 2: Valorization of Sargassum Biomass as Potential Material for the Remediation of Heavy-Metals-Contaminated Waters

Journal: International Journal of Environmental Research and Public Health

Impact Factor (at time of publication): 4.614

Quartile (at time of publication): Q2

Volume: 20(3)

ISSN: 1660-4601

https://doi.org/10.3390/ijerph20032559

https://www.mdpi.com/1660-4601/20/3/2559

Cd(II) and Pb(II) multicomponent adsorption onto *Sargassum spp.* untreated biomass in aqueous solution

Lázaro Adrián González Fernández[1], Amado Enrique Navarro Frómeta[2], Candy Carranza Álvarez[1,3], Rogelio Flores Ramírez[1,4], Paola Elizabeth Díaz Flores [1,5], Ventura Castillo Ramos[6], Nahum Andrés Medellín Castillo[1,7].*

[1]*Multidisciplinary Postgraduate Program in Environmental Sciences. Av. Manuel Nava 201, 2nd. floor, University Zone, 78000, San Luis Potosí, S.L.P., Mexico.*

[2]*Technological University of Izúcar de Matamoros. De Reforma 168, Campestre la Paz, 74420, Izúcar de Matamoros, Pue., Mexico.*

[3]*Faculty of Professional Studies Huasteca Zone. Romualdo del Campo 501, Rafael Curiel, 79060, Ciudad Valles, S.L.P, Mexico.*

[4]*Coordination for the Innovation and Application of Science and Technology. Av. Sierra Leona # 550, Col. Lomas 2a. Sección, 78210, San Luis Potosí, S.L.P., Mexico.*

[5]*Faculty of Agronomy and Veterinary Medicine. Carretera San Luis Potosí - Matehuala Km. 14.5 Ejido Palma de la Cruz, 78321, Soledad de Graciano Sánchez, S.L.P., Mexico.*

[6]*Department of Inorganic Chemistry, Faculty of Science, University of Granada, 18071 Granada, Spain.*

[7]*Center for Research and Postgraduate Studies of the Faculty of Engineering. Dr. Manuel Nava No. 8, West University Zone, 78290, San Luis Potosí, S.L.P., Mexico.*

**Corresponding author:* nahum.medellin@uaslp.mx.

Abstract

Sargassum spp. is a species of brown algae that is abundant in the Pacific Ocean and has become a major environmental problem in recent years. Each year hundreds of tons of these algae arrive on the beaches of the Mexican Caribbean, generating large quantities of decomposing organic matter, which has a negative impact on the region's economy and the health of its ecosystems. In this work, the characterization and lead and cadmium biosorption studies are carried out on this biomass. The collected samples were dried, milled, and sieved. Some of the characterization techniques used were Scanning Electron Microscopy with X-ray Dispersive Energy, Infrared Spectroscopy with Fourier Transform, as well as the determination of moisture percent, ashes, carbohydrates, pKa, among others. The single and binary lead and cadmium adsorption studies were carried out in batch experiments using spectroscopic measurements of the remaining

concentration in solution.The physicochemical characterization of the biomass showed that its composition is favourable for the adsorption of metal species. Its morphology, functional groups and surface charge distribution facilitate the interaction of heavy metal ions with the functional groups present in its cell wall. The adsorption capacity for Cd(II) and Pb(II) are slightly higher than 240 mg g^{-1} and 350 mg g^{-1}, respectively and are also higher than the reported for similar species or some conventional adsorbents. In the binary adsorption experiments, Pb(II) exhibited antagonism in the adsorption of Cd(II). The thermodynamic treatment of lead and cadmium adsorption on the biomass indicates that it is a spontaneous process of endothermic nature and provides evidence of the affinity of the adsorbent for lead and cadmium ions in solution.

1. Introduction

The contamination of water resources is a phenomenon of common occurrence. Drinking water in particular has been one of the hardest damaged. An important group of contaminants of interest are metals that are widely used in various industries, including electronics, mining, electroplating and metallurgy. The occurrence of heavy metal ions in industrial effluents is particularly disadvantageous because they are noxious to living organisms (Jaishankar et al., 2014).

Another water quality problem has recently emerged called *Sargassum*, a type of algae that regularly washes up on Caribbean beaches. Most information indicates that *Sargassum* is currently the biggest environmental problem in Mexico, a kind of algae epidemic out of control. Indeed, the Mexican Caribbean faces a serious environmental problem. This species of brown macroalgae has affected coastal ecosystems, causing the death of marine species such as turtles and fish (Devault et al., 2021).

It has also brought economic damage through its impact on tourist activities in the region and represents a threat to human health, due, among other factors, to its decomposition on the beaches and its high content of arsenic and heavy metals. However, the *Sargassum* itself is not the problem; given that if this macroalga were protected by governments, its benefits would be better understood and, in some cases, it could even be used for some environmental purpose (Saetan et al., 2021), for example, as a soil fertilizer.

Recent studies have established the use of alternative methodologies for the adsorption of pollutants, such as heavy metals, which use materials of biological origin such as bacteria, algae and fungi, industrial, agricultural, and urban waste, due to their great viability, low cost, and high

removal efficiency. One of the techniques used for these processes is biosorption, which consists of the selective transfer of one or more solutes from a liquid phase to a batch of solid particles of biological material, and involves the participation of various physical and chemical mechanisms depending on the various factors (González et al., 2011).

The biosorption of heavy metals in algae is mainly attributed to the properties of the cell wall, where both electrostatic attraction and the formation of complex compounds can play an essential role. The cell walls of algae and seagrasses are typically composed of a fibrillar skeleton and an amorphous matrix. Nearly all of the skeleton is made up of cellulose and the amorphous matrix is predominantly made up of alginic acid or its salt (alginate) and a smaller number of sulfated polysaccharides (fucoidans) (Davis et al., 2003).

Marine algae grow naturally on the continental shelves of seas and oceans. The Pacific coasts, in general, are covered with marine algae, which lie on the shores, without any beneficial use. On the contrary, they give a bad appearance and become waste materials that over time cause a bad smell. The great diversity of marine algae allows to increase its selectivity and efficiency. Different adsorption capacities and selectivity have been discovered by red, green, and brown algae against various heavy metals. The chemical composition and presence of different adsorption centers (fucanoids, alginates, phosphated proteins, etc.) allow greater adsorption of certain metals due to their size, degree of solvation, presence of chelating ions, molecular sieves, ion exchange with species present. in the seaweed, etc. (Davis et al., 2003).

Hence, the main objective of this work is to characterize the biomass of Sargassum spp. for use as materials to remove different metallic contaminants (Cd and Pb) from water using mono- and multi-component batch adsorption systems.

2. Materials and methods

2.1 Collection and prior treatment of Sargassum

The collection and selection of the Sargassum buxifolium is carried out from the algal biomass that reaches the Mexican Caribbean. The selection process is carried out *in situ*, considering the taxonomic and morphological characteristics reported in the specialized literature for the region (Mattio et al., 2008). After selection, the samples are washed with plenty of sea water, then dried

in the sun for 72 h and finally packed in polyethylene bags, being stored in suitable environmental conditions.

The collected species are thoroughly washed with distilled water to remove salts and other impregnated solid residues. They are then dried in an oven at 60 ºC for 24 h, and ground in an electric mill. Subsequently, they are sieved in a vibrating sieve with power regulation, using nylon sieves with an opening of 30 to 50. The fractions of each particle size are packed in high-density polyethylene bottles (Piña Leyte-Vidal et al., 2019).

2.2 Physicochemical characterization

2.2.1 Ash, humidity, and carbohydrates content

Fractions of 2 g of the Sargassum are placed in previously weighed porcelain crucibles in an oven with natural circulation at 150 ºC for 5 h, weighing the crucibles after cooling at room temperature for 30 minutes in a desiccator with silica gel. The mass obtained after this step is considered to correspond to the dry bioindicator.

Subsequently, the crucibles are placed in a muffle for 2 h at 600 ºC, repeating the cooling and weighing steps. The mass obtained after this step is considered to correspond to the ashes of the bioindicator. The ash content, expressed as a percentage, is calculated using the following equation:

$$\text{Ashes (\%)} = \frac{w(ashes)}{w(dry\ Sargassum)} \cdot 100$$

For the determination of the total carbohydrate content, the biomass is washed with distilled water to eliminate the excess of salts that could be on its surface. Electrical conductivity is measured after each wash using a conductivity meter until reaching a value equal to or less than 1 mS cm^{-1}. Later, 4.0 g of biomass are weighed and placed in 250 mL of distilled water, stirring for 24 hours in an orbital shaker. In this first step, a supernatant with polysaccharides (fraction A) is obtained.

4.0 g of biomass are weighed again and treated with a 5 % KOH solution (MERCK, quality for analysis) leaving them stirring in an orbital shaker for 24 hours at room temperature. The biomass of the supernatant containing the polysaccharides (fraction B) is centrifuged and

separated. Finally, the biomass is discarded, and fractions A and B are mixed to obtain a single extract, which is used for the determination of total carbohydrates.

For this, 2 mL of the extract are made up to the mark in 20 mL of distilled water, 2 mL of this new solution are taken, mixed with 0.5 mL of 3 % aqueous phenol in test tubes, added quickly add 5 mL of concentrated H_2SO_4 and stir. The tubes are cooled in an ice bath for 30 minutes and the optical density is measured at 490 nm in glass cuvettes with a path length of 1 cm, using a UV-Vis spectrophotometer. The standard curve is prepared by taking 2 mL of solution containing between 6 and 60 µg of glucose, mixing it with 0.5 mL of 3 % aqueous phenol in test tubes and then adding 5 mL of H_2SO_4. Controls are prepared using 2 mL of distilled water, 0.5 mL of 3 % aqueous phenol, and 5 mL of H_2SO_4.

2.2.2 Scanning Electron Microscopy Analysis (SEM/EDS)

The sample used in this analysis was washed with distilled water to remove salts deposited on the surface. Subsequently, they were dried in an oven at 60 °C. Then, the samples were analysed in a ThermoFisher Quanta 250 FEG Scanning Electron Microscope, equipped with an EDAX-DX-4 energy dispersive microanalysis system, to perform a qualitative analysis of the elements in the material surface.

2.2.3 FTIR Analysis

Infrared analysis of the sample was performed in a ThermoFisher Scientific Nicolet iS10 FTIR spectrophotometer. The sample was introduced into the spectrometer and the infrared spectrum was obtained with an ambient background (with corrections for gases present in the atmosphere). The most probable functional groups that correspond to the intensities of the bands as a function of frequency are determined, and the values of the bands are compared with the spectra of reference compounds reported in the literature.

2.2.4 Thermal Analysis

The Thermal Analysis is carried out in a TA Instruments Derivatograph model Q500 using the EA Universal Analysis 2000 Software. All thermograms are obtained with simultaneous recording of the curves DTA (Differential Thermal Analysis), TG (Thermogravimetry), T (Temperature) and DTG (Differential Thermogravimetry).

The data of the TG curves are converted into continuous thermograms with the use of software supplied by the manufacturer of the equipment, compatible with Windows, also obtaining the D1TG thermograms of the first rate of mass change (dm dt^{-1}). The error of the quantitative TG analysis that is reported is ± 2.00 %.

2.2.5 Elemental Content

The EPA PLANT TISSUE digestion procedure is used. The solution resulting from the digestion process is used to carry out the simultaneous determination of the elemental content. Measurements are carried out in an Inductively Coupled Plasma Mass Spectrometer (ICP-MS) and an Inductively Coupled Plasma Optical Emission Spectrometer (ICP-OES), both with simultaneous analysis with a solid-state detector. The blank assay is performed under the preparation conditions previously established in the digestion procedure. The results of this study are expressed in µg of the element per kg of dry material (µg kg^{-1}).

2.2.6 Point of Zero Charge (PZC) determination

PZC is quantified as described by González-Fernández et al., 2021. The adsorbed proton mass is evaluated by the following equation:

$$q_{H+} = \frac{C_N(V_B - V_M)}{m}$$

The surface charge (SC) is estimated using the following equation:

$$\mathrm{SC} = \frac{q_{H+}F}{S}$$

The SC of the materials is plotted against pH to obtain the SC distribution. The PZC is the pH at which the SC is neutral (SC=0).

2.2.7 Potentiometric titration. Determination of the pKa of bioindicators

To determine the pKa of the sorbents, we proceeded according to the method proposed by Cuizano & Navarro, 2008, with some modifications. 1.0 g of biosorbent pretreated with HCl was added to 50 mL of a KCl solution 0.1 mol L^{-1}, in order to maintain a stable ionic strength throughout the titration. It was titrated with a standardized solution of 0.1 mol L^{-1} of NaOH, in the range of pH 2 to approximately 13 using an equipment for automatic titration.

The total concentration of carboxyl groups, $[COOH]_t$ is calculated with the following equation:

$$[COOH]t \quad = \quad \frac{Ve\ [NaOH]}{m}$$

Katchalsky et al., 1954 showed that the titration curve of a polyacid can be represented by the following equation, based on the pK constants and n:

$$pH \quad = \quad \frac{pK \ - \ n\ log\ (1 - \ \alpha)}{\alpha}$$

Where α is the degree of dissociation defined in the following equation and n is an empirical constant. The equation is represented by the following expression:

$$\alpha \ = \ \frac{[COO^-]}{(C_0V_0)/(V_0 + V_b)}$$

Where V_b represents the volume of base used and C_0 is the initial concentration of acid groups calculated previously, but referred to the volume of the solution, where now V_0 replaces m. The variable [COO-] can be calculated using the load balance of the following equation, where C_b represents the concentration of the titrant:

$$[COO^-] \ = \ \frac{[H^+] + (V_bC_b)}{(V_0 + V_b) - {K_w}/{[H^+]}}$$

After pH vs log (1-α)/α linear regression analysis, the pKa and n values for the adsorbent material are determined.

2.3 Cd and Pb determination in aqueous solution.

The determination of the concentration of cadmium and lead in aqueous solution was carried out through Flame Atomic Absorption Spectrometry using Hollow Cathode Lamps and the calibration curve method. For the preparation of the primary standard of 1000 mg L^{-1} of the solutions of each metal, the necessary masses of salts of these metals were weighed and completely dissolved in water until reaching volumes of 1.0 L. From it, a secondary standard was prepared diluting an aliquot of this solution in deionized water to achieve a concentration of 100 mg L^{-1}.

With these solutions, the calibration curve were prepared in a concentration range of 1.0 to 1000 mg L^{-1}, adjusting the pH each time with NaOH and HCl solutions until reaching the desired pH. Then, the concentration of cadmium and lead was measured using a VARIAN SPECTRAA 220 Atomic Absorption Spectrometer.

2.4 Experimental data of the adsorption equilibrium of Cd and Pb.

Experimental data for adsorption equilibrium of cadmium and lead were obtained in a batch absorber using a methodology similar to the described by González-Fernández et al., 2021.

The adsorbed mass of cadmium and/or lead on the biomass of Sargassum is calculated by means of a mass balance:

$$q = \frac{V_0 C_0 - V_f C_f - \sum_{i=1}^{N} V_i C_i}{m}$$

$$V_f = V_0 - \sum_{i=1}^{N} V_i + V_a$$

The modeling of the equilibrium of the adsorption process is carried out by fitting the experimental results to the equations of the Langmuir, Freundlich and Radke-Prausnitz isotherms. These isotherms can be represented by the following expression, respectively:

$$q_e = \frac{q_m K_L C_e}{1 + K_L C_e}$$

$$q_e = K_F C_e^{1/n}$$

$$q_e = \frac{K_R C_e}{1 + a_R C_e^{\beta}}$$

The data obtained in the multicomponent equilibria are evaluated using the following isotherm models: Langmuir's unmodified multicomponent isotherm (NLMI), Langmuir's extended multicomponent isotherm (ELMI), Langmuir's modified multicomponent isotherm (MLMI), Redlich's unmodified multicomponent isotherm. -Peterson (NRPMI), modified Redlich-Peterson multicomponent isotherm with an interaction factor (MRPMI), the Sheindorf-Rebuhn-Sheintuch isotherm (SRSI) and the extended Freundlich multicomponent isotherm (EFMI). The equations of these isotherms are presented in Table 1.

Table 1. Isotherm models used to describe the experimental data in multicomponent systems.

NLMI	$q_i = \frac{q_m K_i C_i}{1 + \sum_{j=1}^{N} K_j C_j}$	ELMI	$q_i = \frac{q_{max} K_{E,i} C_i}{1 + \sum_{j=1}^{N} K_{Ej} C_j}$
MLMI	$q_i = \frac{q_{m,i} K_i (C_i/\eta_i)}{1 + \sum_{j=1}^{N} K_j (C_j/\eta_j)}$	NRPMI	$q_i = \frac{a_i C_i}{1 + \sum_{j=1}^{N} b_j C_i^{\beta_i}}$
MRPMI	$q_i = \frac{a_i (C_i/\eta_i)}{1 + \sum_{j=1}^{N} b_j (C_j/\eta_j)^{\beta_j}}$	SRSI	$q_i = k_i C_i (\sum_{j=1}^{N} a_{ij} C_j)^{\left(\frac{1}{n_i}\right)-1}$
EFMI	$q_1 = \frac{k_1 C_1^{\left(\frac{1}{n_1}\right)+x_1}}{C_1^{x_1} + y_1 C_2^{z_1}}$; $q_2 = \frac{k_2 C_2^{\left(\frac{1}{n_2}\right)+x_2}}{C_2^{x_2} + y_2 C_1^{z_2}}$		

The parameters of the competitive adsorption models were also obtained by minimizing the MC objective function. The average percentage deviation (%Des) was obtained using the following equation:

$$\%Des = 100 \cdot \frac{1}{k} \sum_{i=1}^{k} \frac{q_{ei,exp} - q_{ei,cal}}{q_{ei,exp}}$$

3. Results and Discussions

3.1 Physicochemical characterization of Sargassum

Table 2 shows the characterization of Sargassum using different analytical techniques. The moisture content of the material is conditioned by the nature of the material as reported by Piña Leyte-Vidal et al., 2019. In this case, the moisture percentage is 8.3 ± 0.6, a value that is close to that reported by Silva et al., 2008 for a species of a similar nature. The results of this study allowed corrections to be made to the amounts of each bioindicator needed in subsequent experiments based on the actual content of dry bioindicator.

The value obtained from the ash content for the Sargassum biomass was also in agreement with that reported by Silva et al., 2008. In addition, some correspondence was observed between the ash content obtained by gravimetry and the cationic content determined by ICP-OES and ICP-MS. This determined content corresponds to the amount of inorganic matter present in the biomass of Sargassum.

In the case of the total carbohydrate content (TCC) of the material, the results correspond to those reported by Kumar et al., 2015 for similar algae species. Carbohydrates have a large number of functional groups such as -COH and -OH, among others, which could provide an

effective environment for complexation and interaction with cationic metal species and could play a determining role in the uptake processes of these in aqueous solution.

Table 2. Physical and chemical characteristics of Sargassum.

TCC (ppm)	PZC	pKa	Moisture (%)	Ash (%)	Basic sites (meq g^{-1})	Acid sites (meq g^{-1})			
						Totals	Carb.	Lact.	Fen.
544.5	6.75	2.94	8.3 ± 0.6	22.2 ± 0.4	0.0836	1.3531	0.7355	0.1267	0.4909

The PZC value obtained for the material used is 6.75 (Figure 1), very close to the neutral zone of the pH range. This indicates that it is a slightly acid adsorbent, and that the concentration of basic sites is lower than that of acid sites.

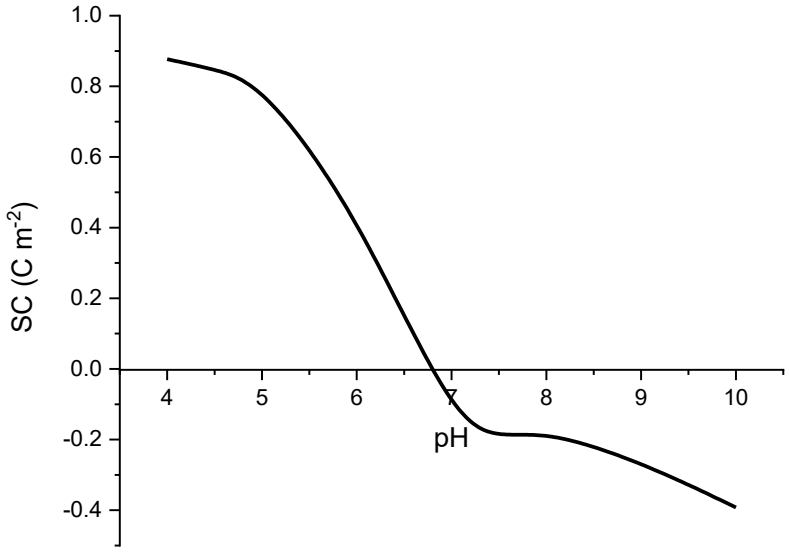

Figure 1. Surface charge change curve vs. pH for Sargassum biomass.

In the literature reviewed in this study, it was found that the PZC for this material ranged from 3.6 (Hannachi & Hafidh, 2020) to 9.0 (Moghazy et al., 2019) depending on the species and the ecosystem where it grows. Authors such as Ahmady-Asbchin & Jafari, 2012 and Kleinübing et al., 2010 have reported PZC value in the range of 6.1 to 7, within which the result obtained in this work is found.

This PZC value is useful to select the pH conditions that favor the electrostatic attraction of metallic species in solution on the absorbent. When the pH is above the PZC, the surface will

carry a negative charge, promoting the uptake of positive species from the medium (Tong et al., 2016).

The pKa of the bioindicator was determined after calculating the necessary parameters to carry out the corresponding linear regression exposed by (Katchalsky & Miller, 1954). Figure 2 shows the result.

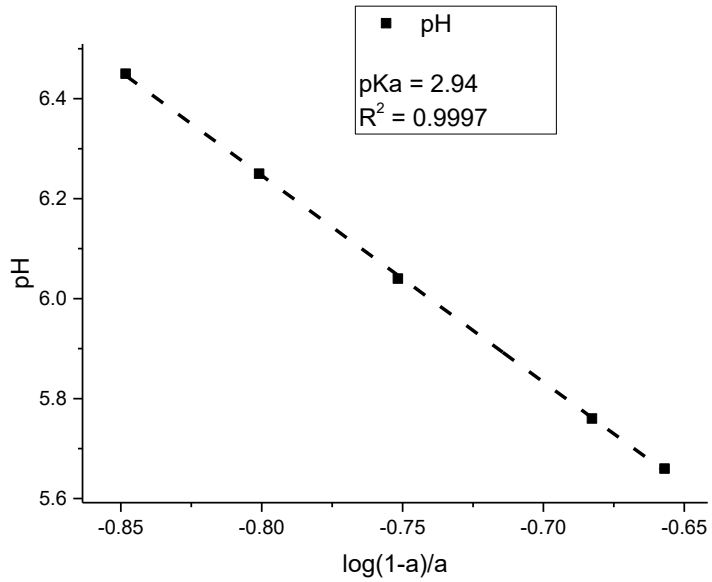

Figure 2. Linear regression to determine the pKa of Sargassum according to the Katchalsky model.

As can be seen, a pKa of 2.94 was obtained, which agrees with the average of the pKa of the functional groups in the cell wall (fucoidan and polyalginates), and supports the elevated uptake capacity for heavy metals at pH value above 3 (Blanco et al., 2005; Sheng et al., 2004).

Sheng et al., 2004 determined that the functional groups that bind to heavy metals in marine algae are carboxyl, phosphates, and sulfonic acids, in the form of phosphated proteins, carboxylic groups, alginate and fucoidans whose pKa are 3-4, 1.8-2.5, 1-4 and 1-2.5 respectively (Davis et al., 2003; Fourest & Volesky, 1995). Unfortunately, the hydroxyl group is not ionizable under these experimental conditions, so its contribution to the adsorption cannot be determined.

The concentrations of the active sites in the adsorbent are also indicated in Table 2. The amount of acid and basic sites agrees with the values reported for Sargassum biomass by Tarbaoui et al., 2016. These authors report concentrations of acidic sites more than five times higher than

those of basic sites. In the case of carboxylic groups, the reported results are consistent with those found in this work, and in the case of lactonic and phenolic groups, the results are similar.

The predominance of acidic sites over basic sites corresponds to the pKa value of the material (a value of a weak acid) and to the point of zero charge of the material, which is slightly acidic.

3.2 Elemental Content of Sargassum (ICP-MS and ICP-OES)

The concentration of minor elements (a) and minor elements (b) is shown in Figure 3. The material has high concentrations of sodium, magnesium and potassium, which is typical of materials that develop in a saline environment, since its cell wall and the polymers that compose it are capable of accumulating these elements (Silva et al., 2008).

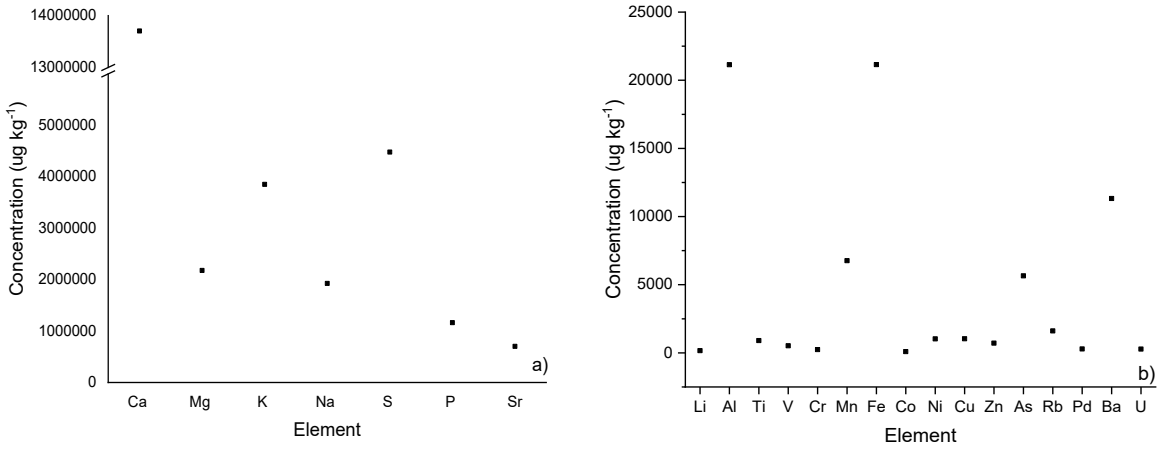

Figure 3. Elemental content (minor (a) and major (b) elements) of Sargassum biomass determined by ICP-MS and ICP-OES.

There are also high concentrations of sulphur, which are associated with sulfonic groups and their derivatives in fucoidan, the second most important and abundant polymer in the algal cell wall (Davis et al., 2003). Additionally, moderately high concentrations of aluminium and iron are noted, which may be evidence of sustained anthropogenic contamination with sources of these metals.

Other metals such as lithium, cobalt, nickel, copper, and zinc are found at low levels, which has been reported by Piña Leyte-Vidal et al., 2019. On the other hand, magnesium was the element determined with the highest concentration in the biomass. of Sargassum. This result was in

correspondence with the elemental analysis of the surface of the bioindicators performed by EDS, where magnesium appears as a major element.

These results affirm that these aforementioned elements almost exclusively determine the cationic content of the materials studied. This result agreed with what was reported in the works by Casas-Valdez et al., 2006, Yang & Chen, 2008 and Sierra-Vélez & Álvarez-León, 2009 for the specific case of *Sargassum spp*.

3.3 FT-IR Spectroscopy

Figure 4 shows the FT-IR spectrum of Sargassum. The presence of a large number of bands in these spectra is indicative of the highly complex composition of the material, associated with the existence of a large number of surface functional groups. The position of the most representative bands is shown in Table 3, together with the assignments according to the literature (Nakamoto, 2006). Through the results of the table, it was possible to verify the existence in the spectrum of signals associated with the functional groups –COOH, $–COO^-$, –OH and –NH.

These functional groups correspond to those most commonly found in the main constituent compounds of the cell wall of brown algae: alginic acid, alginates, proteins, and polysaccharides (Davis et al., 2003). In this way, the presence of these functional groups could explain the surface interaction capacity of the adsorbent with the heavy metals in the medium, either by electrostatic attraction or by complex formation. Similar results were reported by Piña Leyte-Vidal et al., 2019 for a similar material.

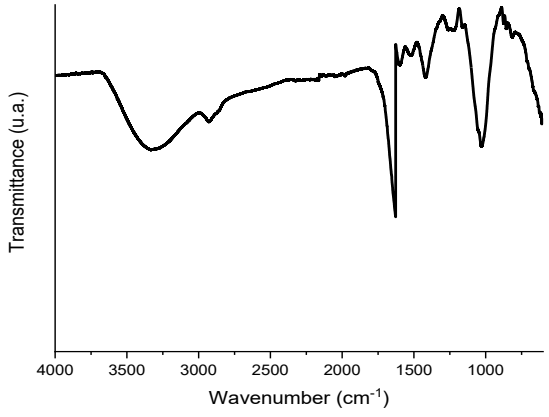

Figure 4. FT-IR spectrum of Sargassum biomass.

Table 3. Main assignments of the FT-IR spectrum of Sargassum.

Sargassum	
ῡ/cm^{-1}	**Assignation**
3350	$\nu^{asoc}_{OH + VN-H}$
2900	ν_{Csp3-H}
1650	$\nu^{as}_{COO^-}$
1400	$\nu^{s}_{COO^-}$
1050	$\nu_{CO\ (-OH)}$

3.4 Thermogravimetric analysis

Figure 5 shows the curves obtained by subjecting the sample to a heat treatment between 35 and 550 ºC. It can be observed in the differential curve (DTG), that a first peak of heat absorption appears around 95 ºC, corresponding to the evaporation of water. At this stage, pyrolysis has not yet started Wang et al., 2017. The exothermic effect generally appears when the temperature is higher than 190 °C. The main reason for this is the breakdown of soluble polysaccharides, proteins, and organic matter (Kim et al., 2013).

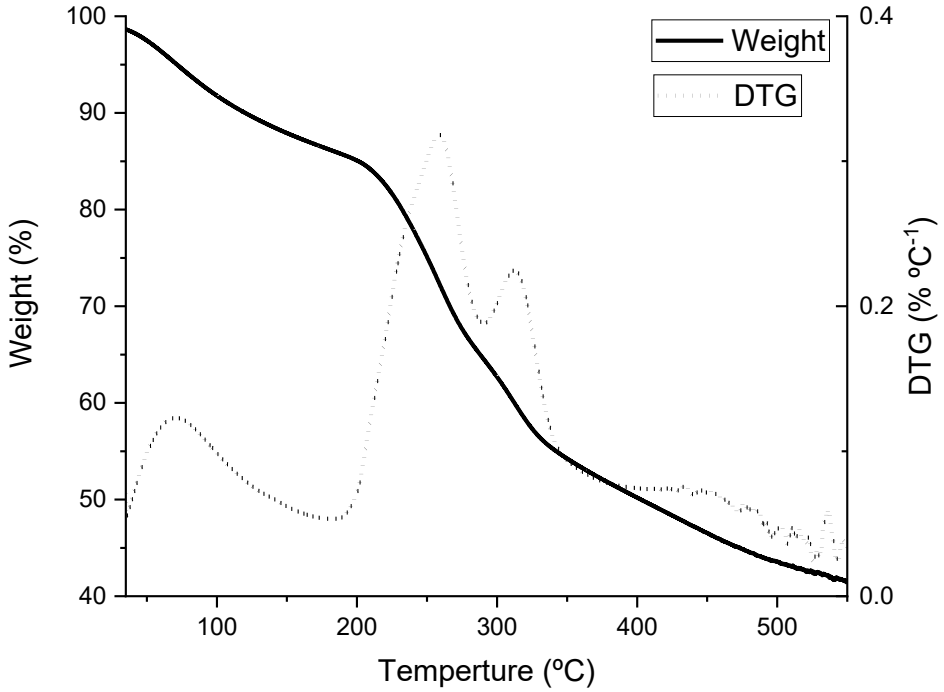

Figure 5. Thermogravimetric curves of Sargassum weight loss.

Starting at 250 °C, the pyrolysis of carbohydrates begins. There is mainly the release of gases such as methane and other derivatives of light hydrocarbons and water vapor due to the

presence of sulfated polysaccharides. CO and CO_2 are gases that evolve during this process. Above 310 °C, the pyrolysis of proteins and amino acids begins, from this reaction gases such as NH_3 are generated (Sanchez-Silva et al., 2012).

A stage can be seen in which the temperature is higher than 350 °C, in which pyrolysis is still observed as an exothermic reaction. Small exothermic peaks are observed. This could be due to the exothermic reaction when ash residues, proteins and polysaccharides participate in pyrolysis.

3.5 Scanning Electron Microscopy

The SEM/EDS analysis allowed the characterization of the adsorbent surface from the study of its morphology and the determination of its elemental composition. Figure 6 shows the SEM micrographs of the adsorbent at different magnification values and the respective EDS spectra.

In the micrographs obtained it was possible to appreciate the great morphological and structural heterogeneity existing on the surface of the material. In the EDS spectra, the signals corresponding to the elements C, O, Na, S, Mg, Cl and K, as well as Ca and Al, were observed. Some of these elements participate in the ion exchange process during biosorption and remain occupying biomass binding sites, blocking them for other metals (Naja & Volesky, 2011).

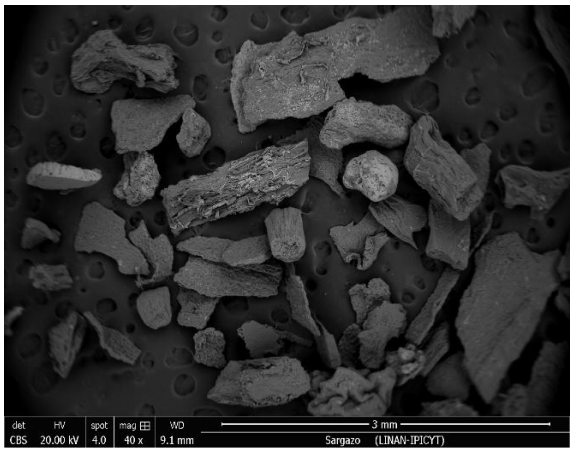

a)

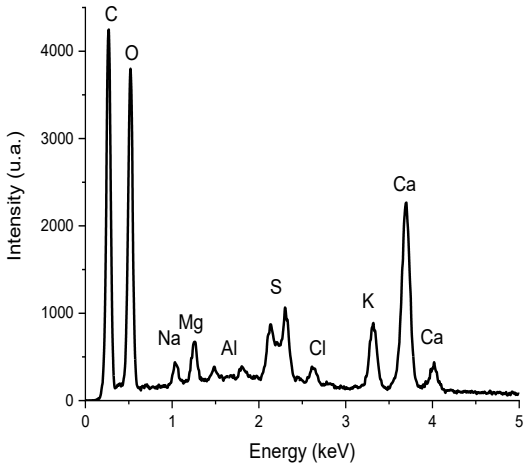

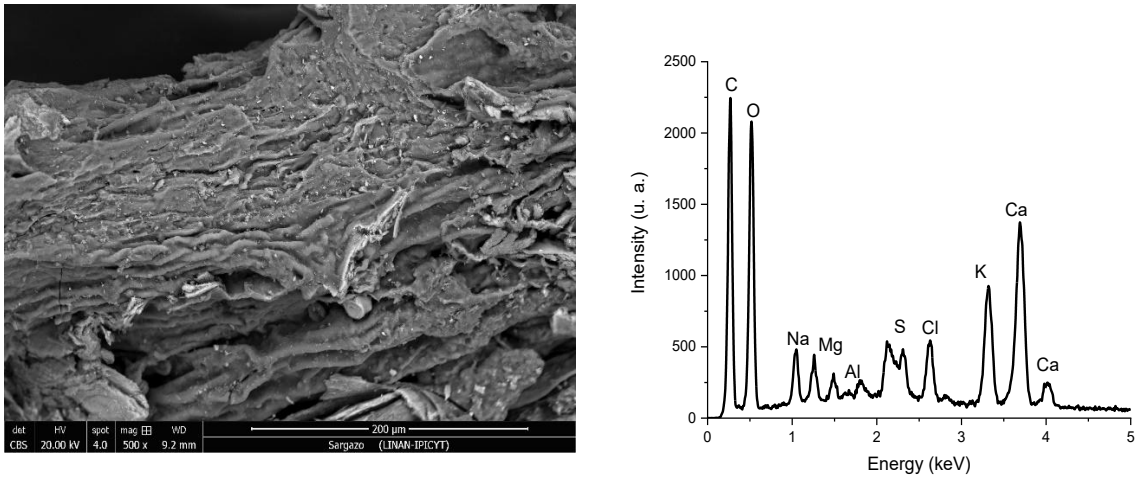

b)

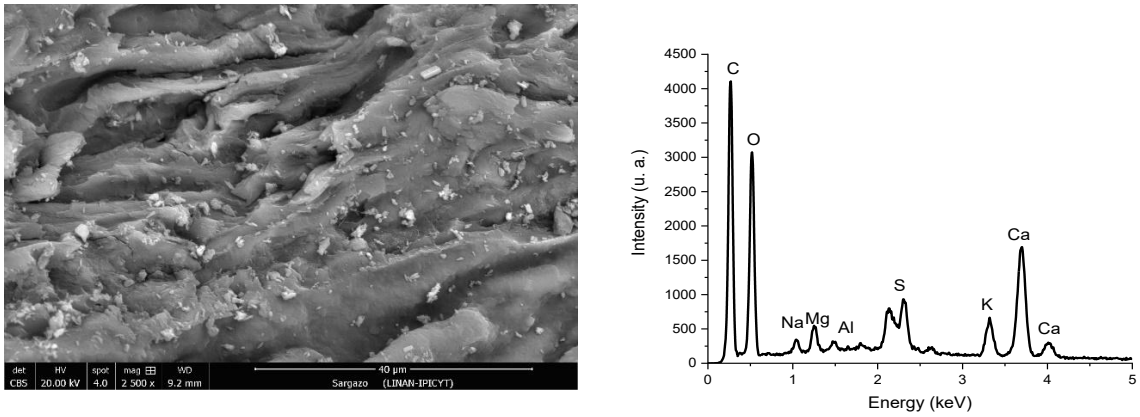

c)

Figure 6. Photomicrographs and EDS spectra of Sargassum at: a) 40 kx, b) 500 kx and c) 2500 kx.

Figure 6 shows that the material particles have a fractured and rough surface. It is also noticed that the shapes and sizes of the fragments are very unpredictable. The size distribution is not regular, and cavities and channels are present. Similar results were reported for species of algal origin by Piña Leyte-Vidal et al., 2019. In the studies of these authors, the irregularity of the coal surfaces, the rupture in their surfaces and the channels that appear can be verified.

3.6 Monocomponent adsorption isotherms

The adsorption isotherms of individual Cd(II) and Pb(II) are shown in Figure 7. In these, the experimental data described by the Radke-Prausnitz mathematical model can be observed.

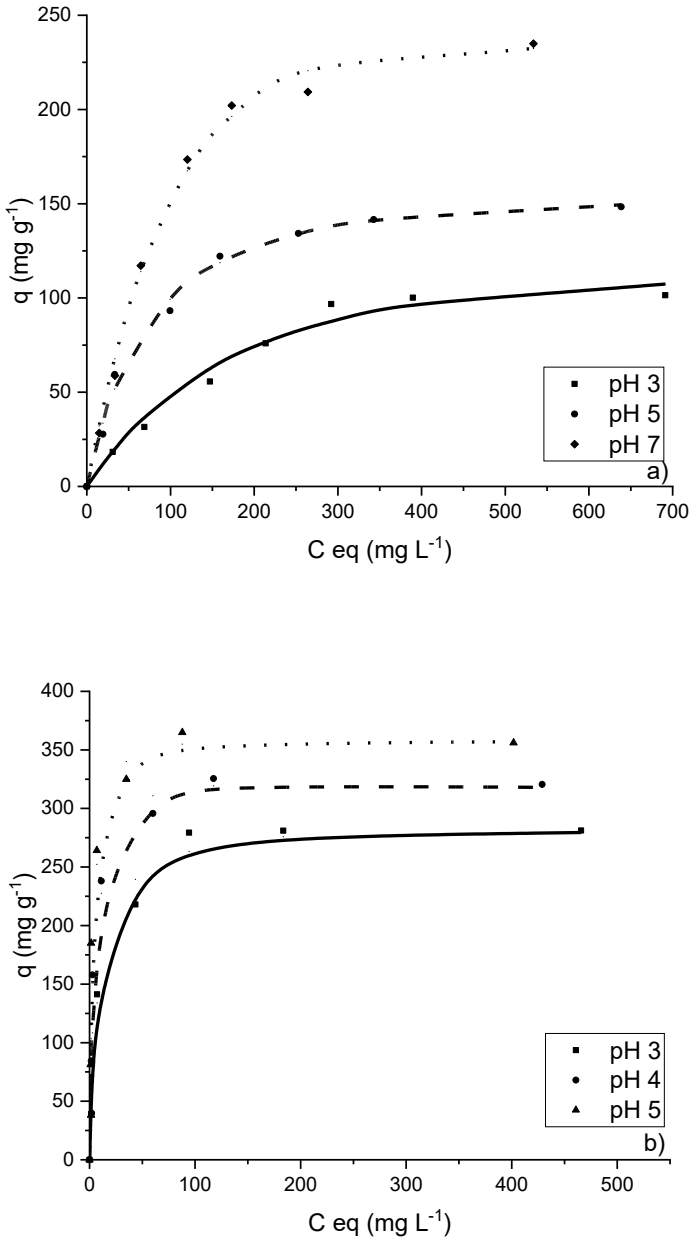

Figure 7. Monocomponent adsorption isotherms for a) Cd(II) and b) Pb(II) at 25 °C.

From the above figure it can be seen that the isotherms show two stages. The first stage with an increase in adsorption capacity with increasing metal concentration at equilibrium. This is because the material initially has a large number of active sites for the retention of metal cations. As the metal concentration increases, these positions become occupied and, for a given concentration, it becomes more difficult for the metal cations to be exchanged. From this point on,

a second stage is observed, with a decrease in the slope representing a saturation level. In this second part of the curves, the maximum experimental adsorption capacity is determined.

Table 4 shows the parameters obtained for each isotherm models for monocomponent systems. The quality of the fit was estimated by the R^2 coefficient and the Durbin-Watson statistical test for the correlation of the residuals, according to the probability values obtained for 95 % confidence (STATGRAPHICS Centurion XV software).

Table 4. Parameters of adsorption isotherm models.

Model	Parameter	Cd			Pb		
		pH 3	pH 5	pH 7	pH 3	pH 4	pH 5
Langmuir	q_m (mg g^{-1})	140 .6	169.7	287.8	286.7	332.5	366.9
	k_L (L mg^{-1})	0.005	0.013	0.011	0.129	0.179	0.304
	R^2 (%)	**95.5**	**98.6**	**97.7**	**97.9**	**93.4**	**89.1**
Freundlich	K_F (mg g^{-1})(L $mg^{-1})^{1/n}$	6.3	19.5	21.6	84.1	109.6	139.8
	n	2.2	3.0	2.5	4.5	5.0	5.5
	R^2 (%)	**87.1**	**88.7**	**87.2**	**85.7**	**75.3**	**70.5**
Redlich-Peterson	K_R (L g^{-1})	0.64	2.06	2.27	36.19	54.66	105.9
	a_R	0.001	0.008	0.001	0.135	0.140	0.267
	β	1.17	1.07	1.27	0.99	1.03	1.01
	R^2 (%)	**97.0**	**98.9**	**99.2**	**98.0**	**93.7**	**89.2**

According to the results, for all materials the best statistical fit is obtained for the R-P model. In this case, the value of the constant β, related to the fit of the experimental data to the model is very close to 1, which indicates that it is adequate for the three biosorbent species studied (Radke & Prausnitz, 1972). In addition, the value of the R-P counter has a relatively high value, indicating a good fit to the model and favorable adsorption of the analyte on the adsorbent (Bayuo et al., 2018). This behavior has also been reported by other authors (Adeogun et al., 2013).

Several studies showed that pH is an important factor influencing heavy metal biosorption (Jaishankar et al., 2014; Villanueva, 2000). pH could have an effect on the protonation of functional groups in biomass as well as metal chemistry. From Fig. 7, it can be observed for both contaminants that the adsorption capacity increases with increasing pH.

A strong pH dependence in the biosorption process is observed. The cell wall of brown algae contains sulfate, carboxyl and amino groups (Andrade et al., 2005). At low pH values, repulsive forces between the cell wall ligands and the metal cations produce a decrease of the adsorption capacity. As pH increases, more groups would become negative and attract metal ions (Aksu, 2001).

The effect of pH can also be described in relation to the competition effect between heavy metal and H^+ ions. When the pH value is low, the H^+ ions appear in higher concentration in the solution and compete for the binding or active site in the adsorbent. When the pH value is higher, the concentration of H^+ decreases and the metal cations can occupy the active sites easier (Matheickal et al., 1999).

3.7 Multicomponent adsorption isotherms

Figure 8 shows the multicomponent isotherms of cadmium (a) and lead (b) in two dimensions. In these, the experimental data are described by the Radke-Prausnitz mathematical model since it was the one that yielded the lowest %D values in all cases.

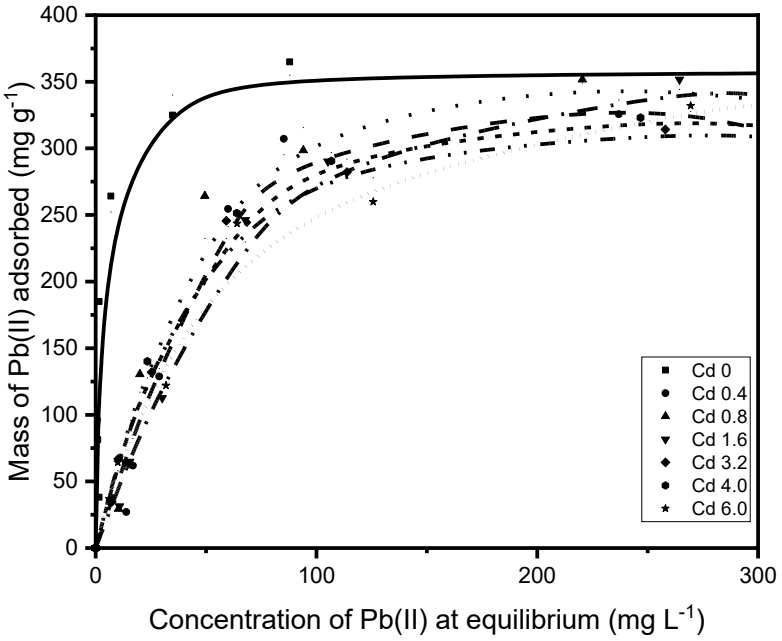

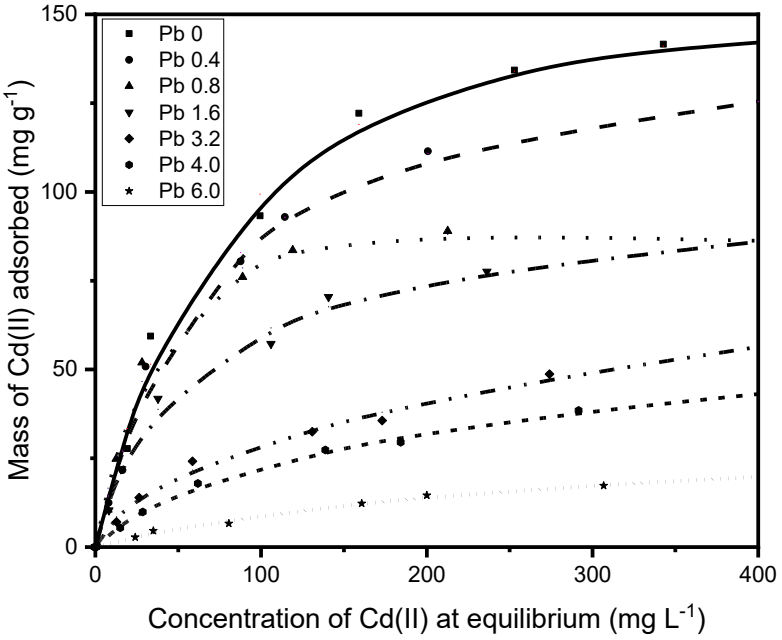

Figure 8. Binary adsorption isotherms of Cd(II)-Pb(II) on Sargassum biomass. (a) Cd(II) and (b) Pb(II) adsorption at T = 25 °C and pH = 5.0.

When analyzing the behavior of the competing isotherms it is evident that they are very similar to the simple adsorption isotherm, however the removal capacity of both Pb(II) and Cd(II) is reduced because the ions in solution can compete for the same active sites. In this case we can observe that the presence of lead significantly affects the adsorption of cadmium, however, the presence of cadmium only slightly affects the adsorption of lead, and even if the concentration of the competitive ion is increased, the capacity varies only slightly.

Figure 9 shows the experimental data in three dimensions, represented by the extended Freundlich multicomponent isotherm (EFMI) model, which reported the lowest percentage deviation among the isotherm models used to describe the data.

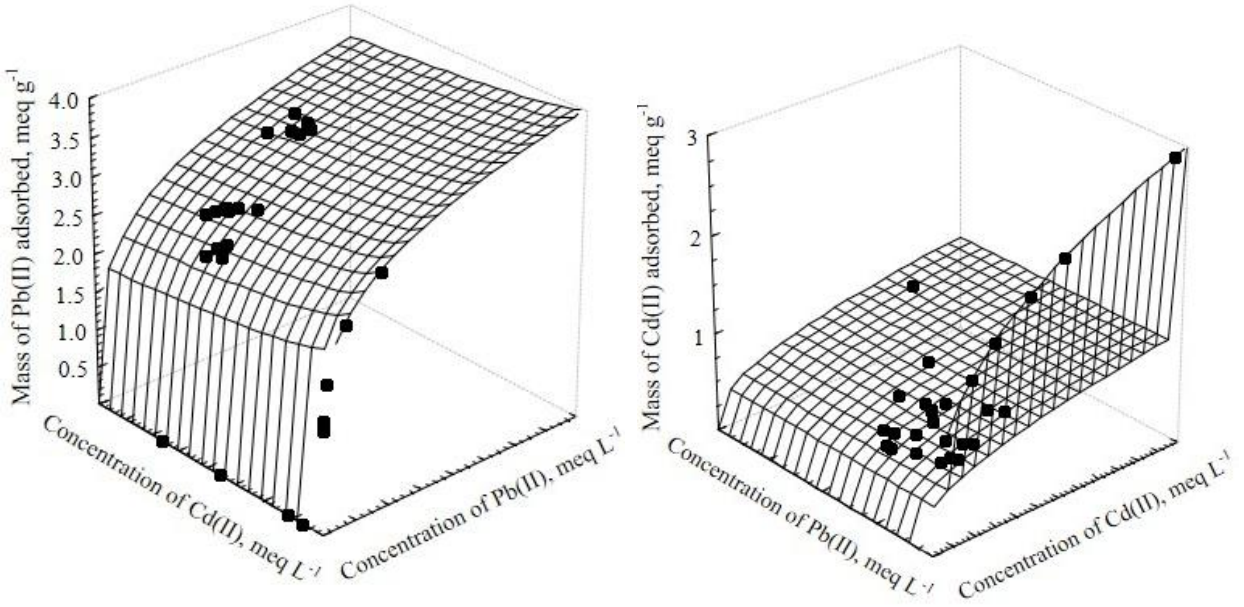

Figure 9. Multicomponent adsorption isotherms of (a) Cd(II) and (b) Pb(II) on Sargassum biomass at T = 25 °C and pH = 5.0. Adsorption surfaces are predicted with the EFMI model.

The dependence of Pb(II) adsorption on the Cd(II) concentration is clearly seen in Fig. 9. The adsorption of Pb(II) was vaguely affected by Cd(II). This results shown that Pb(II) ions show higher affinity for the active sites of Sargassum biomass than for Cd(II) ions, which is also visible in the shape of the single-component isotherms.

The selectivity ratio, S, calculated as reported by Medellin-Castillo et al., 2017, when the Pb(II) and Cd(II) concentration are equal to 4.0 meq L^{-1} (adsorption capacities are predicted from the single adsorption isotherms) has a value of 2.42. Though, S was found to be equal to 5.22 when the adsorption capacities were predicted using the EFMI model. Then, Pb(II) showed strong antagonism in the Cd(II) adsorption, although Cd(II) did not considerably affect the uptake of Pb(II).

3.8 Effect of temperature in the Cd (II) and Pb(II) adsorption onto Sargassum biomass

Fig. 10 demonstrates the effect of temperature on the adsorption capacity of Pb(II) and Cd(II) on Sargassum biomass. The procedure described for monocomponent adsorption was followed with the optimized conditions at 15 and 35 ºC.

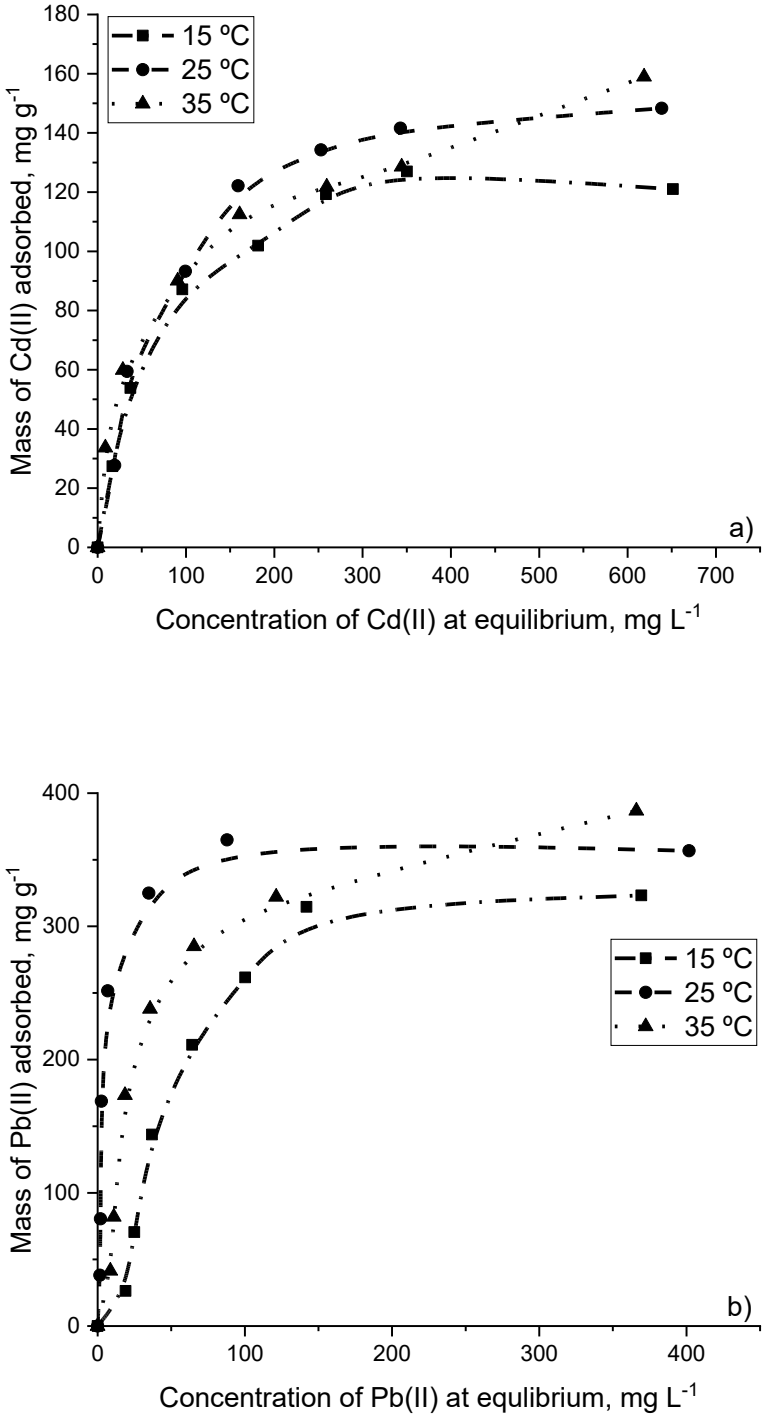

Figure 10. Effect of temperature on the adsorption capacity of (a) Cd(II) and (b) Pb(II) on Sargassum biomass.

In the previous figure it is observed that an increase in temperature during the sorption process brings about an increase in the adsorbent capacity throughout the studied range. Therefore, in this case, the enthalpy variation is positive, being an endothermic adsorption process. Similar results were obtained by Aksu, 2001 for cadmium adsorption on *C. vulgaris* and by Aravindhan et al., 2009 for dye removal on *Caulerpa scalpelliformis*.

The determination of the entropy and enthalpy of the sorption process are key to determine whether the sorption process occurs spontaneously or not from a thermodynamic point of view. The adsorption process of Pb(II), like that of Cd(II), on biomass can be assumed to be the following reversible, heterogeneous equilibrium:

$$Pb^{2+}(aq) \leftrightarrow Pb^{2+} - algae\ biomass$$

For this equilibrium, the ΔG^{o} can be determined by the following equation:

$$\Delta G^{o} = -RTlnK_c^0$$

The relationship between K_c^0 and the temperature is presented in the Van't Hoff equation:

$$lnK_c^0 = \frac{\Delta S^{o}}{R} - \frac{\Delta H^{o}}{RT}$$

The adsorption entropy change, ΔS^{o}, and the enthalpy change, ΔH^{o}, is obtained from the regression line of $\ln K_c^0$ vs 1/T. These parameters are calculated using the Langmuir isotherm, replacing the equilibrium constant K_c^0 by the Langmuir constant (K_L).

Table 5 shows the thermodynamic parameters of adsorption, determined with the values of capacity and concentrations at equilibrium at the three selected temperatures.

Table 5. Thermodynamic parameters for adsorption of Pb(II) and Cd(II) on Sargassum biomass.

T (ºC)	ΔG^{o} ($kJ\ mol^{-1}$)		ΔH^{o} ($kJ\ mol^{-1}$)		ΔS^{o} ($kJ\ mol^{-1}\ K^{-1}$)	
	Cd	**Pb**	**Cd**	**Pb**	**Cd**	**Pb**
15	-1.54	-3.32	24.35	37.06	0.09	0.14
25	-2.31	-4.44				
35	-3.34	-6.12				

The thermodynamic treatment of lead and cadmium adsorption on biomass indicates that the values of ΔG^{o} at all temperatures is negative. This result points out that chemisorption is a favourable and spontaneous mechanism for sorption of the ions on biomass (Pahlavanzadeh et al.,

2010). The positive value for ΔH^o shows the endothermic nature of the process and reaffirms that it is chemisorption that mostly governs the adsorption process in this case (He et al., 2010).

The relatively high modular ΔH^o values reaffirm the possibility that a chemisorption process is occurring (Gupta & Rastogi, 2008; Thilagan et al., 2013). The positive ΔS^o values observed are evidence of the randomness of the solid-solution interface during the adsorption process of lead and cadmium ions to biomass (Pahlavanzadeh et al., 2010), as well as being indicative of the affinity of the adsorbent for ions in solution (Saeed & Sun, 2011; Sivakumar & Palanisamy, 2009).

4. Conclusions

The physicochemical characterization of the biomass of *Sargassum spp.* collected in the Mexican Caribbean showed that both the morphology and the chemical composition of the cell wall favour the process of incorporation of metallic element ions into the cell wall. The study of the equilibrium and the thermodynamic treatment of adsorption allowed verifying that chemisorption processes could exist during the retention of Pb(II) and Cd(II) on the natural biomass of Sargassum spp.

The adsorption capacity for Cd(II) and Pb(II) are slightly higher than 240 mg g^{-1} and 350 mg g^{-1}, respectively. These values are also higher than those reported by other authors for materials of similar nature, and than those obtained for some conventional and novel adsorbents. When both chemical elements are simultaneously in solution, it is observed that *Sargassum spp.* biomass shows higher affinity for Pb(II) than for Cd(II) cations. The thermodynamic treatment of lead and cadmium adsorption on the biomass indicates that the values of ΔG^o at all temperatures is negative indicating a spontaneous process.

The results obtained in this work demonstrate that *Sargassum spp.* biomass is an excellent alternative for the removal of heavy metal elements such as cadmium and lead, compared to other more traditional adsorbents, or even novel adsorbents. The composition of the biomass as well as its physical and chemical properties make it a promising adsorbent, especially because it is a material that is usually considered a waste and that generates enormous damage to the economy and coastal ecosystems of the Caribbean region of Mexico.

5. References

Adeogun, A. I., Idowu, M. A., Ofudje, A. E., Kareem, S. O., & Ahmed, S. A. (2013). Comparative biosorption of Mn (II) and Pb (II) ions on raw and oxalic acid modified maize husk: kinetic,

thermodynamic and isothermal studies. *Applied Water Science*, *3*(1), 167–179.

Ahmady-Asbchin, S., & Jafari, N. (2012). Physicochemical studies of copper (II) biosorption from wastewater by marine brown algae Sargassum angustifolium C. Agardh (Fucales, Phaeophyceae). *International Journal on Algae*, *14*(4).

Aksu, Z. (2001). Equilibrium and kinetic modelling of cadmium (II) biosorption by C. vulgaris in a batch system: effect of temperature. *Separation and Purification Technology*, *21*(3), 285–294.

Andrade, A. D., Rollemberg, M. C. E., & Nóbrega, J. A. (2005). Proton and metal binding capacity of the green freshwater alga Chaetophora elegans. *Process Biochemistry*, *40*(5), 1931–1936.

Aravindhan, R., Rao, J. R., & Nair, B. U. (2009). Preparation and characterization of activated carbon from marine macro-algal biomass. *Journal of Hazardous Materials*, *162*(2–3), 688–694.

Bayuo, J., Pelig-Ba, K. B., & Abukari, M. A. (2018). Isotherm modeling of lead (II) adsorption from aqueous solution using groundnut shell as a low-cost adsorbent. *IOSR J Appl Chem (IOSR-JAC)*, *11*(11), 18–23.

Blanco, D. E., Llanos, B., Cuizano, N. A., Maldonado, H. J., & Navarro, A. E. (2005). Optimizacion de la adsorcion de cadmio divalente en Lessonia trabeculata mediante reticulacion con CaCl~ 2~ 7. *REVISTA-SOCIEDAD QUIMICA DEL PERU*, *71*(4), 237.

Casas-Valdez, M., Hernández-Contreras, H., Marín-Álvarez, A., Aguila-Ramírez, R. N., Hernández-Guerrero, C. J., Sánchez-Rodríguez, I., & Carrillo-Domínguez, S. (2006). El alga marina Sargassum (Sargassaceae): una alternativa tropical para la alimentación de ganado caprino. *Revista de Biología Tropical*, *54*(1), 83–92.

Cuizano, N., & Navarro, A. (2008). Biosorción de metales pesados por algas marinas: Posible solución a la contaminación a bajas concentraciones. In *Anales de la Real Sociedad Española de Química, ISSN 1575-3417, Nº. 2, 2008, pags. 120-125* (Vol. 104).

Davis, T. A., Volesky, B., & Mucci, A. (2003). A review of the biochemistry of heavy metal biosorption by brown algae. *Water Research*, *37*(18), 4311–4330.

Devault, D. A., Modestin, E., Cottereau, V., Vedie, F., Stiger-Pouvreau, V., Pierre, R., Coynel, A.,

& Dolique, F. (2021). The silent spring of Sargassum. *Environmental Science and Pollution Research*, 1–4.

Fourest, E., & Volesky, B. (1995). Contribution of sulfonate groups and alginate to heavy metal biosorption by the dry biomass of Sargassum fluitans. *Environmental Science & Technology*, *30*(1), 277–282.

González-Fernández, L. A., Medellín-Castillo, N. A., Ocampo-Pérez, R., Hernández-Mendoza, H., Berber-Mendoza, M. S., & Aldama-Aguilera, C. (2021). Equilibrium and kinetic modelling of triclosan adsorption on Single-Walled Carbon Nanotubes. *Journal of Environmental Chemical Engineering*, 106382. https://doi.org/10.1016/J.JECE.2021.106382

González, F., Romera, E., Ballester, A., Blázquez, M. L., Muñoz, J. Á., & García-Balboa, C. (2011). Algal biosorption and biosorbents. In *Microbial biosorption of metals* (pp. 159–178). Springer.

Gupta, V. K., & Rastogi, A. (2008). Biosorption of lead from aqueous solutions by green algae Spirogyra species: kinetics and equilibrium studies. *Journal of Hazardous Materials*, *152*(1), 407–414.

Hannachi, Y., & Hafidh, A. (2020). Biosorption potential of Sargassum muticum algal biomass for methylene blue and lead removal from aqueous medium. *International Journal of Environmental Science and Technology*, *17*(9), 3875–3890.

He, J., Hong, S., Zhang, L., Gan, F., & Ho, Y.-S. (2010). Equilibrium and thermodynamic parameters of adsorption of methylene blue onto rectorite. *Fresenius Environmental Bulletin*, *19*(11), 2651–2656.

Jaishankar, M., Tseten, T., Anbalagan, N., Mathew, B. B., & Beeregowda, K. N. (2014). Toxicity, mechanism and health effects of some heavy metals. *Interdisciplinary Toxicology*, *7*(2), 60.

Katchalsky, A., & Miller, I. R. (1954). Polyampholytes. *Journal of Polymer Science*, *13*(68), 57–68.

Katchalsky, A., Shavit, N., & Eisenberg, H. (1954). Dissociation of weak polymeric acids and bases. *Journal of Polymer Science*, *13*(68), 69–84.

Kim, S.-S., Ly, H. V., Kim, J., Choi, J. H., & Woo, H. C. (2013). Thermogravimetric

characteristics and pyrolysis kinetics of Alga Sagarssum sp. biomass. *Bioresource Technology*, *139*, 242–248.

Kleinübing, S. J., Vieira, R. S., Beppu, M. M., Guibal, E., & Silva, M. G. C. da. (2010). Characterization and evaluation of copper and nickel biosorption on acidic algae Sargassum filipendula. *Materials Research*, *13*(4), 541–550.

Kumar, P. S., Pavithra, J., Suriya, S., Ramesh, M., & Kumar, K. A. (2015). Sargassum wightii, a marine alga is the source for the production of algal oil, bio-oil, and application in the dye wastewater treatment. *Desalination and Water Treatment*, *55*(5), 1342–1358.

Matheickal, J. T., Yu, Q., & Woodburn, G. M. (1999). Biosorption of cadmium (II) from aqueous solutions by pre-treated biomass of marine alga Durvillaea potatorum. *Water Research*, *33*(2), 335–342.

Mattio, L., Payri, C. E., & Stiger-Pouvreau, V. (2008). TAXONOMIC REVISION OF SARGASSUM (FUCALES, PHAEOPHYCEAE) FROM FRENCH POLYNESIA BASED ON MORPHOLOGICAL AND MOLECULAR ANALYSES 1. *Journal of Phycology*, *44*(6), 1541–1555.

Medellin-Castillo, N. A., Padilla-Ortega, E., Regules-Martínez, M. C., Leyva-Ramos, R., Ocampo-Pérez, R., & Carranza-Alvarez, C. (2017). Single and competitive adsorption of Cd (II) and Pb (II) ions from aqueous solutions onto industrial chili seeds (Capsicum annuum) waste. *Sustainable Environment Research*, *27*(2), 61–69.

Moghazy, R. M., Labena, A., & Husien, S. (2019). Eco-friendly complementary biosorption process of methylene blue using micro-sized dried biosorbents of two macro-algal species (Ulva fasciata and Sargassum dentifolium): Full factorial design, equilibrium, and kinetic studies. *International Journal of Biological Macromolecules*, *134*, 330–343.

Naja, G., & Volesky, B. (2011). The mechanism of metal cation and anion biosorption. In *Microbial biosorption of metals* (pp. 19–58). Springer.

Nakamoto, K. (2006). Infrared and R aman spectra of inorganic and coordination compounds. *Handbook of Vibrational Spectroscopy*.

Pahlavanzadeh, H., Keshtkar, A. R., Safdari, J., & Abadi, Z. (2010). Biosorption of nickel (II) from aqueous solution by brown algae: Equilibrium, dynamic and thermodynamic studies.

Journal of Hazardous Materials, *175*(1–3), 304–310.

Piña Leyte-Vidal, J. J., González-Fernández, L. A., Gutiérrez-Artiles, O., Márquez-Llauger, L., & Del Cristo, T. A. (2019). Caracterización de tres bioindicadores de contaminación por metales pesados. *Revista Cubana de Química*, *31*(2), 293–308.

Radke, C. J., & Prausnitz, J. M. (1972). Adsorption of organic solutes from dilute aqueous solution of activated carbon. *Industrial & Engineering Chemistry Fundamentals*, *11*(4), 445–451.

Saeed, T., & Sun, G. (2011). A comparative study on the removal of nutrients and organic matter in wetland reactors employing organic media. *Chemical Engineering Journal*, *171*(2), 439–447.

Saetan, U., Nontasak, P., Palasin, K., Saelim, H., Wonglapsuwan, M., Mayakun, J., Pongparadon, S., & Chotigeat, W. (2021). Potential health benefits of fucoidan from the brown seaweeds Sargassum plagiophyllum and Sargassum polycystum. *Journal of Applied Phycology*, 1–8.

Sanchez-Silva, L., López-González, D., Villaseñor, J., Sánchez, P., & Valverde, J. L. (2012). Thermogravimetric–mass spectrometric analysis of lignocellulosic and marine biomass pyrolysis. *Bioresource Technology*, *109*, 163–172.

Sheng, P. X., Ting, Y.-P., Chen, J. P., & Hong, L. (2004). Sorption of lead, copper, cadmium, zinc, and nickel by marine algal biomass: characterization of biosorptive capacity and investigation of mechanisms. *Journal of Colloid and Interface Science*, *275*(1), 131–141.

Sierra-Vélez, L., & Álvarez-León, R. (2009). Comparación Bromatológica de las algas nativas (Gracilariopsis tenuifrons, Sargassum filipendula) y exóticas (Kappaphycus Alvarezii) del caribe colombiano. *Boletín Científico. Centro de Museos. Museo de Historia Natural*, *13*(2), 17–25.

Silva, V. M. da, Silva, L. A., Andrade, J. B. de, Veloso, M. C., & Santos, G. V. (2008). Determination of moisture content and water activity in algae and fish by thermoanalytical techniques. *Quimica Nova*, *31*(4), 901–905.

Sivakumar, P., & Palanisamy, P. N. (2009). Adsorption studies of basic Red 29 by a non-conventional activated carbon prepared from Euphorbia antiquorum L. *Int. J. Chem. Tech. Res*, *1*(3), 502–510.

Tarbaoui, M., Oumam, M., Fourmentin, S., Benzina, M., Bennamara, A., & Abourriche, A. (2016). Development of A New Biosorbent Based on The Extract Residue of Marine Alga Sargassum Vulgare: Application in Biosorption of Volatile Organic Compounds. *World Journal of Innovative Research*, *1*(2), 262563.

Thilagan, J., Gopalakrishnan, S., & Kannadasan, T. (2013). Thermodynamic study on adsorption of Copper (II) ions in aqueous solution by Chitosan blended with Cellulose & cross linked by Formaldehyde, Chitosan immobilised on Red Soil, Chitosan reinforced by Banana stem fibre. *International Journal of Scientific Research Engineering & Technology*, *2*(1).

Tong, Y., Mayer, B. K., & McNamara, P. J. (2016). Triclosan adsorption using wastewater biosolids-derived biochar. *Environmental Science: Water Research & Technology*, *2*(4), 761–768.

Villanueva, R. O. C. (2000). Biosorption of heavy metals by use of microbial biomass. *Revista Latinoamericana de Microbiología*, *42*(3), 131–143.

Wang, S., Hu, Y., He, Z., Wang, Q., & Xu, S. (2017). Study of pyrolytic mechanisms of seaweed based on different components (soluble polysaccharides, proteins, and ash). *Journal of Renewable and Sustainable Energy*, *9*(2), 23102.

Yang, L., & Chen, J. P. (2008). Biosorption of hexavalent chromium onto raw and chemically modified Sargassum sp. *Bioresource Technology*, *99*(2), 297–307.

Paper 3: Algal-Based Carbonaceous Materials for Environmental Remediation: Advances in Wastewater Treatment, Carbon Sequestration, and Biofuel Applications

Journal: Processes

Impact Factor (JCR): 2.8

Quartile: Q2

Volume: 13(2)

ISSN (electronic): 2227-9717

https://doi.org/10.3390/pr13020556

https://www.mdpi.com/2227-9717/13/2/556

Algal-Based Carbonaceous Materials for Environmental Remediation: Advances in Wastewater Treatment, Carbon Sequestration, and Biofuel Applications

Lázaro Adrián González Fernández [1,2,], Nahum Andrés Medellín Castillo [1,3,*], Manuel Sánchez Polo [2], Amado Enrique Navarro Frómeta [4] and Javier Ernesto Vilasó Cadre [5]*

[1] *Multidisciplinary Postgraduate Program in Environmental Sciences, Av. Manuel Nava 201, 2nd. Floor, University Zone, San Luis Potosí 78000, Mexico*

[2] *Faculty of Sciences, University of Granada, 18071 Granada, Spain; mansanch@ugr.es*

[3] *Center for Research and Postgraduate Studies, Faculty of Engineering, Autonomous University of San Luis Potosi, Dr. Manuel Nava No. 8, West University Zone, San Luis Potosí 78290, Mexico*

[4] *Food and Environmental Technology Department, Technological University of Izucar de Matamoros, De Reforma 168, Campestre La Paz, Izúcar de Matamoros 74420, Mexico; navarro4899@gmail.com*

[5] *Institute of Metallurgy, Autonomous University of San Luis Potosí, Sierra Leona Av. 550, Lomas 2nd Section, San Luis Potosí 78210, Mexico; a321418@alumnos.uaslp.mx*

***** *Correspondence: lazaroadrian1995@gmail.com (L.A.G.F.); nahum.medellin@uaslp.mx (N.A.M.C.)*

Abstract: Water pollution from industrial, municipal, and agricultural sources is a pressing global concern, necessitating the development of sustainable and efficient treatment solutions. Algal biomass has emerged as a promising feedstock for the production of carbonaceous adsorbents due to its rapid growth, high photosynthetic efficiency, and ability to thrive in wastewater. This review examines the conversion of algal biomass into biochar and hydrochar through pyrolysis and hydrothermal processes, respectively, and evaluates their potential applications in wastewater treatment, carbon sequestration, and biofuel production. Pyrolyzed algal biochars typically exhibit a moderate to high carbon content and a porous structure but require activation treatments (e.g., KOH or $ZnCl_2$) to enhance their surface area and adsorption capabilities. Hydrothermal carbonization, conducted at lower temperatures (180–260 °C), produces hydrochars rich in oxygenated functional groups with enhanced cation exchange capacities, making them effective for pollutant removal. Algal-derived biochars and hydrochars have been successfully applied for the adsorption of heavy metals, dyes, and pharmaceutical contaminants, with adsorption capacities significantly increasing through post-treatment modifications. Beyond wastewater treatment, algal biochars serve as effective carbon sequestration materials due to their stable structure and high carbon retention. Their application as soil amendments enhances long-term carbon storage and improves soil fertility. Additionally, algal biomass plays a key role in biofuel production, particularly for biodiesel synthesis, where microalgae's high lipid content facilitates bio-oil

generation. Hydrochars, with energy values in the range of 20–26 MJ/kg, are viable solid fuels for combustion and co-firing, supporting renewable energy generation. Furthermore, the integration of these materials into bioenergy systems allows for waste valorization, pollution control, and energy recovery, contributing to a sustainable circular economy. This review provides a comprehensive analysis of algal-derived biochars and hydrochars, emphasizing their physicochemical properties, adsorption performance, and post-treatment modifications. It explores their feasibility for large-scale wastewater remediation, carbon capture, and bioenergy applications, addressing current challenges and future research directions. By advancing the understanding of algal biomass as a multifunctional resource, this study highlights its potential for environmental sustainability and energy innovation.

Keywords: algal biochar; hydrothermal carbonization; wastewater treatment; carbon sequestration; biofuel production

1. Introduction

Water pollution from industrial, municipal, and agricultural sources remains a critical global challenge, necessitating innovative and sustainable approaches for wastewater treatment. Conventional treatment methods, such as coagulation, flocculation, ion exchange, and membrane technologies, while effective, are often hindered by high operational costs, energy consumption, and the generation of secondary pollutants [1]. Consequently, the development of cost-effective, environmentally friendly, and efficient adsorbents has become imperative. Algal biomass, characterized by rapid growth rates, high photosynthetic efficiency, and the ability to thrive on non-arable land and wastewater, emerges as a promising feedstock for the production of carbonaceous adsorbents [2]. Conventional methods, such as activated carbon adsorption, membrane filtration, and advanced oxidation processes, are widely used for removing contaminants from water. Activated carbon, for instance, is highly effective in adsorbing organic pollutants, but its high operational cost and limited reusability are key drawbacks. Membrane filtration techniques, including reverse osmosis, provide excellent removal of dissolved contaminants but often suffer from issues like membrane fouling and high energy consumption. Advanced oxidation processes, such as ozonation and UV-H_2O_2, are effective in degrading persistent contaminants but can be energy-intensive and require careful handling of reactive chemicals [3]. In contrast, biochar and hydrochar are emerging as promising alternatives in the

field of water treatment. Derived from biomass via pyrolysis or hydrothermal carbonization, both materials offer high surface areas and porous structures, making them efficient adsorbents for various contaminants. Biochar and hydrochar are not only cost-effective and sustainable but also exhibit the potential for reusability and regeneration, thus addressing some of the limitations of traditional methods. This paper explores the effectiveness of these materials for water remediation, comparing them to conventional techniques in terms of performance, sustainability, and economic feasibility [4].

Among the various conversion techniques, pyrolysis stands out as a widely used thermochemical method for transforming algal biomass into biochar under oxygen-limited conditions. Algal biochar typically exhibits a porous structure, a moderate to high carbon content, and oxygenated functional groups, with pyrolysis temperatures ranging from 300 to 650 °C. However, its surface area (1–50 m^2/g) is often smaller than that of terrestrial biochars, necessitating activation processes, such as KOH or $ZnCl_2$ treatments, to enhance adsorptive performance [5,6]. Alternatively, hydrothermal processes provide efficient pathways for wet algal biomass conversion. Hydrothermal carbonization, conducted at moderate temperatures (180–260 °C), produces hydrochar, a carbon-rich solid with high concentrations of oxygenated functional groups and enhanced cation-exchange capacities, making it particularly effective for wastewater treatment [7].

Hydrothermal liquefaction, primarily designed for biocrude oil production, also generates solid residues with potential adsorptive applications [8]. Post-treatment modifications play a crucial role in optimizing the performance of algal-derived biochars and hydrochars. Chemical activation using agents such as KOH, $ZnCl_2$, or acidic treatments significantly enhances surface area, porosity, and functional group diversity, which are essential for efficient pollutant adsorption. For instance, KOH activation has been reported to increase the BET surface area of algal hydrochar by up to two orders of magnitude, leading to improved removal efficiencies for heavy metals and organic dyes [9]. Additionally, algal chars exhibit a moderate to high carbon content (10–60%) and high ash levels, which, while detrimental for fuel applications, can be advantageous for wastewater treatment due to the presence of mineral components that enhance cation-exchange capacity [10]. In practical applications, algal-derived carbonaceous materials have demonstrated efficacy in removing heavy metals such as Pb, Cd, Cu, and Cr through mechanisms such as ion exchange and surface complexation. For example, HTC-derived hydrochar from *Sargassum*

hornerri has shown high efficiency in Cr removal, while biochars from *Chlorella vulgaris* exhibit significant Cd adsorption capacities. Furthermore, algal-based adsorbents have proven effective in mitigating dye pollution from the textile industry, with activated hydrochars achieving adsorption capacities of up to 714 mg/g for methylene blue (MB), facilitated by an optimized surface area and functional group composition [11]. Similarly, pharmaceutical contaminants, including antibiotics and endocrine disruptors, have been effectively removed using chemically activated algal chars, which exhibit increased nitrogen-rich functional groups that enhance affinity for pharmaceutical molecules. Beyond wastewater treatment, algal biochars and hydrochars offer additional environmental benefits, including their use as soil amendments. Their nutrient-rich composition improves soil fertility and water retention, promoting sustainable agricultural practices.

Beyond wastewater treatment, algal chars have demonstrated significant potential in carbon capture, sequestration, and storage. Due to their high carbon content and stable structure, these materials can act as long-term carbon sinks, effectively reducing atmospheric CO_2 levels. Algal biochars have been explored for their ability to adsorb CO_2 and store it in a stable form, making them valuable in climate change mitigation strategies. Their porous nature and functional group composition enhance their CO_2 uptake capacity, providing a renewable and sustainable approach to carbon sequestration. Furthermore, algal biochars can be utilized as soil amendments to promote carbon retention in agricultural lands, further contributing to long-term carbon storage and improved soil health [12].

Algal biomass also plays a crucial role in biofuel production, offering a renewable alternative to fossil fuels. Microalgae, with their high lipid content and rapid growth rates, are particularly promising candidates for biodiesel production. Thermochemical processes such as pyrolysis and hydrothermal liquefaction can convert algal biomass into bio-oil, which can be further upgraded into transportation fuels. Additionally, algal biochars derived from biofuel production residues can be repurposed for environmental applications, creating a closed-loop system that maximizes resource efficiency. The integration of algal biochars into bioenergy systems not only supports sustainable fuel production but also provides additional environmental benefits, such as waste valorization and carbon reduction [13].

Moreover, the use of algal hydrochars in bioenergy applications extends beyond liquid fuels. With energy values ranging from 20 to 26 MJ/kg, algal hydrochars can be utilized as solid fuels for direct combustion or co-firing with conventional fuels. Their high carbon content and

energy density make them a viable option for renewable energy generation. Additionally, advancements in hydrochar activation techniques can enhance their properties, making them suitable for use in fuel cells, gasification, and other advanced energy applications [14]. By integrating algal-derived biochars and hydrochars into carbon capture and bioenergy frameworks, a sustainable and multifunctional approach to environmental management can be achieved.

This review aims to provide a comprehensive analysis of the potential of algal-derived biochars and hydrochars as adsorbents for wastewater treatment while evaluating their physicochemical properties and the role of post-treatment modifications in enhancing adsorption efficiency. Additionally, it explores the feasibility of integrating these materials into large-scale wastewater remediation processes and their potential applications in bioenergy generation, carbon capture, and sequestration. By critically examining the current state of research and identifying key challenges, this study seeks to advance the understanding of algal biomass as a versatile and sustainable solution for environmental remediation.

2. Bibliography Analysis

This review was carried out through a structured approach involving the collection, classification, analysis, and synthesis of information following the PRISMA guidelines [15]. The process commenced with comprehensive literature searches across prominent academic databases, such as Web of Science, Scopus, and CNKI, with a focus on peer-reviewed journal articles to compile the most recent advancements in algae-based technologies for environmental applications. After a thorough screening of abstracts based on predefined inclusion criteria (relevance to algae-based environmental applications, peer-reviewed journal articles, publication date, availability of full text, language, scientific quality, and exclusion of redundant studies), 1245 papers were selected for an in-depth full-text review. Ultimately, approximately 190 studies were incorporated into this analysis. Furthermore, additional data were gathered from publicly accessible sources, including reports from international organizations, governmental publications, and corporate websites. The reviewed literature spans several decades, covering research from the 1970s to 2024. By critically evaluating existing algae-based technologies for environmental applications, this review highlights current limitations and challenges while suggesting potential solutions and future research directions for further development.

3. Algae and Algal-Based Materials

Algae are a diverse group of photosynthetic organisms commonly found in aquatic environments. They exhibit a wide range of structural complexities, from unicellular microscopic forms to large multicellular species. As a polyphyletic group, algae include both prokaryotic species, such as cyanobacteria (blue-green algae), and eukaryotic species like green algae (*Chlorophyceae*), diatoms (*Bacillariophyceae*), and golden algae (*Chrysophyceae*) [16]. These organisms play a fundamental role in global ecosystems by contributing to primary production, supporting food chains, and maintaining biodiversity [17].

Algae are composed of essential biological compounds, including proteins, lipids, carbohydrates, cellulose, vitamins, minerals, and unique bioactive substances such as polysaccharides and pigments. The precise composition varies among species, influencing their applications in various industries. Key biochemical components—lipids, carbohydrates, and proteins—are particularly valuable for producing biofuels, pharmaceuticals, cosmetics, and food products [8,18].

Algae are generally categorized into two main groups based on their size and structural characteristics: macroalgae and microalgae (Figure 1). Macroalgae, often referred to as seaweeds, are large, multicellular organisms commonly found in marine environments, where they attach to surfaces such as rocks and coral reefs. Although their growth rate is relatively slow, their substantial biomass contributes significantly to carbon sequestration [19].

In contrast, microalgae are microscopic, single-celled organisms that thrive in a wide range of aquatic environments, including freshwater, brackish water, and marine systems. These organisms exhibit high photosynthetic efficiency and rapid reproduction, making them well-suited for large-scale biomass production [20]. Despite their structural differences, both macroalgae and microalgae play critical roles in carbon capture, utilization, and storage, making them valuable components of sustainable environmental and bioenergy solutions.

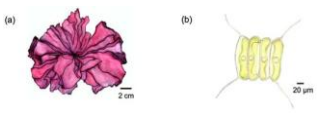

Figure 1. Diagram of algal structures: (**a**) *Porphyra umbilicalis* (macroalgae); (**b**) *Scenedesmus* (microalgae). Reproduced from Pereira, 2021 [21], under terms of Creative Commons Attribution (CC BY) license.

Environmental conditions exert a significant influence on the biochemical composition of algae, thereby affecting the characteristics of the carbon materials derived from them. Light intensity, for instance, plays a critical role in photosynthetic efficiency and carbon fixation. Under optimal light conditions, algae efficiently convert inorganic carbon into organic molecules, resulting in a biomass rich in structural carbohydrates and other carbon-based compounds. However, excessive light exposure can induce photo-oxidative stress, prompting the algae to synthesize protective compounds such as carotenoids and specific polysaccharides. These adaptations not only mitigate cellular damage but also modify the overall carbon profile of the algal biomass [22].

Temperature is another crucial factor that affects metabolic rates and enzymatic activities in algae. Moderate increases in temperature generally enhance metabolic processes and promote efficient carbon assimilation, while extreme temperatures may lead to stress responses that shift metabolic pathways. Under such stress, algae often redirect carbon flux from growth-related processes to the accumulation of storage compounds, including lipids and carbohydrates. This shift in metabolic balance can alter both the quality and the quantity of carbon materials available for downstream applications [23]. Nutrient availability further modulates the carbon composition; nutrient-limited conditions typically result in an elevated carbon-to-nitrogen ratio as algae divert fixed carbon into storage molecules rather than growth. Elevated CO_2 concentrations also enhance photosynthetic carbon fixation, potentially increasing the proportion of carbon incorporated into structural and storage compounds [24].

Additionally, variations in pH and salinity introduce osmotic and ionic stresses that influence cell wall composition and the synthesis of compatible solutes. Such environmental stresses lead to modifications in the types and arrangements of carbon-rich biomolecules within the cells, ultimately impacting the structural properties and reactivity of the derived carbon materials. The cumulative effects of these environmental parameters are especially important when algal biomass is employed as a feedstock for biofuels, biochar, or activated carbon production, where the nature of the precursor material directly determines the performance characteristics of the final product [22].

Future global conditions, particularly those driven by climate change, are poised to significantly influence the production and exploitation of new carbon materials. Climate change, characterized by rising global temperatures, altered precipitation patterns, and increased

atmospheric CO_2 concentrations, directly impacts the biomass sources used as precursors in carbon material production. For instance, variations in these environmental parameters may affect the growth rates and biochemical composition of algae, a critical feedstock, thereby altering both the efficiency of carbon fixation and the quality of the resulting carbon materials [2].

In addition to these direct impacts on biomass productivity, the increased frequency and intensity of extreme weather events—such as droughts, floods, and storms—pose considerable challenges to the stability of biomass production systems. Such events can disrupt the availability of essential resources, including water and nutrients, which are vital for consistent and high-quality biomass cultivation. Consequently, these fluctuations can lead to variability in the raw materials used for carbon synthesis, potentially affecting the efficiency, scalability, and economic viability of production processes. Moreover, the broader implications of climate change are expected to drive significant shifts in environmental policies and regulatory frameworks. As governments and international bodies implement more stringent measures to mitigate climate change, industries involved in the production of carbon materials may be compelled to adopt more sustainable practices and technologies. This regulatory evolution is likely to incentivize investments in research and development aimed at enhancing process efficiency, reducing environmental footprints, and integrating renewable energy sources into production chains [25].

Given these multifaceted challenges and opportunities, it is imperative to adopt a multidisciplinary approach that considers both the direct environmental impacts on biomass precursors and the indirect effects mediated through policy and regulatory changes. Future research should focus on developing adaptive strategies and robust process models that integrate climate projections with technological innovations. Such an approach will be essential for ensuring that the production and exploitation of new carbon materials remain resilient and sustainable in the context of evolving global environmental conditions.

4. Algal-Based Hydrochars and Biochars for Pollutants Uptake

Over time, water used in industrial processes that becomes contaminated with heavy metals has emerged as a critical environmental and public health issue. The rapid pace of industrialization and urban growth has led to the persistent release of hazardous substances—including heavy metals, synthetic dyes, pesticides, and various organic compounds—into river systems [26]. These contaminants primarily originate from wastewater produced by industries such as textiles,

electroplating, paper manufacturing, leather tanning, and food processing [27]. Given their toxic and non-biodegradable nature, these pollutants tend to accumulate in the tissues of flora, fauna, and humans, leading to severe health consequences such as central nervous system damage, dermatitis, cancer, kidney failure, and impairments to liver and reproductive functions [2].

As a result, it is essential to devise efficient and cost-effective methods for the removal of heavy metals and other contaminants from industrial wastewater before its discharge into natural water bodies. In an effort to overcome the limitations of traditional purification techniques, recent research has increasingly explored the use of novel sorbents derived from renewable resources, such as hydrochars [28,29]. Hydrochar is a carbon-rich material produced through the HTC process, which involves the conversion of wet biomass into a solid, charcoal-like substance under high temperature and pressure, typically in the presence of water. Unlike biochar, which is produced through pyrolysis in the absence of oxygen, hydrochar is generated in an aqueous environment, making it particularly suitable for processing moist feedstocks such as food waste, agricultural residues, and algae. The HTC process typically occurs at temperatures ranging from 180 to 250 °C and pressures between 2 and 6 MPa [30]. Although hydrochars typically exhibit relatively low surface area and porosity, the presence of chemically active functional groups—namely ketone, carboxyl (COOH), and hydroxyl groups—on their surfaces endows them with adequate adsorption capabilities [31]. Numerous studies have investigated the potential of hydrochars produced from various precursors to adsorb heavy metals [32–34], dyes [11,35–37], and pharmaceuticals [38–41] from aqueous solutions. Moreover, a range of modification techniques have been applied to further enhance their adsorption capacity toward specific pollutants. Figure 2 outlines the potential binding mechanisms involved.

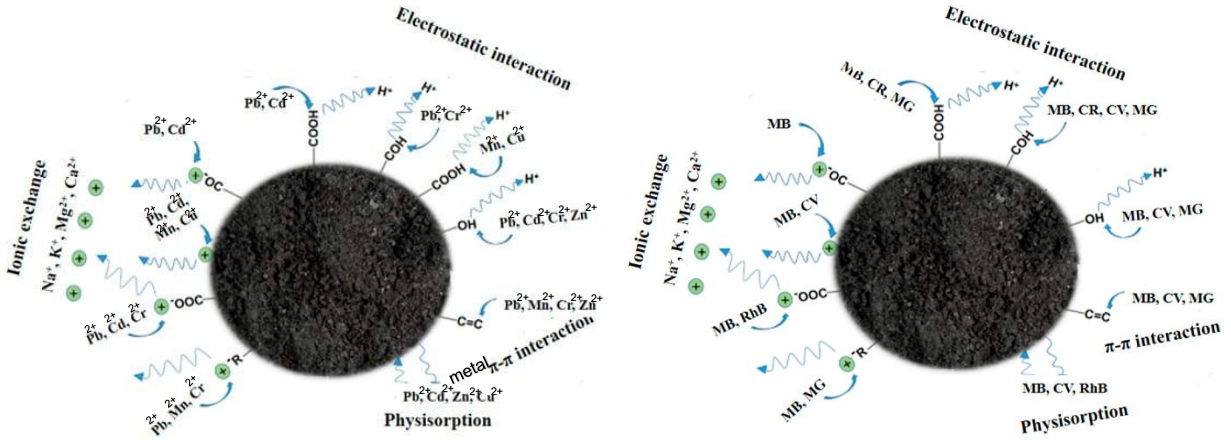

(**a**) (**b**)

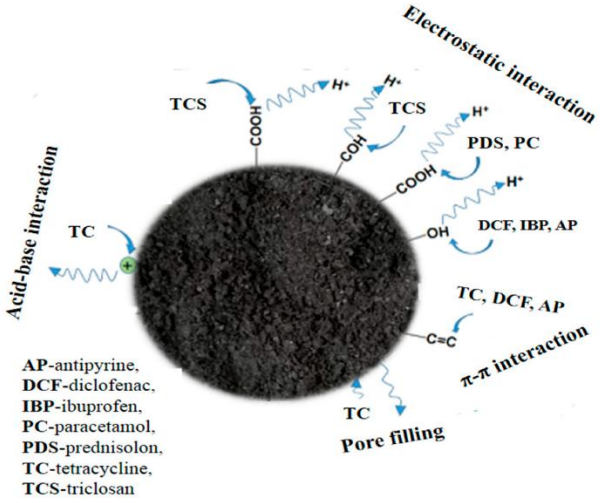

(**c**)

Figure 2. Possible mechanisms of interaction between hydrochar surfaces and (**a**) heavy metals, (**b**) dyes, and (**c**) pharmaceuticals. Images reused from Petrović et al., 2024 [42], in accordance with Creative Commons Attribution license (CC BY).

Algal biomass has gained increasing attention as a renewable feedstock for the development of sustainable carbonaceous materials. Among the various methods employed, HTC has emerged as a versatile and eco-friendly technique for converting algae into hydrochars with a high carbon content, a large surface area, and functional versatility. This section delves into studies on hydrochars derived from *Sargassum horneri*, *Sargassum muticum*, and related algal sources, focusing on their synthesis, physicochemical properties, and environmental applications (see Table 1).

Table 1. Physicochemical properties and adsorptive applications of algal-derived carbonaceous materials.

Adsorbent/Feedstock	Conditions	Surface Area (m^2/g)	HHV (MJ/kg)	Adsorption Capacity (mg/g)	Key Applications	Refs.
Sargassum horneri	180–210 °C, 2–16 h, citric acid	0.6–31.8	20.8–25.1	-	Solid fuel, energy recovery	[29]
Sargassum muticum	180–300 °C, 60–300 min	22.8–24.2	-	90% (Rhodamine B)	Dye adsorption	[11]
Sargassum-derived SAH	180–260 °C, KOH activation	1216–1404	-	714.29 (MB)	Advanced adsorption	[10]
Lignocellulosic biomass	200–300 °C, HTC and activation	800–1200	22.0–26.5	600 (MB)	Adsorption and catalysis	[6]

Poultry litter hydrochar	150–300 °C, HTC	10–50	15.0–22.0	80–150 (various dyes)	Wastewater treatment	[43]
Enteromorpha prolifera	800 °C pyrolysis, $ZnCl_2$/$FeCl_3$ activation	-	-	90 (Naphthalene, NAP), 51 (Acetaminophen, ACE), 86 (Phenanthrene, PHE)	PAH removal	[44]
Aegagropila linnaei	700 °C pyrolysis, KOH/Fe_3O_4 loading	-	-	69.8% (Bisphenol A, BPA)	Organic pollutant removal	[45]
Microalgae-derived biochar	450–600 °C pyrolysis	-	-	218.4 and 744 (Sulfamethoxazole, STZ)	Pharmaceutical waste removal	[46,47]
Macroalgae-based biochar	800 °C pyrolysis, KOH activation	-	-	841.64 (MB)	Dye removal	[48]
Nannochloropsis sp.	250 °C HTC, $ZnCl_2$ activation	12.56	-	34.15 (Cu)	Heavy metal removal	[49]
Spirulina platensis	450 °C pyrolysis	7.65	-	128.6 (MB)	Dye adsorption	[50]
Cladophora glomerata	350 °C pyrolysis	-	-	104 (MB)	Dye adsorption	[51]
Eucheuma spinosum	600 °C pyrolysis	200.74	-	331.97 (RR-120 azo dye)	Textile dye removal	[52]
Chlorella vulgaris	250 °C HTC	8.5	-	24.39 (Cd)	Heavy metal removal	[32]
Sargassum hornerri	523 K HTC	14.12	-	330.84 (Cr)	Heavy metal adsorption	[53]

A recent study by Rasam et al., 2021 [29], explored the HTC of *Sargassum horneri* under varying conditions of temperature (180–210 °C), time (2–16 h), and catalyst loading (citric acid). The hydrochar yield and properties were evaluated, including the Brunauer–Emmett–Teller (BET) surface area, higher heating value (HHV), and energy recovery. The BET surface area of the hydrochars varied significantly, ranging from 0.6 to 31.8 m^2/g. The HHV ranged from 20.8 to 25.1 MJ/kg, highlighting the potential of *S. horneri*-derived hydrochar as a solid fuel. The energy densification ratios increased with reaction severity, indicating effective dehydration and decarboxylation during HTC. The optimization of HTC parameters was achieved using machine learning models such as support vector machines and artificial neural networks. These predictive tools enhanced the understanding of complex parameter interdependencies, enabling the design of hydrochars with tailored properties for specific applications. For instance, small particle sizes and higher catalyst loads were associated with higher BET surface areas and energy recovery efficiencies, demonstrating the role of feedstock preparation and process intensification.

Another study performed by Spagnuolo et al., 2023 [11], investigated hydrochars derived from *Sargassum muticum*, emphasizing their application in removing Rhodamine B dye from wastewater. Hydrochars were synthesized under HTC conditions ranging from 180 to 300 °C for durations of 60 to 300 min. Characterization using FTIR, XPS, and SEM-EDX revealed the presence of macroporous structures and oxygen-containing functional groups that enhanced adsorption capabilities. Hydrochars obtained at lower temperatures (≤180 °C) and shorter durations (≤60 min) showed the highest adsorption capacities for Rhodamine B, attributed to their higher surface area and optimal functional group composition. Adsorption tests demonstrated removal efficiencies exceeding 90% for Rhodamine B, even without chemical or physical activation. The adsorption kinetics followed a pseudo-second-order model, indicating chemisorption as the dominant mechanism. Chambers et al., 2024 [10], examined the production of ultraporous superactivated hydrochar (SAH) from Sargassum using HTC followed by KOH activation. The HTC process was conducted at temperatures of 180, 220, and 260 °C, while activation enhanced the surface area, reaching up to 1404 m^2/g. The resulting SAHs demonstrated remarkable adsorption capacities for MB, reaching up to 714.29 mg/g at 37 °C.

This study identified key factors influencing adsorption, including solution pH, contact time, and temperature. The optimal adsorption occurred at pH 12, with equilibrium reached within 24 h. Mechanistic insights revealed that pore filling and electrostatic attractions played critical roles in the adsorption process. The Langmuir isotherm model provided the best fit for the data, affirming monolayer adsorption behavior. Thermodynamic studies confirmed the spontaneity and endothermic nature of the adsorption process, with increased temperatures enhancing dye uptake. Comparing these studies highlights the versatility of HTC-derived hydrochars in addressing environmental challenges. While *S. horneri*-based hydrochars excel in energy recovery and fuel applications, *S. muticum*-derived hydrochars showcase high efficiency in dye removal from aqueous solutions. The addition of KOH activation further transforms hydrochars into ultraporous materials suitable for advanced adsorption applications. These findings underscore the potential of algal biomass valorization to mitigate water pollution and reduce reliance on fossil-derived adsorbents.

To promote environmental sustainability, Kim et al., 2023 [54], investigated the simultaneous removal of Cu(II) and Cr(VI) ions using a nitrogen-doped hydrochar synthesized from corncob biomass. The hydrochar was chemically modified with NH_4Cl, which significantly

enhanced its adsorption efficiency, achieving capacities of 1.223 mmol/g for Cu(II) and 1.995 mmol/g for Cr(VI), surpassing those of the unmodified hydrochar. An infrared spectroscopy analysis indicated that redox reactions on the hydrochar surface led to an increase in deprotonated imine groups, which contributed to additional Cu(II) binding sites. Furthermore, under acidic conditions (pH < pHpzc), the N-doped hydrochar exhibited a stronger affinity for Cr(VI) than Cu(II) due to electrostatic attraction. Additionally, a protonated amino-functionalized bamboo hydrochar was synthesized by modifying bamboo-derived hydrochar with acryloyl chloride, amine, and hydrochloric acid, and subsequently used for Cr(VI) adsorption [55]. The researchers highlighted that the introduction of amine groups played a crucial role in enhancing adsorption performance, achieving a capacity of 523.57 mg/g through electrostatic interactions that facilitated pollutant removal.

A novel, cost-effective hydrochar composite synthesized from sawdust and modified with magnesium and silicon (MgSi-HC) was employed for Cu(II) and Zn(II) removal. This modification resulted in an increased specific area and a highly porous structure, significantly improving its adsorption potential. Adsorption isotherm studies determined the maximum adsorption capacities for Cu(II) and Zn(II) as 214.7 mg/g and 227.3 mg/g, respectively [47]. The adsorption mechanism involved multiple interactions, including electrostatic forces, hydrogen bonding, π–π interactions, and pore filling. Furthermore, a calcium-enriched pyro-hydrochar derived from spent mushroom substrate was evaluated for its ability to capture Pb(II) and Cd(II) from aqueous solutions. Based on the Freundlich isotherm model, the maximum sorption capacities were 297 mg/g for Pb(II) and 131 mg/g for Cd(II) [56]. The removal process was attributed to several mechanisms, including ion exchange, surface complexation, mineral precipitation, and cation–π interactions.

The studies reviewed here highlight significant advancements in the modification of hydrochar-based sorbents for heavy metal removal. These materials have shown remarkable adsorption capacities and tunable surface chemistries, making them strong candidates for scalable water purification technologies. However, despite these promising developments, several research gaps remain unaddressed. One of the most pressing challenges is the limited real-world applicability of these hydrochar-based adsorbents. Most adsorption studies are conducted in controlled laboratory environments with synthetic wastewater, which does not accurately reflect the complexity of real industrial effluents. Future studies should focus on evaluating these

hydrochars under realistic conditions, including multi-component wastewater systems where competition among ions might reduce adsorption efficiency. Another crucial gap lies in the long-term stability and regeneration capacity of modified hydrochars. While adsorption efficiencies are often reported, limited studies have assessed the desorption and reusability potential of these materials. Investigating cost-effective and environmentally friendly regeneration techniques is essential to making hydrochar-based sorbents viable for large-scale use.

Additionally, mechanistic insights into adsorption processes require further exploration. While electrostatic interactions, hydrogen bonding, and π–π interactions have been proposed as key adsorption mechanisms, advanced characterization techniques such as X-ray photoelectron spectroscopy (XPS) and in situ spectroscopy should be more widely used to provide a molecular-level understanding of metal binding on hydrochar surfaces. Another area of potential advancement is the integration of hydrochar-based materials into engineered water treatment systems. Rather than using hydrochars as standalone sorbents, incorporating them into hybrid filtration systems or coupling them with membrane technologies could enhance their effectiveness and sustainability. Research in this direction could improve metal ion capture rates while ensuring the materials remain structurally intact over extended operational cycles.

Lastly, while hydrochar modifications using nitrogen, magnesium, silicon, and calcium have shown great promise, exploring alternative modification strategies—such as bio-inspired functionalization or nano-enhanced composites—could unlock even greater adsorption efficiencies. In particular, the use of biopolymer coatings or graphene-based hybrids may improve surface chemistry and expand the range of pollutants that hydrochars can target. As can be observed, hydrochar-based sorbents offer a sustainable and cost-effective approach for heavy metal removal, but their full potential remains untapped. Addressing the current limitations through real-world testing, improved regeneration strategies, deeper mechanistic studies, and advanced material integration will be critical to transitioning these adsorbents from the laboratory to large-scale environmental applications. Algal-derived hydrochars offer a sustainable approach to environmental remediation and energy recovery. Advancements in HTC and post-treatment processes, such as activation, enable the tailoring of hydrochar properties to meet specific application demands. Future research should focus on scaling up production, exploring hybrid processes, and broadening the range of pollutants addressed by these versatile materials.

Recent studies in the literature explore the applications and advancements of algae-based biochar (ABB) in environmental remediation, emphasizing its role in water treatment, air pollution control, and soil restoration. ABB is a specific type of biochar produced from algae biomass through pyrolysis, a thermochemical process that involves heating the algae in the absence of oxygen. Algae, being rich in carbon and other organic compounds, undergoes decomposition at temperatures typically ranging from 300 to 700 °C, resulting in a porous, carbon-rich material. The properties of algae-based biochar can vary depending on the species of algae used, as well as the pyrolysis conditions [46]. Algae, owing to their rapid growth, ability to thrive in adverse environments, and minimal resource demands, serve as an excellent feedstock for biochar production [57]. ABB emerges as a sustainable solution for addressing global environmental challenges due to its versatility, low cost, and renewable nature [58]. Biochar, produced through pyrolysis, gasification, and other thermal processes, is renowned for its high porosity, large specific surface area, and exceptional adsorption capacities [59] (see Table 1). Algae-based biochars, derived from both microalgae and macroalgae, outperform terrestrial plant-based biochars in several applications, primarily because of the unique composition of algae. Rich in proteins, lipids, and carbohydrates, algae contribute to the creation of biochars with enhanced functional groups and superior pollutant adsorption capabilities [60].

In water treatment, ABB has proven highly effective in removing a range of pollutants. For instance, it demonstrates remarkable efficiency in adsorbing persistent organic pollutants like polycyclic aromatic hydrocarbons (PAHs) [61,62], endocrine-disrupting chemicals (EDCs) [45], and pharmaceutical residues [47,63,64]. Studies show that *Enteromorpha prolifera*-derived biochar, activated with $ZnCl_2$ and $FeCl_3$, exhibited adsorption capacities of 90 mg/g for NAP, 51 mg/g for ACE, and 86 mg/g for PHE [44], showcasing its potential in wastewater treatment. Similarly, algae-based biochars have been employed in the adsorption of antibiotics such as tetracycline [65] and ciprofloxacin [64], with adsorption capacities reaching up to 384.6 mg/g when biochars were modified with activators like $ZnCl_2$. Furthermore, ABB is widely used in dye removal, a significant challenge posed by the textile industry. Certain macroalgae-based biochars demonstrated exceptional dye adsorption capacities, with malachite green removal reaching 5306.2 mg/g after pyrolysis at 800 °C [66]. These results underline ABB's adaptability in treating various industrial wastewater pollutants.

In the realm of soil remediation, ABB plays a dual role in reducing contamination and enhancing soil fertility [67]. Heavy metal contamination, a persistent issue in industrial and agricultural zones, is effectively mitigated using ABB. For instance, biochars derived from blue algae immobilized cadmium with an adsorption capacity of 135.7 mg/g [68]. In addition to heavy metal remediation, ABB has shown promise in reducing pesticide residues and fluoride contamination in soils. Hydroxyapatite-activated biochars have achieved defluorination efficiencies of 79% [69], while biochars tailored for pesticide residue adsorption have reduced environmental availability by over 80% [57]. Beyond pollutant mitigation, ABB significantly improves soil properties by enhancing nutrient retention [70], cation exchange capacity [71], and water-holding abilities [72]. When incorporated into agricultural practices, such as soybean cultivation, ABB has been observed to boost yields by 119% [73].

ABB also demonstrates notable performance in air pollution control, particularly in greenhouse gas adsorption and toxic gas removal [74]. For example, biochars doped with nitrogen exhibit enhanced CO_2 adsorption capacities, reaching up to 4.21 mmol/g through advanced activation methods like microwave-assisted KOH modification [75]. Similarly, ABB has been utilized in the capture of hydrogen sulfide (H_2S), a toxic gas commonly found in industrial emissions, with adsorption capacities exceeding 8500 mg/kg when activated with H_2SO_4/H_2O_2 [76]. The ability to modify ABB for specific pollutants makes it a versatile tool in combating air pollution, particularly for challenging contaminants like mercury, where halide-modified biochars have demonstrated removal efficiencies of over 90% [77].

Some studies thoroughly examine the various activation and modification techniques employed to enhance ABB's properties. Chemical activations, such as acid or alkali treatments, improve porosity and introduce functional groups that boost adsorption performance. For instance, KOH-modified biochars exhibited a 127% increase in CO_2 adsorption capacity [78]. Halide modifications with agents like $FeCl_3$ and $ZnCl_2$ further enhance the removal efficiency of heavy metals and organic pollutants [79,80]. Meanwhile, the integration of metal oxides like Fe_2O_3 into biochar structures not only improves catalytic properties but also facilitates the removal of complex contaminants like uranium [81]. Among the more sustainable approaches, UV/H_2O_2 advanced oxidation processes provide a green alternative to conventional modification methods, significantly enhancing ABB's performance without contributing to secondary pollution.

Despite its potential, ABB faces challenges that hinder its widespread application. Many ABBs suffer from underdeveloped pore structures and limited active sites, which reduce their adsorption capacities. Furthermore, preparation processes can sometimes release secondary pollutants, necessitating a careful evaluation of ABB's lifecycle impact, including its carbon footprint and energy consumption. Economic feasibility also poses a significant challenge, as scaling ABB production to industrial levels while maintaining performance enhancements can be cost-prohibitive [46].

To address these limitations, future research should focus on developing multifunctional biochars with co-doped elements and multidimensional structures to broaden their applicability. Additionally, synergistic activation techniques combining physical and chemical methods could overcome structural deficiencies. Comprehensive lifecycle assessments are essential to evaluate ABB's long-term environmental and economic impacts. Lastly, transitioning from laboratory studies to field-scale applications will be crucial in validating ABB's effectiveness and scalability under real-world conditions. As a partial conclusion, algae-based biochar represents a transformative material in environmental remediation, offering sustainable solutions for water, soil, and air pollution. By addressing its current challenges through innovative modification strategies and rigorous assessments, ABB holds the potential to become a cornerstone of sustainable environmental management.

The adsorption capacities of various macroalgae and microalgae-derived biochars for heavy metal removal from aqueous solutions have been extensively investigated under different preparation conditions. Among the macroalgae, *Macrocystis pyrifera* exhibited a significant Cu^{2+} adsorption capacity of 119.9 mg/g when subjected to pyrolysis at 450 °C under a N_2 atmosphere for one hour, with intra-particle diffusion governing the adsorption kinetics [82]. Similarly, red macroalgae treated via hydrothermal carbonization at 200 °C with $FeCl_3$ impregnation achieved an As^{3+} adsorption capacity of 3.8314 mg/g, following a Langmuir isotherm model and pseudo-second-order kinetics [83].

Enteromorpha prolifera demonstrated notable Cd^{2+} adsorption properties under different preparation methods. When pyrolyzed at 500 °C with KOH activation at 700 °C, the resulting biochar had a Cd^{2+} adsorption capacity of 5.84 mg/g, following the Langmuir isotherm and pseudo-second-order kinetics [84]. However, when pretreated with H_3PO_4 for 12 h before undergoing pyrolysis at 500 °C, the adsorption capacity significantly increased to 423 mg/g, with intra-particle

diffusion playing a crucial role [85]. Meanwhile, *Ascophyllum nodosum* biochar, derived from pyrolysis at 700 °C followed by $FeCl_3$ and $FeCl_2$ coprecipitation, achieved a Cu^{2+} adsorption capacity of 53.19 mg/g, with pseudo-second-order kinetics dominating the adsorption process [86]. Among microalgae, *Chlorella pyrenoidosa* showed a remarkably high Ni^{2+} adsorption capacity of 201.18 mg/g when pyrolyzed at 600 °C with KOH activation, following the Langmuir isotherm and pseudo-second-order kinetics [87]. *Scenedesmus dimorphus* exhibited a lower Co^{2+} adsorption capacity of 0.672 mg/g when subjected to fast pyrolysis at 500 °C, following the Freundlich isotherm and pseudo-second-order kinetics [88].

Other notable microalgae include *Spirulina* sp., which demonstrated Cu^{2+} adsorption after pyrolysis at 200 °C, with adsorption behavior aligning with the Redlich–Peterson isotherm and pseudo-second-order kinetics [89]. Additionally, *Chlorella* sp. and *Spirulina* sp. biochars pyrolyzed at 600 °C exhibited Pb^{2+} adsorption capacities of 131.41 mg/g and 154.51 mg/g, respectively, both following Langmuir isotherm models and pseudo-second-order kinetics [90]. These findings underscore the potential of algae-derived biochars for heavy metal removal, with adsorption efficiency being highly dependent on biomass type, preparation conditions, and activation methods.

While algae-derived biochars and hydrochars show great promise for heavy metal removal from aqueous environments, several challenges and research gaps must be addressed to optimize their practical application. One of the primary concerns is the variability in the adsorption capacity of these carbon materials, which depends on the algal species used as feedstock and the preparation methods employed. As evident from previous studies, factors such as the pyrolysis temperature, activation techniques, and chemical modifications significantly influence adsorption performance. However, there is a lack of standardized protocols for optimizing these parameters, making it difficult to compare results across studies and scale up the technology for real-world applications.

Additionally, while some biochars exhibit impressive adsorption capacities, others show relatively low efficiency, particularly for metals such as Co^{2+} and As^{3+}. This raises concerns about the selectivity of these materials and their ability to remove multiple contaminants simultaneously. Future research should focus on enhancing the functionalization of biochars to improve selectivity and binding affinity toward diverse pollutants. Advanced surface modification techniques, such as doping with nanomaterials or introducing functional groups, could be explored further. Another critical limitation is the regeneration and reusability of algal biochars. While adsorption studies

highlight their high initial efficiency, there is limited research on their long-term stability and desorption performance. Repeated adsorption–desorption cycles could lead to structural degradation or reduced adsorption capacity, which may affect economic feasibility for large-scale applications [46]. Investigating effective regeneration strategies, such as thermal reactivation or chemical treatments, is crucial to ensure sustainability and cost-effectiveness.

Moreover, the economic and environmental implications of large-scale biochar production require further evaluation. Algal biomass cultivation and harvesting can be resource-intensive, particularly when grown under controlled conditions. Additionally, the energy requirements for high-temperature pyrolysis or hydrothermal processing could offset the environmental benefits if not optimized. Life cycle assessments and techno-economic analyses should be conducted to determine the true sustainability of this approach compared to conventional wastewater treatment methods. From a practical standpoint, the real-world applicability of these adsorbents depends on their performance in complex wastewater matrices, where competing ions and organic matter may interfere with adsorption. Most studies are conducted under controlled laboratory conditions with synthetic solutions, which may not accurately represent industrial or municipal wastewater. Field-scale trials are necessary to validate laboratory findings and identify potential challenges in real-world scenarios.

5. Algal-Based Materials for Carbon Capture and Energy and Biofuel Production

The integration of algal biofuel production and carbon capture catalytic approaches represents a promising frontier in sustainable energy and environmental preservation. These photosynthetic organisms, ranging from unicellular microalgae to multicellular macroalgae, possess unique characteristics that make them particularly attractive for sustainable energy solutions [91]. The increasing global demand for renewable energy sources, coupled with the urgency to mitigate greenhouse gas emissions, has intensified research into alternative bioenergy pathways. Among these, algal-based biofuels have emerged as a promising solution due to their high photosynthetic efficiency, rapid growth rates, and ability to thrive on non-arable land [92].

Microalgae and macroalgae are photosynthetic organisms that convert solar energy and carbon dioxide (CO_2) into organic compounds through photosynthesis. Their high growth rates and superior biomass productivity make them attractive candidates for biofuel production. Unlike

terrestrial energy crops, algae do not compete with food production since they can be cultivated in saline, brackish, or wastewater, thereby reducing pressure on arable land. Algae are exceptional carbon fixers, utilizing photosynthesis to absorb CO_2 from the atmosphere and convert it into organic substances, primarily lipids and carbohydrates (Figure 3). This inherent ability establishes algae as natural carbon sinks, with their cultivation playing a pivotal role in mitigating CO_2 emissions and contributing to climate change abatement.

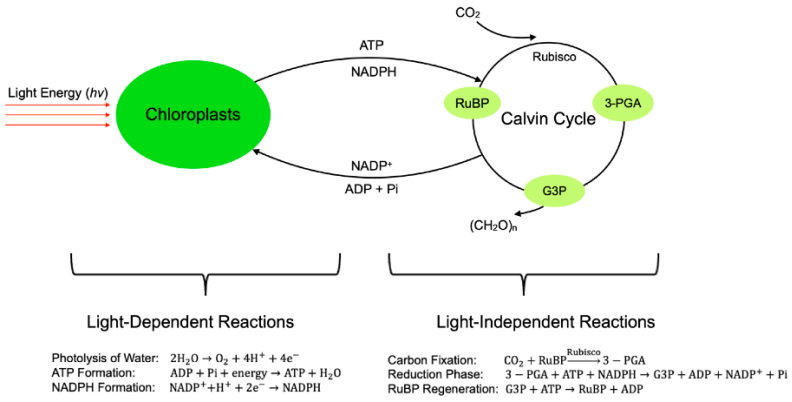

Figure 3. Photosynthetic carbon assimilation process in algae. Image reused from Li and Yao, 2024 [93], in accordance with Creative Commons Attribution license (CC BY).

The capacity of many algal species to accumulate significant amounts of lipids is a cornerstone of their utility in biodiesel production. Lipid biosynthesis in algae is intricately regulated by environmental factors such as nutrient availability, light intensity, and temperature. Under nutrient stress conditions, certain species can divert metabolic flux from growth to storage, resulting in an increased lipid content. Algal cultivation systems are broadly classified into open pond systems and closed photobioreactors (PBRs). Open ponds, due to their low operational costs, are widely used for large-scale production, albeit with limited control over environmental conditions. In contrast, PBRs offer superior control over parameters such as light, temperature, and nutrient supply, leading to higher biomass yields and more consistent product quality [94].

The cultivation of algae for biofuel production involves a range of technologies designed to maximize growth and productivity (Table 2). Open pond systems, such as shallow, sunny ponds in which algae thrive, represent a traditional and economic method. These systems are scalable and have low operating costs but may face challenges related to evaporation and contamination. Closed photobioreactors, on the other hand, offer precisely controlled environments that enable

the management of temperature, light, and nutrient levels. While more expensive to set up, photobioreactors have the potential for year-round cultivation, lower contamination risks, and increased production.

The efficient harvesting of algal biomass remains one of the most critical challenges in algal biofuel production. Techniques such as flocculation, centrifugation, and membrane filtration are commonly employed [95]. Emerging methods, including bio-flocculation and electrocoagulation, have shown promise in reducing energy consumption and operational costs. Thermochemical processes, such as pyrolysis, gasification, and hydrothermal liquefaction, convert algal biomass into liquid and gaseous fuels. Pyrolysis involves the thermal decomposition of biomass in the absence of oxygen, yielding bio-oil, char, and syngas. Gasification, on the other hand, converts biomass into a combustible gas mixture through partial oxidation. Hydrothermal liquefaction operates at high pressures and moderate temperatures to produce bio-crude oil, which can be further refined into transportation fuels. These processes benefit from the high moisture content of algae, which can be advantageous under certain processing conditions [96].

Biochemical conversion routes include anaerobic digestion and fermentation. The anaerobic digestion of algal biomass produces biogas, primarily composed of methane, while fermentation processes convert carbohydrates into ethanol and other bioalcohols. The biochemical conversion of algal biomass is often limited by the structural complexity of the cell wall; thus, pretreatment methods such as mechanical disruption, enzymatic hydrolysis, or acid treatments are required to improve conversion efficiency. The integration of biochemical conversion with advanced biotechnological approaches has the potential to enhance overall yields and reduce processing costs [97]. Recent research has focused on integrating thermochemical and biochemical conversion techniques to optimize biofuel production. Hybrid processes that combine hydrothermal liquefaction with subsequent catalytic upgrading have shown enhanced conversion efficiencies and improved fuel properties. These integrated approaches leverage the strengths of each conversion pathway, resulting in biofuels that meet stringent performance and emission standards [98].

Table 2. Algal processes for carbon capture and biofuel production.

Process	Description	Key Advantages	Challenges
CO_2 capture by algae	Algae absorbs CO_2 via photosynthesis, converting it into biomass	High CO_2 fixation rates, renewable process	Requires optimized growth conditions and nutrient supply
Open-pond cultivation	Algae grow in large outdoor ponds under natural sunlight	Low-cost and scalable	Susceptible to contamination and low productivity
Photobioreactor cultivation	Algae cultivated in enclosed systems with controlled light and nutrients	High biomass yield, reduced contamination	High capital and operational costs
Biofuel production (transesterification)	Converts algal lipids into biodiesel using catalysts	Produces clean, renewable fuel	Energy-intensive lipid extraction and purification required
Hydrothermal liquefaction	Converts whole algal biomass into biocrude oil using high temperature and pressure	Utilizes wet biomass, high energy content fuel	High processing costs, catalyst deactivation
Pyrolysis	Thermal decomposition of algae to produce syngas and bio-oil	Efficient energy recovery	Complex upgrading processes required
Carbon storage in biochar	Converts algal biomass into stable carbon-rich biochar	Long-term carbon sequestration potential	Requires large-scale applications for impact

Catalytic processes play a crucial role in harnessing the immense potential of algae as a biofuel source. In the context of algae-based biofuel production (Figure 4), catalysis is indispensable for several critical steps. Transesterification, a primary process in biodiesel production, relies heavily on catalysts such as sodium hydroxide or potassium hydroxide to convert algal lipids into biodiesel efficiently [99]. This transformation yields biodiesel and glycerol while ensuring reaction efficiency and the production of high-quality fuel. Hydrothermal liquefaction offers another promising route, subjecting algal biomass to high temperatures and pressures to break it down into valuable biocrude oil [100]. Catalysts are instrumental in enhancing reaction rates and yields, rendering the process economically viable. Additionally, the gasification of algal biomass generates synthesis gas (syngas) that can be further refined into liquid biofuels or valuable chemicals. Catalysts optimize the gasification process, facilitating the efficient conversion of abundant raw algal materials into refined, energy-dense biofuels suitable for diverse applications, including transportation, industry, and power generation [101].

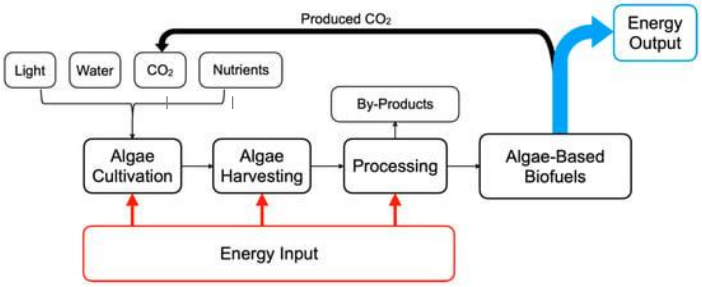

Figure 4. Biofuel generation process from algae. Image reused from Li and Yao, 2024 [93], in accordance with Creative Commons Attribution license (CC BY).

The cultivation of algae for biofuel production involves a range of technologies designed to maximize growth and productivity. Open pond systems, such as shallow, sunny ponds in which algae thrive, represent a traditional and economic method. These systems are scalable and have low operating costs but may face challenges related to evaporation and contamination [102]. Closed photobioreactors, on the other hand, offer precisely controlled environments that enable the management of temperature, light, and nutrient levels. While more expensive to set up, photobioreactors have the potential for year-round cultivation, lower contamination risks, and increased production [94]. Emerging technologies such as raceway ponds and vertical tube bioreactors combine the advantages of open ponds and photobioreactors, aiming to maximize productivity while reducing costs and operational complexity [103].

Technological advancements in algae cultivation focus on improving productivity, resource efficiency, and sustainability. Innovative approaches utilize genetic engineering to develop high-yielding algae strains that are more resilient to environmental stressors or have a higher lipid content. Integration with wastewater treatment plants enables nutrient recycling, reducing production costs and environmental impact. Furthermore, combining biomass production with carbon capture technologies enhances environmental sustainability by reducing greenhouse gas emissions.

A multitude of factors influence the cultivation of microalgae species, playing a pivotal role in determining overall productivity and economic viability. Environmental factors such as light intensity and quality, temperature, pH, and carbon dioxide concentration are critical in ensuring optimal growth conditions. Operational factors, including nutrient availability, mixing and turbulence, efficient harvesting and dewatering methods, and contamination control, are equally crucial for maintaining high biomass yields and preventing losses. Biological factors, like

strain selection, genetic modifications, life cycle stage, and metabolic pathways, significantly impact the production of desired compounds and the overall performance of the cultivation system. The design of the cultivation system itself, whether open or closed, and its scale and geometry, can profoundly affect factors such as light penetration, mixing, gas exchange, and compatibility with downstream processing steps [104].

Recent innovations in genetic engineering, metabolic engineering, and synthetic biology have revolutionized the ability to enhance algal traits with greater speed and precision. These advancements provide promising avenues for improving algae's efficiency in carbon capture and biofuel production. Yang et al., 2017 [105], employed genetic engineering to enhance the photosynthetic performance of *Chlorella vulgaris*. By introducing cyanobacterial fructose-1,6-bisphosphate aldolase via a plastid transit peptide, they significantly boosted photosynthetic capacity and cell growth. Their research suggests that overexpressing this enzyme facilitates the regeneration of ribulose-1,5-bisphosphate in the Calvin cycle, improving energy transfer within photosystems and ultimately enhancing carbon fixation efficiency. Similarly, Hlavova et al., 2015 [106], conducted an extensive review of genetic engineering strategies for modifying microalgal traits. These techniques enable the precise insertion of exogenous DNA or external induction mechanisms, leading to genetically optimized strains with enhanced biomass production, increased cell density, and improved CO_2 capture efficiency.

Beyond genetic modifications, metabolic engineering has emerged as a critical tool for fine-tuning algal biochemical pathways. Brar et al., 2021 [107], highlighted strategies such as modifying enzyme expression levels, altering protein structures for increased stability, and optimizing key metabolic reactions to enhance CO_2-to-biomass conversion. These approaches have been instrumental in improving algal productivity under varying environmental conditions. Synthetic biology further expands the potential for algal biotechnology by integrating artificial genetic modifications with metabolic pathway engineering. Among the most promising tools in this field, CRISPR-Cas systems have been successfully adapted to enhance algal carbon sequestration and biofuel synthesis. For instance, modifications to *Chlamydomonas reinhardtii* and *Synechocystis sp.* have improved their resilience to environmental stressors while optimizing light-harvesting pathways for accelerated growth. Additionally, combining CRISPR-based techniques with high-throughput screening holds significant potential for scaling up algae-based carbon capture and bioenergy applications [108]. By optimizing key enzymatic steps and

redirecting metabolic fluxes, researchers have achieved significant improvements in biomass composition and biofuel precursor synthesis [109]. Computational models and high-throughput screening techniques are now routinely used to predict and validate genetic modifications, thus accelerating the development of high-performance algal strains. These advances are critical for overcoming bottlenecks in the conversion of CO_2 to biofuels and enhancing overall process efficiency.

Despite these promising advances, a critical gap remains in transitioning these laboratory successes to large-scale, real-world applications. While genetically engineered algae have demonstrated enhanced performance in controlled environments, their stability and efficiency in open-pond or industrial-scale bioreactors remain uncertain. Factors such as genetic drift, regulatory challenges, ecological risks, and cost-effectiveness need further exploration. Future research should focus on bridging this gap by conducting extensive field trials and developing robust biocontainment strategies to ensure the viability and safety of engineered algal strains in large-scale carbon capture, utilization, and storage (CCUS) systems. Addressing these challenges will be key to unlocking the full potential of algae as a sustainable solution for carbon mitigation and biofuel production.

Extracting lipids from microalgal biomass is also a critical step in the production of biofuels and other valuable compounds. Several extraction techniques have been developed and employed, each with its own advantages and limitations. Conventional solvent extraction methods, such as hexane extraction [110] or the Bligh and Dyer method [111], are widely used for their efficiency in extracting lipids. However, these techniques often require large volumes of toxic organic solvents, raising environmental and safety concerns. Emerging techniques like supercritical fluid extraction, using carbon dioxide or other solvents under high pressure and temperature, offer a greener and more selective approach but may require specialized equipment and higher operational costs [112].

Innovative techniques like enzymatic extraction, utilizing lipase enzymes to break down cell walls and release lipids, and ultrasound-assisted extraction, employing high-frequency sound waves to disrupt cell membranes, have gained attention for their potential to improve extraction efficiency and reduce solvent usage. Microwave-assisted extraction and pulsed electric field extraction have shown promise in enhancing the permeability of cell membranes and facilitating lipid recovery. The choice of extraction technique often depends on factors such as the microalgal

species, desired lipid quality, scalability, environmental impact, and economic viability, necessitating a careful evaluation of the trade-offs between efficiency, sustainability, and cost [12].

Microalgae species such as *Chlorella*, *Nannochloropsis*, and *Scenedesmus* are frequently chosen for biodiesel production due to their high lipid content and rapid growth rates. These microalgae can accumulate triacylglycerols, which can be transesterified to produce biodiesel. Chlorella has been extensively studied for biodiesel production due to its high lipid content and adaptability to various environmental conditions. *Nannochloropsis* is another promising option for biodiesel feedstock because of its robust growth and lipid-rich biomass. Similarly, *Scenedesmus* has shown potential for biodiesel production due to its ability to accumulate lipids under various cultivation conditions [104].

The integration of algae-based technologies into existing energy infrastructure presents both opportunities and challenges. Understanding the synergies and trade-offs between algal biofuel production and carbon capture is crucial for maximizing their impact on climate change mitigation and sustainable development. Scalability remains a significant hurdle in translating laboratory success to large-scale industrial applications. Optimizing cultivation techniques, improving strain selection for higher lipid content, and developing efficient harvesting methods are essential steps in addressing this challenge.

To overcome challenges associated with large-scale algal cultivation, researchers have explored mixed-culture systems, where multiple algal species are cultivated together [113–117]. This approach takes advantage of species diversity, allowing cultures to better adapt to fluctuating environmental conditions such as light availability, temperature shifts, and pH variations. Additionally, mixed cultures can suppress the proliferation of pathogens and unwanted contaminants, reducing the risk of culture crashes. By fostering complementary nutrient utilization among species, these systems not only enhance biomass productivity but also lower operational costs, making large-scale cultivation more economically viable. One promising method for optimizing mixed-culture systems involves leveraging natural density differences between algal strains. This allows for the selective enrichment of lipid-rich or carbohydrate-rich species, simplifying biomass harvesting and improving the efficiency of biofuel and bioproduct generation. Such strategies provide a cost-effective alternative to traditional separation techniques, which are often energy-intensive and expensive [118].

In addition to mixed cultures, integrating algal cultivation with industrial byproducts such as wastewater and CO_2-rich emissions presents another sustainable solution. Wastewater from agricultural and food processing industries contains essential nutrients like nitrogen and phosphorus, which can serve as a growth medium for algae. By utilizing this resource, algal cultivation systems not only achieve higher biomass yields but also contribute to wastewater remediation, reducing the environmental impact of nutrient pollution. Studies have shown that microalgal strains can thrive in wastewater conditions, effectively removing excess nutrients while simultaneously increasing biomass production [119].

Similarly, the direct utilization of CO_2-rich industrial emissions has been explored as a way to enhance algal carbon capture efficiency. Positioning cultivation systems near emission sources, such as power plants or industrial facilities, minimizes the costs associated with CO_2 transportation while improving carbon fixation rates. Certain thermotolerant microalgal strains have been successfully cultivated using exhaust gases from industrial burners, demonstrating the feasibility of large-scale integration with existing infrastructure. Open raceway ponds located near power plants have also been used to capture flue gas emissions, highlighting the potential for synergy between carbon-emitting industries and sustainable algal production [120].

Despite these advancements, several challenges remain. The long-term stability of mixed-culture systems under outdoor conditions is still not fully understood, as interactions between species can shift over time, potentially leading to competitive imbalances. Additionally, while wastewater and flue gas integration offer promising cost reductions, optimizing nutrient availability and CO_2 transfer rates for consistent biomass productivity requires further investigation. Future research should focus on developing more predictive models for species interactions in mixed cultures and refining scalable methods for nutrient and carbon delivery in industrial applications. Addressing these gaps will be crucial in realizing the full potential of algae as a sustainable solution for carbon capture and biofuel production.

Moreover, the development of cost-effective and durable catalysts is necessary to enhance carbon capture efficiency and address challenges such as low stability and high cost. Research efforts are focused on designing novel catalysts that can withstand the harsh conditions of carbon capture processes while maintaining high efficiency and selectivity. Nanomaterials and hybrid catalysts have shown promise in this regard, offering improved performance and longevity compared to traditional catalysts. The environmental benefits of algae-based catalysis extend

beyond carbon capture and biofuel production. Algae-based systems can be utilized for wastewater treatment, removing nutrients and contaminants while simultaneously producing valuable biomass. This dual-purpose approach addresses water pollution issues while generating feedstock for biofuel production. Additionally, algae-derived materials have shown potential in photocatalytic and electrocatalytic applications, offering sustainable alternatives for various industrial processes.

As research in algae-based technologies progresses, addressing current challenges and exploring future directions are crucial for realizing their full potential. Improving the efficiency of lipid extraction and conversion processes, developing more robust and productive algal strains through genetic engineering, and optimizing large-scale cultivation systems are key areas of focus. Furthermore, integrating algae-based technologies with other renewable energy sources and industrial processes can create synergistic effects, enhancing overall sustainability and economic viability.

The integration of algal biofuel production and carbon capture catalytic approaches represents a promising pathway towards a more sustainable and environmentally friendly energy future. By harnessing the unique capabilities of algae and leveraging advanced catalytic technologies, these integrated systems offer solutions to multiple global challenges, including climate change mitigation, energy security, and environmental preservation. Continued research, innovation, and interdisciplinary collaboration will be essential in overcoming current limitations and unlocking the full potential of algae-based technologies. As the world transitions towards a low-carbon economy, algae-based solutions are poised to play a significant role in shaping a cleaner, more sustainable future.

6. Algae-Based Solid Biomass Pellets

Algae-based solid biomass pellets have emerged as a promising renewable fuel source, offering high energy density and efficient combustion with minimal carbon emissions. These pellets, primarily derived from microalgae, undergo densification processes that improve their storage, transport, and usability in existing combustion systems. Their compatibility with coal-fired boilers makes them a viable alternative to traditional fossil fuels while also contributing to carbon recycling [121]. The production of algae-based biomass pellets involves several key stages: drying, crushing, screening, and palletization. Drying, often achieved through solar dryers or

mechanical drying equipment, is crucial for reducing moisture content, thereby increasing combustion efficiency. Once dried, the biomass is crushed and screened to ensure a uniform particle size before being compressed into dense pellets. This densification step enhances their transportability and energy output [122].

To further improve pellet performance, researchers have explored techniques such as increasing compression pressure, incorporating additives, and using higher processing temperatures. One particularly effective method is torrefaction palletization, which involves mild thermal treatment (200–300 °C) in an oxygen-limited environment. This process removes excess moisture and volatile compounds, yielding pellets with superior energy density, structural integrity, and durability [123]. A significant advantage of algae-based pellets is their clean combustion profile. When burned, they primarily release CO_2 and ash—both of which can be reintegrated into algal cultivation systems. The emitted CO_2 acts as a carbon source for photosynthesis, while ash, rich in essential minerals, serves as a nutrient supplement for further algae growth. Studies have shown that these pellets can achieve high energy densities comparable to or exceeding conventional biomass fuels, underscoring their potential for bioenergy applications [124,125].

To address cost challenges and enhance fuel performance, researchers have explored blending algae with other biomass materials, such as wood waste, agricultural residues, and rice husks. Even in small proportions, algae contribute to improved combustion efficiency, higher energy density, and enhanced durability of the pellets. Their fine particle size allows them to fill voids in biomass mixtures, increasing pellet density, while their lipid content improves structural cohesion, reducing fragmentation during burning. Additionally, the natural oils in algae act as lubricants, lowering energy requirements during the palletization process.

Beyond standalone pellets, algae-based fuels have been tested in dual-fuel applications, where they are co-combusted with coal, sludge, or oil shale [126–129]. These combinations offer multiple advantages, such as reducing ignition temperatures, accelerating burnout rates, and enhancing overall combustion performance. Algae can also facilitate the breakdown of sludge residues and contribute to more stable combustion reactions, lowering emissions of harmful pollutants such as nitrogen oxides. While algae-based biomass pellets demonstrate significant potential, challenges remain in scaling up their production and optimizing their economic feasibility. One key research gap lies in the long-term stability and combustion behavior of algae-

blended fuels in real-world industrial applications. Additionally, refining torrefaction conditions to maximize energy retention while minimizing production costs remains an ongoing area of investigation. Future studies should also focus on integrating algae-based pellets into existing energy infrastructure, assessing their performance in different combustion environments, and developing predictive models for their large-scale deployment. By addressing these challenges, algae-based biomass pellets could become a pivotal solution in sustainable energy production, reducing dependence on fossil fuels while advancing carbon-neutral bioenergy technologies.

7. Conclusions

Algal-based biochar and hydrochar have emerged as promising and sustainable materials for wastewater treatment, offering efficient removal of heavy metals, dyes, pharmaceuticals, and other pollutants. Their production through pyrolysis, HTC, or HTL allows for the development of highly tunable adsorbents, whose performance can be further enhanced through advanced activation and modification techniques. Beyond water remediation, algal-derived chars provide additional benefits, including soil amendment and energy recovery, reinforcing their potential as a versatile tool in environmental engineering. However, challenges related to feedstock variability, production costs, and large-scale implementation must still be addressed to unlock their full potential. Future research should focus on refining processing techniques, optimizing activation methods, and improving regeneration strategies to ensure long-term stability and effectiveness.

As can be observed, while algal-based biochars and hydrochars offer a sustainable and innovative approach to heavy metal, dye, and pharmaceutical removal, addressing these gaps is crucial for their widespread adoption. Future research should focus on improving selectivity, enhancing regeneration strategies, reducing production costs, and conducting real-world trials to bridge the gap between laboratory research and practical implementation. By tackling these limitations, algal-based adsorbents could become a key component of sustainable wastewater treatment technologies.

This review also highlights the broader role of algae-based CCUS technologies in mitigating climate change while contributing to sustainable energy solutions. Recent advances in algal biotechnology, including genetic modifications, optimized cultivation methods, and enhanced carbon capture efficiency, have significantly improved the conversion of CO_2 into valuable biomass. This biomass serves as a feedstock for various biofuels—solid, liquid (biodiesel

and bioethanol), and gaseous (biohydrogen, biogas, and syngas)—with technological innovations continuously increasing fuel yields. Despite these advancements, economic feasibility remains a major barrier to widespread adoption. Reducing cultivation costs, improving conversion efficiency, and minimizing energy inputs are critical areas for future development. Additionally, integrating algae-based biofuels into existing energy infrastructure and exploring biorefinery models could enhance their commercial viability.

HTC has also gained attention as an efficient thermochemical process for converting wet biomass into hydrochars, which have diverse applications in energy storage, adsorption, and soil conditioning. Understanding key process parameters—such as temperature, pressure, and residence time—has allowed better control over hydrochar properties, optimizing them for specific environmental applications. While significant progress has been made in elucidating the mechanisms of hydrothermal conversion, further research is needed to improve hydrochar performance, particularly through surface modifications and regeneration strategies. Enhancing hydrochar stability and adsorption capacity is crucial for its large-scale application in environmental remediation.

Algal-based biofuels and carbon materials present a multifaceted solution to the twin challenges of energy security and environmental sustainability. Their high photosynthetic efficiency, rapid growth rates, and diverse biochemical composition offer key advantages over conventional energy crops. However, the successful commercialization of these technologies will require a concerted effort across multiple disciplines, including genetic engineering, process optimization, and integrated system design. Moving forward, the combination of innovative research, technological advancements, and supportive policies will be essential in transforming algae-based solutions from a promising concept into a viable alternative for carbon mitigation, biofuel production, and environmental restoration.

Author Contributions: L.A.G.F.: Conceptualization, Methodology, Software, Formal Analysis, Investigation, Data Curation, Writing—Original Draft, and Visualization. N.A.M.C.: Conceptualization, Methodology, Software, Formal Analysis, Investigation, Data Curation, Writing—Original Draft, Visualization, Resources, and Supervision. M.S.P.: Visualization, Resources, and Supervision. A.E.N.F.: Visualization, Resources, and Supervision. J.E.V.C.: Conceptualization, Methodology, and Writing—Original Draft. All authors have read and agreed to the published version of the manuscript.

Funding: The authors thank CONAHCyT (CVU 1014829) for funding this research. This work forms part of a doctoral thesis in Chemistry at the University of Granada (Spain) and in Environmental Sciences at the Autonomous University of San Luis Potosi (Mexico).

Data availability: Data will be made available upon request.

Conflicts of Interest: The authors declare that they have no known competing financial interests or personal relationships that could have appeared to influence the work reported in this paper.

References

1. Briffa, J.; Sinagra, E.; Blundell, R. Heavy Metal Pollution in the Environment and Their Toxicological Effects on Humans. *Heliyon* **2020**, *6*, e04691. https://doi.org/10.1016/j.heliyon.2020.e04691.
2. Ramesh, B.; Saravanan, A.; Senthil Kumar, P.; Yaashikaa, P.R.; Thamarai, P.; Shaji, A.; Rangasamy, G. A Review on Algae Biosorption for the Removal of Hazardous Pollutants from Wastewater: Limiting Factors, Prospects and Recommendations. *Environ. Pollut.* **2023**, *327*, 121572. https://doi.org/10.1016/j.envpol.2023.121572.
3. Qi, Y.; He, K. Science and Technology for Water Purification: Achievements and Strategies. *Water* **2025**, *17*, 91.
4. Arora, N.; Tripathi, S.; Bhatnagar, P.; Gururani, P.; Philippidis, G.P.; Kumar, V.; Mohan Poluri, K.; Nanda, M. Algal-Based Biochar and Hydrochar: A Holistic and Sustainable Approach to Wastewater Treatment. *Chem. Eng. J.* **2024**, *496*, 153953. https://doi.org/10.1016/j.cej.2024.153953.
5. Nguyen, M.H.; Zbair, M.; Dutournié, P.; Gervasini, A.; Vaulot, C.; Bennici, S. Toward New Low-Temperature Thermochemical Heat Storage Materials: Investigation of Hydration/Dehydration Behaviors of $MgSO_4$/Hydroxyapatite Composite. *Sol. Energy Mater. Sol. Cells* **2022**, *240*, 111696. https://doi.org/10.1016/j.solmat.2022.111696.
6. Zeng, G.; Lou, S.; Ying, H.; Wu, X.; Dou, X.; Ai, N.; Wang, J. Preparation of Microporous Carbon from Sargassum Horneri by Hydrothermal Carbonization and KOH Activation for CO_2 Capture. *J. Chem.* **2018**, *2018*, 4319149. https://doi.org/10.1155/2018/4319149.
7. Magdziarz, A.; Wilk, M.; Wądrzyk, M. Pyrolysis of Hydrochar Derived from Biomass—Experimental Investigation. In Proceedings of the ECOS 2019—Proceedings of the 32nd International Conference on Efficiency, Cost, Optimization, Simulation and Environmental

Impact of Energy Systems, Wroclaw, Poland, 23–28 June 2019; Volume 2019-June, pp. 4465–4476.

8. Borah, D.; Rout, J.; Nooruddin, T. Application of Nanotechnology in Bioenergy Production from Algae and Cyanobacteria. In *Modern Nanotechnology: Volume 2: Green Synthesis, Sustainable Energy and Impacts*; Springer: Berlin/Heidelberg, Germany, 2023; pp. 267–291. ISBN 9783031311048.
9. El Ouadrhiri, F.; Elyemni, M.; Lahkimi, A.; Lhassani, A.; Chaouch, M.; Taleb, M. Mesoporous Carbon from Optimized Date Stone Hydrochar by Catalytic Hydrothermal Carbonization Using Response Surface Methodology: Application to Dyes Adsorption. *Int. J. Chem. Eng.* **2021**, *2021*, 1–16. https://doi.org/10.1155/2021/5555406.
10. Chambers, C.; Saha, S.; Grimes, S.; Calhoun, J.; Reza, M.T. Physical and Morphological Alteration of Sargassum-Derived Ultraporous Superactivated Hydrochar with Remarkable Cationic Dye Adsorption. *Biomass Convers. Biorefinery* **2023**, *14*, 29131–29144. https://doi.org/10.1007/s13399-023-04326-2.
11. Spagnuolo, D.; Iannazzo, D.; Len, T.; Balu, A.M.; Morabito, M.; Genovese, G.; Espro, C.; Bressi, V. Hydrochar from Sargassum Muticum: A Sustainable Approach for High-Capacity Removal of Rhodamine B Dye. *RSC Sustain.* **2023**, *1*, 1404–1415. https://doi.org/10.1039/d3su00134b.
12. Sahu, S.; Kunj, P.; Kaur, A.; Khatri, M.; Singh, G.; Arya, S.K. Catalytic Strategies for Algal-Based Carbon Capture and Renewable Energy: A Review on a Sustainable Approach. *Energy Convers. Manag.* **2024**, *310*, 118467. https://doi.org/10.1016/j.enconman.2024.118467.
13. Thanigaivel, S.; Rajendran, S.; Gnanasekaran, L.; Chew, K.W.; Tran, D.T.; Tran, H.D.; Nghia, N.K.; Show, P.L. Nanotechnology for Improved Production of Algal Biofuels: A Review. *Environ. Chem. Lett.* **2023**, *21*, 821–837. https://doi.org/10.1007/s10311-022-01529-3.
14. Baghel, R.S.; Suthar, P.; Gajaria, T.K.; Bhattacharya, S.; Anil, A.; Reddy, C.R.K. Seaweed Biorefinery: A Sustainable Process for Valorising the Biomass of Brown Seaweed. *J. Clean. Prod.* **2020**, *263*, 121359. https://doi.org/10.1016/j.jclepro.2020.121359.
15. Selcuk, A.A. A Guide for Systematic Reviews: PRISMA. *Turk. Arch. Otorhinolaryngol.* **2019**, *57*, 57–58. https://doi.org/10.5152/tao.2019.4058.
16. Kumar, B.R.; Mathimani, T.; Sudhakar, M.P.; Rajendran, K.; Nizami, A.S.; Brindhadevi, K.; Pugazhendhi, A. A State of the Art Review on the Cultivation of Algae for Energy and Other

Valuable Products: Application, Challenges, and Opportunities. *Renew. Sustain. Energy Rev.* **2021**, *138*, 110649. https://doi.org/10.1016/j.rser.2020.110649.

17. Vatsha, P.; Alam, M.R. Environmental Aspects of Biofuels Used as Sustainable Energy Resources: Current Situation and Future Trends. In *Biofuels and Sustainability Life Cycle Assessments, System Biology, Policies, and Emerging Technologies*; Elsevier: Amsterdam, The Netherlands, 2024; pp. 19–31. https://doi.org/10.1016/B978-0-443-21433-2.00019-0.
18. Davis, T.A.; Volesky, B.; Mucci, A. A Review of the Biochemistry of Heavy Metal Biosorption by Brown Algae. *Water Res.* **2003**, *37*, 4311–4330. https://doi.org/10.1016/S0043-1354(03)00293-8.
19. Moreda, U.; Mazarrasa, I.; Cebrian, E.; Kaal, J.; Ricart, A.M.; Serrano, E.; Serrano, O. Role of Macroalgal Forests within Mediterranean Shallow Bays in Blue Carbon Storage. *Sci. Total Environ.* **2024**, *934*, 173219. https://doi.org/10.1016/j.scitotenv.2024.173219.
20. Gaurav, K.; Neeti, K.; Singh, R. Microalgae-Based Biodiesel Production and Its Challenges and Future Opportunities: A Review. *Green Technol. Sustain.* **2024**, *2*, 100060. https://doi.org/10.1016/j.grets.2023.100060.
21. Pereira, L. Macroalgae. *Encyclopedia* **2021**, *1*, 177–188.
22. Hu, Q. Environmental Effects on Cell Composition. In *Handbook of Microalgal Culture: Applied Phycology and Biotechnology*, 2nd ed.; Wiley: Hoboken, NJ, USA, 2013; pp. 114–122. https://doi.org/10.1002/9781118567166.ch7.
23. Davison, I.R. Environmental Effects on Algal Photosynthesis: Temperature. *J. Phycol.* **1991**, *27*, 2–8. https://doi.org/10.1111/j.0022-3646.1991.00002.x.
24. Richmond, A. Cell Response to Environmental Factors. In *CRC Handbook of Microalgal Mass Culture*; CRC Press: Boca Raton, FL, USA, 2017; pp. 69–99. ISBN 9781351362702.
25. Stevenson, J. Ecological Assessments with Algae: A Review and Synthesis. *J. Phycol.* **2014**, *50*, 437–461. https://doi.org/10.1111/jpy.12189.
26. Zamora-Ledezma, C.; Negrete-Bolagay, D.; Figueroa, F.; Zamora-Ledezma, E.; Ni, M.; Alexis, F.; Guerrero, V.H. Heavy Metal Water Pollution: A Fresh Look about Hazards, Novel and Conventional Remediation Methods. *Environ. Technol. Innov.* **2021**, *22*, 101504. https://doi.org/10.1016/j.eti.2021.101504.

27. Akbar, S.A.; Khairunnisa, K. Seaweed-Based Biosorbent for the Removal of Organic and Inorganic Contaminants from Water: A Systematic Review. In *BIO Web of Conferences*; EDP Sciences: Les Ulis, France, 2024; Volume 87, p. 2011.
28. Periyavaram, S.R.; Bella, K.; Uppala, L.; Reddy, P.H.P. Hydrothermal Carbonization of Food Waste: Process Parameters Optimization and Biomethane Potential Evaluation of Process Water. *J. Environ. Manag.* **2023**, *347*, 119132. https://doi.org/10.1016/j.jenvman.2023.119132.
29. Rasam, S.; Talebkeikhah, F.; Talebkeikhah, M.; Salimi, A.; Moraveji, M.K. Physico-Chemical Properties Prediction of Hydrochar in Macroalgae Sargassum Horneri Hydrothermal Carbonisation. *Int. J. Environ. Anal. Chem.* **2021**, *101*, 2297–2318. https://doi.org/10.1080/03067319.2019.1700973.
30. Zhang, Z.; Zhu, Z.; Shen, B.; Liu, L. Insights into Biochar and Hydrochar Production and Applications: A Review. *Energy* **2019**, *171*, 581–598.
31. Santos Santana, M.; Pereira Alves, R.; da Silva Borges, W.M.; Francisquini, E.; Guerreiro, M.C. Hydrochar Production from Defective Coffee Beans by Hydrothermal Carbonization. *Bioresour. Technol.* **2020**, *300*, 122653. https://doi.org/10.1016/j.biortech.2019.122653.
32. Jafar Sufian, Marchelli, F.; Fiori, L. Algal Biomass, Biochar and Hydrochar from Chlorella Vulgaris for Cadmium Removal from Aqueous Streams. *Res. Sq.* **2023**, 0–17. https://doi.org/10.21203/rs.3.rs-2943751/v1.
33. Zhang, X.; Gao, Z.; Fan, X.; Tan, L.; Jiang, Y.; Zheng, W.; Han, F.X.; Liang, Y. A Comparative Study on Adsorption of Cadmium and Lead by Hydrochars and Biochars Derived from Rice Husk and Zizania Latifolia Straw. *Environ. Sci. Pollut. Res.* **2022**, *29*, 63768–63781. https://doi.org/10.1007/s11356-022-20263-5.
34. Wang, J.; Wang, Y.; Wang, J.; Du, G.; Khan, K.Y.; Song, Y.; Cui, X.; Cheng, Z.; Yan, B.; Chen, G. Comparison of Cadmium Adsorption by Hydrochar and Pyrochar Derived from Napier Grass. *Chemosphere* **2022**, *308*, 136389. https://doi.org/10.1016/j.chemosphere.2022.136389.
35. Haris, M.; Khan, M.W.; Paz-Ferreiro, J.; Mahmood, N.; Eshtiaghi, N. Synthesis of Functional Hydrochar from Olive Waste for Simultaneous Removal of Azo and Non-Azo Dyes from Water. *Chem. Eng. J. Adv.* **2022**, *9*, 100233. https://doi.org/10.1016/j.ceja.2021.100233.

36. Kohzadi, S.; Marzban, N.; Libra, J.A.; Bundschuh, M.; Maleki, A. Removal of RhB from Water by Fe-Modified Hydrochar and Biochar—An Experimental Evaluation Supported by Genetic Programming. *J. Mol. Liq.* **2023**, *369*, 120971. https://doi.org/10.1016/j.molliq.2022.120971.
37. Algethami, J.S.; Alhamami, M.A.M.; Alqadami, A.A.; Melhi, S.; Seliem, A.F. Magnetic Hydrochar Grafted-Chitosan for Enhanced Efficient Adsorption of Malachite Green Dye from Aqueous Solutions: Modeling, Adsorption Behavior, and Mechanism Analysis. *Int. J. Biol. Macromol.* **2024**, *254*, 127767. https://doi.org/10.1016/j.ijbiomac.2023.127767.
38. Delgado-Moreno, L.; Bazhari, S.; Gasco, G.; Méndez, A.; El Azzouzi, M.; Romero, E. New Insights into the Efficient Removal of Emerging Contaminants by Biochars and Hydrochars Derived from Olive Oil Wastes. *Sci. Total Environ.* **2021**, *752*, 141838. https://doi.org/10.1016/j.scitotenv.2020.141838.
39. Yudha, S.P.; Tekasakul, S.; Phoungthong, K.; Chuenchom, L. Green Synthesis of Low-Cost and Eco-Friendly Adsorbent for Dye and Pharmaceutical Adsorption: Kinetic, Isotherm, Thermodynamic and Regeneration Studies. *Mater. Res. Express* **2019**, *6*, 125526. https://doi.org/10.1088/2053-1591/ab58ae.
40. Senthil Kumar, P.; Shanmugapriya, M.; Prasannamedha, G.; Rangasamy, G. Immobilization of Hydrochar in Cellulose Beads for Eradicating Paracetamol from Synthetic and Sewage Water. *Environ. Pollut.* **2024**, *342*, 123035. https://doi.org/10.1016/j.envpol.2023.123035.
41. Hayoun, B.; Escudero-Curiel, S.; Bourouina, M.; Bourouina-Bacha, S.; Angeles Sanromán, M.; Pazos, M. Preparation and Characterization of High Performance Hydrochar for Efficient Adsorption of Drugs Mixture. *J. Mol. Liq.* **2022**, *353*, 118797. https://doi.org/10.1016/j.molliq.2022.118797.
42. Petrović, J.; Ercegović, M.; Simić, M.; Koprivica, M.; Dimitrijević, J.; Jovanović, A.; Janković Pantić, J. Hydrothermal Carbonization of Waste Biomass: A Review of Hydrochar Preparation and Environmental Application. *Processes* **2024**, *12*, 207. https://doi.org/10.3390/pr12010207.
43. Ismail, H.Y.; Shirazian, S.; Skoretska, I.; Mynko, O.; Ghanim, B.; Leahy, J.J.; Walker, G.M.; Kwapinski, W. ANN-Kriging Hybrid Model for Predicting Carbon and Inorganic Phosphorus Recovery in Hydrothermal Carbonization. *Waste Manag.* **2019**, *85*, 242–252. https://doi.org/10.1016/j.wasman.2018.12.044.

44. Cheng, H.; Ji, R.; Bian, Y.; Jiang, X.; Song, Y. From Macroalgae to Porous Graphitized Nitrogen-Doped Biochars—Using Aquatic Biota to Treat Polycyclic Aromatic Hydrocarbons-Contaminated Water. *Bioresour. Technol.* **2020**, *303*, 122947. https://doi.org/10.1016/j.biortech.2020.122947.
45. Yu, C.; Tang, J.; Su, H.; Huang, J.; Liu, F.; Wang, L.; Sun, H. Development of a Novel Biochar/Iron Oxide Composite from Green Algae for Bisphenol-A Removal: Adsorption and Fenton-like Reaction. *Environ. Technol. Innov.* **2022**, *28*, 102647. https://doi.org/10.1016/j.eti.2022.102647.
46. Wang, Y.; Ma, C.; Kong, D.; Lian, L.; Liu, Y. Review on Application of Algae-Based Biochars in Environmental Remediation: Progress, Challenge and Perspectives. *J. Environ. Chem. Eng.* **2023**, *11*, 111263. https://doi.org/10.1016/j.jece.2023.111263.
47. Wu, Y.; Cheng, H.; Pan, D.; Zhang, L.; Li, W.; Song, Y.; Bian, Y.; Jiang, X.; Han, J. Potassium Hydroxide-Modified Algae-Based Biochar for the Removal of Sulfamethoxazole: Sorption Performance and Mechanisms. *J. Environ. Manag.* **2021**, *293*, 112912. https://doi.org/10.1016/j.jenvman.2021.112912.
48. Amin, M.; Chetpattananondh, P.; Khan, M.N. Ultrasound Assisted Adsorption of Reactive Dye-145 by Biochars from Marine Chlorella Sp. Extracted Solid Waste Pyrolyzed at Various Temperatures. *J. Environ. Chem. Eng.* **2020**, *8*, 104403. https://doi.org/10.1016/j.jece.2020.104403.
49. Saber, M.; Takahashi, F.; Yoshikawa, K. Characterization and Application of Microalgae Hydrochar as a Low-Cost Adsorbent for Cu(II) Ion Removal from Aqueous Solutions. *Environ. Sci. Pollut. Res.* **2018**, *25*, 32721–32734. https://doi.org/10.1007/s11356-018-3106-8.
50. Leng, L.J.; Yuan, X.Z.; Huang, H.J.; Wang, H.; Wu, Z. Bin; Fu, L.H.; Peng, X.; Chen, X.H.; Zeng, G.M. Characterization and Application of Bio-Chars from Liquefaction of Microalgae, Lignocellulosic Biomass and Sewage Sludge. *Fuel Process. Technol.* **2015**, *129*, 8–14. https://doi.org/10.1016/j.fuproc.2014.08.016.
51. Parsa, M.; Nourani, M.; Baghdadi, M.; Hosseinzadeh, M.; Pejman, M. Biochars Derived from Marine Macroalgae as a Mesoporous By-Product of Hydrothermal Liquefaction Process: Characterization and Application in Wastewater Treatment. *J. Water Process Eng.* **2019**, *32*, 100942. https://doi.org/10.1016/j.jwpe.2019.100942.

52. Gurav, R.; Bhatia, S.K.; Choi, T.R.; Choi, Y.K.; Kim, H.J.; Song, H.S.; Lee, S.M.; Lee Park, S.; Lee, H.S.; Koh, J.; et al. Application of Macroalgal Biomass Derived Biochar and Bioelectrochemical System with Shewanella for the Adsorptive Removal and Biodegradation of Toxic Azo Dye. *Chemosphere* **2021**, *264*, 128539. https://doi.org/10.1016/j.chemosphere.2020.128539.
53. Wang, J.; Xie, Q.; Li, A.; Liu, X.; Yu, F.; Ji, J. Biosorption of Hexavalent Chromium from Aqueous Solution by Polyethyleneimine-Modified Ultrasonic-Assisted Acid Hydrochar from Sargassum Horneri. *Water Sci. Technol.* **2020**, *81*, 1114–1129. https://doi.org/10.2166/wst.2020.167.
54. Kim, H.; Lee, S.Y.; Choi, J.W.; Jung, K.W. Synergistic Effect in Simultaneous Removal of Cationic and Anionic Heavy Metals by Nitrogen Heteroatom Doped Hydrochar from Aqueous Solutions. *Chemosphere* **2023**, *323*, 138269. https://doi.org/10.1016/j.chemosphere.2023.138269.
55. Chen, Z.-L.; Xu, H.; Bai, L.Q.; Feng, Y.L.; Li, B. Protonated-Amino-Functionalized Bamboo Hydrochar for Efficient Removal of Hexavalent Chromium and Methyl Orange. *Prog. Nat. Sci. Mater. Int.* **2023**, *33*, 501–507. https://doi.org/10.1016/j.pnsc.2023.08.005.
56. Kojić, M.; Mihajlović, M.; Marinović-Cincović, M.; Petrović, J.; Katnić, Đ.; Krstić, A.; Butulija, S.; Onjia, A. Calcium-Pyro-Hydrochar Derived from the Spent Mushroom Substrate as a Functional Sorbent of Pb2+ and Cd2+ from Aqueous Solutions. *Waste Manag. Res.* **2022**, *40*, 1629–1636. https://doi.org/10.1177/0734242X221093951.
57. Ranguin, R.; Delannoy, M.; Yacou, C.; Jean-Marius, C.; Feidt, C.; Rychen, G.; Gaspard, S. Biochar and Activated Carbons Preparation from Invasive *Algae Sargassum* Spp. For Chlordecone Availability Reduction in Contaminated Soils. *J. Environ. Chem. Eng.* **2021**, *9*, 105280. https://doi.org/10.1016/j.jece.2021.105280.
58. Jazie, A.A.; Hydary, J.; Abed, S.A.; Al-Dawody, M.F. Hydrothermal Liquefaction of Fucus Vesiculosus Algae Catalyzed by Hβ Zeolite Catalyst for Biocrude Oil Production. *Algal Res.* **2022**, *61*, 102596. https://doi.org/10.1016/j.algal.2021.102596.
59. Cavali, M.; Libardi Junior, N.; de Sena, J.D.; Woiciechowski, A.L.; Soccol, C.R.; Belli Filho, P.; Bayard, R.; Benbelkacem, H.; de Castilhos Junior, A.B. A Review on Hydrothermal Carbonization of Potential Biomass Wastes, Characterization and Environmental

Applications of Hydrochar, and Biorefinery Perspectives of the Process. *Sci. Total Environ.* **2023**, *857*, 159627. https://doi.org/10.1016/j.scitotenv.2022.159627.

60. Martínez-Meraz, C.; González-Fernández, L.A.; Medellín-Castillo, N.A.; López-Cruz, C.M.; Reyes-Hernández, J.; Castillo-Ramos, V.; Sánchez-Polo, M. Sargassum Biomass-Derived Biochars for Ibuprofen Removal from Water: Adsorption and Kinetics. *MRS Adv.* **2023**, *8*, 1377–1384. https://doi.org/10.1557/s43580-023-00720-0.
61. Hung, C.M.; Chen, C.W.; Huang, C.P.; Dong, C. Di Activation of Peroxymonosulfate by Nitrogen-Doped Carbocatalysts Derived from Brown Algal (*Sargassum Duplicatum*) for the Degradation of Polycyclic Aromatic Hydrocarbons in Marine Sediments. *J. Environ. Chem. Eng.* **2021**, *9*, 106420. https://doi.org/10.1016/j.jece.2021.106420.
62. Hung, C.M.; Chen, C.W.; Huang, C.P.; Cheng, J.W.; Dong, C. Di Algae-Derived Metal-Free Boron-Doped Biochar as an Efficient Bioremediation Pretreatment for Persistent Organic Pollutants in Marine Sediments. *J. Clean. Prod.* **2022**, *336*, 130448. https://doi.org/10.1016/j.jclepro.2022.130448.
63. Atugoda, T.; Gunawardane, C.; Ahmad, M.; Vithanage, M. Mechanistic Interaction of Ciprofloxacin on Zeolite Modified Seaweed (*Sargassum Crassifolium*) Derived Biochar: Kinetics, Isotherm and Thermodynamics. *Chemosphere* **2021**, *281*, 130676. https://doi.org/10.1016/j.chemosphere.2021.130676.
64. Nguyen, T.B.; Truong, Q.M.; Chen, C.W.; Doong, R.A.; Chen, W.H.; Dong, C. Di Mesoporous and Adsorption Behavior of Algal Biochar Prepared via Sequential Hydrothermal Carbonization and ZnCl2 Activation. *Bioresour. Technol.* **2022**, *346*, 126351. https://doi.org/10.1016/j.biortech.2021.126351.
65. Chabi, N.; Baghdadi, M.; Sani, A.H.; Golzary, A.; Hosseinzadeh, M. Removal of Tetracycline with Aluminum Boride Carbide and Boehmite Particles Decorated Biochar Derived from Algae. *Bioresour. Technol.* **2020**, *316*, 123950. https://doi.org/10.1016/j.biortech.2020.123950.
66. Chen, Y.D.; Lin, Y.C.; Ho, S.H.; Zhou, Y.; Ren, N. qi Highly Efficient Adsorption of Dyes by Biochar Derived from Pigments-Extracted Macroalgae Pyrolyzed at Different Temperature. *Bioresour. Technol.* **2018**, *259*, 104–110. https://doi.org/10.1016/j.biortech.2018.02.094.

67. Ighalo, J.O.; Ohoro, C.R.; Ojukwu, V.E.; Oniye, M.; Shaikh, W.A.; Biswas, J.K.; Seth, C.S.; Mohan, G.B.M.; Chandran, S.A.; Rangabhashiyam, S. Biochar for Ameliorating Soil Fertility and Microbial Diversity: From Production to Action of the Black Gold. *iScience* **2025**, *28*, 11152. https://doi.org/10.1016/j.isci.2024.111524.
68. Liu, P.; Rao, D.; Zou, L.; Teng, Y.; Yu, H. Capacity and Potential Mechanisms of Cd(II) Adsorption from Aqueous Solution by Blue Algae-Derived Biochars. *Sci. Total Environ.* **2021**, *767*, 145447. https://doi.org/10.1016/j.scitotenv.2021.145447.
69. Moirana, R.L.; Mkunda, J.; Machunda, R.; Paradelo, M.; Mtei, K. Hydroxyapatite-Activated Seaweed Biochar for Enhanced Remediation of Fluoride Contaminated Soil at Various PH Ranges. *Environ. Adv.* **2023**, *11*, 100329. https://doi.org/10.1016/j.envadv.2022.100329.
70. Yu, H.; Zou, W.; Chen, J.; Chen, H.; Yu, Z.; Huang, J.; Tang, H.; Wei, X.; Gao, B. Biochar Amendment Improves Crop Production in Problem Soils: A Review. *J. Environ. Manag.* **2019**, *232*, 8–21. https://doi.org/10.1016/j.jenvman.2018.10.117.
71. Pandey, D.; Singh, S.V.; Savio, N.; Bhutto, J.K.; Srivastava, R.K.; Yadav, K.K.; Sharma, R.; Nandipamu, T.M.K.; Sarkar, B. Biochar Application in Constructed Wetlands for Wastewater Treatment: A Critical Review. *J. Water Process Eng.* **2025**, *69*, 106713. https://doi.org/10.1016/j.jwpe.2024.106713.
72. Waheed, A.; Xu, H.; Qiao, X.; Aili, A.; Yiremaikebayi, Y.; Haitao, D.; Muhammad, M. Biochar in Sustainable Agriculture and Climate Mitigation: Mechanisms, Challenges, and Applications in the Circular Bioeconomy. *Biomass Bioenergy* **2025**, *193*, 107531. https://doi.org/10.1016/j.biombioe.2024.107531.
73. Liu, Y.N.; He, L.Y. Effects of Alkali-Activated Algae Biochar on Soil Improvement after Phosphorus Absorption: Efficiency and Mechanism. *Sustainability* **2021**, *13*, 11973. https://doi.org/10.3390/su132111973.
74. Yang, X.; Jiang, D.; Cheng, X.; Yuan, C.; Wang, S.; He, Z.; Esakkimuthu, S. Adsorption Properties of Seaweed-Based Biochar with the Greenhouse Gases (CO_2, CH_4, N_2O) through Density Functional Theory (DFT). *Biomass Bioenergy* **2022**, *163*, 106519. https://doi.org/10.1016/j.biombioe.2022.106519.
75. Shi, S.; Liu, Y. Nitrogen-Doped Activated Carbons Derived from Microalgae Pyrolysis by-Products by Microwave/KOH Activation for CO_2 Adsorption. *Fuel* **2021**, *306*, 121762. https://doi.org/10.1016/j.fuel.2021.121762.

76. Chen, H.; Han, X.; Liu, Y. Gaseous Hydrogen Sulfide Removal Using Macroalgae Biochars Modified Synergistically by H_2SO_4/H_2O_2. *Chem. Eng. Technol.* **2021**, *44*, 698–709. https://doi.org/10.1002/ceat.202000461.
77. Liu, Z.; Yang, W.; Xu, W.; Liu, Y. Removal of Elemental Mercury by Bio-Chars Derived from Seaweed Impregnated with Potassium Iodine. *Chem. Eng. J.* **2018**, *339*, 468–478. https://doi.org/10.1016/j.cej.2018.01.148.
78. Balahmar, N.; Al-Jumialy, A.S.; Mokaya, R. Biomass to Porous Carbon in One Step: Directly Activated Biomass for High Performance CO_2 Storage. *J. Mater. Chem. A* **2017**, *5*, 12330–12339. https://doi.org/10.1039/c7ta01722g.
79. Wang, Y.; Yang, Q.; Chen, J.; Yang, J.; Zhang, Y.; Chen, Y.; Li, X.; Du, W.; Liang, A.; Ho, S.H.; et al. Adsorption Behavior of Cr(VI) by Magnetically Modified Enteromorpha Prolifera Based Biochar and the Toxicity Analysis. *J. Hazard. Mater.* **2020**, *395*, 122658. https://doi.org/10.1016/j.jhazmat.2020.122658.
80. Liu, Z.; Adewuyi, Y.G.; Shi, S.; Chen, H.; Li, Y.; Liu, D.; Liu, Y. Removal of Gaseous Hg0 Using Novel Seaweed Biomass-Based Activated Carbon. *Chem. Eng. J.* **2019**, *366*, 41–49. https://doi.org/10.1016/j.cej.2019.02.025.
81. Wang, H.; Wang, H.; Zhao, H.; Yan, Q. Adsorption and Fenton-like Removal of Chelated Nickel from Zn-Ni Alloy Electroplating Wastewater Using Activated Biochar Composite Derived from Taihu Blue Algae. *Chem. Eng. J.* **2020**, *379*, 122372. https://doi.org/10.1016/j.cej.2019.122372.
82. Araya, M.; Rivas, J.; Sepúlveda, G.; Espinoza-González, C.; Lira, S.; Meynard, A.; Blanco, E.; Escalona, N.; Ginocchio, R.; Garrido-Ramírez, E.; et al. Effect of Pyrolysis Temperature on Copper Aqueous Removal Capability of Biochar Derived from the Kelp Macrocystis Pyrifera. *Appl. Sci.* **2021**, *11*, 9223. https://doi.org/10.3390/app11199223.
83. Khanzada, A.K.; Rizwan, M.; Al-Hazmi, H.E.; Majtacz, J.; Kurniawan, T.A.; Mąkinia, J. Removal of Arsenic from Wastewater Using Hydrochar Prepared from Red Macroalgae: Investigating Its Adsorption Efficiency and Mechanism. *Water* **2023**, *15*, 3866. https://doi.org/10.3390/w15213866.
84. Wang, C.; Li, X.; Wu, W.; Chen, G.; Tao, J. Removal of Cadmium in Water by Potassium Hydroxide Activated Biochar Produced from Enteromorpha Prolifera. *J. Water Process Eng.* **2021**, *42*, 102201. https://doi.org/10.1016/j.jwpe.2021.102201.

85. Li, X.; Wang, C.; Tian, J.; Liu, J.; Chen, G. Comparison of Adsorption Properties for Cadmium Removal from Aqueous Solution by Enteromorpha Prolifera Biochar Modified with Different Chemical Reagents. *Environ. Res.* **2020**, *186*, 109502. https://doi.org/10.1016/j.envres.2020.109502.
86. Kumar, P.; Patel, A.K.; Singhania, R.R.; Chen, C.W.; Saratale, R.G.; Dong, C. Di Enhanced Copper (II) Bioremediation from Wastewater Using Nano Magnetite (Fe3O4) Modified Biochar of Ascophyllum Nodosum. *Bioresour. Technol.* **2023**, *388*, 129654. https://doi.org/10.1016/j.biortech.2023.129654.
87. Tan, L.; Nie, Y.; Chang, H.; Zhu, L.; Guo, K.; Ran, X.; Zhong, N.; Zhong, D.; Xu, Y.; Ho, S.H. Adsorption Performance of Ni(II) by KOH-Modified Biochar Derived from Different Microalgae Species. *Bioresour. Technol.* **2024**, *394*, 130287. https://doi.org/10.1016/j.biortech.2023.130287.
88. Kumar, M.; Singh, A.K.; Sikandar, M. Biosorption of Hg (II) from Aqueous Solution Using Algal Biomass: Kinetics and Isotherm Studies. *Heliyon* **2020**, *6*, 1465–1469. https://doi.org/10.1016/j.heliyon.2020.e03321.
89. Moon, S.; Lee, Y.J.; Choi, M.Y.; Lee, C.G.; Park, S.J. Adsorption of Heavy Metals and Bisphenol A from Wastewater Using Spirulina Sp.-Based Biochar as an Effective Adsorbent: A Preliminary Study. *J. Appl. Phycol.* **2023**, *35*, 2257–2269. https://doi.org/10.1007/s10811-023-03070-4.
90. Yang, Z.; Hou, J.; Wu, J.; Miao, L. The Effect of Carbonization Temperature on the Capacity and Mechanisms of Pb(II) Adsorption by Microalgae Residue-Derived Biochar. *Ecotoxicol. Environ. Saf.* **2021**, *225*, 112750. https://doi.org/10.1016/j.ecoenv.2021.112750.
91. Yaashikaa, P.R.; Keerthana Devi, M.; Senthil Kumar, P.; Pandian, E. A Review on Biodiesel Paroduction by Algal Biomass: Outlook on Lifecycle Assessment and Techno-Economic Analysis. *Fuel* **2022**, *324*, 124774. https://doi.org/10.1016/j.fuel.2022.124774.
92. Kumar, S.; Tirlangi, S.; Kumar, A.; Imran, M.; Pillai HP, J.S.; Kumar Koshariya, A.; Sathish, T.; Ubaidullah, M.; Ayub, R.; Minnam Reddy, V.R.; et al. A Review on the Contribution of Nanotechnology for Biofuel Production from Algal Biomass: A Bridge to the Reduction of Carbon Footprint. *Sustain. Energy Technol. Assess.* **2023**, *60*, 103498. https://doi.org/10.1016/j.seta.2023.103498.

93. Li, G.; Yao, J. A Review of Algae-Based Carbon Capture, Utilization, and Storage (Algae-Based CCUS). *Gases* **2024**, *4*, 468–503. https://doi.org/10.3390/gases4040024.
94. Zhang, Q.; Guan, Y.; Zhang, Z.; Dong, S.; Yuan, T.; Ruan, Z.; Chen, M. Sustainable Microalgae Cultivation: A Comprehensive Review of Open and Enclosed Systems for Biofuel and High Value Compound Production. In *E3S Web of Conferences*; EDP Sciences: Les Ulis, France, 2024; Volume 577, p. 1008.
95. Ijaola, A.O.; Akamo, D.O.; George, T.T.; Sengul, A.; Adediji, M.Y.; Asmatulu, E. Algae as a Potential Source of Protein: A Review on Cultivation, Harvesting, Extraction, and Applications. *Algal Res.* **2024**, *77*, 103329. https://doi.org/10.1016/j.algal.2023.103329.
96. Sun, J.; Norouzi, O.; Mašek, O. A State-of-the-Art Review on Algae Pyrolysis for Bioenergy and Biochar Production. *Bioresour. Technol.* **2022**, *346*, 126258. https://doi.org/10.1016/j.biortech.2021.126258.
97. Kannah, R.Y.; Kavitha, S.; Banu, J.R.; Sivashanmugam, P.; Gunasekaran, M.; Kumar, G. A Mini Review of Biochemical Conversion of Algal Biorefinery. *Energy Fuels* **2021**, *35*, 16995–17007. https://doi.org/10.1021/acs.energyfuels.1c02294.
98. Poornima, S.; Manikandan, S.; Prakash, R.; Deena, S.R.; Subbaiya, R.; Karmegam, N.; Kim, W.; Govarthanan, M. Biofuel and Biochemical Production through Biomass Transformation Using Advanced Thermochemical and Biochemical Processes—A Review. *Fuel* **2024**, *372*, 132204. https://doi.org/10.1016/j.fuel.2024.132204.
99. Farouk, S.M.; Tayeb, A.M.; Abdel-Hamid, S.M.S.; Osman, R.M. Recent Advances in Transesterification for Sustainable Biodiesel Production, Challenges, and Prospects: A Comprehensive Review. *Environ. Sci. Pollut. Res.* **2024**, *31*, 12722–12747. https://doi.org/10.1007/s11356-024-32027-4.
100. Bassoli, S.C.; da Fonseca, Y.A.; Wandurraga, H.J.L.; Baeta, B.E.L.; de Souza Amaral, M. Research Progress, Trends, and Future Prospects on Hydrothermal Liquefaction of Algae for Biocrude Production: A Bibliometric Analysis. *Biomass Convers. Biorefinery* **2023**, *14*, 28781–28796. https://doi.org/10.1007/s13399-023-03905-7.
101. El-Araby, R. Biofuel Production: Exploring Renewable Energy Solutions for a Greener Future. *Biotechnol. Biofuels Bioprod.* **2024**, *17*, 129. https://doi.org/10.1186/s13068-024-02571-9.

102. Quiroz, D.; McGowen, J.; Quinn, J.C. Implications of Pond Reliability on the Techno-Economic and Life Cycle Environmental Impacts of Algal Biofuels. *J. Clean. Prod.* **2024**, *469*, 143178. https://doi.org/10.1016/j.jclepro.2024.143178.
103. Zarei, Z.; Malekshahi, P.; Morowvat, M.H.; Trzcinski, A.P. Hydrodynamic Performance of Algal Bioreactors. *Algal Bioreact. Sci. Eng. Technol. Upstream Process.* **2024**, *1*, 121–133. https://doi.org/10.1016/B978-0-443-14058-7.00043-9.
104. Pandey, S.; Narayanan, I.; Selvaraj, R.; Varadavenkatesan, T.; Vinayagam, R. Biodiesel Production from Microalgae: A Comprehensive Review on Influential Factors, Transesterification Processes, and Challenges. *Fuel* **2024**, *367*, 131547. https://doi.org/10.1016/j.fuel.2024.131547.
105. Yang, B.; Liu, J.; Ma, X.; Guo, B.; Liu, B.; Wu, T.; Jiang, Y.; Chen, F. Genetic Engineering of the Calvin Cycle toward Enhanced Photosynthetic CO_2 Fixation in Microalgae. *Biotechnol. Biofuels* **2017**, *10*, 1–13. https://doi.org/10.1186/s13068-017-0916-8.
106. Hlavova, M.; Turoczy, Z.; Bisova, K. Improving Microalgae for Biotechnology—From Genetics to Synthetic Biology. *Biotechnol. Adv.* **2015**, *33*, 1194–1203. https://doi.org/10.1016/j.biotechadv.2015.01.009.
107. Brar, A.; Kumar, M.; Soni, T.; Vivekanand, V.; Pareek, N. Insights into the Genetic and Metabolic Engineering Approaches to Enhance the Competence of Microalgae as Biofuel Resource: A Review. *Bioresour. Technol.* **2021**, *339*, 125597. https://doi.org/10.1016/j.biortech.2021.125597.
108. Patel, V.K.; Das, A.; Kumari, R.; Kajla, S. Recent Progress and Challenges in CRISPR-Cas9 Engineered Algae and Cyanobacteria. *Algal Res.* **2023**, *71*, 103068. https://doi.org/10.1016/j.algal.2023.103068.
109. Joshi, S.; Mishra, S.D. Recent Advances in Biofuel Production through Metabolic Engineering. *Bioresour. Technol.* **2022**, *352*, 127037. https://doi.org/10.1016/j.biortech.2022.127037.
110. Valizadeh Derakhshan, M.; Nasernejad, B.; Abbaspour-Aghdam, F.; Hamidi, M. Oil Extraction from Algae: A Comparative Approach. *Biotechnol. Appl. Biochem.* **2015**, *62*, 375–382. https://doi.org/10.1002/bab.1270.
111. Rathinavel, L.; Ravikumar, Y.; Jothinathan, D.; Pandey, A.; Mahata, C. Extraction and Enrichment of Fatty Acids from Marine Microalgae. In *Marine Molecules from Algae and*

Cyanobacteria: Extraction, Purification, Toxicology and Applications; Elsevier: Amsterdam, The Netherlands, 2024; pp. 41–57. ISBN 9780443216749.

112. Ezhumalai, G.; Arun, M.; Manavalan, A.; Rajkumar, R.; Heese, K. A Holistic Approach to Circular Bioeconomy Through the Sustainable Utilization of Microalgal Biomass for Biofuel and Other Value-Added Products. *Microb. Ecol.* **2024**, *87*, 1–16. https://doi.org/10.1007/s00248-024-02376-1.
113. Gentili, F.G.; Fick, J. Algal Cultivation in Urban Wastewater: An Efficient Way to Reduce Pharmaceutical Pollutants. *J. Appl. Phycol.* **2017**, *29*, 255–262. https://doi.org/10.1007/s10811-016-0950-0.
114. Bakonyi, P.; Peter, J.; Koter, S.; Mateos, R.; Kumar, G.; Koók, L.; Rózsenberszki, T.; Pientka, Z.; Kujawski, W.; Kim, S.H.; et al. Possibilities for the Biologically-Assisted Utilization of CO_2-Rich Gaseous Waste Streams Generated during Membrane Technological Separation of Biohydrogen. *J. CO2 Util.* **2020**, *36*, 231–243. https://doi.org/10.1016/j.jcou.2019.11.008.
115. Comley, J.G.; Scott, J.A.; Laamanen, C.A. Utilizing CO_2 in Industrial Off-Gas for Microalgae Cultivation: Considerations and Solutions. *Crit. Rev. Biotechnol.* **2024**, *44*, 910–923. https://doi.org/10.1080/07388551.2023.2233692.
116. Vieira Costa, J.A.; Cruz, C.G.; Centeno da Rosa, A.P. Insights into the Technology Utilized to Cultivate Microalgae in Dairy Effluents. *Biocatal. Agric. Biotechnol.* **2021**, *35*, 102106. https://doi.org/10.1016/j.bcab.2021.102106.
117. Zewdie, D.T.; Ali, A.Y. Cultivation of Microalgae for Biofuel Production: Coupling with Sugarcane-Processing Factories. *Energy. Sustain. Soc.* **2020**, *10*, 1–16. https://doi.org/10.1186/s13705-020-00262-5.
118. Thomas, P.K.; Dunn, G.P.; Coats, E.R.; Newby, D.T.; Feris, K.P. Algal Diversity and Traits Predict Biomass Yield and Grazing Resistance in Wastewater Cultivation. *J. Appl. Phycol.* **2019**, *31*, 2323–2334. https://doi.org/10.1007/s10811-019-01764-2.
119. Sathinathan, P.; Parab, H.M.; Yusoff, R.; Ibrahim, S.; Vello, V.; Ngoh, G.C. Photobioreactor Design and Parameters Essential for Algal Cultivation Using Industrial Wastewater: A Review. *Renew. Sustain. Energy Rev.* **2023**, *173*, 113096. https://doi.org/10.1016/j.rser.2022.113096.
120. Hekmatmehr, H.; Esmaeili, A.; Pourmahdi, M.; Atashrouz, S.; Abedi, A.; Ali Abuswer, M.; Nedeljkovic, D.; Latifi, M.; Farag, S.; Mohaddespour, A. Carbon Capture Technologies: A

Review on Technology Readiness Level. *Fuel* **2024**, *363*, 130898. https://doi.org/10.1016/j.fuel.2024.130898.

121. Yang, J.; Zhao, T.; Cui, X.; Peng, M.; Wang, X.; Mao, H.; Cui, M. New Insights into the Carbon Neutrality of Microalgae from Culture to Utilization: A Critical Review on the Algae-Based Solid Biofuels. *Biomass Bioenergy* **2022**, *166*, 106599. https://doi.org/10.1016/j.biombioe.2022.106599.
122. Chia, S.R.; Nomanbhay, S.B.H.M.; Chew, K.W.; Munawaroh, H.S.H.; Shamsuddin, A.H.; Show, P.L. Algae as Potential Feedstock for Various Bioenergy Production. *Chemosphere* **2022**, *287*, 131944. https://doi.org/10.1016/j.chemosphere.2021.131944.
123. Jiang, Y.; Zhou, G.; Zhang, H.; Xu, J.; Ge, H.; Shen, L.; Song, T. Coupling Effects of Heating Pelleting and Torrefaction on Black Pellets Production from Microalga Nannochloropsis Oceanica Residues. *Fuel* **2023**, *353*, 129007. https://doi.org/10.1016/j.fuel.2023.129007.
124. Kosowska-Golachowska, M.; Musiał, T.; Urbaniak, D.; Otwinowski, H. Analysis of Microalgae Pellets Combustion in a Circulating Fluidized-Bed. In *E3S Web of Conferences*; EDP Sciences: Les Ulis, France, 2017; Volume 14, p. 2035.
125. Miranda, M.T.; Sepúlveda, F.J.; Arranz, J.I.; Montero, I.; Rojas, C.V. Physical-Energy Characterization of Microalgae Scenedesmus and Experimental Pellets. *Fuel* **2018**, *226*, 121–126. https://doi.org/10.1016/j.fuel.2018.03.097.
126. Kastanaki, E.; Vamvuka, D. A Comparative Reactivity and Kinetic Study on the Combustion of Coal-Biomass Char Blends. *Fuel* **2006**, *85*, 1186–1193. https://doi.org/10.1016/j.fuel.2005.11.004.
127. Gong, Z.; Wang, Z.; Wang, Z.; Du, A.; Fang, P.; Sun, Z.; Li, X. Study on Pyrolysis of Oil Sludge with Microalgae Residue Additive. *Can. J. Chem. Eng.* **2018**, *96*, 1919–1925. https://doi.org/10.1002/cjce.23143.
128. Wu, X.; Liu, J.; Wei, Z.; Chen, Z.; Evrendilek, F.; Huang, W. Oxy-Fuel Co-Combustion Dynamics of Phytoremediation Biomass and Textile Dyeing Sludge: Gas-to-Ash Pollution Abatement. *Sci. Total Environ.* **2022**, *825*, 153656. https://doi.org/10.1016/j.scitotenv.2022.153656.
129. Chen, C.; Chen, F.; Cheng, Z.; Chan, Q.N.; Kook, S.; Yeoh, G.H. Emissions Characteristics of NOx and SO_2 in the Combustion of Microalgae Biomass Using a Tube Furnace. *J. Energy Inst.* **2017**, *90*, 806–812. https://doi.org/10.1016/j.joei.2016.06.003.

Paper 4: Sargassum biomass-derived biochars for ibuprofen removal from water: Adsorption and kinetics

Journal: MRS Advances

Impact Factor (JCR): 0.8

Quartile: Q4

Volume: 8

ISSN (electronic): 2059-8521

ISSN (print): 2731-5894

https://doi.org/10.1557/s43580-023-00720-0

https://link.springer.com/article/10.1557/s43580-023-00720-0

Sargassum biomass-derived biochars for ibuprofen removal from water: Adsorption and kinetics

Carolina Martínez-Meraz[1], Lázaro Adrián González-Fernández[2], Nahum Andrés Medellín-Castillo[1,2], Claudia Maricela López-Cruz[3], Jaime Reyes-Hernández[4], Ventura Castillo-Ramos[5] and Manuel Sánchez-Polo[5]*

[1]*School of Engineering, Autonomous University of San Luis Potosi, San Luis Potosí 78290, Mexico*

[2]*Multidisciplinary Graduate Program in Environmental Sciences, Autonomous University of San Luis Potosi, San Luis Potosí 78000, Mexico*

[3]*Graduate Studies and Research Center, Faculty of Engineering, Autonomous University of San Luis Potosi, Zona Universitaria, S.L.P., 78290, Mexico.*

[4]*School of Nursing and Nutrition, Autonomous University of San Luis Potosi, Zona Universitaria, S.L.P., 78290, Mexico.*

[5]*Department of Inorganic Chemistry, School of Science, University of Granada, 18071 Granada, Spain.*

**Corresponding author: lazaroadrian1995@gmail.com*

Abstract

Water contamination, particularly in drinking water sources, presents a significant global challenge. In recent times, the widespread use of pharmaceuticals like ibuprofen has emerged as a concerning factor. Concurrently, the accumulation of Sargassum, a marine algae, along the Caribbean coastlines has caused severe socioeconomic and ecological impacts. To address the challenges posed by both pharmaceutical contamination and Sargassum accumulation, an innovative approach is proposed. This approach involves utilizing Sargassum biomass to create carbonaceous materials, which can effectively decontaminate water polluted with ibuprofen. Through batch adsorption experiments, these materials have demonstrated exceptional adsorption capacities, surpassing conventional adsorbents, with capacities of up to 21.7 mg g^{-1}. Additionally, the kinetics of ibuprofen removal was investigated, revealing that the second-order model provides the best fit for the experimental data. The use of Sargassum-derived materials not only aligns with principles of the circular economy but also serves as a crucial solution for remediating water resources.

1. Introduction

Pharmaceuticals are a vital part of modern medicine, helping to treat and cure a wide range of illnesses and diseases. However, as with any substance, they can have unintended consequences when they enter the environment. Pharmaceuticals can enter the environment through a variety of pathways, including human and animal waste, runoff from agricultural fields, and improper

disposal of unused medications. Once in the environment, they can persist for long periods of time and potentially have harmful effects on wildlife and ecosystems [1].

One of the main concerns with pharmaceuticals in the environment is their potential impact on aquatic ecosystems. Many pharmaceuticals are designed to be biologically active, meaning they can have effects on living organisms even at low concentrations. When these substances enter waterways, they can accumulate in the tissues of aquatic organisms, potentially causing harm to fish, amphibians, and other wildlife. In addition, some pharmaceuticals have been shown to disrupt the endocrine systems of aquatic organisms, leading to reproductive and developmental problems [2].

Another concern with pharmaceuticals in the environment is the potential for them to enter the food chain. When animals consume contaminated water or food, they can accumulate pharmaceuticals in their tissues, potentially exposing humans who consume those animals to these substances. While the long-term effects of this exposure are not yet fully understood, there is growing concern about the potential risks to human health. As a result, there is increasing interest in finding ways to reduce the amount of pharmaceuticals that enter the environment and to better understand their potential impacts [3].

Various methods have been used to remove pharmaceuticals from water. Biological degradation involves the use of microorganisms to break down pharmaceutical compounds, and while it can be effective for certain types of pharmaceuticals, its efficiency depends on the specific microorganisms and conditions. Membrane filtration techniques, such as reverse osmosis and nanofiltration, can effectively remove pharmaceuticals from water by physically separating them from the water molecules, but these methods can be expensive and require high energy input. Advanced oxidation processes (AOPs) involve the use of powerful oxidants, such as ozone, hydrogen peroxide, or UV light, to break down pharmaceutical compounds. While AOPs can be effective for removing a wide range of pharmaceuticals, they can also generate harmful by-products. Electrochemical oxidation processes use an electric current to generate oxidants that can break down pharmaceuticals, and this method has been increasingly studied for its potential to remove pharmaceuticals from water. Adsorption, on the other hand, is a process in which pharmaceuticals are attracted to and bound to a solid surface, such as activated carbon or graphene oxide beads. This method is often cost-effective and highly efficient [4].

Carbonaceous materials have shown promise as a potential solution for removing pharmaceuticals from water. These materials, which include activated carbon, biochar, and graphene oxide, have a high surface area and a strong affinity for organic compounds. When added to water, they can adsorb pharmaceuticals and other contaminants, effectively removing them from the water [5]. Biochar is a form of charcoal that is produced by heating organic materials, such as wood, crop residues, or animal manure, in a low-oxygen environment through a pyrolysis process. This results in a porous and stable carbon-rich material that has a wide range of applications, including soil improvement, carbon sequestration, and water remediation [6]. Biochar has a highly porous structure with a large surface area, which makes it an excellent adsorbent for various contaminants in water. It can adsorb pollutants such as heavy metals (e.g., lead, cadmium), organic compounds (e.g., pesticides, pharmaceuticals), and nutrients (e.g., nitrogen and phosphorus) [7].

The Sargassum problem in Mexico has become a significant environmental and economic challenge in recent years. Sargassum is a type of brown algae that originates from the Sargasso Sea in the Atlantic Ocean. However, in recent years, massive amounts of Sargassum have been washing up on the shores of Mexico's Caribbean coast, particularly in popular tourist destinations such as Cancun, Playa del Carmen, and Tulum. The excessive influx of Sargassum has had detrimental effects on the region's pristine beaches, marine ecosystems, and tourism industry [8].

The arrival of Sargassum poses several problems for Mexico. Firstly, the seaweed accumulates on the beaches, forming thick mats that release an unpleasant odor as they decompose. This not only affects the aesthetic appeal of the beaches but also discourages tourists from visiting. The tourism industry, a vital source of revenue for the region, has suffered as a result. Additionally, the excessive amounts of Sargassum can smother and suffocate coral reefs, seagrasses, and other marine life, disrupting the delicate balance of the coastal ecosystem. The decomposition of Sargassum also consumes oxygen, leading to hypoxic conditions that further harm marine organisms [9].

Efforts are being made to address the Sargassum problem, including the deployment of barriers and the development of innovative technologies for its collection and disposal. However, finding a long-term solution remains a challenge as the influx of Sargassum can be unpredictable and difficult to manage effectively [10]. In the absence of effective management programs for the macroalgae Sargassum, the collected biomass is typically disposed of in waste sites that do not

adhere to proper protocols. As a result, there is a growing interest in identifying alternative applications for this biomass, which is commonly considered as waste. These potential applications encompass various fields, with particular emphasis on fertilizer and biogas production.

The primary aim of this study is to conduct a comprehensive characterization of the biochars derived from Sargassum biomass via pyrolysis. Furthermore, the study seeks to assess the potential applicability of these derivatives for the removal of ibuprofen from aqueous environments, employing batch adsorption techniques. Additionally, the investigation includes an examination of the impact of time on the removal efficiency of ibuprofen, applying first and second order kinetic models.

2. Materials and methods

2.1 Biochar synthesis from Sargassum

Biochar is obtained by the slow pyrolysis process which must be carried out in an atmosphere in the absence of oxygen, so nitrogen is used as an inert gas (80 mL min^{-1}) in the process to displace the oxygen in the furnace. Three residence time values are used in this process, for which three stainless steel vessels are used, each containing 50 g of Sargassum and are introduced into a synthesis oven, causing the temperature to rise at a heating rate of approximately 10 °C min^{-1} to the desired temperature of 600 °C, then this temperature is kept constant for the residence times of 1, 3 and 5 h. The samples (identified as Bio1h, Bio3h, Bio5h depending on the residence time) are allowed to cool in the oven itself under the nitrogen stream and are passed into a desiccator and finally weighed on an analytical balance.

2.2 Conversion efficiency

The efficiency of the conversion of natural material to biochar is calculated with the equation (1):

$$\%_{Conv} = \frac{m_i - m_f}{m_i} \cdot 100 \quad (1)$$

Where $\%_{Conv}$ refers to the conversion rate of biomass to biochar and m_i and m_f are the masses of natural material and biochar obtained, respectively.

2.3 Characterization of biochars

FTIR analysis was performed on the raw material (RM) and the three synthesized materials to identify their primary functional groups, utilizing a ThermoFisher Scientific Nicolet iS10 FTIR spectrophotometer. Furthermore, the synthesized materials underwent a comprehensive physicochemical characterization. This characterization encompassed nitrogen physisorption, which was utilized to determine the specific area (S_{BET}) and pore volume (V_{pore}) and size of the materials [11]. Additionally, the point of zero charge (PZC) was determined, following the methodology outlined by Dávila-Rodríguez et al. [12] and Pérez-Escobedo et al. [13]. Additionally, the materials were subjected to elemental analysis to determine their composition on a Thermo Scientific Elemental Analyzer Model Flash 2000. The Boehm titration method [14] was employed to determine the total sites. In 50 mL centrifuge tubes, 50 mL of NaOH and 0.01 N HNO_3 were separately introduced. Subsequently, 0.1 g of each material was placed in the respective tubes. The tubes were maintained at 25 °C and shaken every 24 hours for a duration of 5 days. Following this period, 20 mL aliquots were extracted and titrated with the corresponding acidic or basic solution. The concentrations of the active sites were calculated using Eq. (2), while the final concentration of the neutralizing solution was determined using Eq. (3).

$$C_{AS} = \frac{V_i(C_i - C_f)}{m} \times 1000 \tag{2}$$

$$C_i = \frac{V_T C_T}{V_a} \tag{3}$$

In this context, C_{AS} represents the concentration of active sites (meq g^{-1}), C_i denotes the initial concentration of the neutralizing solution (Eq L^{-1}), C_f indicates the final concentration of the neutralizing solution (Eq L^{-1}), m represents the mass of the adsorbent material (g), V_i stands for the initial volume of the neutralizing solution (L), C_T is the concentration of the titrating solution (Eq L^{-1}), V_T corresponds to the used volume of the titrating solution (mL), and V_a indicates the volume of the aliquot of the neutralizing solution (mL).

2.4 Removal of ibuprofen using biochars. Kinetic study

The synthesized materials underwent analysis for ibuprofen adsorption within batch systems, aiming to investigate the kinetic behaviour of the removal process. In 50 mL centrifuge tubes, a

50 mL portion of a contaminant solution with a concentration of 20 mg L^{-1} was introduced. For each tube, 0.05 g of the synthesized materials were incorporated, and the pH was precisely adjusted to 7.0 using diluted solutions of NaOH and HCl as required. The pH values were systematically monitored over a 7-day period, during which each tube was consistently agitated within a temperature-controlled bath set at 25 ºC. Samples of the solution were extracted at specific time intervals spanning from 0.25 to 168 h. Subsequently, these samples were analysed using UV/Vis spectroscopy to determine their respective concentrations.

The ibuprofen adsorption capacity experimental data, in relation to time, are interpreted through application of the first and second-order kinetic models. The mathematical representations of these kinetic models, describing the adsorption rates for the first and second order reactions, are expressed as equations (4) and (5) correspondingly:

$$q = q_e(1 - e^{-k_1 t}) \tag{4}$$

$$\frac{1}{q_e - q} - \frac{1}{q_e} = k_2 t \tag{5}$$

Where k_1 and k_2 are the first order reaction rate constants, in min^{-1}, and second-order, in g mg^{-1} min^{-1}, respectively, and q_e is the mass of ibuprofen adsorbed when equilibrium is reached, in mg g^{-1}. The process of data fitting for the estimation of the constants, in accordance with the kinetic models, was executed through an optimization methodology based on the least squares method. This procedure was conducted using the Statistica® software.

3. Results and discussions

3.1 Biochar yield and characterization

After the slow pyrolysis, three biochars were obtained at the three residence times evaluated. The materials were allowed to cool and weighed to calculate the $\%_{Conv}$. Table 1 shows the results obtained, both in terms of mass and $\%_{Conv}$. As can be seen, the $\%_{Conv}$ of biochar synthesis was found to be between 43.5 and 59.8 %.

Table 1. Performance of biochar synthesis from Sargassum biomass and physicochemical characterization

Sample	$\%_{Conv}$	Elemental Analysis (%)					PZC	Active Sites					S_{BET} (m^2 g^{-1})	V_{pore} (cm^3 g^{-1})	Pore size (nm)
		C	H	N	S	O*		Basic Sites (meq g^{-1})	Acid Sites (meq g^{-1})						
									Total	Carboxylic	Lactonic	Phenolic			
Bio1h	59.8	45.04	5.70	1.36	0.29	47.61	6.32	0.0263	1.0101	0.3522	0.3594	0.2985	2.7	0.005	9.7
Bio3h	45.9	48.37	2.17	0.96	0.05	48.45	6.50	0.0535	1.5241	0.4208	0.1121	0.9912	5.3	0.006	3.5
Bio5h	43.5	50.59	2.41	1.16	0.11	45.73	6.62	0.0989	1.1412	0.7185	0.1015	0.3212	14.7	0.011	2.9

*Calculated by difference

As the residence time is increased, the material's $\%_{Conv}$ reduces due to increased removal of organic matter and the decomposition of other compounds caused by prolonged exposure to elevated temperatures [15]. The specific composition and yield of the pyrolysis products and the resulting biochar depends on the type of biomass and the pyrolysis conditions, such as heating rate, residence time, and temperature. In this case, the residence or synthesis time is the variable that affects the conversion rate of the material. As the pyrolysis time increases, more carbohydrates and other components of the starting material may volatilize, resulting in a loss of mass in the sample.

These materials underwent various tests to facilitate their characterization. Initially, they underwent Elemental Analysis, and the results are also presented in Table 1. As can be noticed, an increase in residence time causes an increase in carbon content in the prepared biochars as reported for biochars prepared from other biomasses [16,17].

The PZC and active sites concentration were estimated, and the results are reported in Table 1. As can be seen, the materials are acidic, as the concentration of acidic sites is higher than that of basic sites, which corresponds with the slightly acidic PZC also found. This behaviour has also been reported by other authors such as Atugoda [18]. As can be observed, as pyrolysis time increases, the PZC also increases, as does the concentration of basic and acidic sites, in all cases.

The specific area of the biochars that were synthesized ranged from 2.7 to 14.7 m^2 g^{-1}, while the pore volume values spanned from 0.005 to 0.011 cm^3 g^{-1}. Furthermore, the pore diameters varied between 2.9 and 9.7 nm. These observations indicate that the calcination process applied to the raw material led to an increase in specific area. According to the IUPAC classification, all the prepared biochars can be classified as essentially mesoporous materials [19] (Fig. 1).

This increase in specific surface of the biochars can be attributed to the calcination method employed during their synthesis, wherein the thermal treatment facilitates the decomposition of organic matter, thereby promoting pore formation with the increase of time [20]. As can also be observed, with increasing residence time, the diameter of the pores decreases, which is directly related to the increase in the area of the material, since as the pores become smaller and smaller, the internal surface area of the synthesized materials increases.

In the case of Sargassum-derived biochars, specific characteristics of the precursor material, Sargassum seaweed, contribute to the properties of the resulting biochars. Sargassum-derived biochars may exhibit relatively low specific surface areas due to the composition of seaweed biomass, which may not inherently possess the porous structure found in certain carbonaceous materials. The carbonization conditions applied to Sargassum may also influence the development of the biochar's porous framework. The cellular structure of Sargassum, along with the potential presence of compounds such as alginates and other organic constituents, can impact the overall porosity of the resulting biochars. While the specific surface area of Sargassum-derived biochars can be influenced by various factors, their natural composition and the conditions of carbonization contribute to their characteristic surface properties.

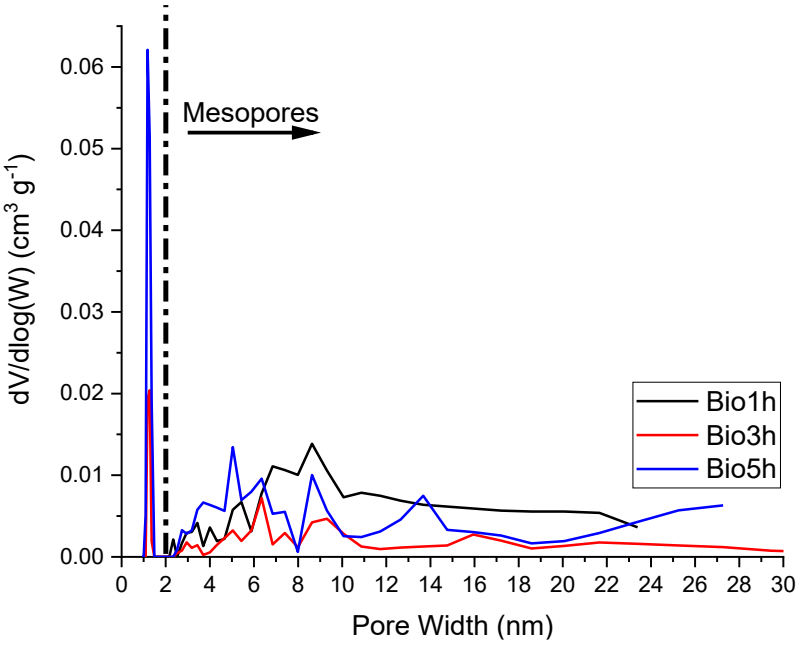

Figure 1. Pore size distribution for the synthesized biochars

Figure 2 illustrates the principal functional groups identified within the synthesized materials. The analysis reveals the presence of distinct functional groups, including carboxylic, carbonyl (associated with lactones), and aromatic structures, which are indicative of the presence of phenolic groups within the material's structure. These functional groups play an essential role in the removal of the contaminant studied from the solution, primarily through mechanisms involving electrostatic interactions with the electron cloud of the contaminants and due to the formation of chemical bonds between the adsorbate and the adsorbent [21].

It is important to note that the most notable change when going from the RM spectra to that of the synthesized biochars is the absence of the band associated with the asymmetric vibration of the carboxyl group (1650 cm^{-1}), which is related to the concentration of carboxyl sites in the materials. It can also be observed that the materials synthesized with the highest residence times (3h and 5h) do not show the band associated with hydroxyl groups and nitrogen-bearing bonds (3300 cm^{-1}), which may mean that the materials are more dehydrated than the RM and hydrochar synthesized with the shortest residence time.

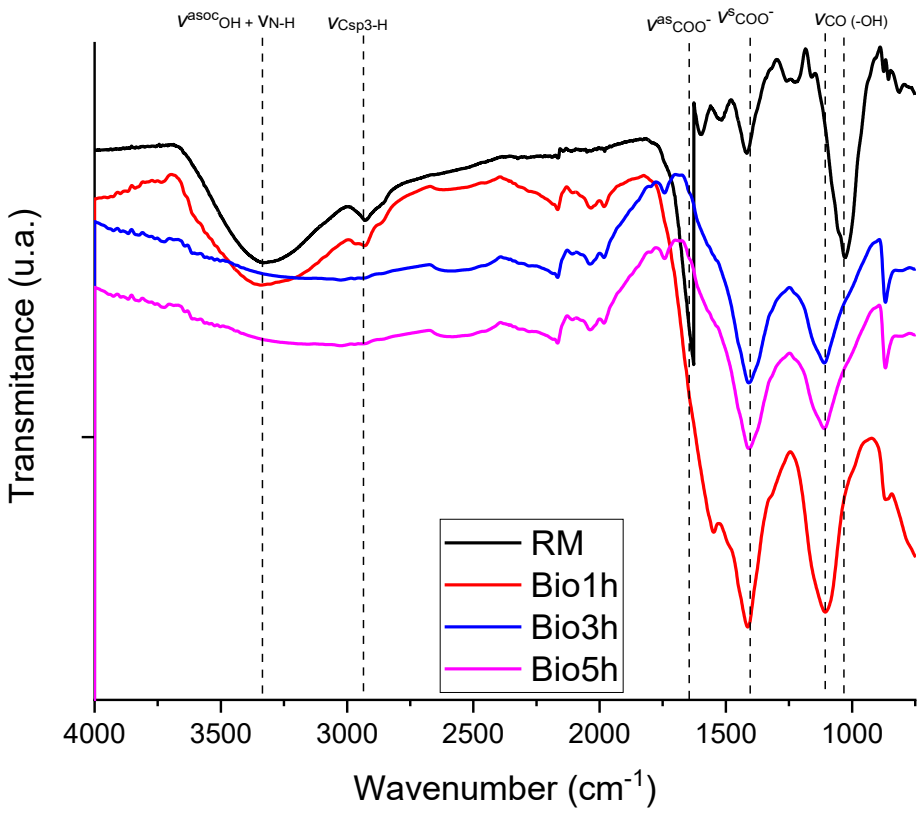

Figure 2. Infrared spectrum of the RM and the three synthesized biochars

3.2 Ibuprofen adsorption

The three synthesized materials and the RM were subjected to ibuprofen adsorption experiments in batch conditions. Figure 3a shows the adsorption capacities achieved as well as the associated removal percentages.

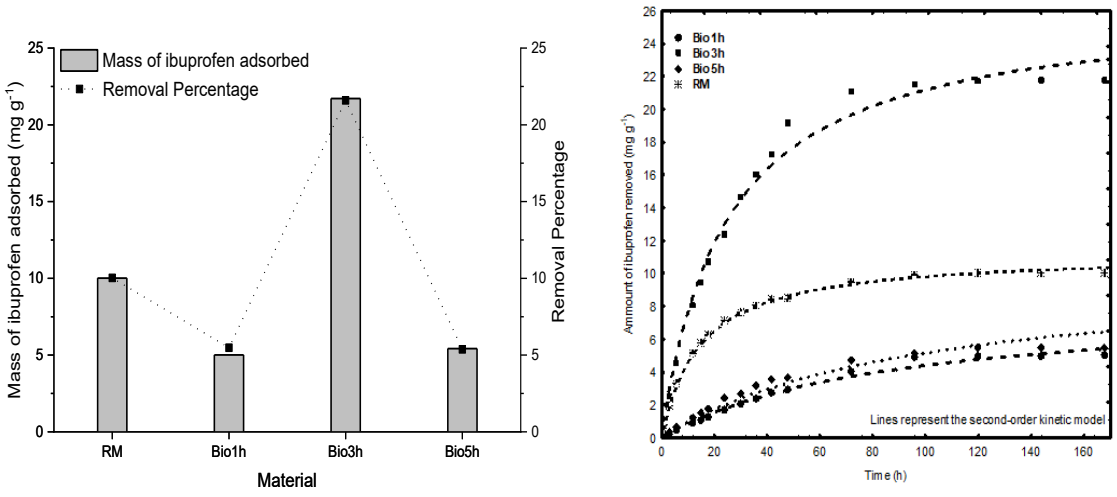

a) b)

Figure 3. a) Adsorption capacities and removal percentages of ibuprofen in the RM and the synthesized biochars and b) Time-dependent variation curves of ibuprofen adsorption capacity for raw material and synthesized biochars

Figure 3a shows that the adsorption capacity of biochars synthesized with residence time of 1 and 5 h decrease with respect to RM sample. This may be due to the lower concentration of active sites of the synthesized materials compared to those of RM, which are previously reported [22]. By decreasing the number of functional groups there are fewer effective sites for the adsorption phenomenon to occur. The opposite occurs with the material synthesized using 3 h of pyrolysis time, which shows a concentration of active sites comparable to that in the RM. In addition to this, the latter material has the highest concentration of phenolic sites, which imply more aromaticity in the material, an environment that promotes the π- π interaction of the delocalized electronic clouds of the aromatic rings in the adsorbent and in the adsorbate [23].

The adsorption capacity shown by the RM is similar to that reported by Pimentel-Almeida [24], however, that of the materials synthesized with 1 and 5 h of synthesis time is lower than that

reported for materials of similar origin and synthesis conditions [25]. In the case of the biochar synthesized using 3 h of residence time during the pyrolysis, its adsorption capacity is comparable, or higher than that reported for other materials obtained using synthesis processes and raw materials of similar nature [26], which evidences its applicability and viability for the removal of ibuprofen (Table 2).

Table 2. Biochars synthesized from different biomasses used for the removal of ibuprofen from aqueous solutions.

Material	Treatment	pH	Temp. °C	Dosage g L^{-1}	q mg g^{-1}	Ref.
Pine wood biochar	Fast pyrolysis	3.0	35	4.0	10.74	[27]
Papel stem biochar	O_2 limited pyrolysis	7.0	20	1.0	569.6	[28]
Walnut shell biochar	Pyrolysis and acid activation	4.0	25	1.0	69.7	[29]
Chili seeds biochar	Pyrolysis	7.0	25	2.5	19.1	[30]
Chrysanthemum wastes biochar	Pyrolysis	2.0	25	2.0	167	[31]
Sugarcane bagasse biochar	Pyrolysis and steam activation	2.0	25	2.33	11.9	[32]
Sugarcane bagasse biochar	Pyrolysis and H_3PO_4 activation	2.0	25	1.66	13.5	[32]
Rice husk biochar	Aluminium modified	2.0	30	2.0	30.2	[33]
Tamarind seeds	Pyrolysis and H_3PO_4 activation	2.0	35	2.0	10.57	[34]
Holm wood biochar	Pyrolysis	7.2-7.6	20	1.0	2.5	[35]
Sargassum biochar	**Pyrolysis**	**7.0**	**25**	**1.0**	**22.4**	**This study**

3.3 Kinetic Study

The kinetics of ibuprofen adsorption were initially analysed by interpreting the experimental data regarding its adsorption capacity over time. A data fitting procedure was employed to determine the respective rate constants of the kinetic models, denoted as k_1 and k_2. The resulting values for these parameters, in addition to the corresponding mean absolute deviation percentages (%D) and correlation coefficients (R^2), are detailed in Table 3. Upon careful examination of the kinetic modelling outcomes, it becomes apparent that both employed models offer satisfactory fits to the experimental data, with an overall commendable performance. However, the second-order kinetic model notably exhibits several advantageous attributes, including the lowest %D and an evidently higher R^2 (%). These compelling statistical indicators collectively establish the second-order model as the most apt and fitting description for the experimental data under consideration.

Table 3. Kinetic parameters for the first and second order models for the ibuprofen adsorption on biochars.

Sample	First-order				Second-order			
	q_e ($mg \cdot g^{-1}$)	$k_1 \cdot 10^2$ (h^{-1})	%D	R^2 (%)	q_e ($mg \cdot g^{-1}$)	$k_2 \cdot 10^3$ ($g\ mg^{-1}\ h^{-1}$)	%D	R^2 (%)
RM	9.7	5.6	8.75	95.25	11.1	6.5	1.51	99.71
Bio 1h	5.7	1.5	8.74	95.27	8.2	1.4	4.64	99.22
Bio 3h	22.0	3.7	7.86	96.78	26.4	1.5	2.71	99.00
Bio 5h	5.7	2.2	7.47	96.01	10.3	1.0	4.25	99.31

This preference for the second-order model is indicative of a chemisorption phenomenon or chemical adsorption mechanism, which implies the formation of chemical bonds between the adsorbent and the adsorbate. This interaction typically emerges within a monolayer configuration on the surface of the adsorbent material [36,37]. This chemisorption mechanism suggests a heightened level of affinity and binding strength between the adsorbent and the adsorbate, which contributes to the attainment of equilibrium conditions with notable efficiency.

These findings display similarity to prior research works conducted by Mestre [38] and Xiong [39], wherein analogous outcomes were reported in the context of ibuprofen removal employing carbonaceous and innovative materials. This consistency in outcomes across diverse studies underscores the robustness and reliability of the second-order kinetic model as a predictive tool for describing ibuprofen adsorption processes.

The graphical representation of the evolution of adsorption capacity over time, along with the overlaid second-order kinetic curves, is depicted in Figure 2b. This figure elucidates the temporal dynamics of the materials' adsorption behaviour in response to the presence of the contaminant. Upon close examination of Figure 2b, a discernible trend becomes apparent: the materials tend to approach their maximum of adsorption capacity at approximately 72 hours following their initial contact with the contaminant. This observation aligns with findings previously reported by Guedidi [40]. It underscores the temporal progression inherent in the adsorption process, where the materials steadily augment their capacity to adsorb the target pollutant over the course of this 72-hour interval.

This phenomenon encapsulates a fundamental aspect of the adsorption kinetics, revealing the intricate interplay of factors that influence the rate and extent of adsorption. It underscores the importance of temporal considerations in optimizing adsorption processes and offers valuable insights for the design and implementation of efficient contaminant removal strategies.

4. Conclusions

In this comprehensive study, we addressed the critical issue of water contamination, with a particular focus on the presence of pharmaceutical contaminants, notably ibuprofen, and the ecological and socioeconomic challenges posed by Sargassum accumulation along the Mexican Caribbean coast. Through an innovative approach, we leveraged Sargassum biomass as a precursor to develop carbonaceous materials for the efficient removal of ibuprofen from contaminated water sources. The discoveries revealed that the synthesized biochars exhibited adsorption capacities superior to conventional adsorbents. This demonstrates their efficacy as potent tools for the removal of ibuprofen contaminants from aqueous environments. Moreover, it was conducted a thorough investigation into the kinetics of ibuprofen adsorption, with the second-order kinetic model emerging as the most suitable for describing the experimental data. This suggests that chemisorption, characterized by chemical bonding between the adsorbent and adsorbate, plays a dominant role in this process. The multifaceted approach of utilizing Sargassum-derived materials not only aligns with the principles of the circular economy but also offers a sustainable solution for remediating water resources contaminated by emerging pharmaceutical contaminants. This research not only emphasizes the significant potential of biomass waste utilization but also underscores the importance of innovative and environmentally conscious strategies in addressing complex environmental challenges. Furthermore, this study contributes to the growing body of knowledge concerning the application of carbonaceous materials for water purification, highlighting the viability and effectiveness of Sargassum-derived biochars in particular.

Acknowledgements

The authors would like to acknowledge the National Council of Science and Technology of Mexico (CONACyT) for supporting this work with Grant Number 800642 and Project CB-286990-2016.

Data availability

The authors can confirm that all relevant data are included in the article.

Declarations

Conflict of interests: On behalf of all authors, the corresponding author states that there is no conflict of interest.

References

1. H. B. Quesada, A. T. A. Baptista, L. F. Cusioli, D. Seibert, C. de Oliveira Bezerra, R. Bergamasco, *Chemosphere*. **222**, 766–780 (2019). DOI:10.1016/j.chemosphere.2019.02.009.

2. B. Ng, N. Quinete, S. Maldonado, K. Lugo, J. Purrinos, H. Briceño, P. Gardinali, *Sci. Total Environ.* **757**, 143720 (2021). DOI:10.1016/j.scitotenv.2020.143720.

3. N. Patel, Z. A. Khan, S. Shahane, D. Rai, D. Chauhan, C. Kant, V. K. Chaudhary, *Pollution*. **6**, 99–113 (2020). DOI:10.22059/POLL.2019.285116.646.

4. M. Patel, R. Kumar, K. Kishor, T. Mlsna, C. U. Pittman Jr, D. Mohan, *Chem. Rev.* **119**, 3510–3673 (2019).

5. H. E. Reynel-Avila, D. I. Mendoza-Castillo, A. Bonilla-Petriciolet, J. Silvestre-Albero, *J. Mol. Liq.* **209**, 187–195 (2015). DOI:10.1016/j.molliq.2015.05.013.

6. H. S. Kambo, A. Dutta, *Renew. Sustain. Energy Rev.* **45**, 359–378 (2015). DOI:10.1016/j.rser.2015.01.050.

7. M. Wang, Y. Liu, Y. Yao, L. Han, X. Liu, *Sci. Total Environ.* **700**, 134470 (2020). DOI:10.1016/j.scitotenv.2019.134470.

8. F. Andrade-Canto, F. J. Beron-Vera, G. J. Goni, D. Karrasch, M. J. Olascoaga, J. Triñanes, *Phys. Fluids*. **34** (2022), doi:10.1063/5.0079055. DOI:10.1063/5.0079055.

9. V. Chávez, A. Uribe-Martínez, E. Cuevas, R. E. Rodríguez-Martínez, B. I. van Tussenbroek, V. Francisco, M. Estévez, L. B. Celis, L. V. Monroy-Velázquez, R. Leal-Bautista, L. Álvarez-Filip, M. García-Sánchez, L. Masia, R. Silva, *Water (Switzerland)*. **12**, 1–24 (2020). DOI:10.3390/w12102908.

10. R. E. Rodríguez-Martínez, E. G. Torres-Conde, E. Jordán-Dahlgren, *Ocean Coast. Manag.* **237**, 106542 (2023). DOI:10.1016/j.ocecoaman.2023.106542.

11. M. Nahata, C. Y. Seo, P. Krishnakumar, J. Schwank, *Front. Chem. Sci. Eng.* **12**, 194–208 (2018). DOI:10.1007/s11705-017-1647-x.

12. J. L. Davila-Rodriguez, V. A. Escobar-Barrios, K. Shirai, J. R. Rangel-Mendez, *J. Fluor. Chem.* **130**, 718–726 (2009). DOI:10.1016/j.jfluchem.2009.05.012.

13. A. Pérez-Escobedo, P. E. Díaz-Flores, J. R. Rangel-Méndez, F. J. Cerino-Cordova, V. M. Ovando-Medina, J. A. Alcalá-Jáuregui, *Rev. Mex. Ing. Quim.* **15**, 139–147 (2016).

14. H. P. Boehm, *Carbon N. Y.* **32**, 759–769 (1994). DOI:10.1016/0008-6223(94)90031-0.

15. H. G. Cisneros-Ontiveros, N. A. Medellín-Castillo, C. Aldama-Aguilera, C. A. Ilizaliturri-Hernández, S. A. Cruz-Briano, G. J. Labrada-Delgado, A. I. Flores-Rojas, *MRS Adv.* **7**, 997–1003 (2022). DOI:10.1557/s43580-022-00456-3.

16. S. Guo, X. Dong, T. Wu, F. Shi, C. Zhu, *J. Anal. Appl. Pyrolysis*. **116**, 1–9 (2015). DOI:10.1016/j.jaap.2015.10.015.

17. K. Nakason, B. Panyapinyopol, V. Kanokkantapong, N. Viriya-empikul, W. Kraithong, P. Pavasant, *Biomass Convers. Biorefinery*. **8**, 199–210 (2018). DOI:10.1007/s13399-017-0279-1.

18. T. Atugoda, C. Gunawardane, M. Ahmad, M. Vithanage, *Chemosphere*. **281**, 130676 (2021). DOI:10.1016/j.chemosphere.2021.130676.

19. F. J. Sotomayor, A. P. Quantatec, K. A. Cychosz, M. Thommes, *Acc. Mater. Surf. Res*. **3**, 34–50 (2018).

20. Q. M. Truong, T. B. Nguyen, W. H. Chen, C. W. Chen, A. K. Patel, X. T. Bui, R. R. Singhania, C. Di Dong, *Bioresour. Technol.* **370**, 128524 (2023). DOI:10.1016/j.biortech.2022.128524.

21. S. Aguirre-Contreras, R. Leyva-Ramos, R. Ocampo-Pérez, C. G. Aguilar-Madera, J. V. Flores-Cano, N. A. Medellín-Castillo, *J. Water Process Eng.* **54**, 103967 (2023). DOI:10.1016/j.jwpe.2023.103967.

22. L. A. González Fernández, A. E. Navarro Frómeta, C. Carranza Álvarez, R. Flores Ramírez, P. E. Díaz Flores, V. Castillo Ramos, M. Sánchez Polo, F. Carrasco Marín, N. A. Medellín Castillo, *Int. J. Environ. Res. Public Health*. **20**, 2559 (2023). DOI:10.3390/ijerph20032559.

23. L. Yi, L. Zuo, C. Wei, H. Fu, X. Qu, S. Zheng, Z. Xu, Y. Guo, H. Li, D. Zhu, *Sci. Total Environ.* **719**, 137389 (2020). DOI:10.1016/j.scitotenv.2020.137389.

24. W. Pimentel-Almeida, A. G. Itokazu, H. A. G. Bazani, M. Maraschin, O. H. C. Rodrigues,

R. G. Corrêa, S. Lopes, G. I. Almerindo, R. Moresco, *Environ. Technol. (United Kingdom)*. **44**, 974–987 (2023). DOI:10.1080/09593330.2021.1989058.

25. J. Shin, J. Kwak, S. Kim, C. Son, Y. G. Lee, S. Baek, Y. Park, K. J. Chae, E. Yang, K. Chon, *J. Environ. Chem. Eng.* **10**, 107914 (2022). DOI:10.1016/j.jece.2022.107914.

26. X. Yang, X. Zhang, H. H. Ngo, W. Guo, J. Huo, Q. Du, Y. Zhang, C. Li, F. Yang, *J. Water Process Eng.* **46**, 102627 (2022). DOI:10.1016/j.jwpe.2022.102627.

27. M. Essandoh, B. Kunwar, C. U. Pittman Jr, D. Mohan, T. Mlsna, *Chem. Eng. J.* **265**, 219–227 (2015).

28. A. Naima, F. Ammar, O. Abdelkader, C. Rachid, H. Lynda, A. Syafiuddin, R. Boopathy, *Bioresour. Technol.* **347**, 126685 (2022).

29. M. Patel, A. K. Chaubey, C. U. Pittman, D. Mohan, *Environ. Sci. Adv.* **1**, 530–545 (2022).

30. R. Ocampo-Perez, E. Padilla-Ortega, N. A. Medellin-Castillo, P. Coronado-Oyarvide, C. G. Aguilar-Madera, S. J. Segovia-Sandoval, R. Flores-Ramírez, A. Parra-Marfil, *Sci. Total Environ.* **655**, 1397–1408 (2019).

31. Y. Ngernyen, D. Petsri, K. Sribanthao, K. Kongpennit, P. Pinijnam, R. Pedsakul, A. J. Hunt, *RSC Adv.* **13**, 14712–14728 (2023).

32. P. Chakraborty, S. Show, S. Banerjee, *Chem. Eng*. **6**, 5287–5300 (2018).

33. D. Yu, S. Zeng, Y. Wu, Y. Li, H. Tian, T. Xie, Y. Yu, *Environ. Sci. Pollut. Res.*, 1–11 (2023).

34. S. Show, B. Karmakar, G. Halder, *Biomass Convers. Biorefinery*, 1–19 (2020).

35. L. Delgado-Moreno, S. Bazhari, G. Gasco, A. Méndez, M. El Azzouzi, E. Romero, *Sci. Total Environ.* **752**, 141838 (2021).

36. D. Kavitha, C. Namasivayam, *Bioresour. Technol.* **98**, 14–21 (2007). DOI:10.1016/j.biortech.2005.12.008.

37. B. H. Hameed, I. A. W. Tan, A. L. Ahmad, *Chem. Eng. J.* **144**, 235–244 (2008). DOI:10.1016/j.cej.2008.01.028.

38. A. S. Mestre, J. Pires, J. M. F. Nogueira, A. P. Carvalho, *Carbon N. Y.* **45**, 1979–1988

(2007). DOI:10.1016/j.carbon.2007.06.005.

39. P. Xiong, H. Zhang, G. Li, C. Liao, G. Jiang, *Sci. Total Environ.* **797**, 149179 (2021). DOI:10.1016/j.scitotenv.2021.149179.

40. H. Guedidi, I. Lakehal, L. Reinert, J. M. Lévêque, N. Bellakhal, L. Duclaux, *Arab. J. Chem.* **13**, 258–270 (2020). DOI:10.1016/j.arabjc.2017.04.006.

Paper 5: Hydrochar from Sargassum biomass for water remediation: Insights from synthesis and ibuprofen removal

Journal: MRS Advances

Impact Factor (JCR): 0.8

Quartile: Q4

Volume: 8

ISSN (electronic): 2059-8521

ISSN (print): 2731-5894

https://doi.org/10.1557/s43580-023-00702-2

https://link.springer.com/article/10.1557/s43580-023-00702-2

Hydrochar from Sargassum biomass for water remediation: Insights from synthesis and ibuprofen removal

Carolina Martínez-Meraz[1], Lázaro Adrián González Fernández[2], Nahum Andrés Medellín Castillo[1,2], Roberto Leyva Ramos[3], Laura Guadalupe Hernández de la Rosa[3], Gloria Korina Loredo Martinez[3], Sergio Armando Cruz Briano[2], Hilda Guadalupe Cisneros Ontiveros[2], Alfredo Israel Flores Rojas[1] and Javier Ernesto Vilasó Cadre[4]*

[1]*School of Engineering, Autonomous University of San Luis Potosi, San Luis Potosí 78290, Mexico*

[2]*Multidisciplinary Graduate Program in Environmental Sciences, Autonomous University of San Luis Potosi, San Luis Potosí 78000, Mexico*

[3]*Center for Research and Graduate Studies, School of Chemical Sciences, Autonomous University of San Luis Potosi, San Luis Potosi 78260, Mexico.*

[4]*Institute of Metallurgy, Autonomous University of San Luis Potosí, San Luis Potosí 78210, Mexico.*

[*]*Corresponding author: nahum.medellin@uaslp.mx*

Abstract

Contamination of water resources, especially drinking water, is common. Pharmaceuticals, extensively used nowadays, are now considered as important contaminants. Sargassum, a marine algae that reaches Caribbean beaches, causes socioeconomic and ecological damage by affecting marine species, and is one of the main environmental problems in Mexico today. To mitigate its impact, it is proposed to use Sargassum biomass as a precursor of carbonaceous materials to decontaminate waters contaminated with ibuprofen. This study explored hydrochar synthesis, finding temperature, residence time, and water-to-biomass ratio affected yield. Higher temperature and time reduced yield, with optimal conditions for yield and ibuprofen adsorption at lower settings, minimizing biomass changes. The materials were subjected to adsorption experiments in batch regime and proved to be effective adsorbents with adsorption capacities up to 33.5 mg g^{-1}, exceeding other conventional and novel adsorbents. Their use could contribute to creating a circular economy and to the remediation of water contaminated with emerging contaminants.

1. Introduction

Pharmaceuticals have become a significant concern as emerging contaminants in the environment. While there has been limited research on their presence in aquatic environments since the 1950s, it wasn't until the early 1990s that the topic gained substantial attention, leading to numerous scientific articles on the subject. The consumption of drugs has been steadily increasing, particularly in industrialized countries with high purchasing power. Commonly prescribed drugs

like non-steroidal anti-inflammatory drugs, antiepileptics, antibiotics, and β-blockers are of particular interest [1].

The existence of pharmaceuticals in the environment is a cause for concern because of their bioactive properties, even when present in minimal concentrations, which can negatively impact both wildlife and humans. This is particularly concerning when pharmaceuticals like ibuprofen, diclofenac, and carbamazepine are found in drinking water, potentially exposing humans through direct consumption or by consuming aquatic organisms containing these residues [2].

Carbonaceous materials are extensively employed for effectively and economically removing contaminants such as pharmaceuticals [3]. Particularly, biomass-derived materials, often sourced from waste, have gained significant attention. Processes like pyrolysis and hydrothermal carbonization are used to create carbon materials from biomass waste, but additional activation treatments are required to achieve high porosity [4]. Hydrochar is a carbon-rich material produced through the hydrothermal carbonization (HTC) process, which involves the conversion of biomass or organic waste materials into a solid carbon-rich product in the presence of water at elevated temperatures and pressures. Hydrochar has gained significant attention in recent years, particularly for its potential applications in water remediation and environmental sustainability [5].

Hydrochar has shown promise in the removal of various water pollutants, including heavy metals (e.g., lead, cadmium, copper), organic contaminants (e.g., pesticides, pharmaceuticals), and nutrients (e.g., phosphorus and nitrogen compounds). Its porous structure and high surface area make hydrochar an effective adsorbent for trapping and immobilizing pollutants from water [6].

Since 2011, a notable phenomenon of Sargassum accumulation has been observed on the coasts of the Mexican Caribbean, the source of which is identified in the Sargassum Sea in the Atlantic Ocean. This Sargassum released into the sea travels towards the Mexican coasts and can double in size due to its nature. In 2015, a significant event caught the attention of the local and national government, as well as the tourism sector [7].

The challenge with this Sargassum lies in its organic nature, which initiates its decomposition during its arrival. Given the abundance of decomposing material, much of it is not removed from the beaches, generating a series of detrimental consequences. This causes a deterioration of the landscape and significantly affects both the tourism sector and the economy. In addition, marine ecosystems are compromised, and the loss of various marine species, both animal and plant, has

been recorded. It should be noted that this Sargassum also contains considerable levels of arsenic and heavy metals, which have adverse effects on human health when in contact with the skin, resulting in dermatological conditions, conjunctivitis, and respiratory disorders [8].

Since there is no efficient program for the proper management of this macroalgae, the collected waste is usually sent to solid waste centers that do not apply the necessary procedures for its disposal [7]. Therefore, the search for alternatives to take advantage of this resource, which is usually considered as waste, has been promoted. These applications cover various fields, being especially useful in the production of fertilizers and biogas. In the present study, the possibility of using the carbonaceous by-products derived from Sargassum biomass to remove ibuprofen from aqueous matrices through batch adsorption is investigated. This study also focuses on characterizing the carbonaceous materials and in optimizing the conditions to achieve optimal removal efficiency.

2. Materials and Methods

2.1 Raw Material

Sargassum spp. was collected from the Mexican Caribbean, adhering to established taxonomic and morphological criteria specified in expert literature [9]. Subsequent to selection, the collected samples underwent a thorough rinse with abundant seawater and were sun-dried for a span of 72 h. Afterward, the dried samples were carefully stored in light-excluded, humidity-controlled conditions using polyethylene bags. In anticipation of analysis, the algae samples underwent a thorough cleansing procedure using distilled water to eliminate salts and any other solid residues that may have been present. Afterward, they underwent a drying process in an oven at 110 °C lasting for 24 h, followed by grinding using an electric mill. The obtained material was passed through vibrating sieves with openings from 30 to 50 μm. Afterward, the separated portions of particles of various sizes were carefully stored [10].

2.2 Synthesis of hydrochar

The study involved conducting hydrocarbonization experiments, varying carbonization temperature, residence time, and water-to-biomass ratio. A response surface experimental design was employed to analyse how operating conditions affected material properties. The design (see

Table 1), based on response surface methodology, comprised 15 experiments in a Box-Behnken setup with 3 factors and 3 central point replications.

Carbonization aimed for hydrochar production, with temperature (T) range set at 180-220 °C. Residence time (t) ranged from 2 to 8 h, allowing material transformation. Hydrocarbonization required dispersing raw material in water, with water-to-biomass ratios (R) from 5 to 10 mL g^{-1}. A second-order polynomial regression model, as described by equation (1), was employed to fit the experimental data:

$$\%Y = \beta_0 + \beta_1 \cdot T + \beta_2 \cdot t + \beta_3 \cdot R + \beta_4 \cdot T \cdot t + \beta_5 \cdot T \cdot R + \beta_6 \cdot t \cdot R + \beta_7 \cdot T^2 + \beta_8 \cdot t^2 + \beta_9 \cdot R^2 \quad (1)$$

where $\beta_{0\text{-}9}$, are the regression coefficients.

In the process, about 10 g of Sargassum biomass and specified water amounts were placed in a Teflon vessel within a stainless-steel autoclave. Temperature and time were determined, followed by natural cooling. Solid and liquid products were separated via vacuum filtration. Solids underwent water, ethanol, and acetone washing, and were dried at 105 °C for 12 hours. Prepared hydrochars were stored in polyethylene bags for characterization and adsorption tests.

2.3 Adsorption of ibuprofen

The synthesized materials were subjected to ibuprofen adsorption in batch systems. In 50 mL centrifuge tubes, 50 mL of the contaminant solution of concentration 20 mg L^{-1} were added. To each of the tubes 0.05 g of the materials was added and the pH was adjusted to 7.0 with dilute solutions of NaOH and HCl as necessary. The pH was monitored for 7 days, during which each tube was kept in a bath with constant agitation at 25 ºC. At the end of this time the samples were allowed to settle, 5 mL aliquots were taken and filtered through 45 µm membranes to be analyzed by UV/Vis Spectroscopy using a wavelength of 234 nm. With the adsorption capacities obtained from the mass balance (Eq 2), a response surface was constructed, and the best conditions were determined through optimization with the Microsoft Excel 2023 Solver tool.

$$q = \frac{V(C_0 - C_e)}{m} \quad (2)$$

where, C_0 and C_e are the initial and final concentration of ibuprofen (mg L^{-1}), V is the volume of the solution (L) and m is the adsorbent mass (g) added to the experiments.

2.4 Raw Material and Hydrochar characterization

The Raw Material (RM) and the hydrochar that showed the highest capacity to adsorb ibuprofen (HCS-3) were subjected to a physicochemical characterization that included the determination of their specific area (S_{BET}) and pore volume (V_{pore}) and the point of zero charge (PZC) as reported by González-Fernández et al. [10], in addition to the determination of the acidic and basic sites of the materials following the Boehm titration method reported elsewhere [11].

Additionally, the HCS-3 sample before and after adsorption (saturated with ibuprofen) was subjected to FTIR analysis to identify the main functional groups of the material as well as the presence of ibuprofen in the saturated material. A ThermoFisher Scientific Nicolet iS10 FTIR spectrophotometer (Waltham, MA, USA) was utilized to collect the FTIR spectrum. The identification of functional groups was based on the strengths of the spectral bands relative to their frequencies. Furthermore, the recorded band values were contrasted with reference compound spectra documented in existing literature [12].

3. Results and Discussions

3.1 Hydrochar yield and optimization of the synthesis variables

The calculation of the yield (%Y) for the synthesized samples was derived from the ratio indicated in equation (3):

$$\%Y = \frac{Dry\ hydrochar\ weight\ (g)}{Dry\ biomass\ weight\ (g)} \cdot 100 \quad (3)$$

Table 1 presents the experimental design along with the hydrochar yield obtained as a response in each synthesis experiment. Data in Table 1 illustrates a noticeable effect of the explored parameters on hydrochar %Y values. This is evident from the observation that the highest yield was achieved at the lowest time and temperature settings, while the lowest yield corresponded to higher time and temperature values. This observation aligns with findings from Nizamuddin et al. [13], who also reported that elevated carbonization time and temperature lead to decreased yield values. The %Y spanned from 39 to 58%. An analysis of variance (ANOVA) was conducted to ascertain the significance of the factors and to evaluate the model's goodness of fit. The statistical assessment of the factors relied on hypothesis testing (p-value) and Fisher's-F test, maintaining a 95 % confidence interval.

Table 1. Experimental design of HTC treatment and response variables.

Exp.	T (°C)	t (h)	R (mL g^{-1})	%Y	q_{IBU} (mg g^{-1})
HCS-1	200	2.0	5.0	50.28	32.5
HCS-2	200	8.0	5.0	48.06	31.4
HCS-3	180	2.0	7.5	58.04	33.5
HCS-4	200	2.0	10	47.28	32.2
HCS-5	220	8.0	7.5	43.23	31.6
HCS-6	200	5.0	7.5	45.85	30.9
HCS-7	180	8.0	7.5	50.50	28.9
HCS-8	220	5.0	5.0	45.99	31.0
HCS-9	200	5.0	7.5	47.25	30.6
HCS-10	220	5.0	10	42.27	30.9
HCS-11	200	8.0	10	39.01	29.5
HCS-12	220	2.0	7.5	46.88	31.3
HCS-13	200	5.0	7.5	48.98	30.3
HCS-14	180	5.0	5.0	51.03	29.1
HCS-15	180	5.0	10	50.21	29.5

As per the ANOVA results, the three linear terms emerged as significant factors, boasting p-values below 0.05. Consequently, it can be deduced that the variables exerting influence on hydrochar yield are carbonization temperature, residence time, and water-to-biomass ratio. The regression model fitted to %Y, considering the meaningful factors and disregarding non-significant terms, is represented by equation (4):

$$\%Y = 246.06 - 1.93T - 3.24t + 7.27R \quad (4)$$

The negative coefficients for temperature and time (β_1 and β_2), shown in the above equation indicate that an increase in the values of these factors promotes a decrease in the response. The interaction between temperature, time and water-to-biomass ratio and their effects on the response were analyzed from the three-dimensional response surface, as shown in Figure 1. As can be observed in Figure 1a), the highest yield values are obtained when both factors are at their lower levels, which is due to the fact that under these conditions the biomass does not undergo severe changes during the treatment and, therefore, there is less mass loss.

With the parameters of the equation that describes the model, an optimization of the response variable was carried out using the Solver tool of Microsoft Excel 2023 in such a way that the maximum value of the yield was obtained. The maximum value obtained after optimization is 57.28 % which corresponds to T= 180 ºC, t= 2 h and R= 7.6 mL g^{-1}. The value of the maximum

experimental yield was 58.04 %, so the model has a percentage of deviation with respect to the experimental values of 1.31 %, which is an acceptable value that allows affirming that the model adequately describes the obtained data.

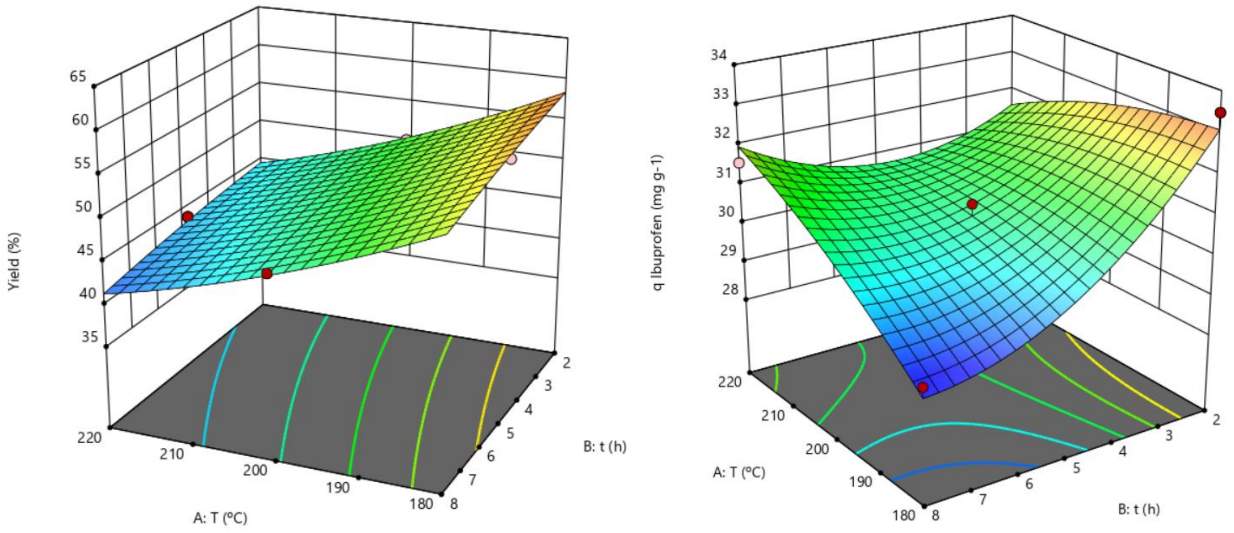

a) b)

Figure 1. Three-dimensional response surface for a) Y% and b) adsorption capacity of the hydrochars to remove ibuprofen.

3.2 Ibuprofen adsorption on hydrochars

Figure 1b) shows the response surface of the adsorption capacity as a function of the synthesis variables. Based on the ANOVA data, it was observed that the linear factor "t" and the quadratic factors "T·t" and "t^2" exhibited p-values below 0.05. This implies that the factors with a substantial impact on hydrochar yield are the linear and quadratic representations of residence time, as well as the interaction between residence time and carbonization temperature. The regression equation, tailored to the significant factors and excluding non-significant terms, describes the relationship of the decoded factors to the q_{IBU} as follows:

$$q_{IBU} = 13.36 - 5.11t + 0.02Tt + 0.11t^2 \quad (5)$$

The interaction between temperature, time and water-to-biomass ratio and their effects on the response (q_{IBU}) were analyzed from the three-dimensional response surface, as shown in Figure 1b). The findings reveal that the adsorption capacities of ibuprofen exhibited a range of 28.8 to

33.5 mg g^{-1}. Particularly, the maximum adsorption capacity values are evident when both factors ("t" and "T") are in their lowest values, corresponding to 2 h and 180°C, respectively. This result can be attributed to the synthesis conditions, which induce the least pronounced alterations in biomass composition, particularly functional groups, during the treatment [14,15]. Additionally, this result can be explained by the comparatively higher specific area of the synthesized material (approximately 100 m^2 g^{-1}), thereby enhancing the pollutant adsorption process [16,17].

These observed adsorption capacity values for all the synthesized materials align with those documented by other researchers [18–20]. Furthermore, it was observed that the adsorption capacity of ibuprofen diminishes as residence time increases, a trend linked to the depletion of functional groups crucial for binding with the contaminant [20,21].

By utilizing the equation's parameters that define the quadratic model, an optimization of the response variable was executed through Microsoft Excel 2023's Solver tool. This optimization aimed to achieve the highest adsorption capacity for ibuprofen. The resulting maximum capacity, post-optimization, was 33.17 %, corresponding to specific conditions T= 180 °C, t= 2 h, and a value of R= 10 mL g^{-1}. Comparatively, the maximal experimental adsorption capacity reached 33.48 %. Consequently, the model displays a mere 0.97 % deviation from the experimental values. This small deviation is deemed acceptable and affirms the model's capability to effectively describe the experimental data.

3.3 Physicochemical characterization

The results derived from the diverse analytical methods for characterizing the RM and the HCS-3 are presented in Table 2. As observed, the RM exhibits a notably small specific area and limited porosity, consistent with the characteristics commonly found in biomass materials [22]. On the contrary, hydrochar synthesized under conditions of 180 °C and a 2 h residence time (HCS-3) exhibits a specific surface of approximately 100 m^2 g^{-1}, signifying an enhancement by two orders of magnitude compared to RM. Concerning to pore volume, the hydrochar shows a value surpassing that of the precursor by three orders of magnitude. The combination of these characteristics in the synthesized material significantly enhances the adsorption capacity for ibuprofen. This is particularly relevant due to the inherent steric limitations associated with ibuprofen adsorption in confined micropores or materials with limited surface [19].

Table 2. Physicochemical characteristics of RM and HCS-3

Material	S_{BET} (m^2 g^{-1})	V_{pore} (m^3 g^{-1})	PZC	Acid sites (meq g^{-1})				Basic sites (meq g^{-1})
				Total	Carboxylic	Lactonic	Phenolic	
RM	0.2	$9 \cdot 10^{-4}$	6.75	1.3531	0.7355	0.1267	0.4909	0.0836
HCS-3	99.3	0.23	6.38	1.5346	0.4512	0.0935	0.9899	1.2456

The RM and HCS-3 obtained PZC were 6.75 and 6.38, respectively. These values are close to the neutral value of pH. Consequently, this adsorbents exhibits a slight acidity, characterized by a relatively lower concentration of basic sites compared to acidic sites. Sheng et al. [23] discovered that functional groups within marine algae, which are accountable for binding or engaging with pollutants, encompass entities like sulfonic acids, carboxyl and phosphates. These components exist in various configurations such as carboxylic groups, phosphate proteins, fucoidans, and alginate. The distribution of acid and basic sites showed in Table 2 corresponds with findings from Tarbaoui et al. [24] regarding Sargassum biomass.

As can be seen, the hydrocarbonization process caused an increase in the concentration of basic sites. These basic sites hold a negative charge density that interacts with the delocalized π electronic cloud of the adsorbate, thus increasing its adsorption on the synthesized material. Additionally, it can be observed that the concentration of acid sites also increased, and within these the concentration of phenolic sites, which also have delocalized electronic clouds that favor the removal of the contaminant through π-π interactions [25] (Figure 2b).

Figure 2a) presents an analysis of the primary functional groups found in synthesized material, particularly in relation to its enhanced capacity for ibuprofen adsorption both before and after adsorption, alongside the RM. The analysis discerns the existence of diverse functional groups within the material, encompassing carboxylic, carbonyl (linked to lactones), and aromatic structures, indicative of the presence of phenolic groups within the material's composition.

These functional groups serve a key role in eliminating the targeted pollutant from the solution. This elimination primarily occurs through mechanisms involving electrostatic interactions with the electron cloud of the pollutants and through the formation of chemical bonds between the adsorbate and the adsorbent [26] (Figure 2b). Furthermore, when comparing both spectra, a distinct band is observed around 1650 cm^{-1} (asymmetric vibration of the carboxyl group), demonstrating the presence of ibuprofen in the ibuprofen-saturated HCS-3 material [27], which is found to be much less wide and intense in the starting material. This observation conclusively demonstrates

the successful removal of this contaminant from the solution, with its presence now detected in the saturated adsorbent.

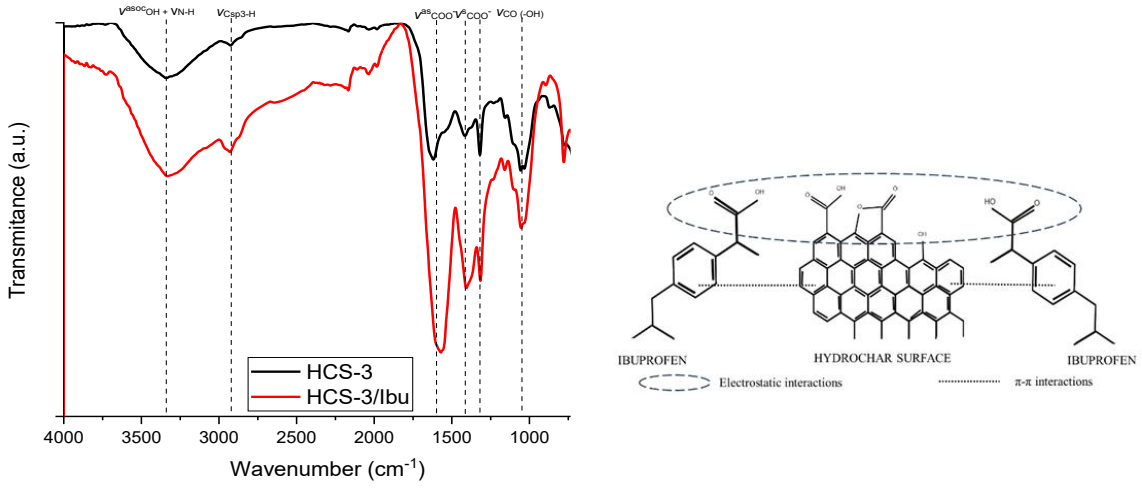

a) b)

Figure 2. a) Infrared spectrum of HCS-3 and HCS-3 saturated with ibuprofen; b) Possible interactions involved in the removal of ibuprofen during the adsorption onto HCS-3

4. Conclusions

This study conducted a comprehensive exploration of hydrochar synthesis, its implications on yield, and its effectiveness in ibuprofen adsorption. Hydrochar yield was notably influenced by temperature, residence time, and water-to-biomass ratio, indicating higher yields at reduced time and temperature settings. Regression models accurately captured this trend (%D < 5 %), revealing that heightened temperature and time corresponded to diminished yields. Optimal conditions for both maximum yield and ibuprofen adsorption were identified at lower time and temperature levels (T = 180 ºC; t = 2h), thus mitigating biomass alteration.

Furthermore, the investigation analyzed how synthesis parameters impacted ibuprofen adsorption, identifying the relevant factors linked to residence time and its interaction with temperature. The models accurately predicted adsorption behaviors, providing crucial insights for refining pollutant elimination processes. Physicochemical evaluation underscored the augmented hydrochar properties versus the raw material, with amplified specific surface area and pore volume significantly enhancing ibuprofen adsorption. This advance is particularly noteworthy, addressing ibuprofen's steric constraints in confined micropores.

Overall, the study illustrated intricate relationships between hydrochar synthesis, yield, and adsorption efficiency, routing the optimization of synthesis for efficacious pollutant removal. The formulated models hold great potential for process enhancement and highlight hydrochar's promise as a potent agent in environmental remediation.

Acknowledgements

The authors would like to acknowledge the National Council of Science and Technology of Mexico (CONACyT) for supporting this work with Grant Number 800642 and Project CB-286990-2016.

Data availability

The authors can confirm that all relevant data are included in the article.

Declarations

Conflict of interests: On behalf of all authors, the corresponding author states that there is no conflict of interest.

References

1. P. Chaturvedi, P. Shukla, B. S. Giri, P. Chowdhary, R. Chandra, P. Gupta, A. Pandey, *Environ. Res.* **194**, 110664 (2021). DOI:10.1016/j.envres.2020.110664.
2. H. B. Quesada, A. T. A. Baptista, L. F. Cusioli, D. Seibert, C. de Oliveira Bezerra, R. Bergamasco, *Chemosphere*. **222**, 766–780 (2019). DOI:10.1016/j.chemosphere.2019.02.009.
3. C. Piccirillo, I. S. Moreira, R. M. Novais, A. J. S. Fernandes, R. C. Pullar, P. M. L. Castro, *J. Environ. Chem. Eng.* **5**, 4884–4894 (2017). DOI:10.1016/j.jece.2017.09.010.
4. J. Scaria, A. Gopinath, N. Ranjith, V. Ravindran, S. Ummar, P. V. Nidheesh, M. S. Kumar, *J. Clean. Prod.* **350**, 131319 (2022). DOI:10.1016/j.jclepro.2022.131319.
5. J. Fang, L. Zhan, Y. S. Ok, B. Gao, *J. Ind. Eng. Chem.* **57**, 15–21 (2018). DOI:10.1016/j.jiec.2017.08.026.
6. S. Yu, X. Yang, P. Zhao, Q. Li, H. Zhou, Y. Zhang, *J. Energy Inst.* **101**, 194–200 (2022). DOI:10.1016/j.joei.2022.01.013.

7. C. León, *Salud Publica Mex.* **61**, 701–703 (2019). DOI:10.21149/10870.

8. W. Farnham, C. Murfin, A. Critchley, S. Morrell, in *International Seaweed Symposium (Xth)* (De Gruyter, 2019), pp. 277–282. DOI:10.1515/9783110865271-030.

9. L. Mattio, C. E. Payri, *J. Phycol.* **45**, 1374–1388 (2009). DOI:10.1111/j.1529-8817.2009.00760.x.

10. L. A. González Fernández, A. E. Navarro Frómeta, C. Carranza Álvarez, R. Flores Ramírez, P. E. Díaz Flores, V. Castillo Ramos, M. Sánchez Polo, F. Carrasco Marín, N. A. Medellín Castillo, *Int. J. Environ. Res. Public Health*. **20**, 2559 (2023). DOI:10.3390/ijerph20032559.

11. H. P. Boehm, *Carbon N. Y.* **32**, 759–769 (1994). DOI:10.1016/0008-6223(94)90031-0.

12. K. Nakamoto, *Handb. Vib. Spectrosc.* (2001), doi:10.1002/0470027320.s4104. DOI:10.1002/0470027320.s4104.

13. S. Nizamuddin, N. M. Mubarak, M. Tiripathi, N. S. Jayakumar, J. N. Sahu, P. Ganesan, *Fuel*. **163**, 88–97 (2016). DOI:10.1016/j.fuel.2015.08.057.

14. M. Ilić, F. H. Haegel, A. Lolić, Z. Nedić, T. Tosti, I. S. Ignjatović, A. Linden, N. D. Jablonowski, H. Hartmann, *PLoS One*. **17**, e0277365 (2022). DOI:10.1371/journal.pone.0277365.

15. N. Saha, A. Saba, M. T. Reza, *J. Anal. Appl. Pyrolysis*. **137**, 138–145 (2019). DOI:10.1016/j.jaap.2018.11.018.

16. H. H. C. Lima, R. S. Maniezzo, M. E. G. Llop, V. L. Kupfer, P. A. Arroyo, M. R. Guilherme, A. F. Rubira, E. M. Girotto, A. W. Rinaldi, *J. Mol. Liq.* **276**, 570–576 (2019). DOI:10.1016/j.molliq.2018.12.010.

17. G. T. Tee, X. Y. Gok, W. F. Yong, *Environ. Res.* **212**, 113248 (2022). DOI:10.1016/j.envres.2022.113248.

18. M. Bouzidi, L. Sellaoui, M. Mohamed, D. S. P. Franco, A. Erto, M. Badawi, *J. Mol. Liq.* **376**, 121457 (2023). DOI:10.1016/j.molliq.2023.121457.

19. A. Ayati, B. Tanhaei, H. Beiki, P. Krivoshapkin, E. Krivoshapkina, C. Tracey, *Chemosphere*. **323**, 138241 (2023). DOI:10.1016/j.chemosphere.2023.138241.

20. S. N. Oba, J. O. Ighalo, C. O. Aniagor, C. A. Igwegbe, *Sci. Total Environ.* **780**, 146608 (2021). DOI:10.1016/j.scitotenv.2021.146608.

21. H. A. Al-Yousef, B. M. Alotaibi, F. Aouaini, L. Sellaoui, A. Bonilla-Petriciolet, *J. Mol. Liq.* **331**, 115697 (2021). DOI:10.1016/j.molliq.2021.115697.

22. K. A. Adegoke, S. O. Akinnawo, T. A. Adebusuyi, O. A. Ajala, R. O. Adegoke, N. W. Maxakato, O. S. Bello, *Int. J. Environ. Sci. Technol.*, 1–30 (2023). DOI:10.1007/s13762-023-04872-2.

23. P. X. Sheng, Y. P. Ting, J. P. Chen, L. Hong, *J. Colloid Interface Sci.* **275**, 131–141 (2004). DOI:10.1016/j.jcis.2004.01.036.

24. M. Tarbaoui, M. Oumam, S. Fourmentin, M. Benzina, A. Bennamara, A. Abourriche, *World J. Innov. Res.* **1**, 5 (2016).

25. S. Aguirre-Contreras, R. Leyva-Ramos, R. Ocampo-Pérez, C. G. Aguilar-Madera, J. V. Flores-Cano, N. A. Medellín-Castillo, *J. Water Process Eng.* **54**, 103967 (2023). DOI:10.1016/j.jwpe.2023.103967.

26. G. Song, Y. Shi, H. Wang, A. Li, W. Li, Y. Sun, G. Ding, *Water Sci. Technol.* **85**, 1999–2014 (2022).

27. M. Mateescu, G. Vlase, M. M. Budiul, B. D. Cernuşcă, T. Vlase, *J. Therm. Anal. Calorim.* **148**, 4601–4614 (2023). DOI:10.1007/s10973-023-12052-0.

Paper 6: Optimization of hydrochar synthesis conditions for enhanced Cd(II) and Pb(II) adsorption in mono and multimetallic systems

Journal: Environmental Research

Impact Factor (JCR): 7.7

Quartile: Q1

Volume: 261

ISSN (electronic): 1096-0953

ISSN (print): 0013-9351

https://doi.org/10.1016/j.envres.2024.119651

https://www.sciencedirect.com/science/article/abs/pii/S0013935124015561

Optimization of hydrochar synthesis conditions for enhanced Cd(II) and Pb(II) adsorption in mono and multimetallic systems

Lázaro Adrián González-Fernández [1,2], Nahum Andrés Medellín-Castillo [1,3,] Amado Enrique Navarro-Frómeta [4], Ventura Castillo-Ramos [2], Manuel Sánchez-Polo [2] and Francisco Carrasco-Marín [2]*

1 *Multidisciplinary Postgraduate Program in Environmental Sciences, Av. Manuel Nava 201, 2nd. Floor, University Zone, San Luis Potosí 78000, Mexico.*

2 *Faculty of Science, University of Granada, 18071 Granada, Spain.*

3 *Center for Research and Postgraduate Studies, Faculty of Engineering, Universidad Autonoma de San Luis Potosi, Dr. Manuel Nava No. 8, West University Zone, San Luis Potosí 78290, Mexico.*

4 *Food and Environmental Technology Department, Technological University of Izucar de Matamoros, De Reforma 168, Campestre la Paz, Izúcar de Matamoros 74420, Mexico*.

Corresponding author: nahum.medellin@uaslp.mx

Abstract

The characterisation of hydrochars derived from Sargassum biomass collected along the Mexican Caribbean coast reveals their favourable morphology and chemical composition for incorporating metal ions, including Cd(II) and Pb(II). Among the synthesized materials, HCS-3, produced at 180 °C with a 2 h residence time, exhibited superior yield, specific area, carbon content, and capacity for removing Cd(II) and Pb(II). Adsorption equilibrium studies demonstrate the presence of adsorption processes during Cd(II) and Pb(II) retention on HCS-3, with adsorption capacities slightly exceeding 140 and 340 mg g^{-1}, respectively. Notably, HCS-3 shows a greater affinity for Pb(II) over Cd(II) when both elements are present concurrently. The physicochemical analysis through FTIR spectroscopy, functional group analysis, point of zero charge determination, SEM/EDS, and other techniques evidenced that HCS-3 possesses favourable characteristics to serve as a heavy metal adsorbent. These findings underscore the efficacy of hydrochars from Sargassum biomass in removing heavy metals, suggesting their potential as superior adsorbents compared to traditional or novel materials, and advising its possible versatility for other pollutants. Utilizing these hydrochars could mitigate the economic and environmental impact of Sargassum biomass by repurposing it for valuable applications.

Keywords: Hydrochars; Sargassum biomass; Heavy metals; Adsorption; Characterisation.

1. Introduction

Water is an essential resource for all living beings, playing a vital role in our daily lives, agriculture, and industrial processes (Morin-Crini et al., 2022). However, in the past few decades,

water contamination has emerged as a critical environmental concern. Of particular concern are heavy metals such as cadmium (Cd) and lead (Pb), which have witnessed a significant surge in their levels over the past decade. The presence of these contaminants poses severe threats to human health, ecosystems, and ecological balance (Vardhan et al., 2019).

Heavy metals, including Cd and Pb, are persistent in nature and exhibit toxic effects even at low concentrations. Industrial activities, inadequate waste management practices, and the use of agrochemicals have been major contributors to the contamination of water sources by these metals. Once released into the environment, heavy metals can enter the food chain, and prolonged exposure can lead to severe health issues, ranging from neurological disorders to organ damage (G. Yu et al., 2022).

Addressing the challenges of heavy metal contamination in water requires effective and economically viable solutions. The most traditional methods for removing heavy metals from water include electrocoagulation, ultrafiltration chemical precipitation, ion exchange, and chemical oxidation, among others. It should be noted that these traditional methods have limitations in terms of efficiency, cost, and waste generation. However, they have been used for a long time and are still implemented in certain contexts where more advanced technology is not available or is economically unfeasible (Yu et al., 2021).

Over the past few years, there has been notable interest in water treatment techniques centred around adsorption, primarily because of their effectiveness in eliminating heavy metals from polluted water sources. Adsorption occurs when the contaminants adhere to the surface of an adsorbent material, effectively removing them from the water. Among the various adsorbents available, biomass-based adsorbents have emerged as a promising solution. Biomass-based adsorbents are derived from organic materials such as plant waste, agricultural residues, and biochars, making them both cost-effective and sustainable (El Atouani et al., 2019; Pimentel-Almeida et al., 2023).

The advantages of biomass-based adsorbents in water decontamination are manifold. Firstly, they exhibit high adsorption capacities due to their abundant surface functional groups, allowing for efficient metal ion binding. Secondly, their porous structure enhances accessibility and facilitates the removal of heavy metals from water. Additionally, their renewable nature contributes towards minimizing environmental impacts, reducing the carbon footprint associated with water treatment

processes. Moreover, the utilization of biomass waste materials as adsorbents promotes waste management and creates a circular economy, turning waste into a valuable resource (S. Yu et al., 2022).

Besides their chemical properties and eco-friendliness, biomass-based adsorbents offer flexibility in terms of customization. Researchers have been able to modify the surface properties of these adsorbents to maximize their selectivity towards specific heavy metals, a crucial advantage for tailored water treatment processes (Raninga et al., 2023). Various adsorbents have been employed to eliminate or decrease heavy metal concentrations to safe levels for human consumption. Table 1 displays several of these adsorbents along with their respective adsorption capacities.

Table 1. Capacities for adsorbing Cd(II) and Pb(II) by various materials

Adsorbent	Adsorbate	Adsorption capacity (mg g^{-1})	Refs.
Brewed tea waste	Pb(II)	1.2	(Çelebi et al., 2020)
Natural clay		25.1	(Kushwaha et al., 2020)
Humic acid		19.2	(Kushwaha et al., 2020)
Porous cellulose nanofiber–sodium alginate hydrogel beads		318.5	(Zhao et al., 2021)
Caragana korshinskii biomass derived biochar		220.9	(Wang et al., 2021)
Functionalized cotton charcoal/chitosan biomass-based hydrogel		1105.8	(Fan et al., 2022)
Moringa oleifera seed biomass		6.2	(Nwagbara et al., 2022)
Hydrochar derived from rice husk and *Zizania latifolia* straw		8.6	(Zhang et al., 2022)
Sargassum spp.		350.0	(González-Fernández et al., 2023a)
Silica aerogel		10.4	(Akhter et al., 2024)
Red algae *Galaxaura oblongata*	Cd(II)	85.5	(Pyrzynska, 2019)
Olive branches activated carbon (AC)		38.2	(Alkherraz et al., 2020)
Brewed tea waste		2.5	(Çelebi et al., 2020)
Litchi chinensis peel biomass		15.3	(Ansari et al., 2020)
Caragana korshinskii biomass derived biochar		42.4	(Wang et al., 2021)
Moringa oleifera seed biomass		5.0	(Nwagbara et al., 2022)
Hydrochar derived from rice husk and *Zizania latifolia* straw		3.9	(Zhang et al., 2022)
Sargassum spp.		240.0	González-Fernández et al., 2023)
Eucalyptus globulus fruit biomass		128.2	(Samimi, 2024)
NaCl-modified zeolite		25.6	(Velarde et al., 2024)

Addressing the pressing issue of water contamination, specifically heavy metals like Cd and Pb, requires innovative and sustainable solutions. Biomass-based adsorbents are gaining recognition as a viable option due to their efficient metal ion binding, accessible porous structure, renewable

nature, and potential for customization. By harnessing the power of adsorption and the benefits of biomass-based materials, we can pave the way for safer and cleaner water sources, ensuring a healthier future for all.

The escalating issue of Sargassum seaweed in Mexico has posed significant challenges to coastal ecosystems and local economies. The excessive influx of Sargassum deposits along the coastlines is not only visually displeasing but also causes ecological imbalances and impacts marine life. However, amidst this predicament lies an innovative opportunity. The biomass derived from Sargassum holds tremendous potential as a precursor for the development of effective adsorbents to address water contamination challenges. Moreover, the utilization of hydrothermal processes for characterization enables the production of high-quality adsorbents from Sargassum biomass, thereby presenting a sustainable and environmentally friendly solution (El Atouani et al., 2019; Pimentel-Almeida et al., 2023).

The proliferation of Sargassum seaweed in coastal areas of Mexico has become a pressing environmental concern. The increase in its frequency and intensity has had significant repercussions on local ecosystems, tourism, and livelihoods. The accumulation of Sargassum on beaches leads to the depletion of oxygen levels in the water, disrupting marine life and creating dead zones. The decomposition of this biomass releases hydrogen sulphide, which not only emits an unpleasant odour but also poses health risks to nearby communities. These challenges necessitate innovative approaches to mitigate the negative impacts of Sargassum while simultaneously generating valuable resources from this abundant biomass (León, 2019).

One notable attribute of Sargassum biomass lies in its excellent characteristics as a precursor for adsorbents. Sargassum is rich in functional groups such as hydroxyl, amine, and carboxyl, which endow it with strong adsorption capabilities for heavy metals and other contaminants. Its high specific area provides ample sites for adsorption, maximizing the removal of pollutants from water sources. Furthermore, Sargassum biomass exhibits remarkable mechanical robustness and chemical stability, ensuring its efficacy as an adsorbent material (Hannachi and Hafidh, 2020; Ma et al., 2020).

To harness the full potential of Sargassum biomass, hydrothermal processes have emerged as a valuable method for its characterization. These processes involve subjecting the biomass to high temperatures and pressure in an aqueous environment. Hydrothermal treatment facilitates the

breakdown of complex organic compounds present in Sargassum, resulting in the generation of adsorbents with enhanced efficiency and durability. The controlled hydrothermal conditions enable the precise tuning of the adsorbent's textural properties, such as pore size and surface area, thereby optimizing its adsorption capacity (Martínez-Meraz et al., 2023a).

The utilization of Sargassum biomass as a precursor for adsorbents not only presents an effective solution to water contamination but also offers a sustainable approach to addressing the Sargassum problem in Mexico. By transforming this invasive seaweed into a valuable resource, we can simultaneously combat water pollution and create economic opportunities. The adoption of hydrothermal processes for the characterization of Sargassum biomass further ensures the production of high-quality adsorbents, thereby enhancing their efficacy in removing heavy metals and other contaminants from water sources.

The primary aim of this investigation was to characterize the hydrochars derived from Sargassum biomass sourced from the Mexican Caribbean and assess their efficacy in removing Cd(II) and Pb(II) from water using single and multicomponent batch adsorption systems. Additionally, optimization of synthesis parameters was conducted to select optimal conditions for achieving the highest yields, carbon contents, surface areas, and adsorption capacities for the targeted pollutants.

The findings suggest that hydrochars derived from Sargassum biomass offer a viable solution for removing metal contaminants such as Pb and Cd, potentially replacing established adsorbent materials. A thorough analysis of the composition, as well as the physical and chemical properties of these adsorbents, is essential to determine their potential effectiveness as highly efficient adsorbents. This evaluation could help alleviate not only the existing economic and coastal ecosystem damages in the Mexican Caribbean region but also the issues related to heavy metal pollution.

The novelty of this work lies in the fact that hydrocarbonized materials with high adsorption capacities are obtained, comparable to traditional materials such as activated carbons, zeolites and clays, and superior to those reported for materials of natural origin such as biomasses, fungi and yeasts. Additionally, the synthesized material has a high specific area, adequate porosity, does not generate colour or taste in the water in which it is used and can also be used to remove other organic contaminants according to other studies carried out (Martínez-Meraz et al., 2023b).

2. Materials & Methods

2.1 Raw Material (RM)

Sargassum spp. sourced from the Mexican Caribbean region were subjected to rigorous taxonomic and morphological assessments based on established criteria outlined in expert literature (Rosado-Espinosa et al., 2020). Following the selection phase, the collected samples underwent a thorough rinsing process using abundant seawater and were subsequently air-dried for 72 h. Following drying, the samples were meticulously stored under controlled humidity conditions and shielded from light using polyethylene bags. Prior to analysis, the algae samples underwent extensive cleansing with distilled water to remove salts and any residual solid particles. Subsequently, they were dried in an oven at 110 °C for 24 h and then finely ground using an electric mill. The resulting material was sifted through vibrating sieves with apertures ranging from 30 to 50 μm. The separated particle fractions of different sizes were then carefully preserved for further analysis (González-Fernández et al., 2023a).

2.2 Synthesis of hydrochar

The hydrothermal carbonization (HCT) experiments entailed controlling parameters such as carbonization temperature (T), residence time (t), and the mass ratio of the RM to water (r) utilized. An experimental design based on response surface methodology (RSM) was employed to evaluate how these operational variables influenced the characteristics of the produced materials. The experimental arrangement, defined in Table 3, was carry out using Design-Expert® software, implementing a Box-Behnken design with 3 factors and 3 centre point replicates, resulting in a total of 15 experiments or hydrochars.

In the pursuit of achieving carbonization and obtaining hydrochars (HCS) as the primary product, the T factor was varied between 180 °C and 220 °C, in accordance with previous studies by Lee et al. (2019) (Lee et al., 2019) and Pauletto et al. (2021) (Pauletto et al., 2021). Considering the literature reports (Cavali et al., 2023; Gong et al., 2023; Soroush et al., 2022; Supee and Zaini, 2024; Wu et al., 2023) indicating a synthesis time of 1 to 8 h for the HTC process with different precursors, the effect of t was explored in this study using lower and upper levels of 2 and 8 h, respectively. This range is deemed sufficient to facilitate the RM transformation and provides a broad scope to discern potential effects of this factor.

In preparation for the HTC process, the RM needed dispersion in water. Preliminary tests were conducted to determine the minimum amount required to cover 1.0 gram of material, establishing a minimum of 5 mL of water per gram of precursor. The maximum level for the R factor was set at 10 mL g^{-1}, considering the capacity of the reactor.

2.3 Hydrochars characterization

2.3.1 Conversion efficiency percentage

The conversion efficiency percentage (CEP) of the RM to hydrochar is calculated with the following equation:

$$\text{CEP}\ (\%) = \frac{w_i - w_f}{w_i} \cdot 100$$

Where w_i and w_f are the masses of the RM and hydrochar obtained, respectively. This equation quantifies the degree to which the RM is converted into hydrochar, providing valuable insights into the efficiency of the conversion process. A higher CEP indicates a more effective utilization of the RM, resulting in a greater proportion being transformed into hydrochar.

2.3.2 Nitrogen physisorption

For the determination of the specific area of the synthesized hydrochars and their related parameters, a sample tube was plugged with a rubber stopper and placed in one of the degassing ports of the Micromeritics Model ASAP 2420 Analyzer. The sample tube was attached to one of the degassing ports and heated by means of the heating basket to a temperature of 110 °C.

The physisorption equipment measured the volume of adsorbed nitrogen at different pressures maintaining constant standard temperature and pressure (274.15 K and 1 atm) with a mass of approximately 0.1 g of each material. With the volumes and pressures obtained at 5-second intervals for each measurement, the specific area of the adsorbent and the pore size distribution was calculated.

2.3.3 C, H, O, N and S determination

Elemental analyses (CHONS) were conducted to determine the chemical composition of both the synthesized hydrochars and the RM. These analyses aimed to assess the compositional variations in the hydrochars resulting from different hydrothermal carbonization (HTC) conditions. The percentage of carbon, hydrogen, nitrogen, and sulphur was analysed using a Thermo Scientific

CHNS-O elemental analyser, FlashSmart model. The oxygen content was estimated independently using the following equation.:

$$\%O = 100\,\% - (\%C + \%H + \%N + \%S)$$

2.3.4 Point of Zero Charge

The determination of the point of zero charge (PZC) follows the method outlined by González-Fernández et al., 2021 (González-Fernández et al., 2021). The mass of adsorbed protons is assessed using the equation provided below.:

$$q_{H+} = \frac{C_N(V_B - V_M)}{m}$$

The application of the following equation is used to estimate the surface charge (SC) of the materials:

$$\mathrm{SC} = \frac{q_{H+}F}{S}$$

The SC distribution is created by plotting pH against the materials' SC. The PZC corresponds to the pH at which the SC is neutral (González-Fernández et al., 2023a). In this equations, q_{H+} indicates the quantity of moles of proton adsorbed on the adsorbent at a specific final pH value (mol g^{-1}), C_N represents the concentration of the neutralizing solution (mol L^{-1}), V_M is the volume of the neutralizing solution (NaOH or HCl) needed to achieve a predetermined final pH value for the solution containing the adsorbent (L), and V_B refers to the volume of neutralizing solution needed for the solution without the adsorbent to achieve a specified final pH value (L).

2.3.5 FTIR analysis

Fourier transform infrared spectroscopy identified the functional groups on the surface of both RM and the synthesized hydrochar which exhibited the highest adsorption for Cd and Pb (HCS-3). Infrared spectra were acquired using the attenuated total reflectance (ATR) method on a *Thermo Scientific* FTIR spectrometer, model Nicolet iS10, equipped with a diamond ATR accessory. The analysis covered the wavenumber range from 3900 to 600 cm^{-1}, with 32 scans conducted at a resolution of 4 cm^{-1}. Background spectra were obtained between each sample during the analysis.

2.3.6 SEM/EDS analysis

Scanning electron microscopy (SEM) was carried out to obtain images of particle size, surface morphology and composition of the RM and the synthesized hydrochar with the highest adsorption for Cd and Pb. Using a *Thermo Fisher* Quanta 250 FEG instrument, images were acquired employing secondary and backscattered electrons. The equipment was also armed with an energy dispersive EDAX-DX-4 microanalysis system to perform qualitative elemental analysis of single points in the material´s surface. For the analysis, the samples underwent pre-drying at 120 °C for 36 h, after which they were directly mounted onto the sample holders.

2.3.7 XPS analysis

The ESCA 5701 spectrometer was employed to capture X-ray photoemission spectra (XPS) of the RM and the synthesized hydrochar with the highest adsorption for Cd and Pb. Operating with a MgKα radiation source ($h\nu$ = 1253.6 eV), and a hemispheric electron analyser at 12 kV and 10 mA, the instrument utilized the carbon C1s peak (284.6 eV) as an internal standard for binding energy determination. To enhance signal-to-noise ratio, each region underwent multiple scans. Analysis involved interpreting the spectra using Lorentzian and Gaussian curves (Voigt profile) after correcting for background signals. Peak positions, areas, and the number of components were determined, and peak assignments were made based on literature information.

2.3.8 Active sites determination

The acid-base titration method introduced by Boehm, 1994 (Boehm, 1994) was employed to identify the active sites of the RM and the synthesized hydrochar with the highest adsorption for Cd and Pb. Neutralization of total acidic and basic sites was carried out using 0.01 mol L^{-1} NaOH and HCl solutions, respectively. Specific acid sites on the adsorbents were neutralized with 0.01 mol L^{-1} solutions of NaOH, Na_2CO_3, and $NaHCO_3$. NaOH solution was used for the total acid sites determination, $NaHCO_3$ for carboxylic sites determination and Na_2CO_3 for carboxylic and lactonic sites (González-Fernández et al., 2023a).

2.4 Analysis of Cd and Pb in aqueous solution

Cd and Pb concentrations in aqueous solution were determined using flame atomic absorption spectrometry (VARIAN SPECTRAA 220 Spectrometer) with hollow cathode lamps and the calibration curve method (1.0 to 1000 mg L^{-1}). A primary standard of 1000 mg L^{-1} for each metal

was prepared by weighing the corresponding masses and fully dissolving them in water to a volume of 1.0 L. Subsequently, a secondary standard was prepared by diluting an aliquot of this solution in deionized water to achieve a concentration of 100 mg L^{-1}.

2.5 Experimental data on the adsorption equilibrium of Cd and Pb

Experimental data regarding the adsorption equilibrium of Cd and Pb were acquired via a batch adsorber, following a methodology similar to that outlined by González-Fernández et al., 2023 (González-Fernández et al., 2023a). The amount of Cd or Pb adsorbed onto the materials was established using the following equations:

$$q = \frac{V_0 C_0 - V_f C_f - \sum_{i=1}^{N} V_i C_i}{m}$$

$$V_f = V_0 - \sum_{i=1}^{N} V_i + V_a$$

Where C_0 represents the initial metal concentration in mg L^{-1}, C_f denotes the final metal concentration also in mg L^{-1}, C_i indicates the metal concentration in the *i* sample measured in mg L^{-1}, m stands for the mass of the adsorbent in grams, N signifies the total number of samples, q signifies the mass of metal adsorbed per unit mass of adsorbent in mg g^{-1}, V_0 represents the initial volume, V_f indicates the final volume, V_i denotes the volume of the *i* sample, and V_a stands for the total volume of acidic and basic solutions added to adjust the pH of the adsorber solution. All the volumes are measured in litters.

The equilibrium of the adsorption process was characterized by matching the experimental data to Langmuir, Freundlich, and Radke–Prausnitz (R–P) isotherm models, expressed by the following equations, respectively:

$$q_e = \frac{q_m K_L C_e}{1 + K_L C_e}$$

$$q_e = K_F C_e^{1/n}$$

$$q_e = \frac{K_R C_e}{1 + a_R C_e^{\beta}}$$

Various isotherms were used to evaluate data from multicomponent equilibria. These included the non-modified Langmuir multicomponent isotherm (NLMI), modified Langmuir multicomponent isotherm (MLMI), extended Langmuir multicomponent isotherm (ELMI), modified Redlich–Peterson multicomponent isotherm with an interaction factor (MRPMI), non-modified Redlich–Peterson multicomponent isotherm (NRPMI), Sheindorf–Rebuhn–Sheintuch isotherm (SRSI) and the extended Freundlich multicomponent isotherm (EFMI). The equations corresponding to these mathematical models are detailed in Table 2.

Table 2. Isotherm models employed to describe the experimental data in multimetallic systems

Model	Equation	Model	Equation
NLMI	$q_i = \frac{q_m K_i C_i}{1 + \sum_{j=1}^{N} K_j C_j}$	**ELMI**	$q_i = \frac{q_{max} K_{E,i} C_i}{1 + \sum_{j=1}^{N} K_{Ej} C_j}$
MLMI	$q_i = \frac{q_{m,i} K_i (C_i/\eta_i)}{1 + \sum_{j=1}^{N} K_j (C_j/\eta_j)}$	**NRPMI**	$q_i = \frac{a_i C_i}{1 + \sum_{j=1}^{N} b_j C_i^{\beta_i}}$
MRPMI	$q_i = \frac{a_i (C_i/\eta_i)}{1 + \sum_{j=1}^{N} b_j (C_j/\eta_j)^{\beta_j}}$	**SRSI**	$q_i = k_i C_i (\sum_{j=1}^{N} a_{ij} C_j)^{\left(\frac{1}{n_i}\right)-1}$
EFMI	$q_1 = \frac{k_1 C_1^{\left(\frac{1}{n_1}\right)+x_1}}{C_1^{x_1} + y_1 C_2^{z_1}}$; $q_2 = \frac{k_2 C_2^{\left(\frac{1}{n_2}\right)+x_2}}{C_2^{x_2} + y_2 C_1^{z_2}}$		

3. Results & discussions

3.1 Conversion efficiency percentage of the HTC

The CEP for each synthesized hydrochar was computed based on the proportion presented previously. Table 3 describes the experimental configuration alongside the hydrochar CEP acquired as a resultant outcome in each synthesis experiment.

The experimental data go through fitting to a regression model based on a second-order polynomial. The CCD methodology was employed by various researchers, including El Ouadrhiri et al., 2021 (El Ouadrhiri et al., 2021), Román et al., 2020 (Román et al., 2020) and Periyavaram et al., 2023 (Periyavaram et al., 2023) to examine the impacts and optimize parameters in the HTC of diverse biomasses such as tomato, peels, olive stone and water hyacinth. The researchers explored the impacts of T, t, and r through a series of 18 randomized experiments. Subsequently, they modelled the resulting solid yield utilizing a second-order function, akin to the approach employed in the present study.

Table 3. HTC treatment experimental design and hydrochar CEP, S_{BET}, PZC and adsorption capacity responses

Exp.	T (°C)	t (h)	r (mL g^{-1})	CEP (%)	A (m^2 g^{-1})	PZC	q_{Cd} (mg g^{-1})	q_{Pb} (mg g^{-1})
HCS-1	200	2.0	5.0	50.14	120.2	6.13	63.97	175.23
HCS-2	200	8.0	5.0	46.84	81.7	6.28	45.55	164.34
HCS-3	180	2.0	7.5	60.35	126.7	6.00	64.82	184.84
HCS-4	200	2.0	10	51.55	99.4	6.16	62.72	172.48
HCS-5	220	8.0	7.5	39.73	52.5	6.81	37.07	165.63
HCS-6	200	5.0	7.5	49.32	101.5	6.25	50.93	158.97
HCS-7	180	8.0	7.5	54.06	86.2	6.14	45.06	138.71
HCS-8	220	5.0	5.0	43.79	62.1	6.63	40.85	159.51
HCS-9	200	5.0	7.5	49.32	75.4	6.24	47.99	155.97
HCS-10	220	5.0	10	43.21	77.5	6.65	41.85	158.57
HCS-11	200	8.0	10	45.26	74.1	6.43	41.53	145.34
HCS-12	220	2.0	7.5	45.02	92.7	6.47	53.98	163.30
HCS-13	200	5.0	7.5	48.32	84.8	6.23	50.57	153.08
HCS-14	180	5.0	5.0	56.12	114.7	6.09	46.75	141.34
HCS-15	180	5.0	10	56.54	105.1	6.09	46.92	144.56

The hydrochar CEPs in this work ranged from 39 to 60 %. There are several investigations in the literature on the effect of operating conditions on the hydrochar CEP obtained. Azaare et al., 2021 (Azaare et al., 2021) performed hydrochar synthesis from softwood to analyse the effect of process conditions on the CEP. For the synthesis they used 90 and 120 min as residence times and temperatures between 180 and 250 °C, obtaining CEPs between 44 and 57 %. Likewise, Güleç et al., 2021 (Güleç et al., 2021) obtained hydrochar CEPs between 58 and 62 % for synthesis from different lignocellulosic biomass feedstocks, using temperature between 75 and 250 ºC.

In a recent study, A DoE-RSM approach was utilized by Afolabi et al., 2020 (Afolabi et al., 2020) to analyse and improve the combined impact of T and T factors on the hydrochar yield derived from spent coffee grounds. They applied a face-centred central composite factorial design to correlate the dual responses with the respective factors. Findings indicate that within the tested range (180 – 220 °C and 1 – 5 h), the optimal hydrochar yield of 63.9 % is attained at a residence time of 1h with a temperature of 216.4 °C.

From Table 3, it is possible to observe that the hydrochar CEP values are influenced by the parameters investigated, since the highest CEP was observed for the lowest time and temperature, while the lowest CEP was found for higher time and temperature values. The above agrees with

that reported by Azaare et al., 2021 (Azaare et al., 2021) who found that high values of carbonization time and temperature promote a decrease in CEP values.

Analysis of variance (ANOVA) was completed to evaluate if the factors are significant and to check the good fit of the model. The statistical analysis of the factors was performed through the hypothesis and Fisher's F test (confidence interval of 95 %). The conclusions obtained in the analysis of variance are presented in Supplementary Table 1.

As per the information presented in Supplementary Table 1, the influential factors involved the three linear terms, each exhibiting p-values below 0.05. Furthermore, the model's p-value, confirms the statement that the linear model effectively characterizes the variability of the experimental response. On the contrary, the p-value for lack-of-fit suggests that the lack-of-fit regarding the error is not statistically significant.

The linear regression model, tailored to the CEP in relation to the encoded factors and omitting the non-significant terms, is expressed by the following equation. The negative coefficients for T and t signify that an increase in the values of these factors correlates with a reduction in the response (CEP).

$$CEP = 246.1 - 1.9T - 3.2t + 7.3r$$

The interplay among T, t, and r, along with their consequential effects on the response, was studied through the examination of the three-dimensional response surface presented in Figure 1. The maximum of the CEP value is achieved when both factors (T and t) are set to their lower levels. This conclusion stems from the circumstance that, under these conditions, the biomass undergoes minimal alterations during the treatment, thereby resulting in reduced mass loss (Martínez-Meraz et al., 2023a).

Utilizing the parameters derived from the model-description equation for CEP, an optimization was conducted utilizing the *Microsoft Excel* Solver tool. The objective was to attain the maximum value. The results of this optimization are presented in Table 4.

The achieved maximum experimental CEP registered at 60.35 % (T = 180 ºC, t = 2 h, r = 7.5 mL g^{-1}), resulting in a percentage deviation of merely 1.31 % when compared to the model-predicted values. This minimal and acceptable deviation underscores the efficacy of the model in accurately depicting the obtained data.

Table 4. Optimization of the parameters for the CEP response

Estimated parameter	Value
T (ºC)	180
t (h)	2
r (mL g^{-1})	7.6
Maximum CEP	57.28

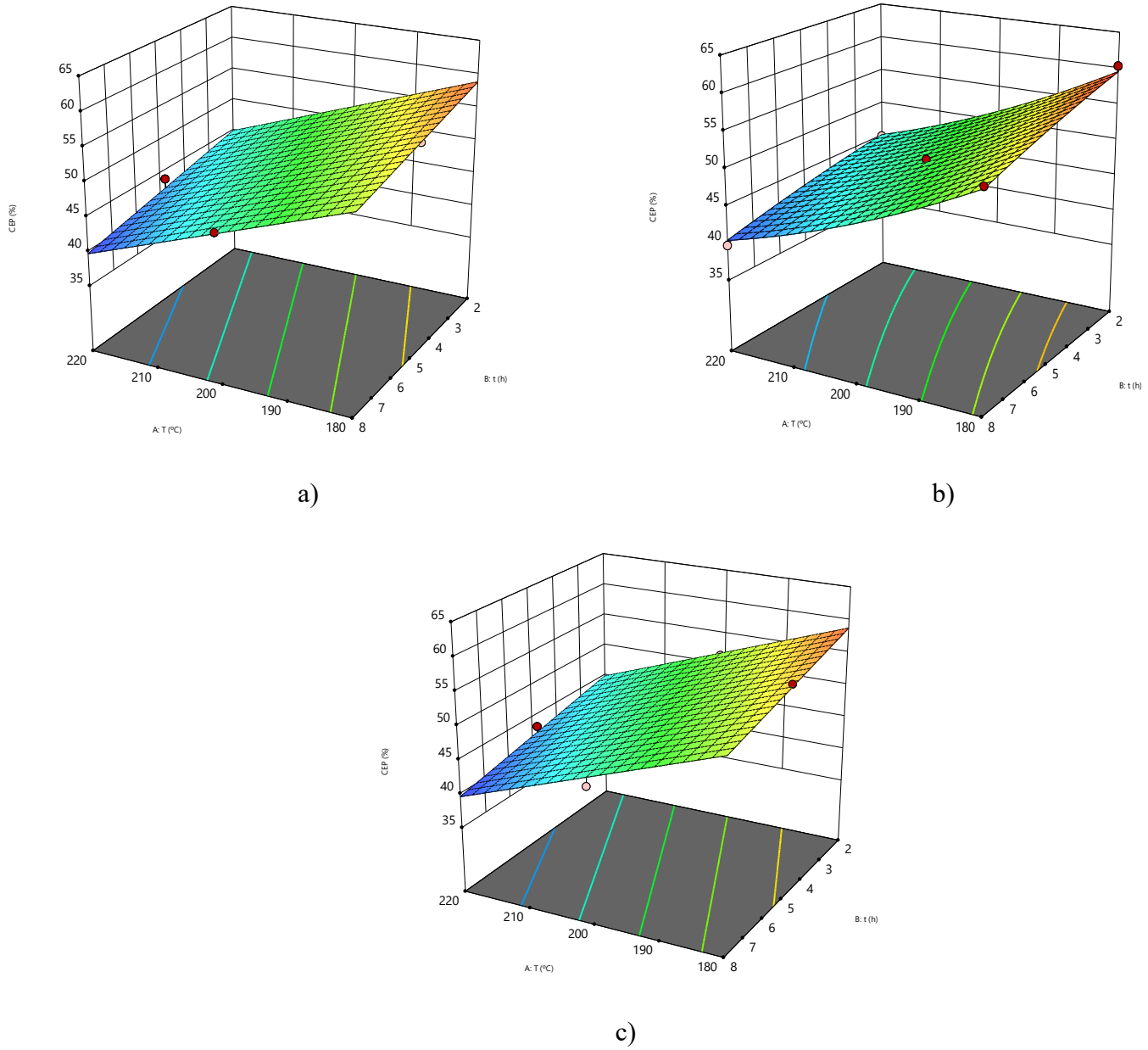

Figure 1. Three-dimensional response surface for CEP: a) r = 5 mL g^{-1}, b) r = 7.5 mL g^{-1} and c) r = 10 mL g^{-1}

3.2 Hydrochars' surface optimisation

The specific area of the synthesised materials was determined using nitrogen physisorption and the Brauner, Emmet and Teller (BET) method. The area values obtained are shown in Table 3 and as can be seen, vary between 52.5 and 120.2 m^2 g^{-1}.

There are limited recent references that provide common values for the specific area of hydrochars prepared from biomass waste. However, one study reported that hydrochars produced from seaweed had a specific area ranging from 0.5 to 1.5 m^2 g^{-1} (Soroush et al., 2022). Another study reported that the specific area of NaOH-activated hydrochar derived from corncobs was 12.8 m^2 g^{-1} (Sivaranjanee and Kumar, 2023). The values found are above the range of values reported in the literature for other hydrochars and similar materials synthesised from biomass waste (Casco et al., 2023; Takaya et al., 2019).

The specific area values achieved were analysed by ANOVA to find the factors or interactions that have a significant influence on the area reached by each material as well as to analyse the corresponding response surface for this variable. The results of the ANOVA and the response surface obtained are shown in Supplementary Table 2 and in Figure 2, respectively.

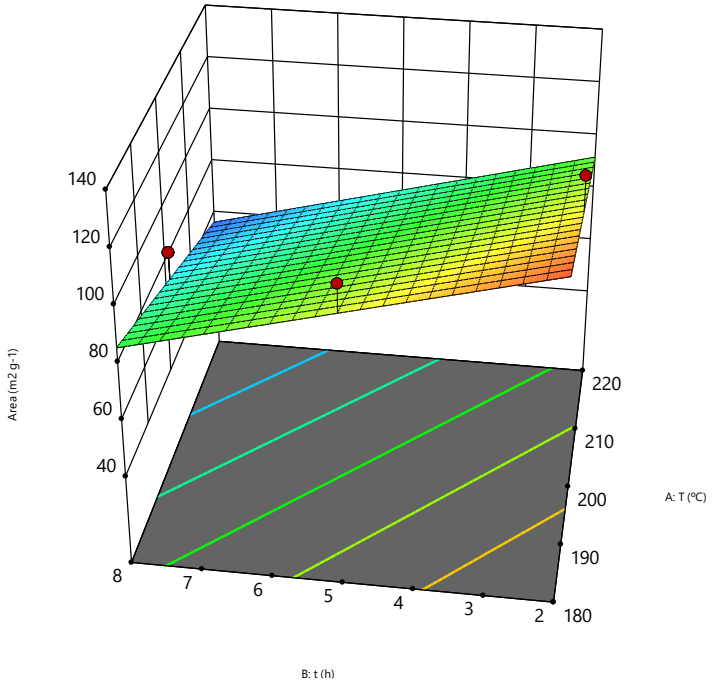

Figure 2. Response surface for the specific area of the synthesised hydrochars at r = 7.5 mL g^{-1}

Supplementary Table 3 reveals that among the factors influencing the area of the synthesized materials, T and t demonstrate significant impacts ($p < 0.05$), whereas the value of R does not exert a significant influence on the mathematical model applied ($p > 0.05$). With this information it was possible to obtain the equation that describes the response surface as a function of the significant variables, which is shown below:

$$A = 269.18 - 0.75T - 6.02t$$

The presence of negative coefficients in the equation for T and t indicates that an increase in their values corresponds to a decrease in the response (A), similar to what was observed in the CEP of the synthesized materials. This phenomenon might be attributed to the generation of porous structures, particularly meso- and macropores, as these variables increase. Conversely, lower levels of the variables favour the formation of micropores (Tee et al., 2022).

An optimization process was conducted on the response variable for this study using the *Microsoft Excel* 2023 Solver tool, utilizing the parameters derived from the model-description equation. The objective was to attain the maximum value. The summarized conclusions of this optimization process are presented in Table 5.

Table 5. Optimization of the parameters for the surface response

Estimated parameter	Value
T (ºC)	180
t (h)	2
Maximum Area (m^2 g^{-1})	121.7

The maximum experimental area reached 126.7 m^2 g^{-1} (T = 180 ºC, t = 2 h, r = 7.5 mL g^{-1}), indicating a percentage deviation of 4.1 % when compared to the values predicted by the model. This slight but acceptable deviation highlights the effectiveness of the model in accurately representing the collected data.

3.3 CHONS determination

Table 6 displays the results of the chemical analysis conducted on all synthesized hydrochars and the RM to assess their elemental composition, focusing on C, H, O, N, and S content.

The data reveals that HTC significantly impacted the chemical composition of the synthesized hydrochars, evident from distinct differences in elemental contents compared to the RM. Notably,

sulphur content remained notably low in both the hydrochars (ranging from 0.03 % to 0.09 % or even undetectable in most of the cases).

Furthermore, nitrogen content was generally higher in the hydrochars, attributed to the absence of nitrogen oxides in the processing liquid using this HTC (Fang et al., 2018). This trend parallels findings from HTC processes involving municipal sludge, organic sludge, and other biomasses (Liu et al., 2021; Magdziarz et al., 2020; Wang et al., 2020), suggesting that elevated temperatures might lead to the precipitation of certain inorganic compounds.

Table 6. CHONS composition of the synthesised hydrochars

Material	C	H	N	S	O[a]
RM	33.82	6.76	1.09	0.32	58.01
HCS-1	44.8	7.25	1.39	0	46.56
HCS-2	47.66	7.69	1.36	0.03	43.26
HCS-3	48.06	7.28	1.36	0.09	43.21
HCS-4	44.46	7.10	1.34	0	47.10
HCS-5	45.61	7.09	1.27	0.04	45.99
HCS-6	48.01	7.83	1.32	0	42.84
HCS-7	44.64	7.80	1.30	0.08	46.18
HCS-8	48.13	7.95	1.30	0.06	42.56
HCS-9	44.43	6.88	1.22	0	47.47
HCS-10	44.16	6.70	1.17	0	47.97
HCS-11	44.85	6.65	1.18	0	47.32
HCS-12	47.00	7.57	1.29	0	44.14
HCS-13	47.65	7.96	1.25	0	43.14
HCS-14	44.36	7.41	1.26	0.05	46.92
HCS-15	46.71	8.13	1.23	0	43.93

[a] Calculated by difference

The HTC process led to a notable increase in carbon content by approximately 30.6 % to 42.3 % across the resulting samples, accompanied by a significant reduction in oxygen content of approximately 26.6 %, going from 58.01 % to 42.56 %. Conversely, hydrogen content exhibited minimal variation, ranging from 6.65 % to 8.13 %.

These findings align with research conducted by Parra-Marfil et al., 2020 (Parra-Marfil et al., 2020), who investigated the HTC of industrial *Capsicum annuum* seeds and examined the impact of temperature, time and water-to-biomass ratio on hydrochar elemental composition. Using between 5 and 10 mL of water per gram of biomass, they observed that as the reaction temperature

increased from 180 °C to 250 °C over 2 to 8 h, carbon content rose from 53.12 % to 7.18 %, while oxygen content decreased from 37.74 % to 18.92 %.

The reduction in oxygen and hydrogen content in hydrochars mainly arises from dehydration and decarboxylation processes, eliminating hydrogen and oxygen in the forms of H_2O and CO_2, respectively. Conversely, the increase in carbon content in hydrochars is attributed to condensation and aromatization processes, resulting in a higher proportion of aromatic carbon compared to the RM.

To represent the changes in the atomic composition of the RM and hydrochars, the atomic H/C and O/C ratios were computed and analysed using a Van Krevelen diagram (Figure 3), with the corresponding data presented in Table 6. These ratios are commonly used to characterize the transformations occurring during the HTC process.

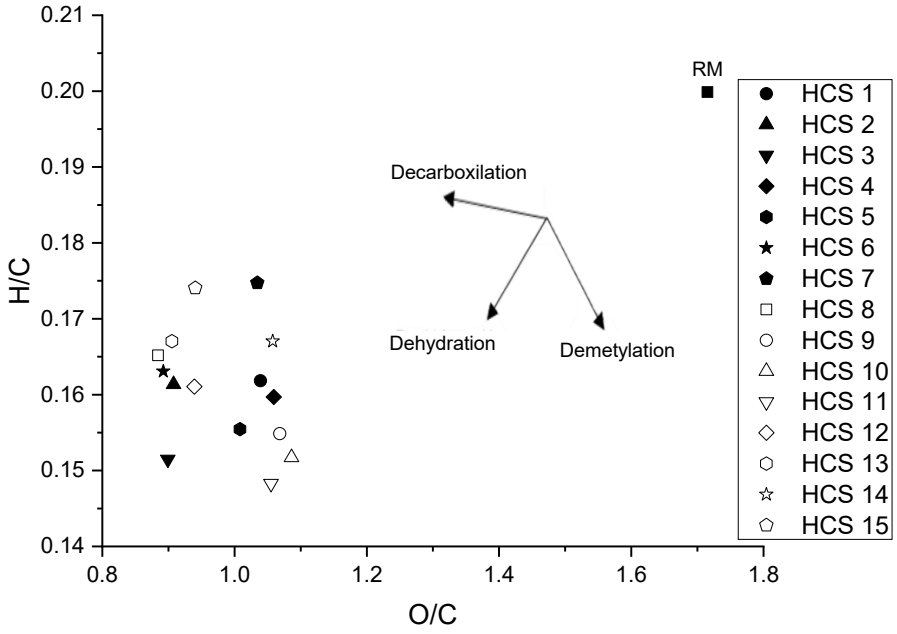

Figure 3. Van Krevelen diagram of RM and HTC-synthesized materials

In the diagram, both ratios decreased, moving from the upper right for the RM to the lower left after the HTC process. This transition is depicted as a vector almost parallel to the reference axis of the dehydration pathway, indicating that dehydration was the primary reaction during treatment. Decarboxylation and demethylation processes also occur, albeit to a lesser extent.

The results obtained for carbon content in the materials were fitted to a polynomial regression model with two interaction factors to obtain a response surface. To assess whether the factors are

significant and to check the good fit of the model, an ANOVA was performed as for the other variables analysed above (Table SuplX3). According to the data, the significant factors were the linear t term, and the quadratic term T·t. The response surface is presented in Figure 4.

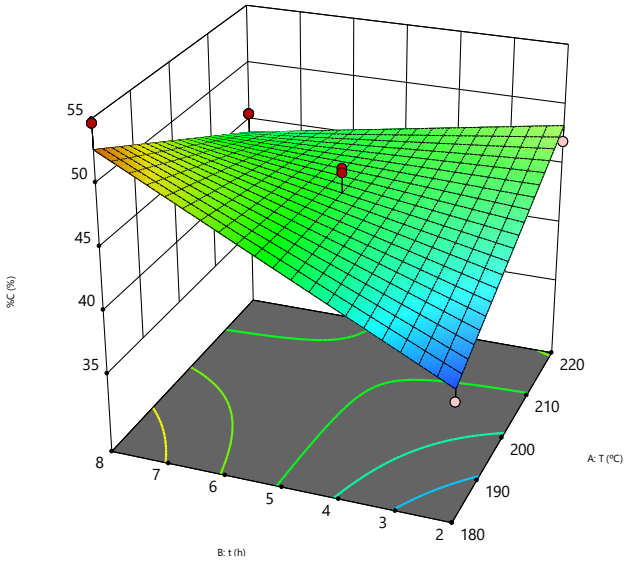

Figure 4. Three-dimensional response surface for the carbon percentage of the synthesised hydrochars at r = 7.5 mL g^{-1}

The response surface analysis reveals that under severe HTC treatment conditions (characterized by high temperatures and durations nearing 8 h), a greater %C is observed in the synthesized hydrochars. This outcome arises because dehydration and decarboxylation reactions are favoured, leading to a reduction in hydrogen and oxygen content and consequently increasing the carbon proportion. The surface primarily tilting towards the t factor underscores the significant influence of this factor on the carbon composition of the hydrochars.

The quadratic regression model, applied to the carbon content in weight percent of hydrochars, is defined by the following equation after decoding factors and eliminating non-significant terms:

$$\%C = -82.79 + 16.36t - 0.07T \cdot t$$

As can be seen from the response surface depicted in Figure 4 and the equation describing it, an increase in residence time during HTC translates into an increase in the mass percentage of carbon in the samples, while an increase in temperature does not produce statistically significant changes in this variable within the ranges studied. Similar results have previously been reported by Parra-

Marfil et al., 2020 (Parra-Marfil et al., 2020) who also obtained increases in the carbon content of the samples with increasing residence time in the HTC process.

3.4 Point of zero charge

The PZC values of the synthesised hydrochars are shown in Table 3. To assess the influence of the synthesis variables on the PZC, an ANOVA for the regression model with two interaction factors was conducted. The results presented in Supplementary Table 4 indicate that the linear factors T and t, as well as the quadratic factors T·t and T^2, are significant in the model, as their p-values are below 0.05. The quadratic regression model, used for the PCC of hydrochars, is described by the following equation eliminating non-significant terms:

$$PZC = 15.90 - 0.11T - 0.16t + 0.00083T \cdot t + 0.00029T^2$$

As the quadratic terms of the model have positive coefficients, increases in these factors would produce increases in the PZC of the materials, which can also be corroborated by analysing the response surface shown in Figure 5. Increases in temperature and residence time within the ranges studied, and their combination, produce increases in the PZC of the synthesised materials.

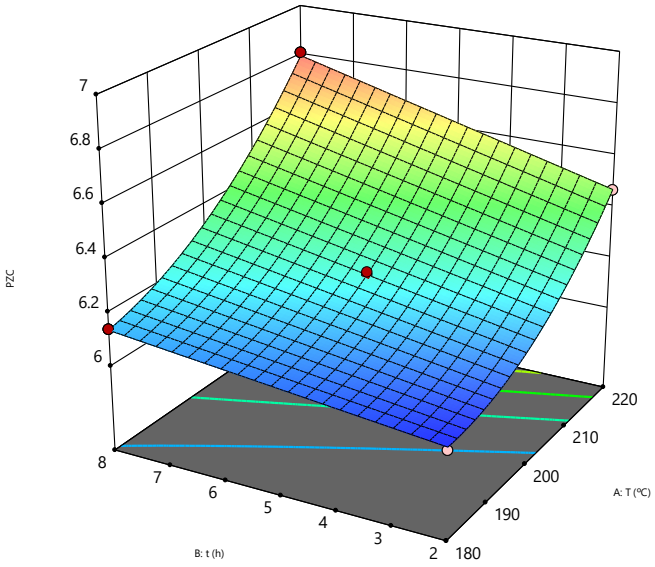

Figure 5. Three-dimensional response surface for the PZC at r = 7.5 mL g^{-1}

3.5 Pb and Cd adsorption

Fifteen synthesized materials underwent Cd and Pb adsorption experiments at pH 5 to assess their capability in removing these pollutants in monometallic systems and to analyse the impact of

synthesis variables. The adsorption capacities of the materials are detailed in Table 3 and depicted in the response surfaces presented in Figure 6.

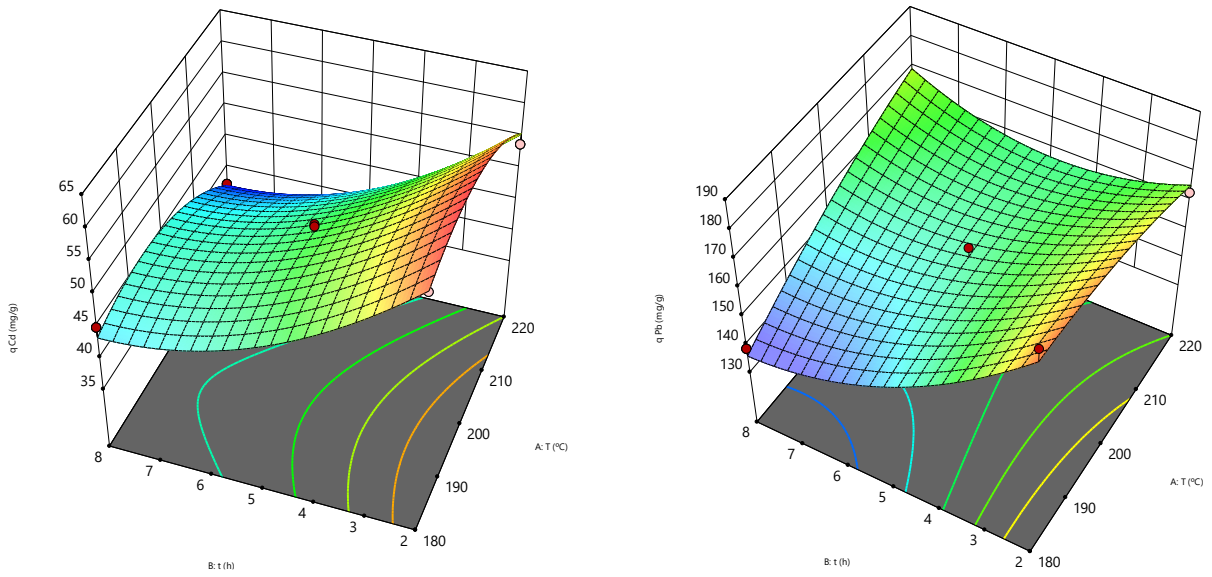

a) b)

Figure 6. Response surface at r = 7.5 mL g^{-1} for a) Cd(II) and b) Pb(II) adsorption capacities in the synthesised materials

The experimental adsorption data for both pollutants underwent an ANOVA to establish the impact of the synthesis variables on the adsorption process. The fits were modelled using quadratic mathematical equations, and the results are presented in Supplementary Table 5 and Supplementary Table 6.

As can be seen in both tables, for Cd adsorption the linear and simple quadratic terms of T and t (T, t, T^2 and t^2) were significant, while for Pb adsorption the linear term t and the quadratic terms T·t and t^2 were significant. This indicates that both temperature and time are variables that influence the adsorption capacity of the materials, but not the ratio of water and biomass used during the synthesis, as previously reported by Parra-Marfil et al., 2020 (Parra-Marfil et al., 2020) and Martínez-Meraz et al., 2023 (Martínez-Meraz et al., 2023a). The equations describing the response surfaces considering only the significant terms are as follows:

$$q_{Cd} = -388.30 + 4.78T - 8.01t - 0.012T^2 + 0.54t^2$$

$$q_{Pb} = -16.44 - 51.11t + 0.20T \cdot t + 1.13t^2$$

The findings indicate that the adsorption capacities for Cd and Pb ranged from 37.07 to 64.82 and 138.71 to 184.84 mg g^{-1}, respectively. This suggests that the material exhibits a higher capacity for removing Pb compared to Cd in terms of mass under identical conditions.

The highest adsorption capacity values occur when t and T are at their lowest values (2 h and 180 °C). This result is due to the synthesis conditions, which lead to the least changes in the biomass composition, especially in the functional groups, during the treatment (Ilić et al., 2022; Saha et al., 2019).

Moreover, this finding can be elucidated by the larger surface area of the material synthesized under these conditions (HCS-3 with approximately 127 m^2 g^{-1}), which enhances the adsorption of metal contaminants (Lima et al., 2019; Tee et al., 2022). Due to the excellent surface properties of this material and its high adsorption capacity for both metals, it was chosen for adsorption experiments on mono- and multimetallic systems of Cd(II) and Pb(II).

3.6 Monocomponent adsorption isotherms

The material denoted as HCS-3, which exhibited superior adsorption capacities for Cd and Pb, was utilized in both single and multi-component adsorption experiments. Figure 7 presents the adsorption isotherms for Cd(II) and Pb(II), depicting the experimental results fitted by the R-P mathematical model. This model is identified as the most suitable fit with the experimental data, as detailed in Table 7.

Table 7. Parameters of adsorption isotherm models

Model	Parameter	Cd			Pb		
		pH 3	pH 5	pH 7	pH 3	pH 4	pH 5
Langmuir	q_m (mg g^{-1})	123.97	132.1	144.8	323.1	290.3	307.9
	k_L (L mg^{-1})	0.005	0.039	0.040	0.009	0.055	0.112
	R^2 (%)	92.5	93.8	97.1	98.1	97.6	95.4
Freundlich	K_F (mg g^{-1})(L mg^{-1})$^{1/n}$	5.48	29.4	29.5	17.6	61.5	78.6
	n	2.20	4.06	3.77	2.22	3.69	3.98
	R^2 (%)	86.1	93.3	91.9	97.2	93.7	91.7
Radke–Prausnitz	K_R (L g^{-1})	0.56	9.12	7.74	4.46	29.08	52.99
	a_R	0.001	0.149	0.088	0.054	0.205	0.309
	β	1.17	0.87	0.92	0.78	0.87	0.89
	R^2 (%)	99.0	99.5	99.7	98.5	95.7	99.2

Based on these findings, the R–P model emerges as the most suitable fit among all materials, with a β constant approaching 1 (Tran et al., 2023). Additionally, the relatively high R–P constant indicates favourable adsorption of the adsorbate on the materials. The suitability of the R–P model in explaining the experimental data in specific adsorption systems suggests the presence of homogeneous and heterogeneous zones on the material's surface in terms of energy for adsorbing cations (González-Fernández et al., 2023a).

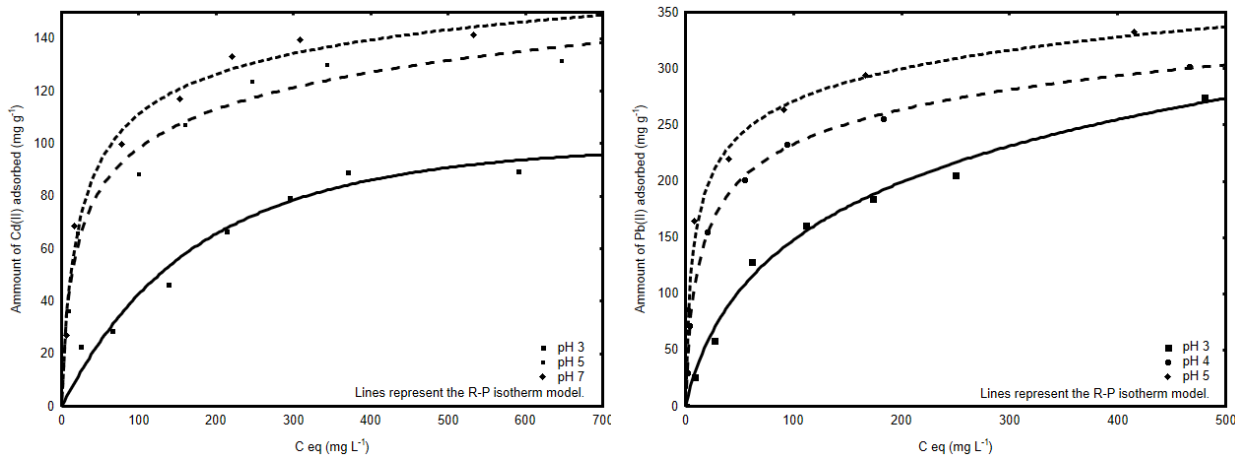

a) b)

Figure 7. Monocomponent adsorption isotherms at 25 °C for (a) Cd(II) and (b) Pb(II)

Figure 7 illustrates two distinct stages. Initially, in the first stage, the adsorption capacity rises as the equilibrium metal concentration increases, as the material possesses numerous active sites initially available for metal cation retention. As the metal concentration increases, these sites become progressively occupied, making it increasingly challenging for cations to undergo exchange. In the second period, a decline is evident in the slope, indicating saturation, where the maximum experimental adsorption capacity is determined (González-Fernández et al., 2023a).

The maximum adsorption capacities obtained in each case were 140 mg g^{-1} of Cd and 325 mg g^{-1} of Pb, so it can be observed that the material has a higher affinity for Pb ions than for Cd, although the capacities obtained for both metals are higher than those reported by other authors for lignocellulosic materials (Hopkins and Hawboldt, 2020), natural materials (Sharma et al., 2022), zeolites (Velarde et al., 2023), and even commercial activated carbons (Wang et al., 2023).This

studies have shown that hydrochars possess a high surface area and porosity, allowing for effective adsorption of a wide range of contaminants in water and air.

In terms of cost-effectiveness, hydrochars have the advantage of being derived from low-cost feedstocks such as Sargassum, making them potentially more economical to produce compared to synthetic materials like activated carbon. Additionally, the synthesis process for hydrochars is relatively simple and can be conducted using conventional equipment, further contributing to their cost-effectiveness (Phuthongkhao et al., 2023).

The impact of pH on heavy metal adsorption is well-documented (Verma and Kuila, 2019). The pH affects the protonation/deprotonation of functional groups in the adsorbents. Figure 8 illustrates that the adsorption capacity for both contaminants rises with an increase in pH, highlighting the significant role of pH in adsorption. At lower pH levels, repulsive forces between the material's ligands and the cations decrease the adsorption capacity. In contrast, with rising pH, more groups develop negative charge that can bind cations (Kaleem et al., 2023).

The pH effect is partly explained by a competitive interaction between heavy metal and hydronium ions. At lower pH values, hydronium ions are present in a considerable concentration, competing for active sites on the materials. Conversely, as pH increases, the concentration of hydronium ions falls, making it easier for cations to occupy active sites (Lucaci and Bulgariu, 2024).

3.7 Multimetallic adsorption isotherms

In two dimensions, Figure 8 illustrates the multicomponent isotherms for Cd(II) (a) and Pb(II) (b). These experimental findings agree to the R-P mathematical model, which consistently produced the lowest %D values across all instances.

In the experiments, the presence of Pb(II) notably influenced the adsorption of Cd(II), while the presence of Cd(II) had minimal impact on the adsorption of Pb(II), with only a slight deviation observed as the concentration of the competitive ion increased. The competitive isotherms demonstrate a striking similarity to the monometallic adsorption isotherm; nevertheless, the capacity to remove Pb(II) or Cd(II) is diminished when the competitive cation is present.

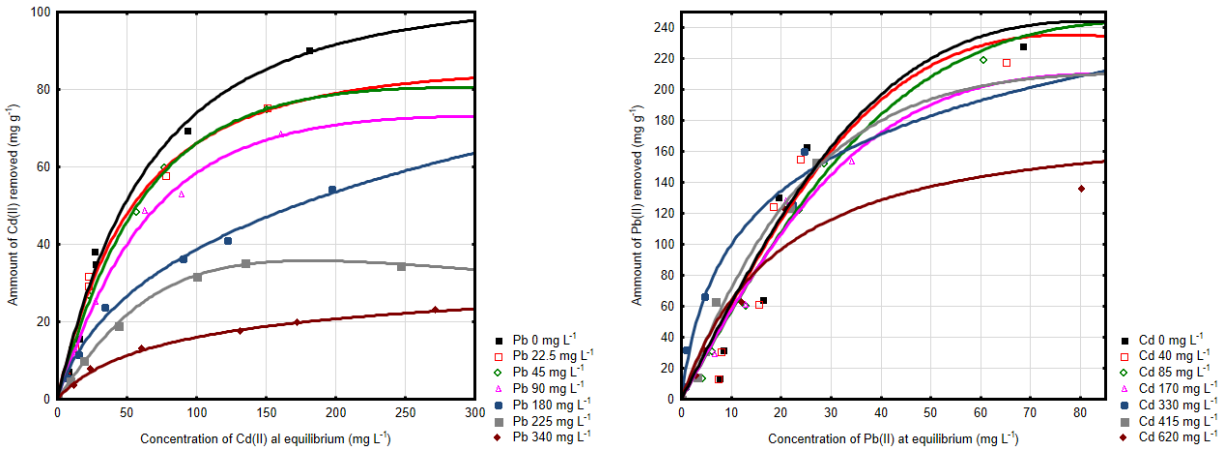

a) b)

Figure 8. (a) Cd(II) and (b) Pb(II) adsorption on HCS-3 at pH = 5.0 and T = 25 °C in the Cd(II)–Pb(II) binary system

Figure 9 depicts the experimental data characterized by the MRPMI model (which exhibited the lowest %D) in 3D.

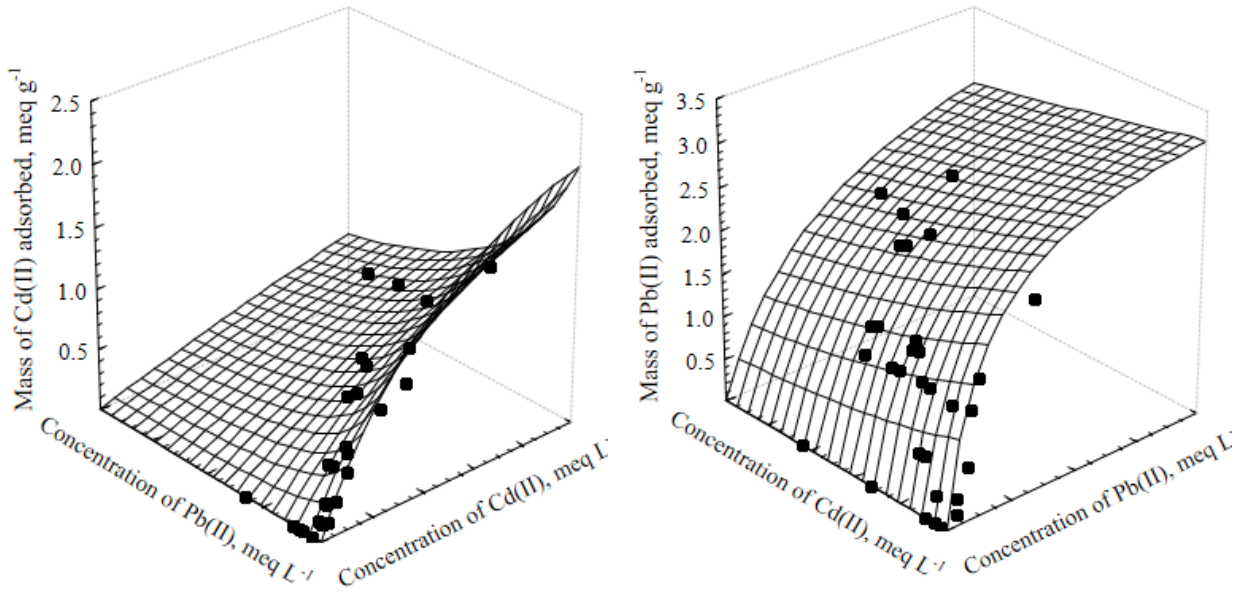

a) b)

Figure 9. MRPMI model representations of the multimetallic adsorption isotherms for (a) Cd(II) and (b) Pb(II) on HCS-3 at T = 25 °C and pH = 5.0

In Figure 9, the relationship between Pb(II) adsorption and the equilibrium concentration of Cd(II) is clearly demonstrated. The adsorption of lead cations was minimally influenced by the presence of cadmium, suggesting that lead ions exhibit a better affinity for the binding sites of HCS-3 compared to cadmium ions, as evidenced by the trend in the monometallic isotherms in Figure 7.

The selectivity ratio calculated following the method outlined by Medellin-Castillo et al., 2017 (Medellin-Castillo et al., 2017), shows a value of 2 when lead and cadmium ions concentrations are 4.0 meq L^{-1}. However, the ratio increases to 11 when the adsorption capacities are estimated using the MRPMI model. Consequently, lead cations exhibit significant (more than fivefold) antagonism in cadmium adsorption, despite cadmium having little impact on the uptake of lead.

The above results can be corroborated by analysing the atomic and mass percentages of the elements in the XPS analysis performed on the samples subjected to adsorption of Cd(II) and Pb(II) (Table 8). As can be seen in the Table, both when this hydrochar is used in a monometallic or multimetallic system, the amount of Pb removed is higher. In the case where both metals are present simultaneously, the amount of Pb present in the material is significantly higher than that of Cd, and the presence of Cd practically does not decrease the amount of Pb detected in the adsorbent.

Table 8. Results of XPS analysis of HCS-3 samples saturated with Cd, Pb, and Cd+Pb

Sample	C_{1s} eV	C % (w)	C % (at)	O_{1s} eV	O % (w)	O % (at)	N_{1s} eV	N % (w)	N % (at)	Cd_{3d} eV	Cd % (w)	Cd % (at)	Pb_{4f} eV	Pb % (w)	Pb % (at)
HCS-3/ Cd	284.6 286.0 287.0 288.2 289.4	70.8	70.0	530.9 532.2 533.1	28.2	25.6	399.5 400.3	2.5	2.6	405.1 411.9	10.6	1.4			
HCS-3/ Pb	284.5 286.0 287.2 288.1 289.6	39.7	67.6	530.8 532.2 533.0	20.1	25.7	399.5 400.2	2.0	2.9				138.4 143.3	37.9	3.7
HCS-3/ Cd,Pb	284.6 286.0 286.9 288.1 289.2	46.0	68.1	530.9 532.2 533.1	19.0	25.0	399.5 400.3	1.2	1.9	405.1 411.9	7.1	1.3	138.4 143.2	33.1	3.4

The equilibrium studies revealed that HCS-3 effectively adsorbs both cadmium and lead ions, with lead showing a stronger affinity than cadmium in multicomponent systems. This phenomenon suggests potential applications in selective metal removal scenarios.

3.8 Physicochemical characterisation of HCS-3

Table 9 presents the results of the characterization of both the RM and the synthesised material with the best performance in the Cd(II) and Pb(II) adsorption (HCS-3). It is evident from the data that the RM exhibits a notably small specific area and limited porosity, which are typical characteristics of biomass materials (Adegoke et al., 2023).

Conversely, HCS-3 shows a specific area of approximately 127 $m^2\ g^{-1}$, representing a two-order-of-magnitude enhancement compared to the RM. Moreover, the hydrochar displays a pore volume that is three orders of magnitude greater than that of the precursor.

The integration of these characteristics in HCS-3 notably improves its ability to adsorb each metal. This is especially remarkable when considering the inherent steric limitations linked to the adsorption of solvated metal ions within micro and mesopores (Ayati et al., 2023).

Table 9. Physicochemical properties of the RM and HCS-3

Material	S_{BET} ($m^2\ g^{-1}$)	V_{pore} ($m^3\ g^{-1}$)	PZC	Acid sites (meq g^{-1})				Basic sites (meq g^{-1})
				Total	Carb.	Lact.	Phen.	
RM	0.2	$9 \cdot 10^{-4}$	6.8	1.35	0.74	0.13	0.49	0.08
HCS-3	126.7	0.23	6.4	1.53	0.45	0.09	0.99	1.25

The PZC values for RM and HCS-3 were determined to be 6.8 and 6.4, respectively, indicating proximity to the neutral pH value. Consequently, these adsorbents exhibit slight acidity, with lower concentration of basic sites than acidic sites. The concentration of acid and basic sites presented in Table 9 aligns with the results previously reported by Tarbaoui et al., 2016 (Tarbaoui et al., 2016) concerning *Sargassum* biomass.

It is notable that the HTC process led to an elevation in the number of basic sites that exhibit a negative charge density that attracts the positive charge of the adsorbate's ions, thereby enhancing its adsorption on the synthesized material. Moreover, the concentration of acid sites also increased, particularly within phenolic sites, which possess delocalized electronic clouds favouring the capture of contaminants through electrostatic interactions (Crist et al., 1988).

Figure 10 illustrates an examination of the functional groups identified in the synthesized HCS, principally concerning its enhanced capacity for Cd(II) and Pb(II) adsorption, in comparison to the RM. This evaluation reveals the presence of aromatic structures, carboxylic (present in phenols) and carbonyl groups (present in lactones).

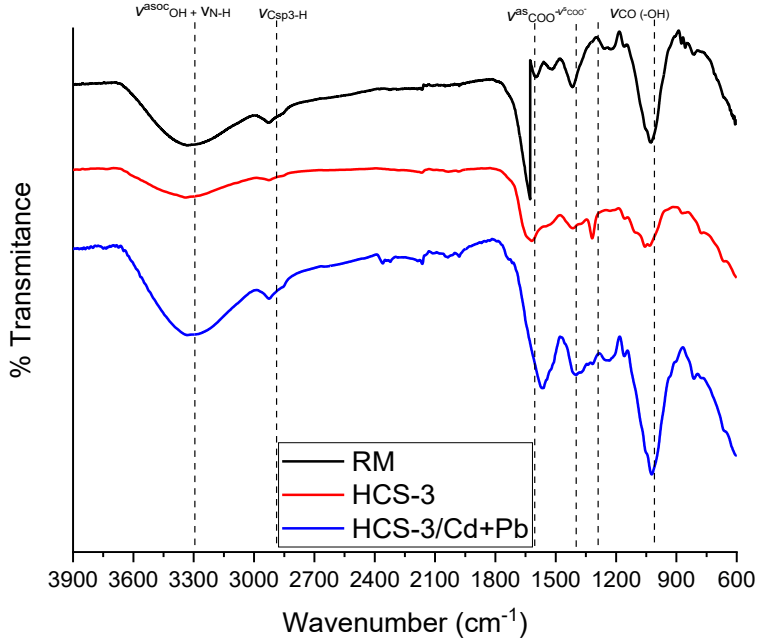

Figure 10. Infrared spectrum of the RM, HCS-3 and HCS-3 saturated with Cd(II) and Pb(II)

In addition to the carboxylic, lactonic and phenolic groups quantified, and the groups detected by FTIR spectroscopy, it was possible to identify other functional groups on the surface of the material by XPS analysis. The functional groups detected are shown in Figure 11. It is possible to notice that most of the groups detected by this technique contain nitrogen atoms, which corresponds to the basic character of the material as shown in Table 9.

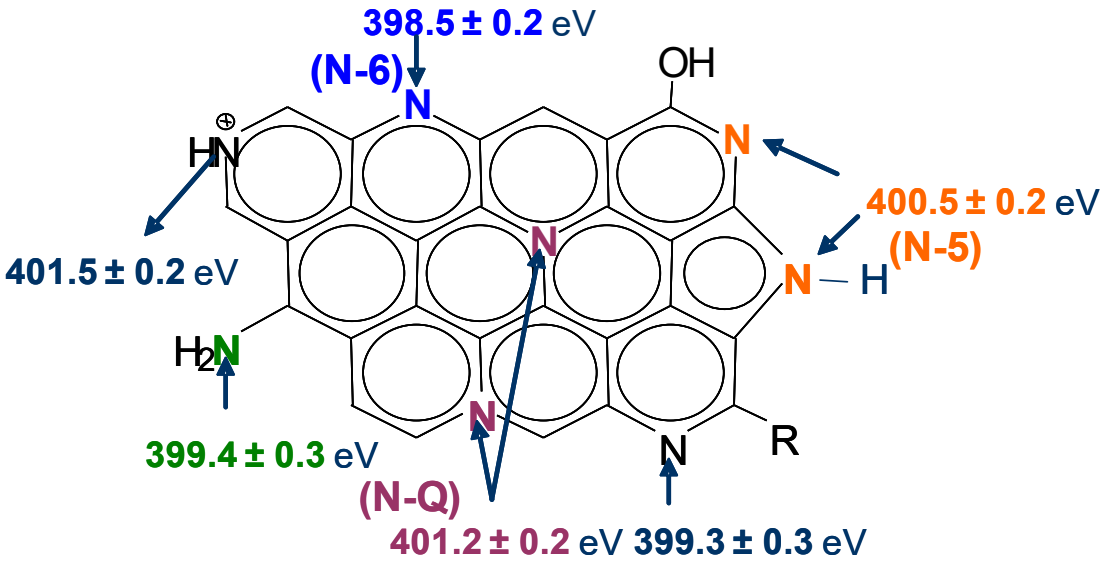

Figure 11. Functional groups in the surface of HCS3 detected by XPS

The groups detected play a crucial function in removing Cd(II) and Pb(II) (S. Yu et al., 2022). This removal predominantly happens through mechanisms that involve electrostatic attractions and the formation of chemical bonds between the adsorbate and the adsorbent (Aguirre-Contreras et al., 2023). Furthermore, upon comparing all the spectra, a distinct behaviour is observed around 1650 cm^{-1} and 1000 cm^{-1}, which appears less wide and more intense in the RM but changes in the HCS-3 material and then again in the saturated hydrochar. These changes in these bands are associated with the interactions of the functional groups with the metallic species that restrict or enhance the vibrations observed in the spectrum (Naseem et al., 2023). This observation confirms the presence of this contaminants in the adsorbent.

In Figure 12 a), b) and c), SEM micrographs of the HCS-3 hydrochar are depicted at various magnification levels that reveal the extensive structural and morphological diversity on the material's external surface. EDS spectra indicate peaks attributed to carbon, oxygen, and calcium. Among these, calcium actively participates in the ion exchange mechanism during biosorption, occupying biomass binding sites and thereby impeding access to other metals (González-Fernández et al., 2023a; Naja and Volesky, 2011).

Figure 12 c) illustrates that the material particles possess fractured and rough surfaces, with highly irregular shapes and sizes. The presence of cavities and channels is evident. Analogous findings were documented for algal species by Piña Leyte-Vidal et al., 2019 (Piña Leyte-Vidal et al., 2019).

These authors outlined the irregularity and fragmentation of a similar material, accompanied by the emergence of canals.

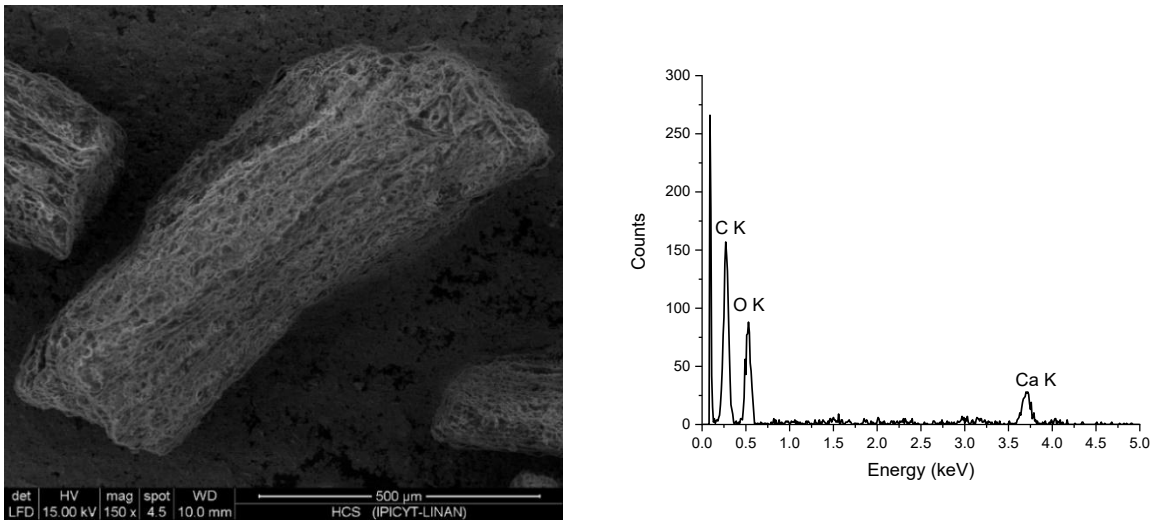

a)

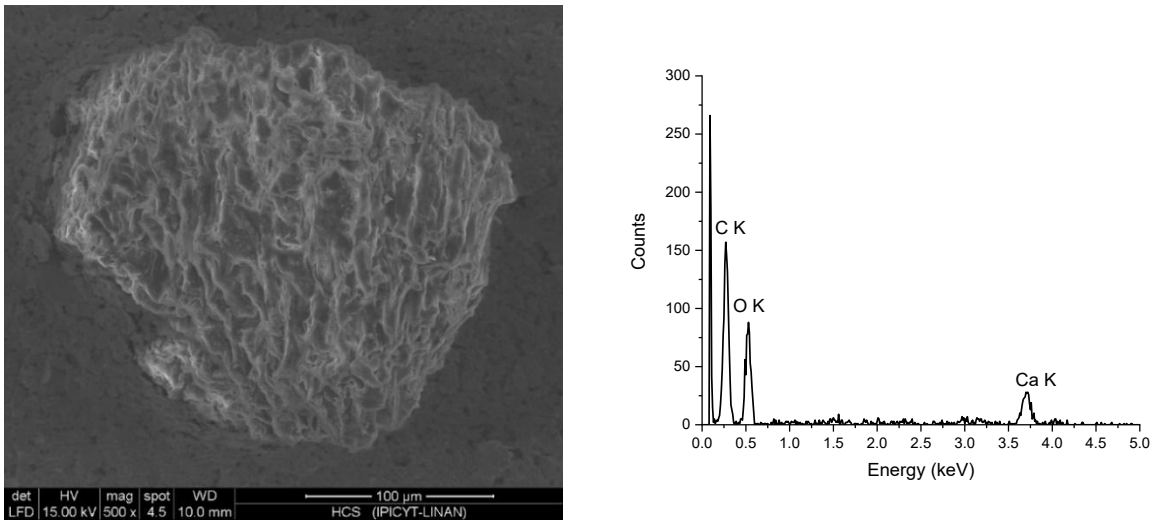

b)

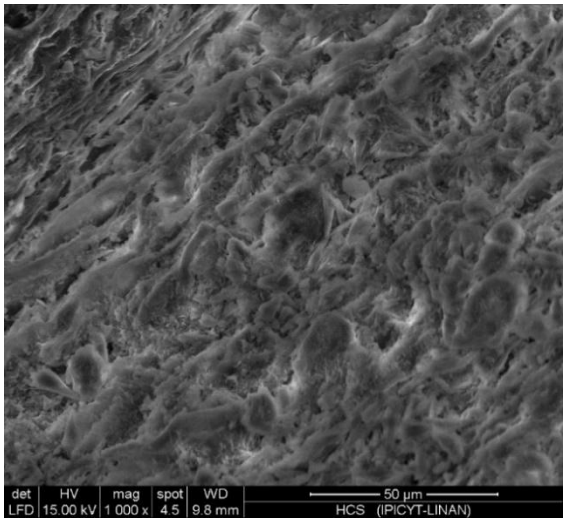
det HV mag spot WD
LFD 15.00 kV 1 000 x 4.5 9.8 mm
50 µm
HCS (IPICYT-LINAN)

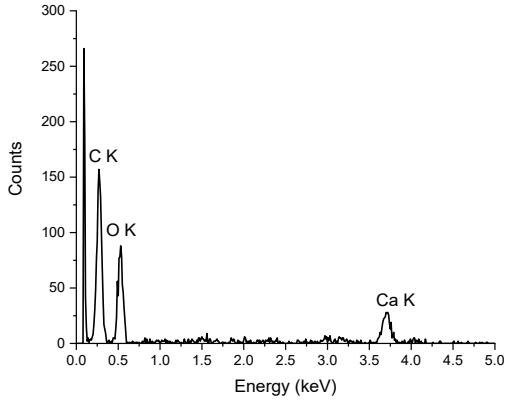
Counts
Energy (keV)
C K
O K
Ca K
300
250
200
150
100
50
0
0.0
0.5
1.0
1.5
2.0
2.5
3.0
3.5
4.0
4.5
5.0

c)

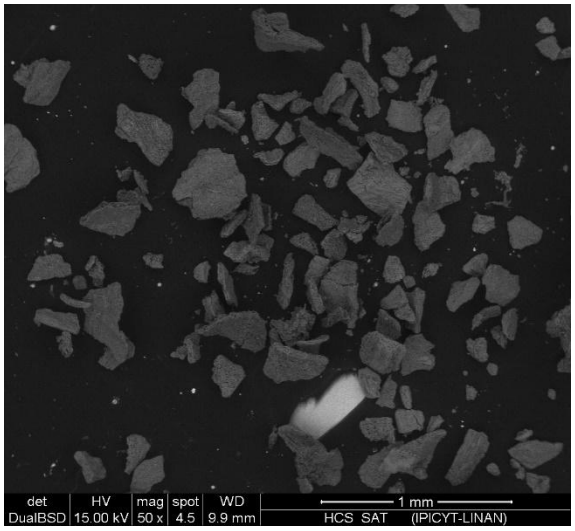
det HV mag spot WD
DualBSD 15.00 kV 50 x 4.5 9.9 mm
1 mm
HCS SAT (IPICYT-LINAN)

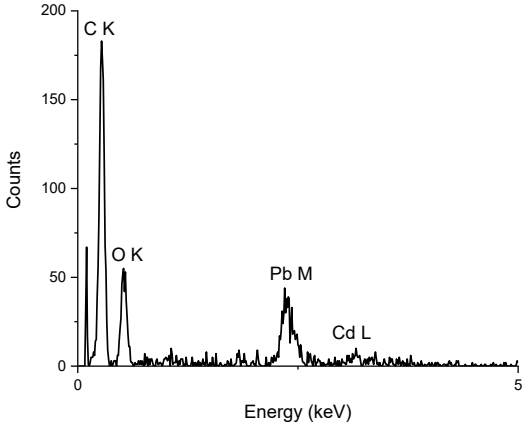
Counts
Energy (keV)
C K
O K
Pb M
Cd L
200
150
100
50
0
0
5

d)

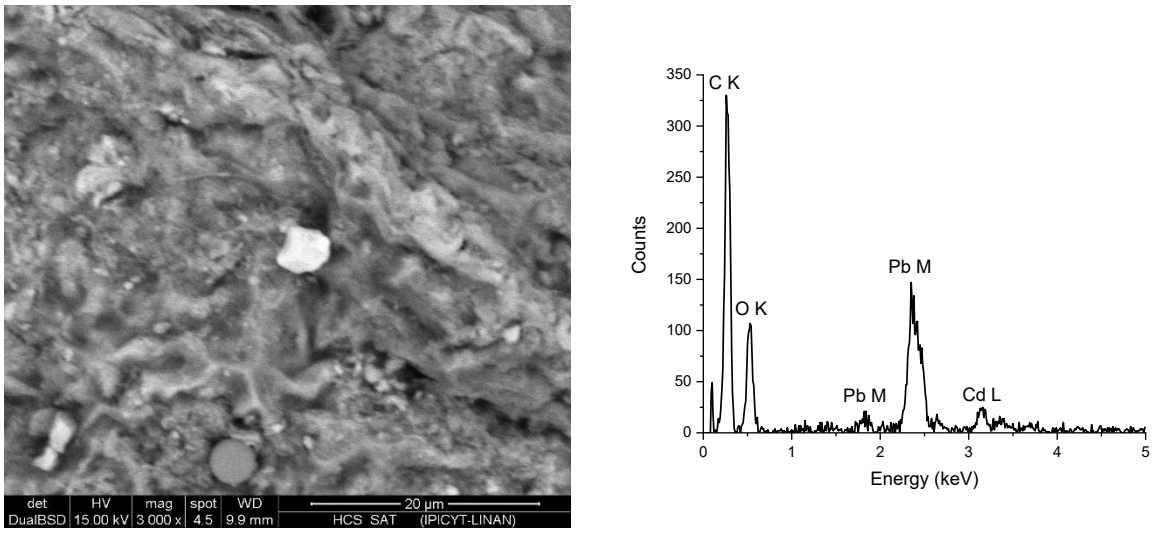

e)

Figure 12. SEM secondary electron micrographs and EDS spectra of HCS-3 at: (a) 150×, (b) 500×, and (c) 1000×; and backscattered electron images and EDS spectra of HCS-3 saturated with Cd(II) and Pb(II) at: (d) 50× and (e) 3000×.

Figure 12 d) and e) show the images of backscattered electrons with different shades (the darker ones corresponding to C and the lighter ones to heavier atoms). These microphotographs and the EDS spectra confirm the existence of the elements cadmium and lead on the material surface post-adsorption, validating that these contaminants have indeed adhered to the material during the adsorption process.

By means of XPS analysis it was possible to detect the Cd and Pb species generated during the adsorption process, which are shown in Table 10. As can be seen, in all cases, these are species in which the metal cations are attached to O- or -COO present on the surface of the adsorbent.

Table 10. Species generated during the adsorption process of Cd(II) and/or Pb(II) using HCS-3 as adsorbent in mono and multimetallic systems

Species	Assignation (eV)	Ref.
$CdCO_3$	405.1	(Chastain and King Jr, 1992)
$Cd(OH)_2$	405.1	(Hammond et al., 1975a)
$Pb_3(OH)_2(CO_3)_2$	138.4	(Pederson, 1982)
$Pb(OH)_2$	138.4	(Nefedov et al., 1980)

The removal of Cd(II) and Pb(II) contaminants by HCS-3 hydrochar reveals crucial insights into the adsorption mechanisms. Electrostatic attractions and chemical bond formations between the

adsorbate and adsorbent are identified as predominant removal pathways according to the previous discussion. Infrared spectra analysis indicates distinct changes attributed to functional group interactions with metallic species, affirming successful contaminant immobilization. EDS spectra confirm the presence of the metals in the adsorbent, aiding ion exchange mechanisms. Backscattered electron images validate contaminant adherence post-adsorption, while XPS analysis detects Cd(II) and Pb(II) species bound to surface oxygen or carboxyl groups, revealing that the main adsorption mechanism controlling the contaminant´s adsorption is chemisorption as previously reported by González-Fernández et al., 2023b; Hammond et al., 1975b; Ho and McKay, 1998 and Martínez-Meraz et al., 2023b (González-Fernández et al., 2023b; Hammond et al., 1975b; Ho and McKay, 1998; Martínez-Meraz et al., 2023b).

4. Conclusions

The physicochemical analysis of hydrochars derived from Sargassum biomass collected along the Mexican Caribbean coast indicates that the morphology and chemical composition of these materials are favourable to the incorporation of metal ions such as Cd(II) and Pb(II).

Among the synthesized materials, the one produced at 180°C with a 2-hour residence time (HCS-3) exhibited the highest yield, specific area, carbon content, and capacity for removing cadmium and lead. Consequently, HCS-3 was chosen for adsorption experiments in both mono and multicomponent systems.

The adsorption equilibrium study revealed the occurrence of adsorption mechanisms during the removal of lead and cadmium on the HCS-3 material. The adsorption capacities for cadmium and lead ions slightly exceed 140 mg g^{-1} and 340 mg g^{-1}, respectively, which are superior to the capacities formerly reported for other similar adsorbents.

In the presence of both chemical elements simultaneously, HCS-3 exhibits a greater attraction for lead cations than for cadmium. Consequently, lead demonstrates a strong antagonism in the adsorption of cadmium, while the latter has no significant influence on the lead adsorption within the studied concentration range.

Surface functional groups, pore structure development, and the interaction between a hydrochar adsorbent and heavy metals are critical factors in understanding and optimizing the adsorption process. Surface functional groups present on the hydrochar adsorbent, such as hydroxyl, carboxyl,

and amine groups, play a crucial role in attracting and binding heavy metal ions due to their varied chemical properties. These functional groups can form complexation reactions with heavy metal ions, facilitating their removal through adsorption .

Furthermore, the pore structure of the hydrochar adsorbent is paramount for efficient heavy metal adsorption. Pores act as pathways for the diffusion of metal ions into the adsorbent material. The size distribution and structure of pores influence the accessibility of metal ions to the adsorbent surface, with larger pores allowing for greater penetration and smaller pores providing enhanced surface area for adsorption. By controlling pore characteristics, the adsorption capacity and kinetics of the material can be optimized.

The interaction between the hydrochar adsorbent and heavy metals involves intricate mechanisms such as ion exchange, surface complexation, and chemisorption, all at the same time, being chemisorption the one governing the adsorption equilibrium in our study. Heavy metal ions are attracted to the adsorbent surface through electrostatic forces or chemical bonding. The adsorption process may entail ion exchange between the adsorbent surface and the metal ions in solution, leading to the immobilization of heavy metals on the adsorbent surface.

The findings indicate that hydrochars derived from Sargassum biomass offer a highly effective solution for removing heavy metal elements like Pb(II) and Cd(II) when compared to traditional or newer adsorbents. These materials possess favourable composition and physical-chemical properties, making them promising candidates for adsorption. Their use could help mitigate the current economic and environmental impact of Sargassum biomass, which is currently considered waste, by repurposing it to valuable applications.

While traditional adsorbents like activated carbon require complex activation processes that involve high temperatures and chemical treatments, hydrochars can be prepared through hydrothermal carbonization of biomass at moderate temperatures and pressures, offering a simpler and more environmentally friendly synthesis route. That is why hydrochars present an attractive option due to their renewable and sustainable nature. The use of biomass-derived feedstocks not only reduces reliance on fossil resources but also contributes to carbon sequestration by converting organic waste into stable carbonaceous materials. Furthermore, hydrochars can be regenerated and reused multiple times, reducing overall waste generation and environmental footprint.

Acknowledgements

The authors thank CONAHCyT (CVU 1014829) for funding this research. This work forms part of a doctoral thesis in Chemistry at the University of Granada (Spain) and the Autonomous University of San Luis Potosi (Mexico).

References

Afolabi, O.O.D., Sohail, M., Cheng, Y.L., 2020. Optimisation and characterisation of hydrochar production from spent coffee grounds by hydrothermal carbonisation. Renew Energy 147, 1380–1391. https://doi.org/10.1016/j.renene.2019.09.098

Aguirre-Contreras, S., Leyva-Ramos, R., Ocampo-Pérez, R., Aguilar-Madera, C.G., Flores-Cano, J. V., Medellín-Castillo, N.A., 2023. Mathematical modeling of breakthrough curves for 8-hydroxyquinoline removal from fundamental equilibrium and adsorption rate studies. Journal of Water Process Engineering 54, 103967. https://doi.org/10.1016/j.jwpe.2023.103967

Akhter, F., Khan, W., Jamali, A.R., 2024. Efficient Lead (II) Adsorption onto Mesoporous Silica Aerogels Synthesized via Green Method, Organic Solvents, and Modified Aging. Physical Chemistry Research 12, 1–9.

Alkherraz, A.M., Ali, A.K., Elsherif, K.M., 2020. Removal of Pb (II), Zn (II), Cu (II) and Cd (II) from aqueous solutions by adsorption onto olive branches activated carbon: Equilibrium and thermodynamic studies. Journal of Chemistry International 6, 11–20.

Ansari, T.M., Shaheen, S., Manzoor, S., Naz, S., Hanif, M.A., 2020. Litchi chinensis peel biomass as green adsorbent for cadmium (Cd) ions removal from aqueous solutions. Desalination Water Treat 173, 343–350.

Ayati, A., Tanhaei, B., Beiki, H., Krivoshapkin, P., Krivoshapkina, E., Tracey, C., 2023. Insight into the adsorptive removal of ibuprofen using porous carbonaceous materials: A review. Chemosphere 323, 138241. https://doi.org/10.1016/j.chemosphere.2023.138241

Azaare, L., Commeh, M.K., Smith, A.M., Kemausuor, F., 2021. Co-hydrothermal carbonization of pineapple and watermelon peels: Effects of process parameters on hydrochar yield and energy content. Bioresour Technol Rep 15, 100720.

Boehm, H.P., 1994. Some aspects of the surface chemistry of carbon blacks and other carbons. Carbon N Y 32, 759–769. https://doi.org/10.1016/0008-6223(94)90031-0

Casco, M.E., Moreno, V., Duarte, M., Sapag, K., Cuña, A., 2023. Valorization of Primary Sludge and Biosludge from the Pulp Mill Industry in Uruguay Through Hydrothermal Carbonization. Waste Biomass Valorization 14, 3893–3907. https://doi.org/10.1007/s12649-023-02105-8

Cavali, M., Junior, N.L., de Sena, J.D., Woiciechowski, A.L., Soccol, C.R., Belli Filho, P., Bayard, R., Benbelkacem, H., de Castilhos Junior, A.B., 2023. A review on hydrothermal carbonization of potential biomass wastes, characterization and environmental applications of hydrochar, and biorefinery perspectives of the process. Science of The Total Environment 857, 159627.

Çelebi, H., Gök, G., Gök, O., 2020. Adsorption capability of brewed tea waste in waters containing toxic lead (II), cadmium (II), nickel (II), and zinc (II) heavy metal ions. Sci Rep 10, 17570.

Chastain, J., King Jr, R.C., 1992. Handbook of X-ray photoelectron spectroscopy. Perkin-Elmer Corporation 40, 221.

Crist, R.H., Oberholser, K., Schwartz, D., Marzoff, J., Ryder, D., Crist, D.L.R., 1988. Interactions of Metals and Protons with Algae. Environ Sci Technol 22, 755–760. https://doi.org/10.1021/es00172a002

El Atouani, S., Belattmania, Z., Reani, A., Tahiri, S., Aarfane, A., Bentiss, F., Jama, C., Zrid, R., Sabour, B., 2019. Brown Seaweed Sargassum muticum as Low-Cost Biosorbent of Methylene Blue. Int J Environ Res 13, 131–142. https://doi.org/10.1007/s41742-018-0161-4

El Ouadrhiri, F., Elyemni, M., Lahkimi, A., Lhassani, A., Chaouch, M., Taleb, M., 2021. Mesoporous carbon from optimized date stone hydrochar by catalytic hydrothermal carbonization using response surface methodology: application to dyes adsorption. International Journal of Chemical Engineering 2021, 1–16.

Fan, X., Wang, X., Cai, Y., Xie, H., Han, S., Hao, C., 2022. Functionalized cotton charcoal/chitosan biomass-based hydrogel for capturing Pb2+, Cu2+ and MB. J Hazard Mater 423, 127191.

Fang, J., Zhan, L., Ok, Y.S., Gao, B., 2018. Minireview of potential applications of hydrochar derived from hydrothermal carbonization of biomass. Journal of Industrial and Engineering Chemistry 57, 15–21. https://doi.org/10.1016/j.jiec.2017.08.026

Gong, Y., Xie, L., Chen, C., Liu, J., Antonietti, M., Wang, Y., 2023. Bottom-up hydrothermal carbonization for the precise engineering of carbon materials. Prog Mater Sci 132, 101048.

González-Fernández, L.A., Medellín-Castillo, N.A., Ocampo-Pérez, R., Hernández-Mendoza, H., Berber-Mendoza, M.S., Aldama-Aguilera, C., 2021. Equilibrium and kinetic modelling of triclosan adsorption on Single-Walled Carbon Nanotubes. J Environ Chem Eng 9, 106382. https://doi.org/10.1016/j.jece.2021.106382

González-Fernández, L.A., Navarro Frómeta, A.E., Carranza Álvarez, C., Flores Ramírez, R., Díaz Flores, P.E., Castillo Ramos, V., Sánchez Polo, M., Carrasco Marín, F., Medellín Castillo, N.A., 2023a. Valorization of Sargassum Biomass as Potential Material for the Remediation of Heavy-Metals-Contaminated Waters. Int J Environ Res Public Health 20, 2559. https://doi.org/10.3390/ijerph20032559

González-Fernández, L.A., Navarro Frómeta, A.E., Carranza Álvarez, C., Flores Ramírez, R., Díaz Flores, P.E., Castillo Ramos, V., Sánchez Polo, M., Carrasco Marín, F., Medellín Castillo, N.A., 2023b. Valorization of Sargassum Biomass as Potential Material for the Remediation of Heavy-Metals-Contaminated Waters. Int J Environ Res Public Health 20, 2559. https://doi.org/10.3390/ijerph20032559

Güleç, F., Riesco, L.M.G., Williams, O., Kostas, E.T., Samson, A., Lester, E., 2021. Hydrothermal conversion of different lignocellulosic biomass feedstocks–Effect of the process conditions on hydrochar structures. Fuel 302, 121166.

Hammond, J.S., Gaarenstroom, S.W., Winograd, N., 1975a. X-ray photoelectron spectroscopic studies of cadmium-and silver-oxygen surfaces. Anal Chem 47, 2193–2199.

Hammond, J.S., Gaarenstroom, S.W., Winograd, N., 1975b. X-ray photoelectron spectroscopic studies of cadmium-and silver-oxygen surfaces. Anal Chem 47, 2193–2199.

Hannachi, Y., Hafidh, A., 2020. Biosorption potential of Sargassum muticum algal biomass for methylene blue and lead removal from aqueous medium. International Journal of Environmental Science and Technology 17, 3875–3890. https://doi.org/10.1007/s13762-020-02742-9

Ho, Y.S., McKay, G., 1998. A Comparison of chemisorption kinetic models applied to pollutant removal on various sorbents. Process Safety and Environmental Protection 76, 332–340. https://doi.org/10.1205/095758298529696

Hopkins, D., Hawboldt, K., 2020. Biochar for the removal of metals from solution: A review of lignocellulosic and novel marine feedstocks. J Environ Chem Eng 8, 103975.

Ilić, M., Haegel, F.H., Lolić, A., Nedić, Z., Tosti, T., Ignjatović, I.S., Linden, A., Jablonowski, N.D., Hartmann, H., 2022. Surface functional groups and degree of carbonization of selected chars from different processes and feedstock. PLoS One 17, e0277365. https://doi.org/10.1371/journal.pone.0277365

Kaleem, M., Minhas, L.A., Hashmi, M.Z., Ali, M.A., Mahmoud, R.M., Saqib, S., Nazish, M., Zaman, W., Samad Mumtaz, A., 2023. Biosorption of Cadmium and Lead by Dry Biomass of Nostoc sp. MK-11: Kinetic and Isotherm Study. Molecules 28, 2292. https://doi.org/10.3390/molecules28052292

Kushwaha, A., Rani, R., Patra, J.K., 2020. Adsorption kinetics and molecular interactions of lead [Pb (II)] with natural clay and humic acid. International Journal of Environmental Science and Technology 17, 1325–1336.

Lee, J., Hong, J., Jang, D., Park, K.Y., 2019. Hydrothermal carbonization of waste from leather processing and feasibility of produced hydrochar as an alternative solid fuel. J Environ Manage 247, 115–120. https://doi.org/10.1016/j.jenvman.2019.06.067

León, C., 2019. Sargassum enters the scene. Salud Publica Mex 61, 701–703. https://doi.org/10.21149/10870

Lima, H.H.C., Maniezzo, R.S., Llop, M.E.G., Kupfer, V.L., Arroyo, P.A., Guilherme, M.R., Rubira, A.F., Girotto, E.M., Rinaldi, A.W., 2019. Synthesis and characterization of pecan nutshell-based adsorbent with high specific area and high methylene blue adsorption capacity. J Mol Liq 276, 570–576. https://doi.org/10.1016/j.molliq.2018.12.010

Liu, H., Basar, I.A., Nzihou, A., Eskicioglu, C., 2021. Hydrochar derived from municipal sludge through hydrothermal processing: A critical review on its formation, characterization, and valorization. Water Res 199, 117186.

Lucaci, A.-R., Bulgariu, L., 2024. Biosorption of Technologically Valuable Metal Ions on Algae Wastes: Laboratory Studies and Applicability. Water (Basel) 16, 512.

Ma, M., Ying, H., Cao, F., Wang, Q., Ai, N., 2020. Adsorption of congo red on mesoporous activated carbon prepared by CO2 physical activation. Chin J Chem Eng 28, 1069–1076. https://doi.org/10.1016/j.cjche.2020.01.016

Magdziarz, A., Wilk, M., Wądrzyk, M., 2020. Pyrolysis of hydrochar derived from biomass–Experimental investigation. Fuel 267, 117246.

Martínez-Meraz, C., González-Fernández, L.A., Medellín Castillo, N.A., Leyva Ramos, R., Hernández de la Rosa, L.G., Loredo Martinez, G.K., Cruz Briano, S.A., Cisneros Ontiveros, H.G., Flores Rojas, A.I., Vilasó Cadre, J.E., 2023a. Hydrochar from Sargassum biomass for water remediation: Insights from synthesis and ibuprofen removal. MRS Adv 1–7. https://doi.org/10.1557/s43580-023-00702-2

Martínez-Meraz, C., González-Fernández, L.A., Medellín Castillo, N.A., Leyva Ramos, R., Hernández de la Rosa, L.G., Loredo Martinez, G.K., Cruz Briano, S.A., Cisneros Ontiveros, H.G., Flores Rojas, A.I., Vilasó Cadre, J.E., 2023b. Hydrochar from Sargassum biomass for water remediation: Insights from synthesis and ibuprofen removal. MRS Adv 1–7. https://doi.org/10.1557/s43580-023-00702-2

Medellin-Castillo, N.A., Padilla-Ortega, E., Regules-Martínez, M.C., Leyva-Ramos, R., Ocampo-Pérez, R., Carranza-Alvarez, C., 2017. Single and competitive adsorption of Cd(II) and Pb(II) ions from aqueous solutions onto industrial chili seeds (Capsicum annuum) waste. Sustainable Environment Research 27, 61–69. https://doi.org/10.1016/j.serj.2017.01.004

Morin-Crini, N., Lichtfouse, E., Liu, G., Balaram, V., Ribeiro, A.R.L., Lu, Z., Stock, F., Carmona, E., Teixeira, M.R., Picos-Corrales, L.A., Moreno-Piraján, J.C., Giraldo, L., Li, C., Pandey, A., Hocquet, D., Torri, G., Crini, G., 2022. Worldwide cases of water pollution by emerging contaminants: a review. Environ Chem Lett 20, 2311–2338. https://doi.org/10.1007/s10311-022-01447-4

Naja, G., Volesky, B., 2011. The mechanism of metal cation and anion biosorption, in: Microbial Biosorption of Metals. Springer, pp. 19–58. https://doi.org/10.1007/978-94-007-0443-5_3

Naseem, K., Imran, Q., Ur Rehman, M.Z., Tahir, M.H., Najeeb, J., 2023. Adsorptive removal of heavy metals and dyes from wastewater using Azadirachta indica biomass. International Journal of Environmental Science and Technology 20, 5799–5822.

Nefedov, V.I., Salyn, Y. V, Solozhenkin, P.M., Pulatov, G.Y., 1980. X-ray photoelectron study of surface compounds formed during flotation of minerals. Surface and Interface analysis 2, 170–172.

Nwagbara, V.U., Chigayo, K., Iyama, W.A., Kwaambwa, H.M., 2022. Removal of lead, cadmium, and copper from water using Moringa oleifera seed biomass. Journal of Water and Climate Change 13, 2747–2760.

Parra-Marfíl, A., Ocampo-Pérez, R., Collins-Martínez, V.H., Flores-Vélez, L.M., Gonzalez-Garcia, R., Medellín-Castillo, N.A., Labrada-Delgado, G.J., 2020. Synthesis and characterization of hydrochar from industrial Capsicum annuum seeds and its application for the adsorptive removal of methylene blue from water. Environ Res 184, 109334. https://doi.org/10.1016/j.envres.2020.109334

Pauletto, P.S., Moreno-Pérez, J., Hernández-Hernández, L.E., Bonilla-Petriciolet, A., Dotto, G.L., Salau, N.P.G., 2021. Novel biochar and hydrochar for the adsorption of 2-nitrophenol from aqueous solutions: An approach using the PVSDM model. Chemosphere 269, 126170. https://doi.org/10.1016/j.chemosphere.2020.128748

Pederson, L.R., 1982. Two-dimensional chemical-state plot for lead using XPS. J Electron Spectros Relat Phenomena 28, 203–209.

Periyavaram, S.R., Bella, K., Uppala, L., Reddy, P.H.P., 2023. Hydrothermal carbonization of food waste: Process parameters optimization and biomethane potential evaluation of process water. J Environ Manage 347, 119132.

Phuthongkhao, P., Phasin, K., Boonma, P., Khunphonoi, R., Kanchanatip, E., Suwannaruang, T., Shivaraju, H.P., Wantala, K., 2023. Preparation and characterization of hydrothermally processed carbonaceous hydrochar from pulp and paper sludge waste. Biomass Convers Biorefin 1–18. https://doi.org/10.1007/s13399-023-03761-5

Pimentel-Almeida, W., Itokazu, A.G., Bazani, H.A.G., Maraschin, M., Rodrigues, O.H.C., Corrêa, R.G., Lopes, S., Almerindo, G.I., Moresco, R., 2023. Beach-cast Sargassum cymosum macroalgae: biochar production and apply to adsorption of Acetaminophen in batch and fixed-bed adsorption processes. Environmental Technology (United Kingdom) 44, 974–987. https://doi.org/10.1080/09593330.2021.1989058

Piña Leyte-Vidal, J.J., González-Fernández, L.A., Gutiérrez-Artiles, O., Márquez-Llauger, L., Del Cristo, T.A., 2019. Caracterización de tres bioindicadores de contaminación por metales pesados. Revista Cubana de Química 31, 293–308.

Pyrzynska, K., 2019. Removal of cadmium from wastewaters with low-cost adsorbents. J Environ Chem Eng 7, 102795. https://doi.org/10.1016/j.jece.2018.11.040

Raninga, M., Mudgal, A., Patel, V.K., Patel, J., Sinha, M.K., 2023. Modification of activated carbon-based adsorbent for removal of industrial dyes and heavy metals: A review. Mater Today Proc 77, 286–294.

Román, S., Ledesma, B., Álvarez, A., Coronella, C., Qaramaleki, S. V., 2020. Suitability of hydrothermal carbonization to convert water hyacinth to added-value products. Renew Energy 146, 1649–1658. https://doi.org/10.1016/j.renene.2019.07.157

Rosado-Espinosa, L.A., Freile-Pelegrín, Y., Hernández-Nuñez, E., Robledo, D., 2020. A comparative study of Sargassum species from the Yucatan Peninsula coast: morphological and chemical characterisation. Phycologia 59, 261–271. https://doi.org/10.1080/00318884.2020.1738194

Saha, N., Saba, A., Reza, M.T., 2019. Effect of hydrothermal carbonization temperature on pH, dissociation constants, and acidic functional groups on hydrochar from cellulose and wood. J Anal Appl Pyrolysis 137, 138–145. https://doi.org/10.1016/j.jaap.2018.11.018

Samimi, M., 2024. Efficient biosorption of cadmium by Eucalyptus globulus fruit biomass using process parameters optimization. Global Journal of Environmental Science and Management 10, 27–38.

Sharma, A., Anjana, Rana, H., Goswami, S., 2022. A comprehensive review on the heavy metal removal for water remediation by the application of lignocellulosic biomass-derived nanocellulose. J Polym Environ 30, 1–18.

Sivaranjanee, R., Kumar, P.S., 2023. Enhanced Adsorption of Rose Bengal Dye from Aqueous Solution Using NaOH Activated Hydrochar Derived from Corncob Waste. Adsorption Science and Technology 2023. https://doi.org/10.1155/2023/6695350

Soroush, S., Ronsse, F., Verberckmoes, A., Verpoort, F., Park, J., Wu, D., Heynderickx, P.M., 2022. Production of solid hydrochar from waste seaweed by hydrothermal carbonization: effect of

process variables. Biomass Convers Biorefin 14, 183–197. https://doi.org/10.1007/s13399-022-02365-9

Supee, A.H., Zaini, M.A.A., 2024. Hydrothermal carbonization of biomass: a commentary. Fullerenes, Nanotubes and Carbon Nanostructures 32, 119–127.

Takaya, C.A., Parmar, K.R., Fletcher, L.A., Ross, A.B., 2019. Biomass-derived carbonaceous adsorbents for trapping ammonia. Agriculture (Switzerland) 9, 16. https://doi.org/10.3390/agriculture9010016

Tarbaoui, M., Oumam, M., Fourmentin, S., Benzina, M., Bennamara, A., Abourriche, A., 2016. Development of A New Biosorbent Based on The Extract Residue of Marine Alga Sargassum Vulgare : Application in Biosorption of Volatile Organic Compounds. World Journal of Innovative Research 1, 5.

Tee, G.T., Gok, X.Y., Yong, W.F., 2022. Adsorption of pollutants in wastewater via biosorbents, nanoparticles and magnetic biosorbents: A review. Environ Res 212, 113248. https://doi.org/10.1016/j.envres.2022.113248

Tran, H.N., Bollinger, J.-C., Salvestrini, S., Chu, K.H., Juang, R.-S., 2023. Critical Review and Discussion of the Nonlinear Form of Radke–Prausnitz Model in Adsorption Solid–Liquid Phases. Journal of Environmental Engineering 149, 3122006. https://doi.org/10.1061/joeedu.eeeng-7074

Vardhan, K.H., Kumar, P.S., Panda, R.C., 2019. A review on heavy metal pollution, toxicity and remedial measures: Current trends and future perspectives. J Mol Liq 290, 111197. https://doi.org/10.1016/j.molliq.2019.111197

Velarde, L., Nabavi, M.S., Escalera, E., Antti, M.-L., Akhtar, F., 2023. Adsorption of heavy metals on natural zeolites: A review. Chemosphere 138508.

Velarde, L., Nikjoo, D., Escalera, E., Akhtar, F., 2024. Bolivian natural zeolite as a low-cost adsorbent for the adsorption of cadmium: Isotherms and kinetics. Heliyon 10.

Verma, S., Kuila, A., 2019. Bioremediation of heavy metals by microbial process. Environ Technol Innov 14, 100369. https://doi.org/10.1016/j.eti.2019.100369

Wang, B., Lan, J., Bo, C., Gong, B., Ou, J., 2023. Adsorption of heavy metal onto biomass-derived activated carbon. RSC Adv 13, 4275–4302.

Wang, T., Zheng, J., Liu, H., Peng, Q., Zhou, H., Zhang, X., 2021. Adsorption characteristics and mechanisms of Pb 2+ and Cd 2+ by a new agricultural waste–Caragana korshinskii biomass derived biochar. Environmental Science and Pollution Research 28, 13800–13818.

Wang, W., Chen, W.-H., Jang, M.-F., 2020. Characterization of hydrochar produced by hydrothermal carbonization of organic sludge. Future Cities and Environment 6, 13.

Wu, S., Wang, Q., Fang, M., Wu, D., Cui, D., Pan, S., Bai, J., Xu, F., Wang, Z., 2023. Hydrothermal carbonization of food waste for sustainable biofuel production: Advancements, challenges, and future prospects. Science of The Total Environment 165327.

Yu, G., Li, P., Wang, G., Wang, J., Zhang, Y., Wang, S., Yang, K., Du, C., Chen, H., 2021. A review on the removal of heavy metals and metalloids by constructed wetlands: bibliometric, removal pathways, and key factors. World J Microbiol Biotechnol 37, 1–12. https://doi.org/10.1007/s11274-021-03123-1

Yu, G., Wang, G., Chi, T., Du, C., Wang, J., Li, P., Zhang, Y., Wang, S., Yang, K., Long, Y., Chen, H., 2022. Enhanced removal of heavy metals and metalloids by constructed wetlands: A review of approaches and mechanisms. Science of the Total Environment 821, 153516. https://doi.org/10.1016/j.scitotenv.2022.153516

Yu, S., Yang, X., Zhao, P., Li, Q., Zhou, H., Zhang, Y., 2022. From biomass to hydrochar: Evolution on elemental composition, morphology, and chemical structure. Journal of the Energy Institute 101, 194–200. https://doi.org/10.1016/j.joei.2022.01.013

Zhang, X., Gao, Z., Fan, X., Tan, L., Jiang, Y., Zheng, W., Han, F.X., Liang, Y., 2022. A comparative study on adsorption of cadmium and lead by hydrochars and biochars derived from rice husk and Zizania latifolia straw. Environmental Science and Pollution Research 29, 63768–63781.

Zhao, H., Ouyang, X.-K., Yang, L.-Y., 2021. Adsorption of lead ions from aqueous solutions by porous cellulose nanofiber–sodium alginate hydrogel beads. J Mol Liq 324, 115122.

Paper 7: Mathematical modelling of kinetic and breakthrough curves for Cd(II) adsorption onto Sargassum biomass using the Diffusion – Permeation Model

Journal: Journal of Water Process Engineering

Impact Factor (JCR): 6.7

Quartile: Q1

Volume: 77

ISSN (electronic): 2214-7144

https://doi.org/10.1016/j.jwpe.2025.108473

https://www.sciencedirect.com/science/article/pii/S2214714425015466

Mathematical modelling of kinetic and breakthrough curves for Cd(II) adsorption onto Sargassum biomass using the Diffusion – Permeation Model

Lázaro Adrián González-Fernández[1,2]; Samuel Aguirre-Contreras[3]; Nahum Andrés Medellín-Castillo[1,4*]; Manuel Sánchez-Polo[2]; Amado Enrique Navarro-Frómeta[5]; Javier E. Vilasó-Cadre[6]; Raúl Ocampo-Pérez[3]*

[1] Multidisciplinary Postgraduate Program in Environmental Sciences, Av. Manuel Nava 201, 2nd. Floor, University Zone, San Luis Potosí 78000, Mexico.

[2] Faculty of Sciences, University of Granada, 18071 Granada, Spain.

[3] Faculty of Chemical Sciences, Autonomous University of San Luis Potosi, Av. Dr. Manuel Nava No.6, Zona Universitaria, 78210, San Luis Potosi, SLP, Mexico

[4] Center for Research and Postgraduate Studies, Faculty of Engineering, Autonomous University of San Luis Potosi, Dr. Manuel Nava No. 8, West University Zone, San Luis Potosí 78290, Mexico.

[5] Food and Environmental Technology Department, Technological University of Izucar de Matamoros, De Reforma 168, Campestre La Paz, Izúcar de Matamoros, 74420, Mexico.

[6] Institute of Metallurgy, Autonomous University of San Luis Potosí, Sierra Leona Av. 550, Lomas 2nd Section, 78210 San Luis Potosí, Mexico.

Correspondence to: nahum.medellin@uaslp.mx and lazaroadrian@correo.ugr.es

Abstract

Access to clean drinking water remains a pressing global challenge, particularly due to the persistent contamination of water bodies by heavy metals such as Cd(II). Conventional water treatment methods, including chemical precipitation and ion exchange often present limitations such as high operational costs and inefficient removal of low-concentration pollutants. In parallel, the excessive proliferation of Sargassum biomass (SB) has emerged as an environmental crisis, causing severe ecological and economic disruptions in coastal regions. Despite being largely regarded as an ecological nuisance, Sargassum exhibits valuable physicochemical properties that make it a promising material for water treatment. However, existing kinetic models, such as the pseudo-first-order (PFO) and pseudo-second-order (PSO) models, fail to accurately describe the adsorption of Cd(II) onto low-porosity biomasses like SB, as they neglect key transport mechanisms (intraparticle diffusion and permeation). This study explores the adsorption of Cd(II) onto SB using the Diffusion-Permeation Model (DPM) to enhance the predictive accuracy of adsorption kinetics. Furthermore, the kinetic model is integrated with the Axial Dispersion Model (ADM) to better describe breakthrough curves in packed-bed adsorption systems. The results demonstrate that the PFO and PSO models provide inadequate fits for adsorption kinetics, whereas the DPM effectively captures the underlying transport mechanisms (R^2 above 99%). Similarly, the ADM-DPM framework provides an improved mathematical description of the breakthrough

curves, accurately predicting the breakthrough point with an average deviation of 5.3% These findings establish the applicability of the proposed modelling approach for metal adsorption onto SB and highlight its potential for optimizing scalable water treatment solutions.

Keywords: Biosorption; Sargassum biomass; Cadmium removal; Diffusion – Permeation Model; Breakthrough curves.

1. Introduction

Access to clean drinking water remains one of the most critical challenges of the 21st century. The rapid industrialization and urbanization of modern societies have led to the increased discharge of pollutants into aquatic ecosystems, severely compromising water quality (Upton and Macdonald, 2021). Heavy metals, in particular, represent a significant environmental and public health threat due to their persistence, non-biodegradability, and high toxicity even at trace concentrations. Contaminants such as cadmium (Cd^{2+}), lead (Pb^{2+}), and mercury (Hg^{2+}) are known to cause severe health issues, including renal failure, neurological disorders, and carcinogenic effects (Zaynab et al., 2022). Conventional water treatment technologies such as chemical precipitation, ion exchange, reverse osmosis, and electrocoagulation have been extensively used to remove these pollutants; however, these methods often suffer from high operational costs, inefficiencies in treating low-concentration pollutants, and the generation of secondary waste streams. Consequently, there is an urgent need to develop cost-effective, sustainable, and efficient water treatment strategies that can address the limitations of existing technologies while ensuring the long-term protection of water resources (Saravanan et al., 2024).

Simultaneously, the excessive proliferation of Sargassum biomass (SB) in marine ecosystems has emerged as an environmental and economic crisis, particularly in regions such as the Caribbean and the Gulf of Mexico (Robledo et al., 2021). Massive influxes of Sargassum have disrupted marine biodiversity, threatened coastal tourism industries, and imposed substantial costs on governments and local communities due to removal and disposal challenges. Climate change, along with the increased influx of nutrients from agricultural runoff and wastewater discharges, has been identified as a key driver of Sargassum overgrowth, exacerbating the problem year after year (Oxenford et al., 2021). Despite being largely viewed as an ecological nuisance, Sargassum biomass possesses valuable physicochemical properties that make it a promising material for various applications, including biofuel production, fertilizer development, and pollutant

adsorption. The high content of functional groups such as carboxyl, hydroxyl, and sulfonate groups in Sargassum enables it to interact effectively with metal ions, making it a viable candidate for water purification through biosorption (Rekha et al., 2023).

The use of Sargassum as an adsorbent has been widely explored in both batch and continuous adsorption systems (do Nascimento Júnior et al., 2024). Batch adsorption studies have historically served as the primary method for evaluating adsorption capacity, equilibrium isotherms, and kinetic behaviours. These experiments provide fundamental insights into the interaction mechanisms between adsorbates and adsorbents, allowing for the estimation of adsorption parameters through widely used mathematical models. However, batch systems do not accurately replicate the conditions encountered in practical water treatment applications, as they fail to account for the continuous flow dynamics present in industrial-scale processes (Adegoke et al., 2022). For this reason, fixed-bed column adsorption studies have gained increasing attention, as they offer a more realistic representation of adsorption performance under dynamic conditions. The analysis of breakthrough curves in these systems is essential for optimizing operational parameters, assessing adsorbent performance over time, and designing large-scale adsorption units for real-world applications.

Kinetic modelling is crucial for understanding the mechanisms governing adsorption processes. The pseudo-first-order and pseudo-second-order models are among the most commonly employed approaches for describing adsorption kinetics (Ezzati et al., 2024). The pseudo-first-order model, based on the Lagergren equation, assumes that the adsorption rate is proportional to the difference between the equilibrium concentration and the current concentration of the adsorbate (Revellame et al., 2020). The pseudo-second-order model, on the other hand, is derived from the assumption that adsorption follows a second-order reaction mechanism, where the adsorption rate depends on the square of the number of available adsorption sites (Ezzati, 2023). While these models have been extensively used to describe the kinetics of various adsorption systems, they exhibit significant limitations when applied to low-porosity biomasses such as Sargassum (Leyva-Ramos et al., 2021). Specifically, these models do not incorporate the effects of intraparticle diffusion and permeation, which are critical transport mechanisms influencing the overall adsorption process. As a result, their predictive accuracy is often compromised, leading to discrepancies between experimental and theoretical adsorption behaviours.

Similarly, traditional models for breakthrough curve analysis, including the Thomas, Yoon-Nelson, and Bohart-Adams models, have been widely used to describe adsorption dynamics in fixed-bed column systems (Omitola et al., 2022). These models provide valuable insights into the overall adsorption process but are based on simplified assumptions that neglect key transport phenomena such as internal diffusion and permeation. The Thomas model, for instance, assumes that adsorption follows Langmuir-type behaviour, and that no significant axial dispersion occurs within the column (Patel, 2021). The Yoon-Nelson model, which is often employed due to its simplicity, assumes that the probability of adsorbate breakthrough is solely a function of residence time, without considering diffusion resistance within the adsorbent particles (Chu and Hashim, 2024). The Bohart-Adams model, one of the earliest developed breakthrough models, assumes that adsorption is controlled by surface reaction kinetics and does not account for mass transfer limitations (Hu et al., 2021). Due to these inherent limitations, traditional breakthrough models may not accurately capture the adsorption dynamics of heavy metals onto Sargassum, leading to suboptimal design and performance predictions.

To address these challenges, a novel modelling approach incorporating diffusion-permeation effects into adsorption kinetics has been recently proposed by Leyva-Ramos et al., 2021 (Leyva-Ramos et al., 2021). This method represents a significant advancement in adsorption modelling by explicitly considering transport limitations that are particularly relevant for low-porosity biomasses. By integrating diffusion-permeation effects into adsorption equations, this approach provides a more comprehensive understanding of adsorption kinetics and improves the accuracy of predictive models. However, despite its potential, this methodology has not yet been applied to the adsorption of heavy metals onto Sargassum biomass. Moreover, no previous studies have attempted to integrate this kinetic model into mathematical frameworks for breakthrough curve analysis, leaving a critical gap in the literature.

This study aims to bridge this knowledge gap by conducting a mathematical analysis of the equilibrium and kinetics of Cd(II) adsorption onto Sargassum biomass using the diffusion-permeation model (DPM). Furthermore, we seek to couple this kinetic model with the axial dispersion model (ADM) to enhance the accuracy of breakthrough curve predictions. By demonstrating the applicability of this combined approach, we aim to establish a more reliable and robust framework for modelling biosorption processes in continuous-flow systems. This research represents the first attempt to integrate the DPM with ADM for the description of metal adsorption

onto Sargassum, highlighting the novelty and significance of our work. The findings of this study not only contribute to the fundamental understanding of adsorption mechanisms in biosorption systems but also provide valuable insights for the development of scalable and efficient water treatment technologies based on Sargassum-derived adsorbents.

Overall, this study underscores the potential of Sargassum biomass as an effective and sustainable adsorbent for heavy metal removal, while simultaneously addressing a pressing environmental issue associated with its uncontrolled proliferation. By improving the mathematical modelling of adsorption kinetics and breakthrough curves, this research paves the way for the practical implementation of Sargassum-based biosorption technologies in real-world water treatment applications. The integration of advanced modelling approaches will not only enhance the predictive capabilities of adsorption systems but also facilitate the design and optimization of fixed-bed adsorption units for large-scale implementation, ensuring greater efficiency and sustainability in water purification efforts.

2. Materials and Methods

2.1 Adsorbate and chemicals

All chemicals used were analytical grade at least. Cadmium nitrate tetrahydrate ($Cd(NO_3)_2 \cdot 4H_2O$), NaOH and HCl were supplied by Sigma-Aldrich. A stock solution of Cd(II) ions with a concentration of 1000 ppm was prepared by weighing the appropriate amount of cadmium nitrate tetrahydrate and dissolving it in distilled water until the desired volume was reached. From this primary solution, secondary solutions of desired concentration were prepared for adsorption experiments and kinetic studies. In all cases, the pH was adjusted to the desired value and, when necessary, the temperature of the solution was also adjusted.

2.2 Adsorbent

SB collected from the Mexican Caribbean region was thoroughly rinsed with seawater and air-dried for 72 h. The dried samples were then stored under controlled humidity conditions in polyethylene bags, protected from light exposure. Prior to subsequent analysis, the algae samples were rigorously cleansed with distilled water to eliminate salts and residual solid impurities. The cleaned samples were oven-dried at 120 °C for 36 h and subsequently ground using an electric mill. The resulting material was sieved using vibrating sieves with mesh sizes ranging from 30 to 50 μm.

2.3 Adsorbent characterization

For the adsorbent characterization, the samples were pre-dried at 120 °C for 48 h before being directly mounted onto the sample holders. To determine the specific surface and associated parameters of the SB, a sample tube was sealed with a rubber stopper and positioned on a degassing port of the Micromeritics Model ASAP 2420 Analyzer. The tube was connected to the port and heated using a heating basket set to 110 °C. The physisorption analysis involved measuring the volume of nitrogen adsorbed at varying pressures under standard conditions of temperature and pressure (274.15 K and 1 atm). Data collected every 5 seconds, including volumes and pressures, was utilized to calculate the adsorbent's specific surface area and pore size distribution. Scanning electron microscopy (SEM) was employed to capture images revealing the particle size and surface morphology of the SB. A Thermo Fisher Quanta 250 FEG microscope was used, employing secondary electrons to obtain the images.

The thickness ($2T$), width (W), and length (L) of the SB particles were measured using the micrographs of 30 particles. Based on these average dimensions, the longitudinal or external area per unit mass (S_{Ext}), lateral area (S_{Lat}), and particle volume (V_P) were determined using the following equations (1) – (3):

$$S_{Ext} = \frac{2LW}{\rho_p V_P} \tag{1}$$

$$S_{Lat} = \frac{2(L+W)2T}{\rho_p V_P} \tag{2}$$

$$V_P = LW2T \tag{3}$$

2.4 Adsorption rate and equilibrium data

The adsorption kinetics was investigated using a rotating basket adsorber, whose configuration and mechanical specifications have been previously described in the literature (Aguirre-Contreras et al., 2023). A measured quantity of the SB was placed within the baskets, and the agitation speed was maintained at 200 rpm. Subsequently, 1 L of Cd(II) solution, preconditioned to the target temperature and pH, was introduced into the adsorber. Upon contact between the solution and the adsorbent, the adsorption process was initiated, with time measurement commencing immediately.

To maintain the solution's pH within the desired range, incremental additions of 0.01 N NaOH or HCl were employed as necessary. Sampling was performed at regular intervals by extracting 1 mL

aliquots of the solution until equilibrium was achieved. The amount of Cd(II) adsorbed at specific time intervals was determined using the mass balance equation (4):

$$q(t) = \frac{V_0 C_{A0} - \left(V_0 - \sum_i^{i(t)} \quad V_i + V_D(t)\right) C_A(t) - \sum_i^{i(t)} \quad V_i C_{Ai}}{m} \tag{4}$$

Furthermore, the equilibrium adsorption capacity for each kinetic experiment was determined by applying a mass balance at the point where the solution concentration stabilized and exhibited negligible variation over time. The calculation was performed using the following equation (5):

$$q_e = \frac{V_0 C_{A0} - (V_0 - \sum_i^n \quad V_i + V_D) C_{Ae} - \sum_i^N \quad V_i C_{Ai}}{m} \tag{5}$$

Using this methodology, the effect of initial Cd(II) concentration on adsorption was investigated, while other parameters, including temperature (25 ºC), adsorbent mass (1.0 g), and agitation speed (200 rpm), were kept constant. Experiments were conducted with initial Cd(II) concentrations ranging from 50 to 800 mg/L.

2.5 Breakthrough curves

The packed bed system illustrated in Fig. S1 was utilized to determine the BC of Cd(II) on SB. The system included a feed vessel for the solution, a stirring mechanism to maintain homogeneity, a pump for delivering the solution to the column, an acrylic column packed with SB and glass beads, and a container for collecting the effluent, along with various ancillary accessories.

Dynamic adsorption experiments followed a standardized protocol previously reported by Aguirre-Contreras et al., 2023 (Aguirre-Contreras et al., 2023). The column was packed with an initial layer of glass beads to prevent clogging and promote uniform fluid distribution. A measured quantity of SB was then added, followed by a final layer of glass beads. The packed bed was preconditioned by flushing with deionized water for 36 h to remove any trapped air and to avoid any preferential pathway (Lv et al., 2022).

After preconditioning, a solution of Cd(II) with a specified initial concentration and volumetric flow rate was introduced into the column. The adsorption process was initiated upon contact of the solution with the SB particles, and a chronometer was activated to track the experiment's progression. Effluent samples were periodically collected and analysed in a VARIAN SPECTRAA 220 Atomic Adsorption Spectrometer until the effluent concentration matched the initial feed

concentration. This methodology facilitated the analysis of the effects of bed height (h), initial Cd(II) concentration (C_o), and volumetric flow (Q) on the adsorption process.

2.6 Mathematical modelling of equilibrium, adsorption kinetics, and packed bed adsorption dynamics

2.6.1 Cadmium adsorption equilibrium

The equilibrium data was analysed using the Langmuir (6), Freundlich (7), and Radke-Prausnitz (8) isotherms, as described by the following equations:

$$q_e = \frac{q_m K_L C_e}{1 + K_L C_e} \tag{6}$$

$$q_e = K_F C_e^{1/n} \tag{7}$$

$$q_e = \frac{a C_e}{1 + b C_a^{\beta}} \tag{8}$$

The isotherm model constants were determined using a nonlinear fitting algorithm implemented in STATISTICA® software (version 10). The objective function for parameter optimization is expressed in Eq. (6). Parameter optimization was performed using the Rosenbrock and quasi-Newton methods which have been widely used in the literature (Mitrevski et al., 2022). The deviation percentage (%Dev) and coefficient of determination (R^2) for each isotherm was calculated based on Eq. (9) and (10) respectively.

$$\%Dev = \frac{1}{N}\sum_{i}^{N} \left| \frac{q_{exp} - q_{cal}}{q_{exp}} \right| \cdot 100 \tag{9}$$

$$R^2(\%) = 1 - \frac{\sum_i^N (q_{e\,exp} - q_{e\,cal})^2}{\sum_i^N (q_{e\,exp} - \underline{q_{e\,cal}})^2} \tag{10}$$

2.6.2 Pseudo-first and second kinetic modelling

In kinetic models, the overall biosorption rate of a pollutant is determined solely by the rate of its interaction with sorption sites on the biosorbent material. As a result, both intraparticle diffusion and external mass transfer processes are assumed to be rapid enough to disregard. Furthermore, the biosorption rate at active sites can be described analogously to a chemical reaction rate. The pseudo-first order (PFO) kinetic model and the pseud-second order (PSO) model (Revellame et

al., 2020) are among the most widely used kinetic models. These models have been shown to effectively describe the biosorption rate of dyes, anions, cations, pharmaceuticals and contaminants of emerging concern onto biomasses from various sources (Bello et al., 2020; Samimi and Mansouri, 2024; Tavana et al., 2020). Their mathematical formulations can be found elsewhere (Ezzati et al., 2024).

2.6.3 Diffusion-permeation modelling

SB is a complex biomaterial primarily composed of alginate, fucoidan, cellulose, and hemicellulose, with a structure consisting of various distinct cell types and polymers chains (Davis et al., 2003). Water and solute transport within SB occur through both the cell walls and the void spaces, which correspond to the hollow interiors of the cells, also known as lumens. Diffusion, as described by Fick's law, can take place within the solution present in these voids, while mass transfer through the cell walls occurs via permeation. Due to this structural complexity, the mass transfer flux in SB is proposed to be represented by a DPM (Leyva-Ramos et al., 2021), with the mass flux expressed as in Eq. (11):

$$N_{Az} = -DP_M \rho_p \frac{dq}{dz} \tag{11}$$

The following assumptions were considered for the formulation of the DPM equations (12)-(16): the SB particles were modelled as rectangular parallelepipeds; mass transfer predominantly occurred through the longitudinal surface area, with negligible transfer through the lateral area; external mass transport was characterized by a mass transfer coefficient; intraparticle diffusion was attributed to permeation-diffusion; and the biosorption process was assumed to occur instantaneously at active sites.

$$V \frac{dC_A}{dt} = -mS_{Ext} k_L (C_A - C_{Az}|_{z=T}); \; t = 0; \; C_A = C_{A0} \tag{12}$$

$$\frac{\partial q}{\partial t} = \frac{\partial}{\partial z}\left(DP_M \frac{\partial q}{\partial z}\right); \; t = 0; \; C_{Az} = 0; 0 \leq z \geq T \tag{13}$$

$$-DP_M \rho_p \frac{\partial q}{\partial z}|_{z=0} = 0 \tag{14}$$

$$DP_M \rho_p \frac{\partial q}{\partial z}|_{z=T} = k_L (C_A - C_{Az}|_{z=T}) \tag{15}$$

$$q = f(C_{Az}) \tag{16}$$

Eq. (12) demonstrates that the accumulation of Cd(II) in the solution corresponds to the external mass transport along with the initial conditions constraints. Additionally, Eq. (13) indicates that the accumulation of Cd(II) within the particle is governed by intraparticle transport resulting from the diffusion-permeation of the ion, along with its initial restrictions. Eq. (14)–(15), on the other hand, describe the standard initial and boundary conditions typically associated with diffusional models (Leyva-Ramos and Geankoplis, 1994). The adsorption isotherm establishes the relationship between q_e and C_{Az}, assuming the biosorption rate occurs instantaneously (16).

2.6.4 Mathematical modelling of the BCs

A mathematical model was proposed by considering two phases in the packed bed: the liquid phase and the SB (adsorbate). It accounts for axial dispersion within the column, external mass transfer, and intraparticle diffusion in the adsorbent. The following assumptions were made: the SB particles are spherical and uniform (size and density); the column works always at the same temperature (isothermal conditions); radial velocity is absent; axial velocity remains constant in the whole column; radial concentration gradients of the solute in the liquid phase are insignificant; the axial dispersion coefficient is constant; and the convective transport of solute to the particle surface is described by the mass transfer coefficient. Based on these considerations, the ADM for the liquid phase is expressed through the following equations (17)-(20):

$$\varepsilon_b \frac{C_A}{\partial t} = -\varepsilon_b v_z \frac{\partial C_A}{\partial z} + \varepsilon_b D_Z \frac{\partial^2 C_A}{\partial z^2} - (1-\varepsilon_b)\rho_p S k_{Lb}(C_A - C_{Ar}|_{r=Rp}) \tag{17}$$

$$t = 0;\ \forall_z; C_A = 0 \tag{18}$$

$$t \geq 0; z = 0;\ C_A = C_{A0} \tag{19}$$

$$t \geq 0; z = L_b;\ \frac{\partial C_A}{\partial z} = 0 \tag{20}$$

To estimate the concentration at $r = Rp, (C_A - C_{Ar}|_{r=Rp})$ in Equation (17), modelling diffusion-permeation transport is essential. This was achieved by integrating the DPM equations (12) – (16) with the ADM model (17) – (20). In Equation (12), $k_L$was replaced with k_{Lb}, as k_{Lb} represents the mass transfer coefficient in the liquid phase of a packed bed adsorber.

Equations (12) – (16) and (17) – (20) define the ADM-DP model, which incorporates axial dispersion in the liquid phase, diffusion and permeation of the solvent in the adsorbate, and adsorption at active sites. To solve the ADM-DPM system, it is necessary to account for both the adsorption equilibrium relationship and diffusion-permeation parameters, which are experimentally determined in kinetic study as reported by Leyva-Ramos et al., 2021 (Leyva-Ramos et al., 2021) and Aguirre-Contreras et al., 2023 (Aguirre-Contreras et al., 2023). The axial dispersion coefficient and convective mass transport coefficient were computed with the Eq. (21)-(27). The ADM-DP was solved numerically using COMSOL Multiphysics® (version 3.5).

$$Sh = 1.09\varepsilon_b{}^{-2/3} Re^{1/3} Sc^{1/3} \tag{21}$$

$$\frac{1}{Pe} = \frac{20}{\varepsilon_b}\frac{1}{Re \cdot Sc} + \frac{1}{2} \tag{22}$$

$$D_z = \frac{2R_P v_z}{Pe} \tag{23}$$

$$Re = \frac{2R_P v_z \rho_w}{\mu_w} \tag{24}$$

$$Sc = \frac{\mu_w}{\rho_w D_{AB}} \tag{25}$$

$$k_{Lb} = \frac{Sh\ D_{AB}}{2R_P} \tag{26}$$

$$v_z = \frac{Q}{\pi R_b^2 \varepsilon_b} \tag{27}$$

3. Results and discussions

3.1 Morphological and textural characterisation

Table 1 summarises the physicochemical characterisation of SB. The experimental parameters include a surface area of 0.20 m²/g, a pore volume of 0.002 cm³/g, an average pore size of 18.5 nm, and a particle density of 1.46 g/cm³. These results are comparable to those reported for SB and other algae and similar materials (Atugoda et al., 2021; Chaouay et al., 2024; Do Nascimento et al., 2021; Tavana et al., 2020; Thamarai et al., 2024) and supported that the SB is effectively a non-porous material. The density of the particle (ρ_p) was treated as equivalent to ρ_s since the pore volume of SB was reasonably low. Additionally, the thickness (2T) of 0.1296 mm, the width (W) of 0.0324 mm, and the length (L) of 0.0891 mm were calculated followed the methodology

described in Section 2.3 for micrographs images like shown in Fig. S2. These results provide essential data for understanding the material's structural properties, which are critical for evaluating its suitability in adsorption and mass transfer applications.

Table 1. Physicochemical characterisation of the SB.

Parameter	Area (m^2/g)	Pore volume (cm^3/g)	Pore size average (nm)	ρ_s (g/cm^3)	2T (mm)	W (mm)	L (mm)
SB	0.20	0.002	18.5	1.46	0.0043	0.0108	0.0297

The external and lateral surface, and the volume of each particle were calculated from the prior average dimensions and employing equations (1) – (3). The geometric parameters have values of $s_{Ext} = 317.10\ cm^2/g$, $s_{Lat} = 172.98\ cm^2/g$ and $V_P = 1.39 \cdot 10^{-6}\ cm^3$. Notably s_{Ext} is approximately 2 times greater than s_{Lat}. Consequently, mass transfer primarily occurs through the external area, corresponding to previous reports by Leyva-Ramos et al., 2021 (Leyva-Ramos et al., 2021).

3.2 Adsorption equilibrium data

The relationship between the mass of Cd(II) absorbed at equilibrium and the ion concentration is shown in Fig. 1. As can be seen, the isotherm shows L2-type behaviour according to the classification of Giles et al., 1974 (Giles et al., 1974). This type of isotherms is common in systems where the adsorbate is a metal ion that can accumulate in mono and multilayers on the adsorbent and is consistent with those reported by Abdelwaheb et al., 222; Karoke & Jadhao, 2021 and Pessôa et al., 2024 (Abdelwaheb et al., 2022; Korake and Jadhao, 2021; Pessôa et al., 2024).

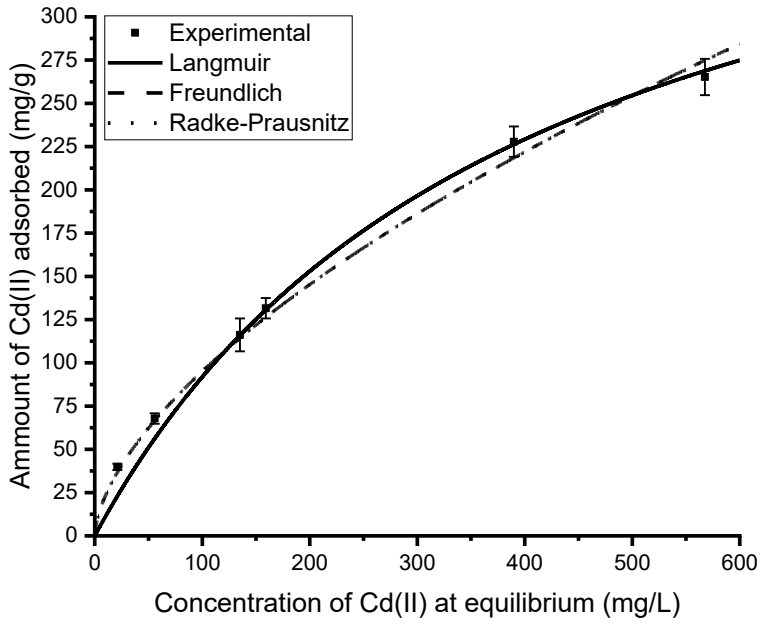

Figure 1. Adsorption behaviour of Cd(II) onto SB in a concentration range between 50 and 800 mg/L at T = 25ºC. Lines represents the isotherm mathematical models.

Fig. 1 depicts two distinct phases in the isotherms. During the initial phase, the adsorption capacity increases rapidly as the equilibrium metal concentration rises. This behaviour is attributed to the abundance of active sites available for cation retention at the outset (Naja and Volesky, 2011). However, as the pollutant concentration continues to grow, these active sites gradually become occupied, making cation exchange more difficult. In the second phase, a noticeable decrease in the slope occurs, signifying saturation, at which point the maximum experimental adsorption capacity is reached.

The experimental adsorption equilibrium data were modelled using isotherm models widely described in the literature such as Langmuir, Freundlich and Radke-Prausnitz (Eq. 6 – 8). The results of these fits are shown in Table S1. As can be seen, all models show a good fit to describe the experimental reality, with correlation coefficients above 95 % in all cases, however the Langmuir mathematical model shows the best fit as well as the lowest $\%Dev$. In practical terms, this suggests that the adsorbent has a homogeneous surface with specific sites that are systematically filled until saturation is reached. This also implies that the behaviour of the system is closer to these ideal conditions than other models, such as the Freundlich model (which considers

heterogeneity in the adsorption sites) (Rajahmundry et al., 2021). It is important to emphasise that the isotherm model will later be applied to solve the ADM and ADM-DP formulations. Therefore, selecting the most suitable isotherm model with the lowest $\%Dev$ and the highest R^2 is essential. Consequently, the Langmuir isotherm model was chosen for the mathematical modelling.

The maximum adsorption capacity achieved experimentally is 265.3 ± 10.5 mg/g, exceeding the values reported by other researchers for lignocellulosic materials (Kayranli, 2022), natural materials (Hebbani et al., 2021; Jellali et al., 2021), zeolites (Kuldeyev et al., 2023; Velarde et al., 2024), commercial activated carbons (Adamu et al., 2023; Mariah et al., 2023), and clays (Bassam et al., 2021; Zhou et al., 2020). Previous studies have highlighted that, despite their relatively low surface area and porosity, biomass wastes like SB possess numerous functional groups. These groups create an effective environment for metal species uptake from solution through mechanisms like complexation and ion exchange (Davis et al., 2003).

3.3 Adsorption kinetic modelling

3.3.1 Pseudo first and second order kinetic models

The experimental data was fitted to the kinetic equations of the models described in Section 2.6.2 to determine the constants of the PFO (q_e and k_1) and the PSO model (q_e and k_2). To identify the optimal parameters, a least-squares approach was employed, utilizing the Rosenbrock – *quasi*-Newton optimization algorithm. The resulting kinetic constants and the corresponding $\%Dev$ values are presented in Table 2. As can be seen from the correlation coefficients, the PFO and PSO model have values that suggest an average to poor adjustment to the experimental data.

Table 2. Parameters of the kinetic models used for describing the Cd(II) adsorption onto SB.

Exp.	$C_0(Cd^{2+})$ mg/L	q_{exp} mg/g	PFO model			PSO model			DP model		
			q_e mg/g	$k_1 \cdot 10^2$ $1/min$	R^2 %	q_e mg/g	$k_2 \cdot 10^4$ $L/min \cdot mg$	R^2 %	$k_L \cdot 10^3$ cm/s	$DP \cdot 10^{10}$ cm^2/s	R^2 %
1	50	39.9	39.4	5.4	78.6	42.9	10.3	91.8	1.5	3.0	99.5
2	100	67.8	64.0	3.8	76.0	73.0	5.7	89.0	4.3	2.5	99.6
3	200	96.2	96.3	2.3	72.0	108.7	5.2	81.4	1.4	3.0	99.8
4	600	217.8	207.0	2.0	17.5	225.6	3.1	34.2	1.5	7.0	99.6
5	800	275.3	253.7	1.7	24.7	278.6	2.7	36.2	1.4	7.0	99.5

When adsorption data cannot be adequately explained by the PFO and PSO, it suggests the possible influence of additional factors or limitations in the assumptions underlying these models. One significant factor could be the presence of additional adsorption mechanisms, such as intraparticle

diffusion or complex electrostatic interactions, which are not accounted for in these models (Wang and Guo, 2022). Similarly, substantial heterogeneity in the adsorbent surface, characterized by a non-uniform distribution of active sites with varying adsorption energies, may lead to discrepancies between experimental data and model predictions (Ebelegi et al., 2020). Another common limitation is the influence of slow diffusion and permeation processes whether external (through the liquid film) or internal (within the adsorbent pores), which the PFO and PSO models typically assume to be either rapid or negligible. Furthermore, interactions between adsorbate molecules, such as aggregation or site-blocking effects, can significantly alter the adsorption rates. Lastly, these models have limited capacity to describe non-linear phenomena, such as atypical initial adsorption rates or complex kinetic behaviours. In such cases, alternative models, such as the Elovich model (Musah et al., 2022), the intraparticle diffusion model (Hu et al., 2024) or the diffusion-permeation model proposed by Leyva-Ramos et al., 2021 (Leyva-Ramos et al., 2021), which incorporate more complex dynamics, may be required.

The observed trends of k_1 and k_2 as the equilibrium mass of Cd(II) adsorbed increases, shown in Fig. 2 (a and b, respectively), highlight distinct relationships between the kinetic rates and the adsorption process. For k_1, the initial decrease followed by stabilization suggests that the adsorption efficiency declines as adsorption progresses, possibly due to the saturation of readily available adsorption sites and the system approaching equilibrium conditions. In contrast, the behavior of k_2 reflects the heterogeneous nature of the adsorbent surface. The observed fluctuations may indicate that variations in site energy or structural changes of the adsorbent influence the adsorption mechanism at different stages. At later stages of the process, factors such as competition for active sites, reduced surface energy, or transport limitations (e.g., intraparticle diffusion) likely become more dominant. These trends imply a complex interplay of surface and diffusion-controlled mechanisms, rather than a purely linear adsorption behaviour. This necessitates a comprehensive evaluation of the underlying kinetic models (Hu et al., 2022).

For k_2, the initial high values at lower Cd(II) adsorption masses suggest that a greater number of adsorption sites are readily accessible, facilitating rapid interaction between the adsorbate and the adsorbent. As the adsorption mass increases, k_2 decreases significantly, indicating progressive occupation of energetically favourable sites. This leaves less favourable sites available, slowing the adsorption process. This behaviour underscores the heterogeneity of the adsorbent and the

coexistence of processes like surface interactions, intraparticle diffusion, and potential agglomeration of Cd(II) on the adsorbent surface (Revellame et al., 2020). Notably, k_1 is consistently two orders of magnitude higher than k_2, suggesting that the adsorption process is predominantly concentration-dependent and diffusion-controlled rather than governed by site-specific interactions. This implies weaker adsorbate-adsorbent interactions and a limited number of active sites on the adsorbent. The higher first-order constant reflects rapid initial adsorption at low concentrations, which is advantageous for applications like water treatment. However, the lower second-order constant indicates reduced efficiency at higher adsorption masses as equilibrium is approached. To better describe the adsorption system's dynamics, alternative kinetic models may be required if first- and second-order models fail to fully capture the process. Incorporating additional factors such as intraparticle diffusion, adsorbent heterogeneity, or complex interaction mechanisms could provide a more accurate representation of the system's behaviour.

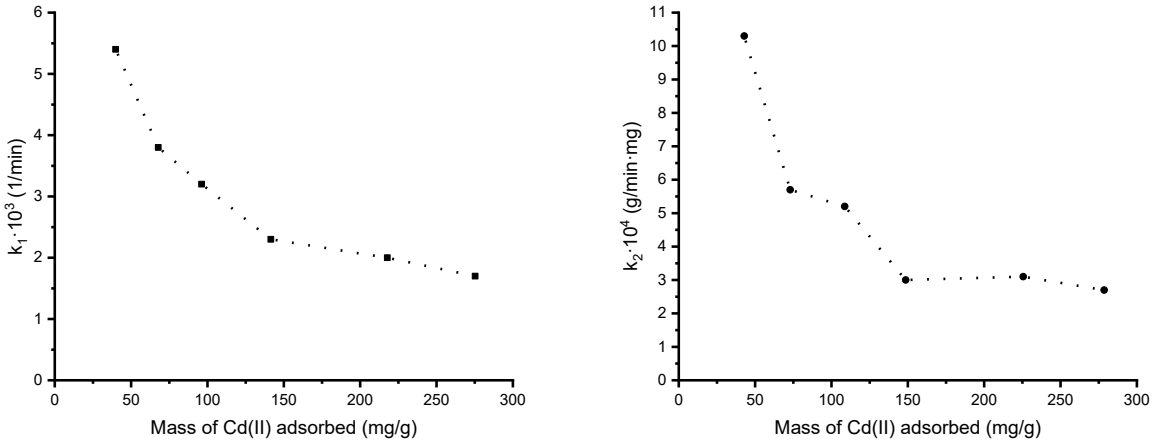

a) b)

Figure 2. Kinetic constants a) k_1 and b) k_2 trend *vs* the adsorbed mass of Cd(II).

3.3.2 Diffusion-permeation model

Aqueous Cd(II) solutions were prepared using cadmium(II) nitrate, which dissociates into Cd^{2+} and NO_3^- ions. In this specific case, the Cd(II) nitrate solutions were considered highly diluted, as Cd(II) concentrations were in the order of part per millions. The diffusivities of these ions in dilute aqueous solutions can be estimated using Eq. (28) previously described by Vanýsek, 1993

(Vanýsek, 1996) who also reported the values for λ_i^0 for mostly all of the most common ions in solution:

$$D_i^o = \frac{RT}{F^2}\lambda_i^0 \tag{28}$$

$$D_{Cd2+}^o = 1.438 \cdot 10^{-5} cm^2/s$$

Additionally, the mass transport coefficient, k_L, was calculated using the method proposed by Furusawa and Smith, 1973 (Furusawa and Smith, 1973). In summary, the boundary condition (Eq. 11) was analysed and reformulated into Eq. (29):

$$\left[\frac{d(\frac{C_A}{C_{A0}})}{dt}\right]_{t=0} = -\frac{mS_{Ext}k_L}{V} \tag{29}$$

The slope on the left-hand side of Eq. 29 was determined using the concentration decay data near $t = 0$. Table 3 presents the calculated k_L values, which range from 1.4 to 7.7 · 10^{-3} cm/s, near to those reported for a similar adsorbent (white pine sawdust) from Leyva-Ramos et al., 2021 (Leyva-Ramos et al., 2021). The DPM model, described by Eq. (12) – (16), was solved numerically using COMSOL Multiphysics software (version 5.5). The mass transfer parameters considered in the DPM model were k_L and DP. The value of k_L was determined as previously described (refer to Table 3), while DP was estimated by aligning the numerical solution of the DPM model with the experimentally observed concentration decay of Cd(II). The optimal value of DP was obtained by minimizing the objective function in Eq. (30):

$$OF(Min) = \sum_{1}^{N} \left((\frac{C_A}{C_{A0}})_{exp} - (\frac{C_A}{C_{A0}})_{predicted}\right)^2 \tag{30}$$

Table 3 provides the optimal DP values for Cd(II) in the SB, which range from 2.5 to 9.0 · 10^{-10} cm^2/s. Fig. 5 illustrate the experimental concentration decay alongside the DPM model predictions using the optimal DP values. As observed in this figure, the DPM model predictions align well with the experimental data ($R^2 \geq 99.5$ %). This indicates that the diffusion-permeation process of Cd(II) within the SB structure is an effective approach for assessing the overall adsorption rate.

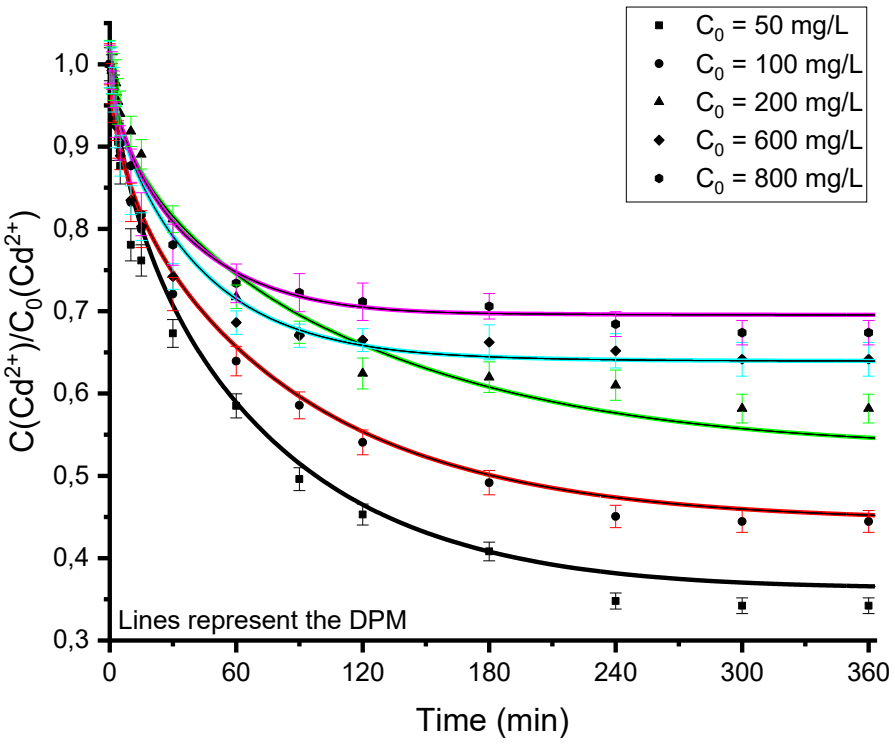

Figure 3. Cd(II) concentration decay curves.

The molecular diffusion coefficient of Cd(II) in water is $1.438 \cdot 10^{-5}$ cm^2/s, which is approximately 16000 to 57500 times greater than DP. This significant difference confirms that the diffusion of Cd(II) within the solution voids alone cannot account for the intraparticle diffusion mechanism. A review of the scientific literature published as of today indicates that the DPM model has not previously been proposed for explaining intraparticle diffusion within SB for heavy metals cations, making this study the first to introduce and apply this model in this type of systems.

Fig. 4(a) establishes the relationship between DP and the amount of Cd(II) adsorbed at equilibrium. As depicted, the DP coefficient remains practically constant for $q_{exp} < 100\ mg/g$, then increases to its maximum value that remain constant again. The DP coefficient is considered stable, as diffusion-permeation depends on the biosorbent's inherent properties and the solute chemical characteristics. The arithmetic mean of DP ($\underline{DP}$) is also shown in Fig. 4(a). Fig. 4(b) illustrates the predictions of the DPM model using $\underline{DP}$ for all experiments. The results indicate that the DPM model, utilizing $\underline{DP}$, predicted the experimental concentration decay data for Cd(II) with reasonable accuracy. The *%Dev* values varied between 2.5 and 5.5 %. Consequently, the $\underline{DP}$ coefficient can be effectively used to predict the overall Cd(II) biosorption rate on SB.

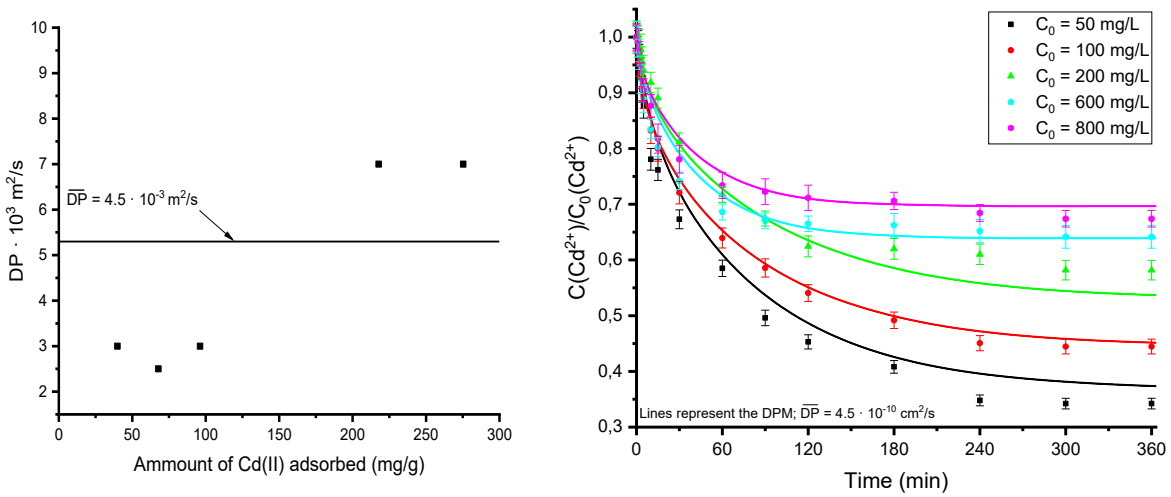

a) b)

Figure 4. a) DP coefficient trend *vs* the amount of Cd(II) adsorbed and b) Cd(II) concentration decay curves using the average DP coefficient.

Fig. 5 presents the adsorption kinetics of Cd(II) at an initial concentration of 100 mg/L, showing the normalized concentration ratio as a function of time. The experimental data demonstrate a consistent decrease in Cd(II) concentration over time as adsorption occurs. The three kinetic models described in this work are compared in this figure (DPM, PFO and PSO). Among these, the DPM shows the closest fit to the experimental data. This highlights the model's suitability for describing the adsorption process, with $DP = 5.3 \cdot 10^{-10} cm^2/s$ reflecting diffusion-limited transport within the adsorbent (Leyva-Ramos et al., 2021).

In contrast, the PFO model significantly deviates from the experimental data, especially in the later stages of the adsorption process. This deviation suggests that the PFO model oversimplifies the adsorption kinetics and fails to capture the complexity of the process. The PSO model provides a better fit compared to the PFO model but still diverges from the experimental data in certain regions. This indicates that while the PSO model accounts for some aspects of the adsorption process, it does not fully describe the underlying mechanisms. Overall, the DPM outperforms both the PFO and PSO models in capturing the adsorption kinetics, supporting its selection as the best-fitting model. The DPM's ability to account for diffusion-controlled transport and other potential mechanisms makes it a more accurate representation of the adsorption behaviour. This emphasizes the importance of considering diffusion-based mechanisms in studies involving similar adsorption

systems, particularly when adsorption kinetics are influenced by transport limitations and heterogeneity within the adsorbent.

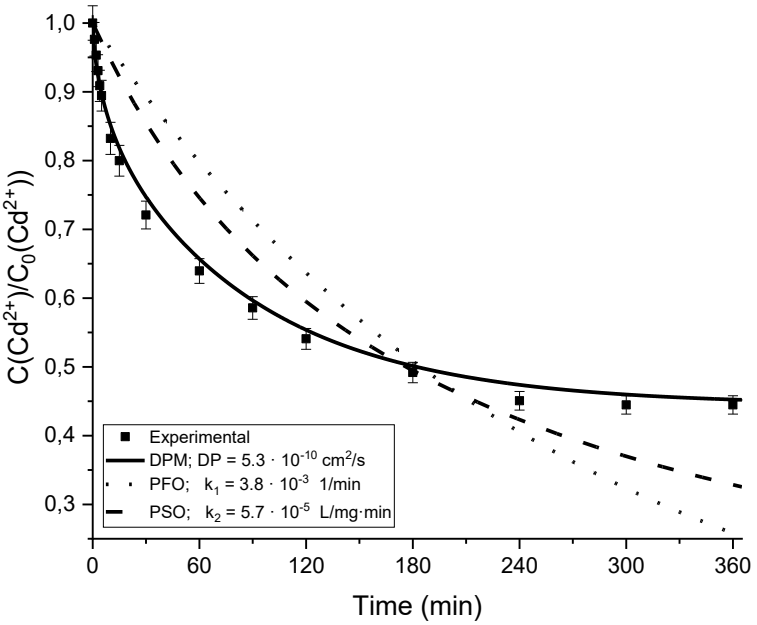

Figure 5. Adsorption kinetics of Cd(II) at an initial concentration of 100 mg/L. Lines represent the kinetic models.

3.3.3 Packed bed adsorption dynamics

The ADM can be combined with the DPM to predict the dynamic adsorption process in a packed bed system. Numerical simulations using the ADM-DP model were compared to experimental data focusing on breakthrough curves under varying conditions: feed concentration (C_0 (Cd^{2+})), packed bed height (L), and volumetric flow rate (Q). A summary of the experimental conditions is provided in Table 3 while the BC are shown in Fig. 6 (a-c). To perform these simulations. the axial fluid velocity (v_z) was calculated, and the dimensionless Reynolds (Re) and Sherwood (Sh) numbers were determined using Eq. (24) and (25), respectively. The computed Re values, presented in Table 3, confirm that the flow regime is laminar across all experiments. Key design parameters, including the breakthrough time (t_b), saturation time (t_s), and the adsorbed mass at t_b (q_b) and t_s (q_s) were estimated from the experimental data. This analysis provides valuable insights for optimizing the design and operational parameters of packed bed adsorption systems.

In general, all curves exhibited a highly symmetrical sigmoidal shape. The Fs values, which represent the symmetry of the breakthrough curves, ranged between 0.5 and 0.7, confirming this

observation. This indicates that intraparticle transport, specifically permeation-diffusion in this case, is sufficiently rapid and does not result in a flattened asymmetric breakthrough curve (Apiratikul and Chu, 2021). On the contrary, the breakthrough curves tend to be similar in extent, indicating a stable mass transfer zone (MTZ) under different operating conditions (Gutierrez-Reyna et al., 2024). This is further corroborated by the observation that the MTZ lengths remained practically constant (see Table 3), with an average of 1.9 cm. Additionally, in all cases, the MTZ was shorter than the bed height (Lb), a necessary condition to confirm that the MTZ reached a steady-state or constant pattern (Worch, 2021).

Varying the operating conditions produced the following effects. Increasing the feed flow rate enhanced the contaminant load processed by the bed within a given time, leading to an earlier breakthrough. Consequently, Fig. 6a illustrates that as the flow rate increases, the breakthrough curves shift to the left. Conversely, a lower flow rate increases the contact time, promoting better utilisation of the adsorbent material. This effect was particularly evident in Experiment 1 ($Q = 0.5\ mL/min$), which had the lowest flow rate and, correspondingly, the highest empty bed contact time (EBCT). Under these conditions, the breakthrough curve exhibited a distinct behaviour compared to the other curves, and the model prediction was only accurate up to the breakthrough point. This suggests that for EBCT values greater than 11.2 minutes, the MTZ behaviour may deviate, marking a limit to the model's validity. Therefore, caution should be exercised when extrapolating model predictions to unvalidated conditions.

Similarly, reducing the bed height produced a comparable effect. Since the amount of adsorbent mass was reduced, the operational duration of the bed under a constant feed load decreased. This was confirmed in the experiments where bed height was varied (Fig. 6b), showing that the breakthrough curves shifted leftward as bed height decreased while maintaining their sigmoidal shape.

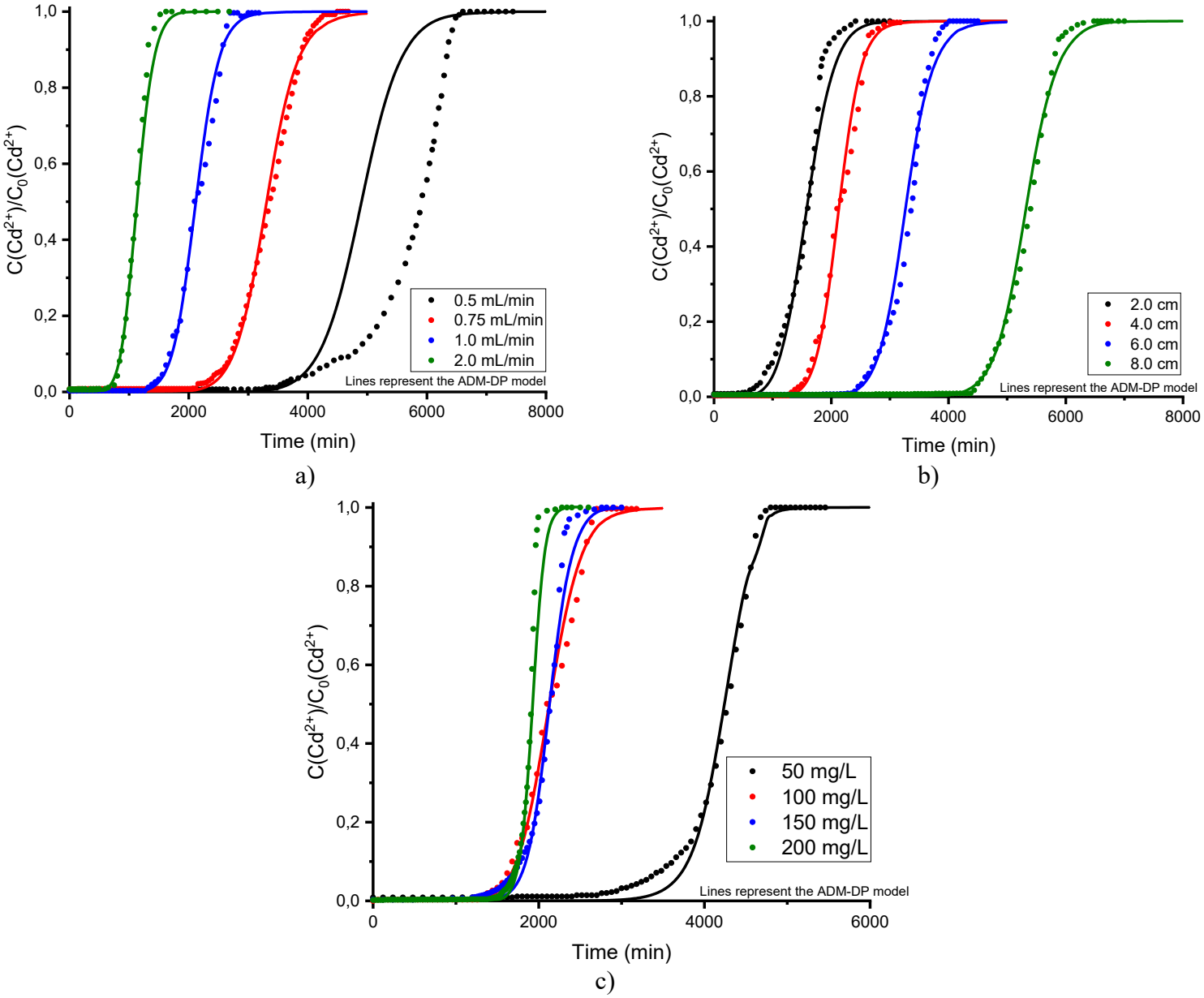

Figure 6. Breakthrough curves for Cd(II) adsorption onto SB varying a) the inlet flow, b) the adsorbent height and c) the inlet flow in the packed columns.

The final studied effect was the variation in initial concentration (Fig. 6c). A lower feed concentration resulted in reduced concentration gradients, thereby decreasing the mass transfer rate (Díaz-Blancas et al., 2020). This can lead to a flattening of the breakthrough curve, as observed in Experiment 5 ($C_0 = 50\ mg/L$), which was conducted at the lowest concentration. In this case, a slight flattening was noted at the beginning of the curve. However, varying the concentration within the range of 100 – 200 mg/L did not produce a significant effect.

It is important to highlight that in predicting the breakthrough curves using the ADM-DPM, no parameter adjustment was performed (see Section 2.6.4), yet the model's predictions remained highly accurate. The characterisation parameters for these curves are also presented in Table 3. A key design parameter is the breakthrough point, making an accurate mathematical modelling prediction highly useful. In this study, the breakthrough point was predicted with an average deviation of 5.3 %, which is lower than the previously reported 10.6 % (Aguirre-Contreras et al., 2023). EBCT is another critical parameter for designing adsorption beds. The variations in flow rate and bed height yielded an EBCT operational range from 11.2 to 2.7 minutes. Fig. 7a) demonstrates that the model's predictions were precise across the entire operational range.

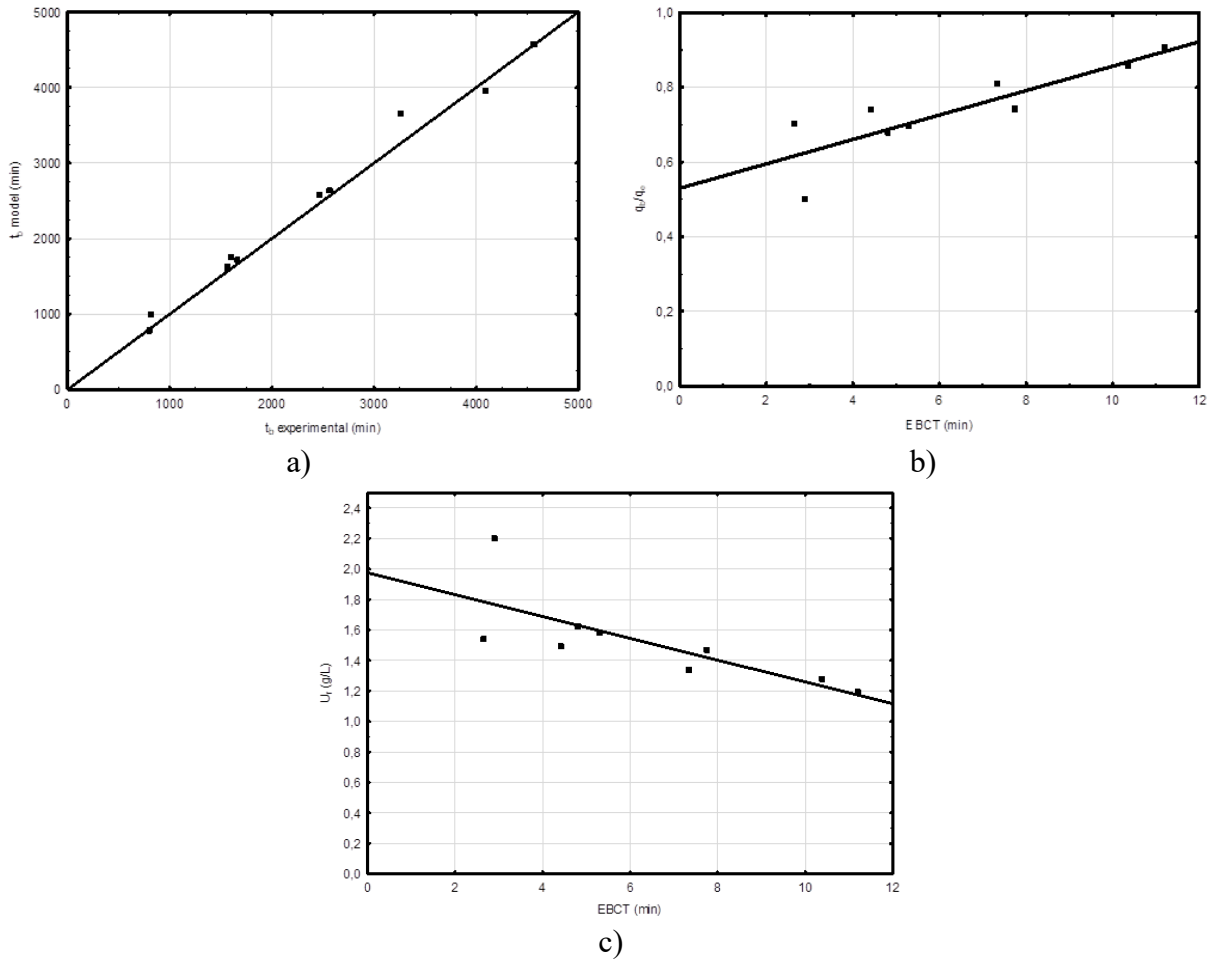

Figure 7. a) Model *vs* experimental prediction of the t_b, b) Efficiency of material utilisation *vs* EBCT and c) Adsorbent usage rate *vs* EBCT. $C_0(Cd^{2+})$ was fixed at 100 mg/L to allow comparison.

Moreover, maximising contaminant adsorption is desirable to optimise the use of the adsorbent material. The dynamic adsorption capacity at the breakthrough point (q_b) represents this quantity,

while the maximum adsorption capacity at equilibrium with the inlet concentration (q_e) defines the material's full potential (Dichiara et al., 2015; Worch, 2021). Thus, the q_b/q_e ratio represents the efficiency of material utilisation. This relationship, depicted in Fig. 7b) as a function of EBCT, shows a tendency for increased material efficiency with increasing EBCT. This trend can be attributed to the extended contact time between the solution and the adsorbent, facilitating more effective interactions. The maximum efficiency observed was 90 %. Another approach to characterising dynamic adsorption performance is the adsorbent usage rate, which indicates the quantity of adsorbent required to treat 1 L of solution. The values obtained were plotted against EBCT, as shown in Fig. 7c). Similarly, the material's performance improved with increasing EBCT, with the lowest adsorbent usage rate recorded at 1.19 g/L. Overall, the results of these dynamic adsorption design parameters demonstrate that the proposed adsorbent material has the potential to be a scalable solution for the removal of Cd(II) from water.

Table 3. Packed bed experiments design and key parameters.

Exp.	C_0 (Cd^{2+}) mg/L	L (cm)	Q (mL/min)	m (g)	FS	MTZ (cm)	v_z (cm/min)	$k_L \cdot 10^5$ (cm/s)	DP · 10^{10} (cm^2/s)	$D_z \cdot 10^4$ (cm^2/s)	Sc	Re	Sh	EBCT (min)	t_b^* (min)	t_s^* (min)	q_b (mg/g)	q_s (mg/g)	Ur (g/L)	R^2 (%)
1	100.91	4.11	0.45	2.1999	0.7	1.67	0.523	1.41	4.75	3.29	1878	0.043	13.2	11.2	4800	6350	83.73	117.14	1.2	94.5
2	100.66	4.13	0.69	2.2799	0.5	1.95	0.813	1.71	4.75	4.37	1878	0.067	15.9	7.3	2720	3915	74.56	100.86	1.3	99.5
3	108.50	4.14	0.96	2.3792	0.5	2.04	1.152	1.95	4.75	5.65	1878	0.095	18.2	5.3	1680	2550	68.24	93.45	1.6	99.4
4	100.15	4.13	1.91	2.3759	0.5	2.24	2.292	2.75	4.75	9.87	1878	0.190	25.7	2.7	876	1320	64.39	88.76	1.5	99.2
5	48.56	4.30	0.90	2.9951	0.7	1.42	1.200	1.64	4.75	5.99	1878	0.099	15.3	5.9	3600	4600	46.93	60.58	1.0	99.0
6	108.50	4.00	1.11	2.5992	0.5	1.97	1.419	1.92	4.75	6.73	1878	0.118	17.9	4.4	1680	2580	72.23	98.91	1.5	99.6
7	150.04	4.05	1.01	2.6013	0.7	1.38	1.283	1.84	4.75	6.22	1878	0.106	17.2	4.9	1770	2300	92.97	121.19	1.6	98.9
8	198.12	4.02	0.97	2.6125	0.7	0.68	1.240	1.79	4.75	6.07	1878	0.103	16.7	5.1	1740	1965	121.76	137.69	1.6	99.1
9	111.14	2.15	0.91	1.6530	0.7	1.45	1.299	1.55	4.75	6.46	1878	0.108	14.5	2.9	1030	1800	49.68	91.47	2.2	98.5
10	108.50	4.00	1.02	2.5992	0.5	1.97	1.304	1.84	4.75	6.31	1878	0.108	17.1	4.8	1680	2550	66.37	90.89	1.6	99.1
11	105.17	6.00	0.95	3.5908	0.6	2.20	1.162	1.88	4.75	5.72	1878	0.096	17.6	7.8	2760	3700	70.96	91.01	1.5	98.9
12	100.57	8.20	0.97	5.6695	0.6	2.01	1.287	1.71	4.75	6.30	1878	0.107	16.0	10.4	4750	5800	78.96	91.21	1.3	99.0

*The breakthrough time (t_b) and saturation time (t_s) were determined at $C/C_0 = 0.05$ and 0.95, respectively.

4. Conclusions

This study investigated the adsorption kinetics and breakthrough behaviour of Cd(II) removal using Sargassum biomass, emphasizing the limitations of traditional kinetic and breakthrough models. The findings revealed that the PFO and PSO models provided suboptimal fits for the adsorption kinetics, indicating that they fail to account for the diffusion and permeation mechanisms critical for low porosity biosorbents. In contrast, the DPM successfully described the adsorption kinetics, incorporating both external and internal transport phenomena. The integration of the DPM with the ADM enabled an accurate prediction of breakthrough curves in packed-bed systems, overcoming the constraints of traditional breakthrough models, which neglect mass transfer limitations. The ADM-DPM framework demonstrated high predictive accuracy across varying operational conditions, with the model effectively capturing the symmetry and mass transfer zone stability of the breakthrough curves. The breakthrough point was predicted with an average deviation of 5.3 %, significantly improving upon previously reported values of 10.6 %.

Experimental results indicated that the EBCT varied between 2.7 and 11.2 min, with a clear trend demonstrating that longer EBCT values improved adsorption efficiency. The highest observed adsorption efficiency reached 90 %, confirming that extending contact time enhances the utilization of the adsorbent. Additionally, the dynamic adsorption capacity at the breakthrough point ranged from 46.93 mg/g to 121.76 mg/g, while the total adsorption capacity at saturation reached a maximum of 137.69 mg/g. These values emphasize the potential of Sargassum biomass as a competitive biosorbent compared to conventional adsorbents. Moreover, the axial dispersion coefficient ranged from $3.29 \cdot 10^{-4}$ cm²/s to $9.87 \cdot 10^{-4}$ cm²/s, indicating a consistent dispersion effect across different operating conditions. The intraparticle diffusion coefficient was determined to be within the range of $2.5 \cdot 10^{-10}$ cm²/s to $9.0 \cdot 10^{-10}$ cm²/s, confirming the relevance of the diffusion-permeation mechanism in controlling mass transfer limitations. The mass transfer coefficient was found to vary between $1.4 \cdot 10^{-3}$ cm/s and $7.7 \cdot 10^{-3}$ cm/s, further supporting the significance of external and internal mass transfer resistances in this adsorption system. The performance of Sargassum biomass in packed-bed adsorption was further highlighted by its low adsorbent usage rate, which was minimized to 1.19 g/L, making it an attractive option for large-scale water treatment applications. The study also demonstrated that reducing the bed height or

increasing the flow rate led to earlier breakthrough times, reinforcing the importance of optimizing operating parameters to maximize adsorbent efficiency.

Overall, this research represents the first attempt to integrate the DPM with ADM for modelling metal adsorption onto Sargassum biomass. The findings provide critical insights for optimizing adsorption-based water treatment processes and contribute to the development of sustainable and cost-effective solutions for heavy metal removal from contaminated water sources. The proposed modelling framework can be extended to other low porosity biosorbents, broadening its applicability to diverse wastewater treatment scenarios. Future studies should focus on scaling up this approach and evaluating its performance in multi-component adsorption systems under real-world conditions.

Funding: This work was supported by the Secretaría de Ciencias, Humanidades, Tecnología e Innovación from Mexico (CVU 1014829). This work is part of a doctoral thesis in Chemistry at the University of Granada (Spain) and in Environmental Sciences at the Autonomous University of San Luis Potosi (Mexico).

Declaration of competing interest: The authors declare that they have no known competing financial interests or personal relationships that could have appeared to influence the work reported in this paper.

Data availability: Data will be made available on request.

Author contributions: L.A.G.F.: Conceptualization, Methodology, Software, Formal Analysis, Investigation, Data Curation, Writing-Original Draft, Visualization. **S.A.C.:** Conceptualization, Methodology, Software, Formal Analysis, Writing-Original Draft, Visualization. **N.A.M.C.:** Conceptualization, Methodology, Software, Formal Analysis, Writing-Original Draft, Visualization, Resources, Supervision. **M.S.P.:** Visualization, Resources, Supervision. **A.E.N.F.:** Visualization, Resources, Supervision. **J.E.V.C.:** Conceptualization, Methodology, Writing-Original Draft. **R.O.P.:** Conceptualization, Methodology, Writing-Original Draft.

References

Abdelwaheb, M., Nedeff, V., Dridi-Dhaouadi, S., Moșneguțu, E., Barsan, N., Chițimus, A.D., 2022. Assessment of Cadmium and Copper Adsorption by Two Agricultural Soils from

Romania and Tunisia: Risk of Water Resource Pollution. Processes 10, 1802. https://doi.org/10.3390/pr10091802

Adamu, A., Sani, B., Muhammad, M., Ahmed, A., 2023. Modelling and Optimization of Cadmium Removal From Wastewater Onto Sugarcane Bagasse Activated Carbon. Niger. J. Eng. 30, 36. https://doi.org/10.5455/nje.2023.30.01.06

Adegoke, K.A., Akinnawo, S.O., Ajala, O.A., Adebusuyi, T.A., Maxakato, N.W., Bello, O.S., 2022. Progress and challenges in batch and optimization studies on the adsorptive removal of heavy metals using modified biomass-based adsorbents. Bioresour. Technol. Reports 19, 101115. https://doi.org/10.1016/j.biteb.2022.101115

Aguirre-Contreras, S., Leyva-Ramos, R., Ocampo-Pérez, R., Aguilar-Madera, C.G., Flores-Cano, J. V., Medellín-Castillo, N.A., 2023. Mathematical modeling of breakthrough curves for 8-hydroxyquinoline removal from fundamental equilibrium and adsorption rate studies. J. Water Process Eng. 54, 103967. https://doi.org/10.1016/j.jwpe.2023.103967

Apiratikul, R., Chu, K.H., 2021. Improved fixed bed models for correlating asymmetric adsorption breakthrough curves. J. Water Process Eng. 40, 101810. https://doi.org/10.1016/j.jwpe.2020.101810

Atugoda, T., Gunawardane, C., Ahmad, M., Vithanage, M., 2021. Mechanistic interaction of ciprofloxacin on zeolite modified seaweed (Sargassum crassifolium) derived biochar: Kinetics, isotherm and thermodynamics. Chemosphere 281, 130676. https://doi.org/10.1016/j.chemosphere.2021.130676

Bassam, R., El Hallaoui, A., El Alouani, M., Jabrane, M., El Khattabi, E.H., Tridane, M., Belaaouad, S., 2021. Studies on the Removal of Cadmium Toxic Metal Ions by Natural Clays from Aqueous Solution by Adsorption Process. J. Chem. 2021, 7873488. https://doi.org/10.1155/2021/7873488

Bello, O.S., Moshood, M.A., Ewetumo, B.A., Afolabi, I.C., 2020. Ibuprofen removal using coconut husk activated Biomass. Chem. Data Collect. 29, 100533. https://doi.org/10.1016/j.cdc.2020.100533

Chaouay, J., Bentiss, F., Zbair, M., Belattmania, Z., Sabour, B., Lamonier, J.F., Duquesne, S.,

Jama, C., 2024. Study of mercury adsorption using biochars derived from the invasive brown seaweed “Sargassum muticum” as a low-cost and ecofriendly adsorbent in the aqueous phase. Int. J. Environ. Sci. Technol. 1–14. https://doi.org/10.1007/s13762-024-05765-8

Chu, K.H., Hashim, M.A., 2024. Comparing different versions of the Yoon–Nelson model in describing organic micropollutant adsorption within fixed bed adsorbers. Environ. Sci. Pollut. Res. 31, 21136–21143. https://doi.org/10.1007/s11356-024-32450-7

Davis, T.A., Volesky, B., Mucci, A., 2003. A review of the biochemistry of heavy metal biosorption by brown algae. Water Res. 37, 4311–4330. https://doi.org/10.1016/S0043-1354(03)00293-8

Díaz-Blancas, V., Aguilar-Madera, C.G., Flores-Cano, J. V., Leyva-Ramos, R., Padilla-Ortega, E., Ocampo-Pérez, R., 2020. Evaluation of mass transfer mechanisms involved during the adsorption of metronidazole on granular activated carbon in fixed bed column. J. Water Process Eng. 36, 101303. https://doi.org/10.1016/j.jwpe.2020.101303

Dichiara, A.B., Weinstein, S.J., Rogers, R.E., 2015. On the Choice of Batch or Fixed Bed Adsorption Processes for Wastewater Treatment. Ind. Eng. Chem. Res. 54, 8579–8586. https://doi.org/10.1021/acs.iecr.5b02350

do Nascimento Júnior, W.J., de Aguiar, G.H., Massarelli, R.C., Landers, R., Vieira, M.G.A., da Motta Sobrinho, M.A., 2024. Multi-pollutant biosorption of organic and inorganic pollutants by brown algae waste from alginate production: batch and fixed-bed investigation. Environ. Sci. Pollut. Res. 31, 53580–53597. https://doi.org/10.1007/s11356-023-30511-x

Do Nascimento, W.J., Landers, R., Gurgel Carlos Da Silva, M., Vieira, M.G.A., 2021. Equilibrium and desorption studies of the competitive binary biosorption of silver(I) and copper(II) ions on brown algae waste. J. Environ. Chem. Eng. 9, 104840. https://doi.org/10.1016/j.jece.2020.104840

Ebelegi, A.N., Ayawei, N., Wankasi, D., 2020. Interpretation of Adsorption Thermodynamics and Kinetics. Open J. Phys. Chem. 10, 166–182. https://doi.org/10.4236/ojpc.2020.103010

Ezzati, R., 2023. A new insight into the pseudo-second-order model and the physical meaning of its rate constant in adsorption. J. Dispers. Sci. Technol. 46, 222–229.

https://doi.org/10.1080/01932691.2023.2288090

Ezzati, R., Azizi, M., Ezzati, S., 2024. A theoretical approach for evaluating the contributions of pseudo-first-order and pseudo-second-order kinetics models in the Langmuir rate equation. Vacuum 222, 113018. https://doi.org/10.1016/j.vacuum.2024.113018

Furusawa, T., Smith, J.M., 1973. Fluid—Particle and Intraparticle Mass Transport Rates in Slurries. Ind. Eng. Chem. Fundam. 12, 197–203. https://doi.org/10.1021/i160046a009

Giles, C.H., Smith, D., Huitson, A., 1974. A general treatment and classification of the solute adsorption isotherm. I. Theoretical. J. Colloid Interface Sci. 47, 755–765. https://doi.org/10.1016/0021-9797(74)90252-5

Gutierrez-Reyna, S.O., Herrera-Hernández, E.C., Aguilar-Madera, C.G., López-Ramón, M.V., Ocampo-Perez, R., Parra-Marfil, A., Garcia-Hernandez, E., Bailon-Garcia, E., 2024. New trends in modelling of breakthrough curves to remove pollutants using adsorption on advanced monoliths geometries. Environ. Res. 243, 117871. https://doi.org/10.1016/j.envres.2023.117871

Hebbani, A.V., Anantha, R., Kasaba Manjunath, G., Kulkarni, A., Sam, R., Mishra, A., 2021. Evaluation of cadmium biosorption property of de-oiled palm kernel cake. Int. J. Phytoremediation 23, 522–529. https://doi.org/10.1080/15226514.2020.1829544

Hu, Q., Ma, S., He, Z., Liu, H., Pei, X., 2024. A revisit on intraparticle diffusion models with analytical solutions: Underlying assumption, application scope and solving method. J. Water Process Eng. 60, 105241. https://doi.org/10.1016/j.jwpe.2024.105241

Hu, Q., Pang, S., Wang, D., 2022. In-depth Insights into Mathematical Characteristics, Selection Criteria and Common Mistakes of Adsorption Kinetic Models: A Critical Review. Sep. Purif. Rev. 51, 281–299. https://doi.org/10.1080/15422119.2021.1922444

Hu, Q., Pang, S., Wang, D., Yang, Y., Liu, H., 2021. Deeper Insights into the Bohart-Adams Model in a Fixed-Bed Column. J. Phys. Chem. B 125, 8494–8501. https://doi.org/10.1021/acs.jpcb.1c03378

Jellali, S., Azzaz, A.A., Jeguirim, M., Hamdi, H., Mlayah, A., 2021. Use of lignite as a low-cost material for cadmium and copper removal from aqueous solutions: Assessment of adsorption

characteristics and exploration of involved mechanisms. Water (Switzerland) 13, 164. https://doi.org/10.3390/w13020164

Kayranli, B., 2022. Cadmium removal mechanisms from aqueous solution by using recycled lignocelluloses. Alexandria Eng. J. 61, 443–457. https://doi.org/10.1016/j.aej.2021.06.036

Korake, S.R., Jadhao, P.D., 2021. Investigation of Taguchi optimization, equilibrium isotherms, and kinetic modeling for cadmium adsorption onto deposited silt. Heliyon 7. https://doi.org/10.1016/j.heliyon.2020.e05755

Kuldeyev, E., Seitzhanova, M., Tanirbergenova, S., Tazhu, K., Doszhanov, E., Mansurov, Z., Azat, S., Nurlybaev, R., Berndtsson, R., 2023. Modifying Natural Zeolites to Improve Heavy Metal Adsorption. Water (Switzerland) 15, 2215. https://doi.org/10.3390/w15122215

Leyva-Ramos, R., Salazar-Rábago, J.J., Ocampo-Pérez, R., 2021. A novel intraparticle mass transfer model for the biosorption rate of methylene blue on white pine (Pinus durangensis) sawdust. Diffusion-permeation. Chem. Eng. Res. Des. 172, 43–52. https://doi.org/10.1016/j.cherd.2021.05.029

Leyva-Ramos, R., Geankoplis, C.J., 1994. Diffusion in liquid-filled pores of activated carbon. I. Pore volume diffusion. Can. J. Chem. Eng. 72, 262–271. https://doi.org/10.1002/cjce.5450720213

Lv, B., Dong, B., Zhang, C., Chen, Z., Zhao, Z., Deng, X., Fang, C., 2022. Effective adsorption of methylene blue from aqueous solution by coal gangue-based zeolite granules in a fluidized bed: Fluidization characteristics and continuous adsorption. Powder Technol. 408, 117764. https://doi.org/10.1016/j.powtec.2022.117764

Mariah, M.A.A., Rovina, K., Vonnie, J.M., Erna, K.H., 2023. Characterization of activated carbon from waste tea (Camellia sinensis) using chemical activation for removal of methylene blue and cadmium ions. South African J. Chem. Eng. 44, 113–122. https://doi.org/10.1016/j.sajce.2023.01.007

Mitrevski, V., Mijakovski, V., Mijakovski, N., Lutovska, M., 2022. Statistical evaluation of some four parameters sorption isotherm models. Ann. Fac. Eng. Hunedoara 20, 2–4.

Musah, M., Azeh, Y., Mathew, J., Umar, M., Abdulhamid, Z., Muhammad, A., 2022. Adsorption

Kinetics and Isotherm Models: A Review. Caliphate J. Sci. Technol. 4, 20–26. https://doi.org/10.4314/cajost.v4i1.3

Naja, G., Volesky, B., 2011. The mechanism of metal cation and anion biosorption, in: Microbial Biosorption of Metals. Springer, pp. 19–58. https://doi.org/10.1007/978-94-007-0443-5_3

Omitola, O.B., Abonyi, M.N., Akpomie, K.G., Dawodu, F.A., 2022. Adams-Bohart, Yoon-Nelson, and Thomas modeling of the fix-bed continuous column adsorption of amoxicillin onto silver nanoparticle-maize leaf composite. Appl. Water Sci. 12, 94. https://doi.org/10.1007/s13201-022-01624-4

Oxenford, H.A., Cox, S.A., van Tussenbroek, B.I., Desrochers, A., 2021. Challenges of Turning the Sargassum Crisis into Gold: Current Constraints and Implications for the Caribbean. Phycology 1, 27–48. https://doi.org/10.3390/phycology1010003

Patel, H., 2021. Comparison of batch and fixed bed column adsorption: a critical review. Int. J. Environ. Sci. Technol. 19, 10409–10426. https://doi.org/10.1007/s13762-021-03492-y

Pessôa, N.T., Sales, D.C.S., Do Nascimento, G.E., dos Santos, J.H.L., Silva, M.N. dos S., Napoleão, D.C., Rodríguez-Díaz, J.M., Duarte, M.M.M.B., 2024. Effective adsorption of cadmium and nickel ions in mono and bicomponent systems using eco-friendly adsorbents prepared from peanut shells. Environ. Res. 247, 118220. https://doi.org/10.1016/j.envres.2024.118220

Rajahmundry, G.K., Garlapati, C., Kumar, P.S., Alwi, R.S., Vo, D.V.N., 2021. Statistical analysis of adsorption isotherm models and its appropriate selection. Chemosphere 276, 130176. https://doi.org/10.1016/j.chemosphere.2021.130176

Rekha, A., Srinivasan, L., S. , P., T. , G., P. N. , S., G. , L., Arumugam, N., Abdulrahman I . , A., Sakkarapalayam M. , M., A. , V., 2023. Biosorption efficacy studies of Sargassum wightii and its biochar on the removal of chromium from aqueous solution. J. Taiwan Inst. Chem. Eng. 166, 105241. https://doi.org/10.1016/j.jtice.2023.105241

Revellame, E.D., Fortela, D.L., Sharp, W., Hernandez, R., Zappi, M.E., 2020. Adsorption kinetic modeling using pseudo-first order and pseudo-second order rate laws: A review. Clean. Eng. Technol. 1, 100032. https://doi.org/10.1016/j.clet.2020.100032

Robledo, D., Vázquez-Delfín, E., Freile-Pelegrín, Y., Vásquez-Elizondo, R.M., Qui-Minet, Z.N., Salazar-Garibay, A., 2021. Challenges and Opportunities in Relation to Sargassum Events Along the Caribbean Sea. Front. Mar. Sci. 8, 699664. https://doi.org/10.3389/fmars.2021.699664

Samimi, M., Mansouri, E., 2024. Efficiency evaluation of Falcaria vulgaris biomass in Co(II) uptake from aquatic environments: characteristics, kinetics and optimization of operational variables. Int. J. Phytoremediation 26, 493–503. https://doi.org/10.1080/15226514.2023.2250462

Saravanan, P., Saravanan, V., Rajeshkannan, R., Arnica, G., Rajasimman, M., Baskar, G., Pugazhendhi, A., 2024. Comprehensive review on toxic heavy metals in the aquatic system: sources, identification, treatment strategies, and health risk assessment. Environ. Res. 258, 119440. https://doi.org/10.1016/j.envres.2024.119440

Tavana, M., Pahlavanzadeh, H., Zarei, M.J., 2020. The novel usage of dead biomass of green algae of Schizomeris leibleinii for biosorption of copper(II) from aqueous solutions: Equilibrium, kinetics and thermodynamics. J. Environ. Chem. Eng. 8, 104272. https://doi.org/10.1016/j.jece.2020.104272

Thamarai, P., Deivayanai, V.C., Karishma, S., Saravanan, A., Yaashikaa, P.R., Vickram, A.S., 2024. Adsorption Strategies in Surface Modification Techniques for Seaweeds in Wastewater Treatment: Exploring Environmental Applications. Rev. Environ. Contam. Toxicol. 262, 18. https://doi.org/10.1007/s44169-024-00071-3

Upton, K., Macdonald, A., 2021. Clean Water and Sanitation, Sustainable Development Goals Series. Springer. https://doi.org/10.1007/978-3-030-38815-7_6

Vanýsek, P., 1996. Ionic conductivity and diffusion at infinite dilution. CRC Handb. Chem. Phys. 96, 5–98.

Velarde, L., Nikjoo, D., Escalera, E., Akhtar, F., 2024. Bolivian natural zeolite as a low-cost adsorbent for the adsorption of cadmium: Isotherms and kinetics. Heliyon 10. https://doi.org/10.1016/j.heliyon.2024.e24006

Wang, J., Guo, X., 2022. Rethinking of the intraparticle diffusion adsorption kinetics model:

Interpretation, solving methods and applications. Chemosphere 309, 136732. https://doi.org/10.1016/j.chemosphere.2022.136732

Worch, E., 2021. Adsorption Technology in Water Treatment, Adsorption Technology in Water Treatment. de Gruyter Berlin. https://doi.org/10.1515/9783110715507

Zaynab, M., Al-Yahyai, R., Ameen, A., Sharif, Y., Ali, L., Fatima, M., Khan, K.A., Li, S., 2022. Health and environmental effects of heavy metals. J. King Saud Univ. - Sci. 34, 101653. https://doi.org/10.1016/j.jksus.2021.101653

Zhou, Q., Liu, Y., Li, T., Zhao, H., Alessi, D.S., Liu, W., Konhauser, K.O., 2020. Cadmium adsorption to clay-microbe aggregates: Implications for marine heavy metals cycling. Geochim. Cosmochim. Acta 290, 124–136. https://doi.org/10.1016/j.gca.2020.09.002

CONCLUSIONS

This research demonstrates the high potential of *Sargassum spp.* biomass, both in its natural and carbonized forms (biochar and hydrochar), as an efficient, low-cost, and sustainable adsorbent for the removal of heavy metals, specifically cadmium (Cd^{2+}) and lead (Pb^{2+}), and the pharmaceutical compound ibuprofen (IBU) from aqueous environments. The study provides a comprehensive approach, combining material synthesis, physicochemical characterization, adsorption performance evaluation in batch and continuous systems, and advanced mathematical modeling.

The natural biomass of *Sargassum spp.* exhibited significant adsorption capacity, attributed to its high content of active functional groups such as carboxylic, hydroxyl, and sulfonic groups. Physicochemical characterization using FTIR, SEM/EDS, TGA, BET, and CHONS elemental analysis confirmed the abundance of reactive sites and the porous nature of the materials. Pyrolytic and hydrothermal carbonization of the biomass significantly enhanced textural properties, achieving specific surface areas up to 240 m^2/g and improving structural stability and adsorption capacity.

In monocomponent systems, the materials achieved maximum adsorption capacities of 157 mg/g for Cd(II), 478 mg/g for Pb(II), and 103 mg/g for ibuprofen under optimized experimental conditions, outperforming many conventional biosorbents reported in the literature. The adsorption processes followed pseudo-second-order kinetics and were best described by Langmuir and Radke–Prausnitz isotherms, suggesting monolayer adsorption on a heterogeneous surface. Thermodynamic analyses confirmed that the adsorption of all contaminants was spontaneous and endothermic, driven by chemisorption mechanisms.

Multicomponent adsorption studies revealed competitive and selective behavior depending on the affinity of each ion or molecule for specific functional groups on the adsorbent surface. Despite competition, the Sargassum-derived materials maintained high removal efficiencies, confirming their suitability for real-world applications where mixed contaminants are present.

Dynamic adsorption experiments using packed-bed columns further validated the materials' practical application. The breakthrough behavior was studied in depth, and a Diffusion–Permeation Model (DPM) was developed and successfully coupled with the Axial Dispersion Model (ADM) to simulate the system. The model accurately predicted breakthrough curves with

deviations under 5 %, demonstrating its robustness and applicability in the design of continuous water treatment systems.

Beyond water decontamination, this thesis also contributes to solving the ecological and economic challenges posed by the massive accumulation of Sargassum in the Mexican Caribbean. By transforming this marine biomass, typically treated as waste, into high-value adsorbent materials, the study supports the principles of circular economy and environmental sustainability. The valorisation of Sargassum not only mitigates the negative impact of algal blooms on tourism and marine ecosystems but also offers a promising solution for the remediation of contaminated water.

In summary, this research provides strong scientific evidence that *Sargassum spp.* biomass is a viable, abundant, and eco-friendly precursor for advanced biosorbent materials. The integration of batch and dynamic adsorption studies, rigorous physicochemical characterization, and predictive mathematical modeling offers a complete framework for the future development and scaling of biosorption technologies. The findings pave the way for broader applications in wastewater treatment, particularly in regions facing challenges with marine algal overgrowth and industrial pollution. Future work should explore long-term operational stability, regeneration and reuse cycles, and the integration of these materials into hybrid treatment systems combining adsorption with other remediation strategies.